

Identification and functional analysis of Trnp1 – a novel DNA associated protein with a key role in neurogenesis

Dissertation der Fakultät für Biologie der
Ludwig-Maximilian-Universität München



Angefertigt in der Arbeitsgruppe von Prof. Dr. Magdalena Götz am
Institut für Physiologische Genomik, LMU München und am
Institut für Stammzellforschung, Helmholtz Zentrum München

Ronny Stahl

12.09.2012

Einreichung der Dissertation bei der Fakultät für Biologie am 12. September 2012

Tag der mündlichen Prüfung (Disputation): 25. Februar 2012

1. Gutachter: Prof. Dr. Heinrich Leonhardt
2. Gutachter: Prof. Dr. Benedikt Grothe
3. Gutachter: PD Dr. Mario Wullimann
4. Gutachter: Prof. Dr. Angelika Böttger
5. Gast: Prof. Dr. Magdalena Götz

Eidesstattliche Erklärung

Ich versichere hiermit an Eides statt, dass die vorgelegte Dissertation von mir selbstständig und ohne unerlaubte Hilfe angefertigt wurde.

München, den

(Unterschrift)

Für meine Familie

For my family

Acknowledgements

First and foremost I would like to thank **Magdalena Götz** for giving me the opportunity to perform my PhD Thesis in her laboratory. I want to thank her for her constant support and for sharing her great knowledge in neuroscience. Her positive character and open-mindedness for new approaches and ideas were very encouraging. Thanks for all the copious discussions we had and for always being available whenever something needed to be discussed. The excellent scientific environment in her lab with outstanding scientists, intellectual exchange and extraordinary technical possibilities has been a great motivation throughout my work.

Thanks to **Robert Blum** for help with the antibody generation and purification, for support in the beginning of my time in the lab and for helpful comments during my thesis committees. Thanks also to **Axel Imhof** for being part of my thesis committee and contributing ideas and experimental know how especially concerning the molecular characterization.

I want to thank **Gabriele Jäger, Andrea Steiner-Mezzadri, Ines Mühlhahn, Carmen Meyer, Detlef Franzen** and **Timu Öztürk** for excellent technical support. Thanks to **Alex Lepier** for help with virus production.

Thanks to my permanent office mate throughout the years **Christophe Heinrich**. Thanks for sharing your broad scientific knowledge. We had great scientific but also non-scientific discussions and without his help I would still search for a suitable chair;-). Thanks to **Elisa Murenu, Christiane Simon, Steffen Tiedt, Melanie Jawerka** and **Andrew Grande** for creating a great office atmosphere with lots of good discussions and a lot of humor.

I am truly glad to have had a lot of great scientific discussions with **Benedikt Berninger, Sergio Gascon, Felipe Ortega de la O, Monika Brill, Matteo Bergami, Marco Canossa, Giacomo Masserdotti, Francesca Vigano, Ruth Beckervordersandforth-Bonk, Judith Fischer-Sternjak, Marcos Costa, Jovica Ninkovic, Filippo Calzolari** and **Aditi Deshpande**. Special thanks to the “spanish connection” Felipe and Sergio without whom the lab-life would have not been the same. Thanks for introducing me to all the special “E-spanenglish” words;-) thanks Felipe for the great canoeing zigzag tour that we did – I guess the poor Spreewald needed to be re-vegetated along the creek after we bumped into literally every tree...

I want to say special thanks to all “embryo club” members and especially **Silvia Cappello, Gregor Pilz, Sven Falk, Pia Johansson, Maki Asami, Franziska Weinandy, Christian Böhringer and Vidya Ramesh** for very fruitful discussions and good inputs concerning my project. Thanks also to **Luisa Pinto** who carried out the screen that was the starting point of this study. I want to thank **Michael Metzger** for being a great Master student. I learned a lot during my time as supervisor. And I want to thank **Lana Polero** and **Suada Ajanovic** for being a great help with administrative and facility issues.

Last but definitely not least I want to thank the most important people in my life: thanks to **Tessa Walcher** for always believing in me and for her constant support. It is truly like in that old song “...you give me hope and consolation, you give me strength to carry on and you’re always there to lend a hand in everything I do - that’s the wonder, the wonder of you!” I am most thankful to my **parents** and **grandparents** that always supported me in everything I did, without them this work would have not been possible.

Table of Contents

1	Abstract.....	1
2	Introduction.....	5
	2.1 Cerebral cortical development - neurogenesis in its natural course.....	6
	2.1.1 Neural stem and progenitor cells during forebrain development	8
	2.1.2 Heterogeneity amongst neurogenic stem cells	10
	2.1.3 Cellular diversity forming the six-layered mammalian cerebral cortex	11
	2.1.4 Control of stem cell proliferation and differentiation by intrinsic and extrinsic factors	12
	2.1.5 Identification of factors involved in direct and indirect neurogenesis	15
	2.2 Cortical Expansion and brain Evolution.....	16
	2.3 Neurogenesis in the adult brain.....	19
	2.4 Trnp1 – a nuclear protein highly conserved within the mammalian lineage.....	21
3	Aim of this study	24
4	Results	25
	4.1 Generation of an antibody raised against Trnp1.....	25
	4.1.1 Antibody recognition site	26
	4.1.2 Test of antibody specificity	27
	4.2 Expression analysis of Trnp1 during murine telencephalic development.....	29
	4.2.1 Analysis of Trnp1 expression during forebrain development	29
	4.2.2 Detailed expression analysis at mid-neurogenesis	31
	4.2.3 Expression analysis of Trnp1 in the adult murine brain	33
	4.3 Investigating the functional role of Trnp1 <i>in vitro</i>.....	35
	4.3.1 Generation of a retroviral construct for forced expression of Trnp1	35
	4.3.2 Overexpression of Trnp1 increases proliferation of neurogenic progenitors in vitro.....	36
	4.4 Functional analysis of Trnp1 <i>in vivo</i>	41
	4.4.1 Forced expression of Trnp1 <i>in vivo</i> by <i>in utero</i> electroporation	41

Table of Contents

4.4.1.1	<i>Forced expression of Trnp1 in vivo increases the number of apical progenitors and causes tangential expansion</i>	41
4.4.1.2	<i>Forced expression of Trnp1 in vivo increases self renewal of Pax6+ radial glial cells</i>	44
4.4.2	Knock down of Trnp1 in vivo by in utero electroporation	45
4.4.2.1	<i>Generation of short hairpin RNAs for the knock down of Trnp1</i>	46
4.4.2.2	<i>Knock down of Trnp1 in vivo leads to radial expansion of the developing forebrain</i>	48
4.4.2.3	<i>Knock down of Trnp1 increases the number of basal progenitors</i>	50
4.4.2.4	<i>Knock down of Trnp1 at mid neurogenesis induces an increase of oRGs and folding of the cortical plate</i>	52
4.4.2.5	<i>Rescue of Trnp1 knock down</i>	57
4.5	Molecular analysis of Trnp1	59
4.5.1	Trnp1 is tightly associated with DNA	59
4.5.2	Bioinformatic analysis of Trnp1 structure	62
4.5.3	Mass Spectrometry analysis to uncover direct binding partners of Trnp1	65
4.5.4	FRAP experiment for Trnp1	66
4.5.5	C-terminal fusion of GFP to Trnp1 inhibits its DNA binding ability	68
4.5.6	Analysis of direct regulation of gene expression through Trnp1	70
4.5.7	Gene Expression analysis of gain and loss of Trnp1	71
5	Discussion	77
5.1	Expression of Trnp1 in the murine brain	77
5.2	The function of Trnp1 in the developing forebrain	79
5.3	The role of Trnp1 in neurogenesis and its potential in reprogramming	84
5.4	TRNP1 in human brain development	84
5.4.1	TRNP1 expression in the developing human brain	84
5.4.2	Investigation of a possible association of TRNP1 with human diseases	86
5.5	The Molecular function of Trnp1	89
5.5.1	Biochemical characteristics of Trnp1	89
5.5.2	The regulatory function of Trnp1 on gene expression	90
5.5.3	Similarities of Trnp1 with other known proteins	91
5.5.4	A possible role of Trnp1 in regulation of chromatin state	94

6	Material and Methods	98
6.1	Materials.....	98
6.1.1	Buffers and Solutions	98
6.1.1.1	10x PBS	98
6.1.1.2	4 % PFA (from initially a 20% PFA Stock).....	98
6.1.1.3	50x TAE-buffer	98
6.1.1.4	10x SDS running-buffer	99
6.1.1.5	Separation Gel buffer for SDS Gels	99
6.1.1.6	Stacking Gel buffer for SDS Gels	99
6.1.1.7	Transfer-buffer (wet blot).....	99
6.1.1.8	Lysis Buffers for Cell/Tissue Lysis	100
6.1.2	Cell lines.....	101
6.1.3	Antibodies.....	101
6.1.3.1	Primary antibodies	101
6.1.3.2	Secondary antibodies.....	102
6.1.4	Oligonucleotides.....	102
6.1.5	Plasmids.....	103
6.2	Methods	105
6.2.1	DNA Methods	105
6.2.1.1	Ethanol precipitation of DNA.....	105
6.2.1.2	PCR.....	105
6.2.1.3	Colony PCR.....	106
6.2.1.4	Restriction digestion of DNA.....	106
6.2.1.5	Analysis of DNA-fragments on agarose gels (Meyers et al., 1976)	106
6.2.1.6	Ligation.....	107
6.2.1.7	Preparation of bacterial agar plates (Sambrook et al., 1989).....	107
6.2.1.8	Generation of chemo-competent E.coli (modified CaCl ₂ -method).....	108
6.2.1.9	Transformation of chemo-competent E.coli	109
6.2.1.10	Small scale DNA-preparation (MiniPrep)	110
6.2.1.11	Large scale DNA-preparation (MaxiPrep)	110
6.2.1.12	Sequencing of DNA.....	110

Table of Contents

6.2.2 Plasmids and Cloning of Constructs	110
6.2.2.1 Cloning of <i>pCAG-Trnp1-GFP/dsRed</i>	110
6.2.2.2 Cloning of <i>pSUPER-shRNA constructs</i>	111
6.2.2.3 Cloning of <i>pLVTHM-shRNA constructs</i>	111
6.2.2.4 Cloning of <i>pSUPER.GFP/Neo-shRNA constructs</i>	112
6.2.3 Biochemical Protein Methods	112
6.2.3.1 Cell / Tissue Lysis.....	112
6.2.3.2 Perchloric Acid Extraction.....	114
6.2.3.3 SDS-Polyacrylamide gel electrophoresis (SDS-PAGE) (Tris-Glycine).....	114
6.2.3.4 Western blot (wet blot).....	115
6.2.3.5 Western blot detection.....	116
6.2.3.6 Reprobing of western blot membranes (stripping).....	117
6.2.3.7 Coomassie staining	117
6.2.3.8 Mass Spectrometry.....	118
6.2.4 Trnp1 Antibody generation	118
6.2.5 Cell- and Tissue-Culture Methods	118
6.2.5.1 Preparation of Coverslips coated with PDL.....	118
6.2.5.2 Cultivation of HEK cells	119
6.2.5.3 Freezing of cells for long term storage	119
6.2.5.4 Thawing cells.....	120
6.2.5.5 Dissociated cell cultures of the embryonic cerebral cortex.....	120
6.2.5.6 Transient transfection of cells with Lipofectamine	120
6.2.5.7 Retroviral production.....	121
6.2.5.8 Time-lapse video microscopy.....	121
6.2.5.9 Dual Luciferase reporter Assay	121
6.2.5.10 Fluorescence recovery after photo bleaching (FRAP)	122
6.2.6 In vivo Methods	123
6.2.6.1 Animals.....	123
6.2.6.2 Anesthesia.....	123
6.2.6.3 In utero Electroporations	123
6.2.6.4 BrdU administration	125
6.2.6.5 Fixation and Sectioning of Mouse Brains	125

Table of Contents

6.2.7	Immuno labeling	125
6.2.8	Fluorescence Activated Cell Sorting	127
6.2.9	Microarray Analysis	127
6.2.10	Data Analysis	128
7	Appendix	130
7.1	Mass Spectrometry Data	130
7.2	Transcriptome Analysis	135
7.2.1	Trnp1 knock down versus control GFP electroporation (152 genes).....	135
7.2.2	Trnp1 overexpression vs. control GFP electroporation (31 genes).....	139
7.3	Abbreviations	140
8	Plasmid maps	144
8.1	pCMV-Sport6- <i>Trnp1</i>	144
8.2	pENTR1A- <i>Trnp1</i>	144
8.3	pCAG- <i>Trnp1</i> -GFP	145
8.4	pCAG- <i>Trnp1</i> -dsRed.....	145
8.5	pSUPER-shRNA	146
8.6	pLVTHM.....	146
8.7	pLVTHM-shRNA	147
8.8	pSUPER.GFP/Neo-shRNA	147
8.9	peGFP- <i>Trnp1</i> -N3.....	148
9	References	149

1 Abstract

Evolution of the mammalian brain encompassed a remarkable increase in size of the cerebral cortex. One key question is how cortical expansion is regulated and what mechanisms distinguish larger brains from smaller ones. During brain development radial glial cells (RG) are stem cells that give rise to neurons and later also to glial cells that then together populate the adult brain. In order to increase the future brain size, initially the stem cell pool needs to be expanded leading to a lateral (also called tangential) expansion of the cerebral cortex. Later, cortical neurogenesis occurs in different modes: first, RGs can give rise to neurons directly by asymmetric cell division thereby re-generating one radial glial cell and producing one neuron at the same time. Second, RGs can give rise to basal progenitor cells (BP) that typically divide once more to give rise to two differentiating neurons. Thereby the neuronal output is increased which then leads to a radial expansion of the cerebral cortex increasing its thickness. At mid-neurogenic stages the pool of RGs is heterogeneous with subpopulations mainly regenerating themselves and giving rise to neurons directly, and others mainly generating BPs. However, the factors determining these different subsets of radial glial cells are mostly unknown. Trnp1, a nuclear protein with previously undescribed *in vivo* function, was recently identified in such RG cells that do not produce BPs (Pinto et al., 2008).

The major aim of my work was to investigate Trnp1 function during cortical neurogenesis. I found Trnp1 protein to be expressed in a subset of radial glial cells at midneurogenesis in the murine cerebral cortex. Trnp1 is absent in BPs but re-expressed in all newborn neurons of the cerebral cortex that then lose Trnp1 expression within the first postnatal week. Expression of Trnp1 in RGs faded at later developmental stages correlating with a more gliogenic potential of the remaining radial glial cells. Additionally, in the adult murine brain Trnp1 is only expressed in the neurogenic subependymal zone, the rostral migratory stream and the olfactory bulb. Therefore, Trnp1 expression is restricted to neurogenic niches of the developing and the adult brain.

Gain- and loss-of-function experiments *in vitro* and *in vivo* identified Trnp1 as a crucial regulator of neural stem cell fate. Trnp1 is important to expand the pool of neural stem cells through self-renewal. Loss of Trnp1 *in vivo* provoked a strong radial expansion of the

developing cerebral cortex by increasing the number of basal progenitors and the recently identified so-called outer radial glial cells (which are normally only sparsely found in the murine brain). Remarkably, loss of *Trnp1* was even able to induce gyrification of the otherwise smooth murine brain. Molecularly, *Trnp1* is tightly associated with DNA and is involved in gene regulation acting in transcriptional activation.

These data suggest that *Trnp1* acts as a molecular switch in neural stem cells with high levels provoking self-renewal and tangential expansion of stem cells whereas low levels of *Trnp1* lead to radial expansion and folding of the murine cerebral cortex reminiscent of larger gyrencephalic brains. Remarkably, *Trnp1* is also expressed in the human developing brain with regional difference, suggesting that control of *Trnp1* expression is crucial for proper cortical development and folding in gyrencephalic brains. Furthermore, these data implicated *Trnp1* in evolutionary processes of brain size expansion.

Zusammenfassung

Die Evolution des Säugetiergehirns umfasst eine bemerkenswerte Vergrößerung der Großhirnrinde. Eine wichtige Frage in diesem Zusammenhang lautet: wie wird die Größenzunahme der Großhirnrinde geregelt und welche Mechanismen unterscheiden sich in der Entstehung von größeren im Vergleich zu kleineren Gehirnen? Während der Entwicklung des Gehirns werden Nervenzellen aus Radialen Gliazellen (RG) – den neuronalen Stammzellen – gebildet. Des Weiteren gehen später in der Entwicklung auch Gliazellen (wie Astrozyten und Oligodendrozyten) aus RG hervor, welche zusammen mit den gebildeten Nervenzellen das erwachsene Gehirn besiedeln. Um das zukünftige Gehirn während der Entwicklung zu vergrößern, muss zunächst die Stammzellpopulation vergrößert werden. Dies führt zu einem lateralen (auch als tangential bezeichneten) Ausbau der Großhirnrinde. Etwas später in der Entwicklung findet dann die Neurogenese der Großhirnrinde in zwei unterschiedlichen Modi statt: erstens können Radiale Gliazellen direkt Neurone durch asymmetrische Zellteilung bilden, dadurch wird eine Radiale Gliazelle erneuert und ein Neuron gebildet. Zweitens können Radiale Gliazellen basale Vorläuferzellen (auch Basale Progenitoren oder einfach BP genannt) bilden, die sich typischerweise ein weiteres Mal teilen und dadurch jeweils zwei Neuronen generieren. Auf diese Art wird die Anzahl der gebildeten Neuronen erhöht, was dann zu einer radialen Ausdehnung der Großhirnrinde führt und somit die Dicke der Großhirnrinde vergrößert. In der zeitlichen Mitte der Neurogenese, ist die Population der neuronalen Stammzellen heterogen. Sie besteht aus solchen Subpopulationen, welche sich vor allem selbst regenerieren und direkt Neurone bilden und jenen Subpopulationen welche vornehmlich basale Vorläuferzellen bilden. Jedoch sind die Faktoren, die diese unterschiedlichen Subpopulationen von Radialen Gliazellen bestimmen weitgehend unbekannt. Trnp1, ein Zellkernprotein mit bisher unbekannter *in vivo* Funktion, wurde vor kurzem in denjenigen neuronalen Stammzellen, die keine BPs bilden identifiziert (Pinto et al., 2008).

Das Hauptziel meiner Arbeit war es die Funktion von Trnp1 während der kortikalen Neurogenese zu untersuchen. Ich konnte zeigen, dass das Protein Trnp1 von einer Subpopulation von Radialen Gliazellen in der sich-entwickelnden Großhirnrinde der Maus exprimiert wird. Zudem konnte ich zeigen, dass Trnp1 nicht mehr in BPs exprimiert wird,

aber dafür in allen neugeborenen Neuronen der Großhirnrinde wieder gebildet wird. Jedoch klingt die Expression von *Trnp1* in Neuronen innerhalb der ersten Lebenswoche auf undetektierbare Spiegel ab. Die Expression von *Trnp1* in Radialen Gliazellen lässt in späteren Entwicklungsstadien nach, was mit dem gliogenen Potenzial der verbleibenden Radialen Gliazellen korreliert. Des Weiteren ist *Trnp1* im erwachsenen Mäusegehirn nur in der neurogenen Subependymalzone entlang des lateralen Ventrikels, dem rostralen Migrationsstrom und im olfaktorischen Bulbus zu finden. Dies bedeutet, dass sich die Expression von *Trnp1* während der Gehirnentwicklung und im erwachsenen Gehirn auf die neurogenen Zonen beschränkt.

In vitro und *in vivo* Experimente bei denen das *Trnp1* Protein über-exprimiert oder aber herunterreguliert wurde konnten zeigen, dass *Trnp1* einen entscheidenden Regulator von neuronalen Stammzellen darstellt. *Trnp1* ist wichtig, um die Population von neuronalen Stammzellen durch Selbsterneuerung zu vergrößern. Verlust von *Trnp1 in vivo*, führte zu einer starken radialen Ausdehnung der sich-entwickelnden Großhirnrinde durch Vermehrung von basalen Vorläuferzellen und den kürzlich identifizierten sogenannten äußeren Radialen Gliazellen (oRG) (die normalerweise nur spärlich im Mäusegehirn vorhanden sind). Bemerkenswerterweise war der Verlust von *Trnp1* sogar in der Lage Gyrierungen (Faltungen) im normalerweise glatten Mäusegehirn zu induzieren. Auf molekularer Ebene ist *Trnp1* stark an DNA gebunden und ist an Genregulationsmechanismen durch Transkriptionsaktivierung beteiligt.

Diese Daten legen nahe, dass *Trnp1* wie ein molekularer Schalter in neuronalen Stammzellen wirkt, wobei hohe *Trnp1* Spiegel Selbsterneuerung und tangential Expansion von Stammzellen hervorrufen, während niedrige *Trnp1* Spiegel zu einer radialen Ausdehnung und Faltung der Großhirnrinde der Maus führen, welche an größere, gyrierte Gehirne erinnert. Bemerkenswerterweise ist *Trnp1* auch im sich-entwickelnden menschlichen Gehirn exprimiert und weist dabei regionale Unterschiede des Expressionsspiegels auf. Dies lässt vermuten, dass die Kontrolle der *Trnp1* Expression entscheidend für die korrekte Entwicklung und Faltung in gyrierten Gehirnen ist und impliziert, dass *Trnp1* eine Rolle in der evolutionären Vergrößerung der Großhirnrinde spielt.

2 Introduction

The central nervous system (CNS), which includes the spinal cord and the brain, represents the biggest part of the nervous system. The CNS consists of two major cell types: nerve cells (neurons) and supporting and protecting elements named after the Greek word for glue (“glia”), so called glial cells. Recent studies have shown that during CNS development radial glial cells (belonging to the glial class of cells) are actually stem cells that give rise to both differentiated glial cells, but also to neurons. Therefore the neural stem cells during development are actually a class of glial cells. For decades it has been a dogma that all neurons in an adult brain are developmentally born and that there is no replacement or addition of neurons (neurogenesis) occurring in the adult brain. The famous Spanish pathologist, histologist and neuroscientist Ramón y Cajal proclaimed in 1928: "once development was ended, the founts of growth and regeneration of the axons and dendrites dried up irrevocably. In the adult centers the nerve paths are something fixed, ended and immutable. Everything must die, nothing may be regenerated. It is for the science of the future to change, if possible, this harsh decree." (Cajal, 1928). This dogma was later revised and Cajal's „science of the future“ indeed unraveled proceeding neurogenesis in the adult brain in specialized niches. However, it also became clear that regeneration of neurons upon neuronal loss is not a ubiquitous, very efficient process. Neuroscientists tried to elucidate the mystery of neurogenesis ever since. The aim persists to understand the molecular and cellular mechanisms of neurogenesis and to make use of the knowledge generated by basic neuroscience to cure neuronal loss resulting from neurodegenerative diseases or CNS injuries such as stroke in the (far) future. Therefore, understanding the factors and temporal happenings involved in neurogenesis is crucial. One way to elucidate these mechanisms is to analyze neurogenesis in its natural course, i.e. during embryogenesis when neurons are born for the first time. Knowledge from the field of developmental neuroscience may then ultimately be applied for approaches aiming to compensate for neuronal loss.

2.1 Cerebral cortical development - neurogenesis in its natural course

For a long time, neurons and glial cells of the CNS have been thought to developmentally originate from different pools of progenitors. In 1846 Rudolf Virchow first suggested the presence of supporting cells within the CNS and called them glia. Virchow believed that glial cells were originating from mesenchymal progenitors as other support cells found within the CNS. The CNS itself however originates from a specific region of the ectoderm (the outer of the three germ layers endo-, meso- and ectoderm), i.e. the neural plate. Later, Wilhelm His demonstrated that glial cells also had an ectodermal origin actually developing within the CNS itself but he still concluded that neurons and glia are derived from different progenitors (for reviews see Rao and Jacobson, 2005; Kriegstein and Alvarez-Buylla, 2009). From observations of the developing human neocortex Wilhelm His defined several key principles: first, germinal cells divide rapidly in the ventricular zone; second, immature neuroblasts migrate from inner to outer zones; and that third, so called spongioblasts form a syncytium through which the neuroblasts migrate (Bentivoglio and Mazzarello, 1999; Lui et al., 2011). For the past century neurons were believed to be derived from specialized neurogenic progenitors (neuroblasts) whereas glia were believed to be derived from spongioblasts that are now called radial glial cells (Rakic, 1971). Radial glial cells have a radial morphology and are attached both to the apical and the basal surface of the developing cortex (see Figure 1). The scaffold generated by radial glial cells was believed to have mainly a guiding function for migrating neurons which are found closely attached to radial glial cells in the developing cortex (Rakic, 1971; 1972). Studies in primates led to the so called “radial unit” hypothesis (Rakic, 1988) claiming, that the neuronal output at the ventricular surface is guided by radial fibers towards the cortical plate and that neurons of the same ontogeny tend to migrate along the same radial columns thereby projecting a ventricular proto-map onto the developing cortex (Rakic, 1988; 2009; Lui et al., 2011) (Figure 2). Therefore, neurons of the same cortical column share their site of origin but have been generated at different time points. However, the radial unit hypothesis did not identify the lineage relationship of radial glial cells and neuronal progenitors in the ventricular zone (VZ) (Lui et al., 2011). First hints towards a neurogenic role of radial glial cells were obtained by analysis in songbirds some twenty years ago (Alvarez-Buylla et al., 1988; 1990). However, this concept was not fully appreciated until

one decade ago, when cell fate analysis in the developing brain proved that RG cells give rise to neurons (Malatesta et al., 2000; Miyata et al., 2001; Noctor et al., 2001). These studies finally showed, that neurons and glia developmentally share a glial origin and that radial glia are the progenitors of nearly all glial cells and neurons in the mammalian cortex (Malatesta et al., 2000; Noctor et al., 2001; Campbell and Götz, 2002; Götz et al., 2002; Kriegstein and Götz, 2003; Pinto and Götz, 2007; Johansson et al., 2010).

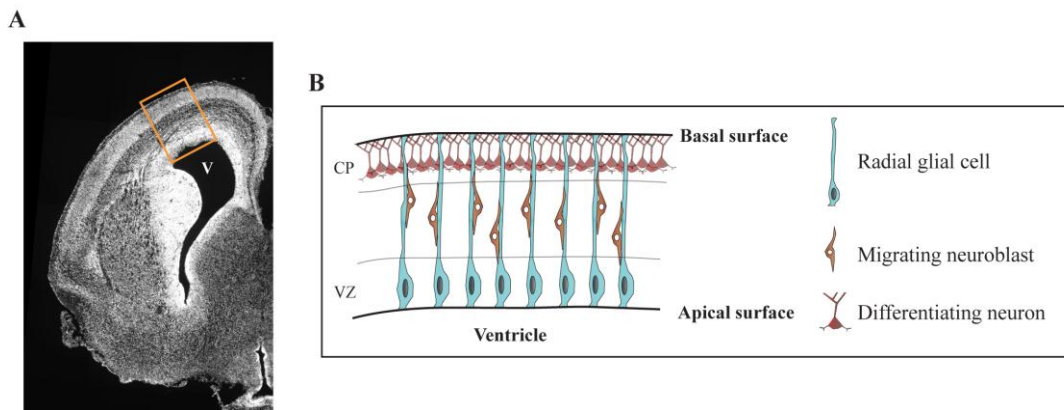
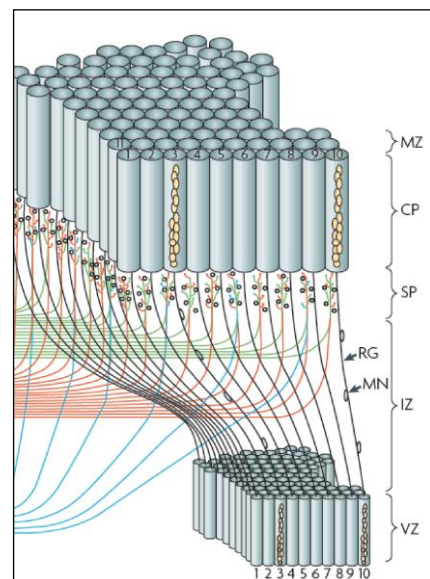


Figure 1: Radial glial cells during brain development

(A) Coronal section of a developing murine brain (embryonic day 16). Cell nuclei are labeled with DAPI, one hemisphere is shown. (B) Simplified Illustration of the region marked with a square in (A). Radial glial cells span from the apical to the basal surface. Cells undergo proliferation at the ventricular surface. Newborn neuroblasts migrate along radial glia fibers towards the cortical plate. V: Ventricle; VZ: ventricular zone; CP: cortical plate.

Figure 2: Radial unit lineage model of cortical neurogenesis

Cartoon illustrating the mode of neuron migration in the developing cerebral cortex. Newborn, migrating neurons (MN) are generated in the ventricular zone (VZ) and migrate along RG fibers through the intermediate zone (IZ), the subplate (SP) and the earlier born deep layer neurons to settle at the top of the cortical plate (CP) at the interface of the CP and the marginal zone (MZ). Newborn neurons form a radial stack of cells in a columnar organization. Cells in one column in the CP share the same site of origin, but are born at different time points. For example neurons born in radial unit 1 in the VZ, will all form the ontogenetic column 1. Neurons then are able to interact with afferents from different sites of the brain. Radial unit hypothesis illustration modified from Rakic (2009).



2.1.1 Neural stem and progenitor cells during forebrain development

Radial glial cells have a bipolar morphology spanning from the ventricle to the pial surface of the developing cerebral cortex. Similar to their ancestors during development - the neuroepithelial cells - their cell bodies reside in the ventricular zone (see Figure 1B). During the cell cycle their somas undergo apical to basal to apical nuclear translocation within the VZ. This somal translocation is called internuclear migration (INM) (in contrast to RGs, internuclear migration of neuroepithelial cells covers the entire distance from the ventricular surface to the pial surface (Götz and Huttner, 2005)). In the course of INM, radial glial cells undergo S-phase and DNA replication at basal positions several cell diameters away from the ventricular surface, and M-Phase at apical positions directly at the ventricle (Sauer and Walker, 1959; Sidman et al., 1959; Fujita, 1962; Hayes and Nowakowski, 2000; Frank and Tsai, 2009; Fietz and Huttner, 2010). Similar to neuroepithelial cells radial glia are able to give rise to neurons directly. However, besides RG so-called basal progenitors (BP also called neurogenic intermediate progenitors or nIPCs) residing more basally are believed to be the major source of amplification and neuronal output in the developing cerebral cortex (Haubensak et al., 2004; Miyata et al., 2004; Götz and Barde, 2005; Malatesta et al., 2007; Sessa et al., 2008; Fietz and Huttner, 2010; Sessa et al., 2010; Borrell and Reillo, 2012) (see Figure 3). Basal progenitors originate from radial glia but retract their apical and basal processes to form a second germinal layer, the so-called subventricular zone (SVZ). BPs usually divide once more to give rise to two postmitotic neurons thereby increasing the neuron number at least two fold (Haubensak et al., 2004; Noctor et al., 2004; Götz and Huttner, 2005; Noctor et al., 2008; Kriegstein and Alvarez-Buylla, 2009). In species with increased brain size, the number of BPs is increased as well, suggesting that the number of this progenitor subtype is crucial for the increase in cortical brain size (Molnár and Kennedy, 2007; Pontious et al., 2008; Cheung et al., 2010; Lui et al., 2011; Molnár, 2011; Borrell and Reillo, 2012).

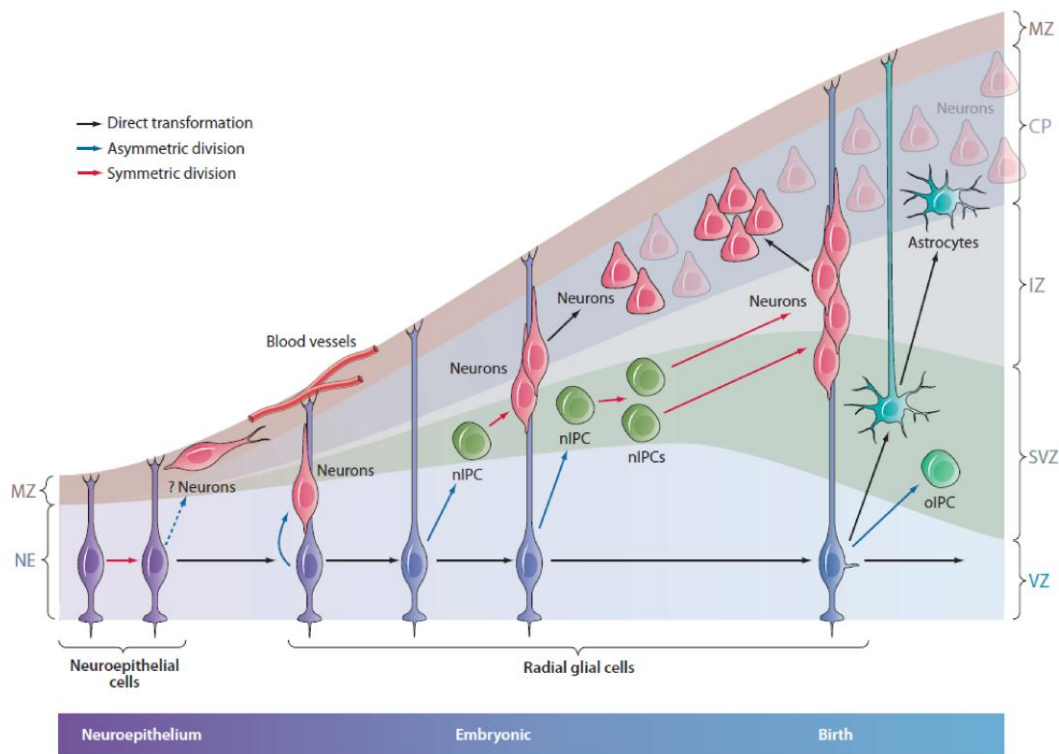


Figure 3: Different modes of neurogenesis during cortical development

Representative drawing of cortical neurogenesis at cellular level during brain development. Radial glia can generate neurons in three different modes: first, RG are able to generate neurons directly, through asymmetric divisions (generating one neuron and regenerating a RG cell at the same time). Second, RG can generate neurons indirectly by generating so-called basal progenitors (BPs) (also called neurogenic intermediate progenitors (nIPC)), which then generate two neurons in the next cell division. Alternatively, RG generate nIPCs but this nIPCs undergo a second round of amplification (regenerating themselves) before they produce neuronal output, thereby increasing the number of neurons. Amplification of the number of BPs/nIPCs is crucial for radial expansion of the cerebral cortex during development. At later stages of development, RG give rise to glial cells such as astrocytes and oligodendrocytic progenitors. BP, basal progenitors (also called nIPCs); CP, cortical plate; IZ, intermediate zone; MZ, marginal zone; nIPC, neurogenic intermediate progenitor cell (also called BP); oIPC, oligodendrocytic progenitor cell; RG, radial glia; SVZ, subventricular zone; VZ, ventricular zone. The time course of brain development is represented from left to right. Figure adapted from Kriegstein and Alvarez Buylla (2009).

Two additional types of neural progenitors, the so called outer radial glial cells (oRGs) and short neural progenitors (SNPs) have recently been described in the developing mammalian cerebral cortex. SNPs have been suggested to be derived from RG (Gal et al., 2006) and imaging studies were able to show that oRGs are directly derived from RGs (Shitamukai et al., 2011; Wang et al., 2011). SNPs lack a basal process and do therefore not contact the pial surface but they still possess apical polarity (Gal et al., 2006). Genetic

fate mapping revealed, that SNPs produce rather neurons directly instead of producing BPs (Gal et al., 2006; Stancik et al., 2010). In contrast to SNPs, oRGs lack their apical process, but still possess a basal process. SNPs and oRGs share expression of the transcription factor Pax6 with radial glial cells. Imaging studies were able to show that oRGs undergo asymmetric self-renewing divisions producing neurons and replicating themselves (Shitamukai et al., 2011; Wang et al., 2011). In contrast to humans and primates that are populated by a large number of oRGs, oRGs are only sparsely present in the murine brain (~5% at E14). In this context, oRGs have been suggested to contribute to cortical expansion in higher mammalian species by representing another type of proliferating progenitors (Fietz et al., 2010; Hansen et al., 2010; Reillo and Borrell, 2011; Reillo et al., 2011; Shitamukai et al., 2011; Wang et al., 2011; Kelava et al., 2012). In summary, BPs and oRGs represent intermediate cell types that are believed to be responsible for the increase in cortical size.

2.1.2 Heterogeneity amongst neurogenic stem cells

Throughout the course of development cellular heterogeneity is crucial for proper formation of the cellular diversity found in an adult organism. In the context of direct versus indirect neurogenesis (via the generation of BPs) from radial glial cells, heterogeneity of the radial glial population has recently been suggested (Sommer et al., 1996; Yaworsky and Kappen, 1999; Malatesta et al., 2003; Gal et al., 2006; Molyneaux et al., 2007; Pinto and Götz, 2007; Pinto et al., 2008; Franco et al., 2012). In contrast to neuroepithelial cells radial glial cells show expression of astrocytic markers such as BLBP, GLAST, GFAP or S100 β but similar to NE cells also specific transcription factors such as Pax6. However, although radial glia share their common morphology and specific marker expression (Götz and Barde, 2005; Götz and Huttner, 2005; Pinto and Götz, 2007), heterogeneity amongst them ensures the proper balance between neuronal output and self-renewal of the stem cell pool. To generate such heterogeneity, cell-internal (intrinsic) as well as environmental (extrinsic) cues play a central role (see also 2.1.4). It has for example been shown, that asymmetric segregation of intrinsic factors during cell division can determine differential cell fate of the daughter cells (Götz and Huttner, 2005; Morin et

al., 2007; Bultje et al., 2009). The existence of cellular heterogeneity is a consequence of the interplay of intrinsic and extrinsic cues together forming individual cellular characters. Encountering different environmental cues can therefore guide initially identical cells into different subpopulations. In the course of development, initially multipotent progenitors become more and more restricted and different subsets of progenitor cells specialize progressively to produce one of the three major cell types: neurons, astrocytes and oligodendrocytes. In this context stem cells produce neurons first before different subsets of them produce astrocytes and oligodendrocytes later. This sequential progression and heterogeneity seems to represent another crucial intrinsic program ensuring the proper organization of the resulting neuron-glia circuitry in the adult brain. However, the factors involved in regulation of radial glial heterogeneity still remain poorly understood.

2.1.3 Cellular diversity forming the six-layered mammalian cerebral cortex

In mammals the dorsal forebrain or pallium gives rise to the neocortex (the biggest part of the cerebral cortex), a highly complex structure that contains a plethora of different neurons and glial cells. A hallmark of the neocortex is the appearance of a six-layered structure (Molyneaux et al., 2007). The generation of this organized structure includes the timed genesis of particular neuronal subtypes. The first neurons arriving in the prospective neocortex around embryonic day (E) 11 are directly generated from neuroepithelial cells and settle in the so-called preplate (Casanova and Trippe, 2006; Pinto and Götz, 2007). With the replacement of neuroepithelial cells by RG, neurons are generated in different modes: either directly by RG or through BPs serving as intermediate progenitors. Newborn neurons settle in the cortical plate in an “inside-out” manner with the latest generated neurons forming the most superficial layers (Rakic, 1988; Bayer et al., 1991; Casanova and Trippe, 2006; Nóbrega-Pereira and Marín, 2009; Rakic, 2009; Marín et al., 2010). In the laminar architecture of the mature neocortex distinct populations of projection neurons are located in different cortical layers and areas, have unique morphological features, express different complements of transcription factors, and ultimately serve different functions (Molyneaux et al., 2007). The different cortical layers are distinguishable by their individual cytoarchitecture and by specific gene expression patterns of their neurons

(Molyneaux et al., 2007). Neurons generated from dorsal progenitors are excitatory cortical projection neurons whereas inhibitory neurons are generated from ventral telencephalic progenitors. Molecularly, dorsal RGs and BPs as well as ventral progenitors are characterized by their specific transcription factor expressions. Radial glial cells in the dorsal telencephalon express the homeobox transcription factor Pax6, whereas BPs can be distinguished from RGs by their expression of Tbr2 (Englund, 2005). Dorsal telencephalic excitatory neurons generated from these progenitors express the transcription factor Tbr1 that can be used as a marker for glutamatergic, pyramidal neurons. On the other hand GABAergic (inhibitory) interneurons of the future neocortex are born in the ganglionic eminence within the ventral forebrain and migrate towards the neocortex (Marín and Rubenstein, 2001; 2003; Marín et al., 2010). The progenitors in these ventral regions express distinct transcription factors such as Dlx1/2, Gsx2 (formerly also called Gsh2), Ascl1 (also called Mash1), Nkx2.1 or Olig2. In this context, transcription factors have been shown to control neural development and subtype specification of these cells. For example, loss of Pax6 leads to a ventralization of the dorsal cerebral cortex (Stoykova et al., 1996; 1997; Chapouton et al., 1999; Yun et al., 2001; Haubst et al., 2004).

Altogether this suggests, that progenitors at any time are restricted to produce layer and subtype specific neurons to constitute the typical six-layered neocortex. Diverse molecular determinants are important for such specification and identification of so far unknown factors is crucial towards a better understanding of brain development.

2.1.4 Control of stem cell proliferation and differentiation by intrinsic and extrinsic factors

Controlling stem cell fate and proliferation versus differentiation is one of the most critical steps during development. First, the stem cell pool needs to be expanded before giving rise to differentiated, specialized cells. Therefore, during brain development a tangential expansion of stem cells is observed first before a radial expansion takes place due to increased neuronal output and differentiation. Tight regulation of such processes is accomplished by cell intrinsic and extrinsic signaling factors. As already mentioned, intrinsic factors play a central role in control of stem cell proliferation, differentiation and

fate specification. Intrinsic regulation of the cell cycle and fate for example comprises the regulation of cell polarity. In this context, knock down of Par3 (which plays a role in apical positioning of the Par complex) leads to premature differentiation of cortical progenitor cells showing, that apico-basal polarity is crucial during development (Costa et al., 2007). It was also reported, that Par3 regulates asymmetric cell division of radial glial cells in a Notch signaling dependent manner (Bultje et al., 2009). Additionally, the small GTPase cdc42 participates in activation of the Par complex and was shown to be required for RG self-renewal (Cappello et al., 2006). Loss of cdc42 function induced RG cells to detach from their apical surface and increased the number of Tbr2 positive progenitors (Cappello et al., 2006).

Transcriptional regulators of cell proliferation and fate comprise members of the basic helix loop helix (bHLH) transcription factor (TF) family such as Ngn1/2, Mash1(Ascl1) or Olig1/2 (Fode et al., 2000; Nieto et al., 2001; Lu et al., 2002; Zhou and Anderson, 2002; Schuurmans et al., 2004; Heng et al., 2008; Pacary et al., 2011) and the homeobox TFs Pax6 and Dlx1/2 (Götz et al., 1998; Heins et al., 2002; Petryniak et al., 2007). For example Pax6 was shown to have a regulatory role on cell proliferation but also to influence the identity of progenitor cells (Götz et al., 1998; Warren et al., 1999; Haubst et al., 2004; Quinn et al., 2007; Tuoc et al., 2009) and its deletion in the dorsal telencephalon resulted in severely defective neurogenesis. Additionally, Tbr2 was also reported to be involved in control of progenitor proliferation (Arnold et al., 2008; Sessa et al., 2008). Moreover, recent studies demonstrated, that such transcription factors are also able to redirect cells with astrocytic characteristics postnatally into the neurogenic lineage (Berninger et al., 2007; Heinrich et al., 2010; Blum et al., 2011). Clonal analysis *in vitro* demonstrated that intrinsic molecular differences are able to govern fate decision, independent of extracellular signals (Williams and Price, 1995; Qian et al., 1998; Malatesta et al., 2000; Heins, 2001; Heins et al., 2002; Shen et al., 2006).

On the other hand, extrinsic signals known to be involved in regulation of cortical development include the Notch and Wnt signaling pathways (Johansson et al., 2010). Notch is a receptor expressed on radial glia cells and activation through its ligands (Delta/DLL) expressed on newborn neurons inhibits neuronal differentiation and leads to self renewal of RGs (Lui et al., 2011). In this context it has been reported, that deletion of

the downstream effectors Hes1, 3 and 5 resulted in extensive cell cycle exit and accelerated differentiation of former stem cells (Hatakeyama et al., 2004; Lui et al., 2011). In addition to the short-range signaling of Notch between adjacent cells, Wnt signaling is considered to be a long-range, diffusive signal that can act in a canonical and a non-canonical way (Michaelidis and Lie, 2008). The canonical Wnt signaling cascade involves β -catenin as an effector (Galceran et al., 2001; Wang et al., 2005; Cho and Cepko, 2006; Gulacsi and Anderson, 2008). Wnt inhibits GSK3 dependent β -catenin phosphorylation and thereby releases β -catenin that is then able to translocate to the nucleus and act as a transcriptional activator (Behrens et al., 1998; Huelsken et al., 2001; Cadigan and Liu, 2006). In this context, overexpression of a constitutively active form of β -catenin blocked cell cycle exit and led to significantly increased cortical size (Chenn and Walsh, 2002; 2003). Differences in cell cycle length of RG versus BP have been shown and the length of the cell cycle may also affect the cellular identity of stem/progenitor cells (Calegari and Huttner, 2003; Calegari et al., 2005). In this context shortening of cell cycle length through overexpression of Cdk4/CyclinD1 was able to delay neurogenesis and cause the expansion of the basal progenitor pool (Lange et al., 2009).

In summary, during brain development a multitude of extrinsic and intrinsic factors interplay together to result in proper cell proliferation, differentiation and fate determination (Farkas and Huttner, 2008; Lui et al., 2011; Tiberi et al., 2012). Such regulation is crucial for the formation of the most complex structure in mammals – the brain.

As all the so far known molecular regulators have not been able to regulate RG versus BP and oRG generation at the same time, it has recently been suggested that there may be novel, so far unknown fate regulators of radial glial cells (Lui et al., 2011). Moreover, understanding the factors involved in different subtypes of radial glial cells may help to understand the regulatory mechanisms that ultimately lead to proper formation of the cerebral cortex. In addition, such factors may also be directly or indirectly involved in regulating cortical expansion and creating differences amongst different species and during evolution. One approach to identify proteins that are specifically up-regulated in RG

subpopulations was performed by Pinto et al and will be discussed specifically in the next section.

2.1.5 Identification of factors involved in direct and indirect neurogenesis

The adult brain is populated by different neuronal and glial cell types that have been generated from heterogeneous progenitor populations during development (Pinto, 2008). In order to identify the molecular differences of such progenitor subpopulations and to find new factors determining heterogeneity during development, Pinto et al. previously performed a transcriptome analysis of different radial glial subsets (Pinto et al., 2008). For this purpose, Pinto et al. used a mouse line expressing GFP under the human version of the GFAP promoter (hGFAP). In order to exclusively isolate radial glia and not their progeny that delaminated from the ventricular surface, the apical membrane protein CD133 (prominin) was additionally used for FACS purification. Cells were sorted for GFP- and prominin expression and pooled as GFP^{high}/prom⁺ and GFP^{low}/prom⁺. Remarkably, GFP expression levels of RGs correlated with their prospective fate (Pinto et al., 2008) and a clear heterogeneity of radial glial cells was observed. Radial glial cells with high level GFP expression mainly formed neurons indirectly through the production of BPs, whereas almost no BPs were detectable from GFP low expressing RG cells that produced neurons directly. This observation is in agreement with the hypothesis that neurogenic radial glial cells down regulate glial markers such as GFAP when they undergo transition to neurons directly (Pinto et al., 2008). Therefore, directly neurogenic RG showed lower GFP expression under the hGFAP promoter at E14 and produced very few BPs as compared to RG that showed high GFP expression and where the main source of BPs (Pinto et al., 2008). In order to identify fate determinants of these two RG subpopulations, transcriptome analysis was performed and revealed strong differences in gene expression (Pinto et al., 2008). One factor that was found in this screen in the indirectly neurogenic lineage generating BPs is AP2 γ (Pinto et al., 2008; 2009). Indeed it was recently shown that AP2 γ is expressed in a subpopulation of RG and is involved in BP cell fate (Pinto et al., 2009). In order to find possible regulators of directly neurogenic radial glial cells, another gene expressed at higher levels in the other, directly neurogenic subset of radial

glial cells was chosen for further investigation. This factor has recently been described as Trnp1 (previously called 2300002d11Rik) and was shown to play a role in proliferation *in vitro* (Volpe et al., 2006 see also 2.4). Analysis of Trnp1 expression and function during forebrain development and its role in neurogenesis was the topic of my work presented in this thesis.

2.2 Cortical Expansion and brain Evolution

In the 17th century, Thomas Willis first proposed that higher cognitive functions originate from the sheer size of the brain (Molnár, 2011). The increase of intellectual capacity during mammalian evolution is believed to highly correlate with the increase in brain size. In this context, the cerebral cortex has undergone an impressive expansion including profound gyrification to accommodate an enormous increase in neuron numbers (Kriegstein et al., 2006; Rakic, 2009; Cheung et al., 2010; Lui et al., 2011; Borrell and Reillo, 2012). In 1664 Willis already realized, that the gyrifications of the human cerebral cortex are larger and more numerous as compared to other species (Willis, 1664).

The evolutionary increase in cortical size correlates with the appearance of the so-called outer subventricular zone in larger brains. Hereby, the subventricular zone is divided into inner (iSVZ) and outer (oSVZ) areas separated by a layer of fibers. The strong expansion of larger brains is believed to be due to an increase in the number of basal progenitors, which subsequently increase the number of neurons. In this context, the strong proliferation of cells residing in the SVZ of primates correlates with the main wave of corticogenesis (Rakic, 1974; Lukaszewicz et al., 2005; Lui et al., 2011). Basal progenitors have been suggested to be the main source of cortical expansion. Indeed, genetic studies in humans showed that the cause of congenital microcephaly was silencing of the transcription factor TBR2 (EOMES) (Baala et al., 2007), a protein shown to be functionally required for SVZ neurogenesis (Arnold et al., 2008; Sessa et al., 2008; 2010) and also used as a marker for basal progenitors (Bulfone et al., 1999; Faedo et al., 2002; Englund, 2005).

Recently, another type of progenitors has been described and implicated in cortical expansion and folding (see also 2.1.1). This type of cell shares several characteristics such

as Pax6 expression with radial glial cells, but in contrast to those has only a basal process lacking the apical contact to the ventricular surface and their cell body resides in the oSVZ. This cell type is called outer radial glial cell (oRG) or basal radial glial cell (bRG). Outer radial glial cells contribute to cortical expansion by representing another type of proliferating progenitor (Fietz et al., 2010; Hansen et al., 2010; Reillo and Borrell, 2011; Reillo et al., 2011; Shitamukai et al., 2011; Wang et al., 2011; Kelava et al., 2012). Expanding the population of radial glia in a distinct germinal zone is a mechanism for increased neuron production that is highly relevant for building a larger brain (Lui et al., 2011). Despite their role in proliferation and expansion of neuron numbers, oRGs are also a crucial part of the migratory scaffold in the developing brain. As expanded, folded brains have a strong increase in basal surface with only slightly increased ventricular surface oRGs are needed to keep the fiber density constant throughout the process of radial expansion (Lui et al., 2011; Reillo and Borrell, 2011; Reillo et al., 2011; Martínez-Cerdeño et al., 2012) (see Figure 4). This interpretation is strongly supported by the appearance of larger numbers of oRGs in brains with a high degree of gyrification (Fietz and Huttner, 2010; Borrell and Reillo, 2012; Martínez-Cerdeño et al., 2012). In contrast, the little and lissencephalic mouse brain has only small numbers of oRGs (Shitamukai et al., 2011; Wang et al., 2011). In human cortical development the number of neurons in the cortical plate increases by about 5 billion new neurons between the 13th and the 20th gestation week. In this context it has been suggested, that on average there must be 1000 neurons arriving every second in the CP during that period indicating that there may be 500-1000 progenitors dividing every second to produce this enormous output (Martínez-Cerdeño et al., 2012). Therefore, tight control of neuronal production and guidance through RGs, BPs and oRGs is crucial for proper brain development.

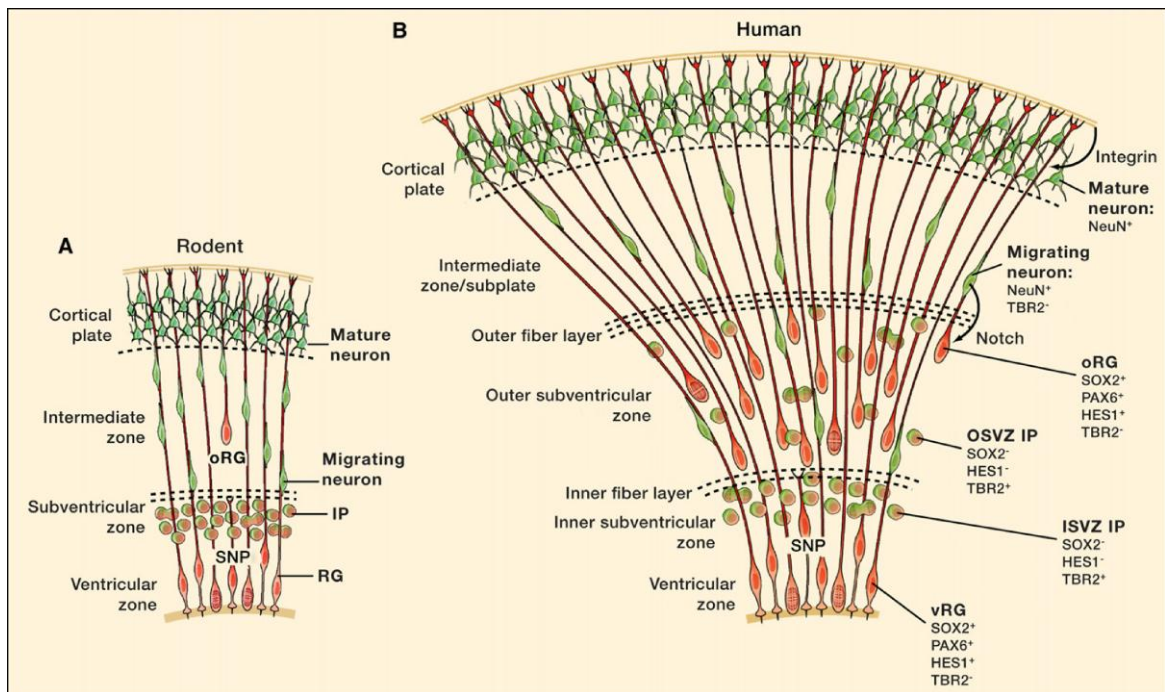


Figure 4: Differences in neocortical development of the rodent and human brain

(A) Model of the current view of rodent corticogenesis. Radial glia (RG) mostly generate intermediate progenitors (IP also called basal progenitors (BP)) that divide again to produce neurons. Newborn neurons migrate along RG fibers towards the cortical plate. Small numbers of outer radial glial cells (oRG) exist in the murine brain. (B) Simplified Model of the human developing neocortex. The increase of the subventricular zone (SVZ) divided into inner- and outer SVZ is illustrated. The number of radial fibers that neurons can use to migrate along is increased due to the abundance of oRGs. Additionally, the number of ontogenetic “units” is significantly increased through the addition of oRG cells to ventricular radial glial cells (vRG). Integrin and Notch signaling are involved in maintenance of oRGs. Additionally, short neuron precursors (SNPs) are depicted in (A) and (B). Transcription factor combinations expressed by the different progenitor types is indicated. Illustration from Lui et al (2011)

In summary, a diversity of progenitors exists in the developing cerebral cortex. Amongst them neuroepithelial cells (that mainly self replicate to initially increase the pool of stem cells), RG cells, SNPs, BPs and oRGs. All of them contribute to the formation and expansion of the cerebral cortex. A general concept of forebrain development indicates that the progenitor pool initially needs to be expanded leading to a tangential expansion at first place. In order to incorporate a large number of neurons, radial expansion takes place later eventually leading to cortical folding and gyrification in higher species (Smart and McSherry, 1986a; 1986b; Rakic, 2009; Lui et al., 2011; Molnár, 2011; Borrell and Reillo, 2012).

2.3 Neurogenesis in the adult brain

Although neurogenesis was initially believed to be restricted to the prenatal phase of development, first studies in the 1960s already indicated the persistence of neurogenesis in the adult brain (Altman, 1963; Altman and Das, 1965; 1966; Altman, 1969). These studies utilized [H^3]-thymidine to label dividing cells by incorporation into DNA during S-phase of the cell cycle. This technique was first described in the 1950s (Sidman et al., 1959). However, little attention was given to these studies, perhaps because they were considered to lack functional relevance (for a review see Ming and Song, 2005). Later studies showed that adult neurogenesis is relevant and that newborn neurons survive for a long period, therefore revealing the significance of neurogenesis in the adult rodent brain (Kaplan and Hinds, 1977; Bayer et al., 1982; Kaplan and Bell, 1983; 1984; Cameron et al., 1993; Seki and Arai, 1995; Kuhn et al., 1996). The synthetic thymidine analogue Bromodeoxyuridine (BrdU) revolutionized the field because (just like [H^3]-thymidine) it incorporates into dividing cells during S-phase but in contrast can easily be detected by immunological approaches (Gratzner, 1982). Before the end of the 20th century adult neurogenesis was observed with BrdU analysis in all mammalian species examined including primates and human patients (BrdU was used in human cancer diagnostics therefore analysis of human neurogenesis post mortem was possible). It has recently become generally accepted that adult neurogenesis occurs in discrete regions of the mammalian CNS (Kempermann and Gage, 1999; Gross, 2000; Rossi and Cattaneo, 2002; Goh et al., 2003; Parent, 2003; Alvarez-Buylla and Lim, 2004; Lie et al., 2004; Lindvall et al., 2004; Ming and Song, 2005). Two main neurogenic regions in the adult mammalian brain have been well described, the subependymal zone (SEZ) of the lateral ventricle (from where newborn neurons migrate through the rostral migratory stream (RMS) to the olfactory bulb (OB)) and the subgranular zone (SGZ) of the dentate gyrus (Kriegstein and Alvarez Buylla, 2009) (see Figure 5). However, neurogenesis outside such specific neurogenic niches seems to be extremely limited, or non-existent, in the intact adult mammalian brain (Ming and Song, 2005). The adult SEZ is related to the embryonic SVZ and contains relatively quiescent neural stem cells called type B cells. These type B cells give then rise to so-called type C cells that are highly proliferative generating immature neuroblasts (also called type A cells)

(see Figure 6), which migrate in chains through the rostral migratory stream to the olfactory bulb. Type B cells of the SEZ as well as the stem cells in the SGZ of the hippocampus show characteristics of astrocytes and have also been frequently called SEZ or SGZ astrocytes (Doetsch et al., 1999; Kriegstein and Alvarez-Buylla, 2009). For type B cells of the adult SEZ it has been shown that they are derived from RG cells during development (Merkle et al., 2004) and the same has been suggested for stem cells of the SGZ (Eckenhoff and Rakic, 1984; Altman and Bayer, 1990; Kriegstein and Alvarez-Buylla, 2009). Moreover, recent studies indicate that NSCs in the adult brain share several important properties with RG (such as an apical contact to the ventricle with a single primary cilium) and a link between embryonic and adult neural stem cells has been suggested (Mirzadeh et al., 2008; for detailed reviews see Ming and Song, 2005; Kriegstein and Alvarez-Buylla, 2009). One major question is what factors distinguish such specialized cells in neurogenic niches of the adult brain from regular, non-neurogenic astrocytes and why neurogenesis in the adult brain is limited to very few restricted regions.

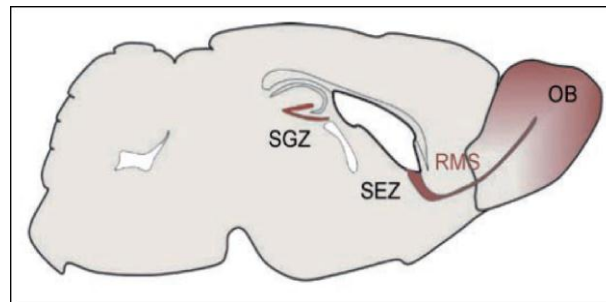


Figure 5: Regions of adult neurogenesis in the rodent brain

Schematic Illustration of the adult rodent brain and its neurogenic niches. Saggital section of the adult murine brain highlighting the SEZ of the lateral ventricle and the SGZ of the hippocampal dentate gyrus as the two well described regions with proceeding neurogenesis. Note also the rostral migratory stream (RMS) along which newborn neurons migrate towards the olfactory bulb. Modified model from Ma et al. (2009).

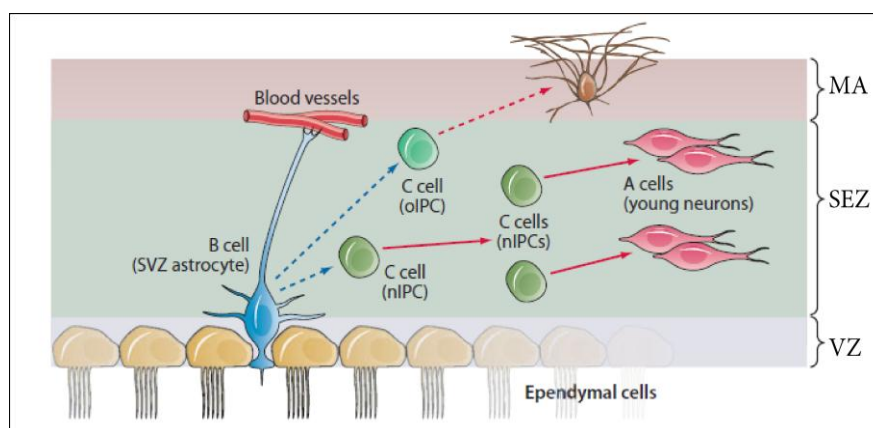


Figure 6: Illustration of progenitor types and lineages in the adult SEZ

Neural stem cells (NSCs) correspond to type B cells and retain epithelial properties, including the extension of a thin apical process contacting the ventricle and a basal process that ends on blood vessels. Type B cells give rise to highly proliferative type C cells (also called intermediate progenitor cell or IPC). These IPCs then give rise to mainly neurons but alternatively also oligodendrocytes. Blue lines represent asymmetric, red lines symmetric cell divisions. oIPC: oligodendrocytic intermediate progenitor cells, nIPC: neuronal intermediate progenitor cells, SEZ: Subependymal zone. (Kriegstein and Alvarez-Buylla, 2009).

2.4 Trnp1 – a nuclear protein highly conserved within the mammalian lineage

Trnp1 has recently been found in a yeast two hybrid screen searching for interacting partners of the TATA Element Modulatory Factor (TMF/ARA160) (Volpe et al., 2006). Trnp1 has been described to be localized to the nucleus and to interact with TMF which leads to proteasomal degradation of Trnp1 in C2C12 cells (Volpe et al., 2006). The gene previously known as 2300002D11Rik was thus named *Trnp1* (for TMF Regulated Nuclear Protein 1). Trnp1 has a single, highly conserved ortholog for each sequenced mammalian genome. A 1607bp cDNA encodes for a 223aa protein in the mouse and a 1745bp cDNA encodes for a 227aa protein in humans with about 90% homology between the human and the murine protein (see Figure 7A). The gene resides at chromosome 1p36.11 in the human genome and at chromosome 4D3 in the murine genome each producing an invariantly spliced, two exon mRNA from an approximately 7,5kb nascent messenger (see Figure 7B). The coding region is entirely located within the first exon and the second exon represents the 3'-UTR of the mRNA (see Figure 7B).

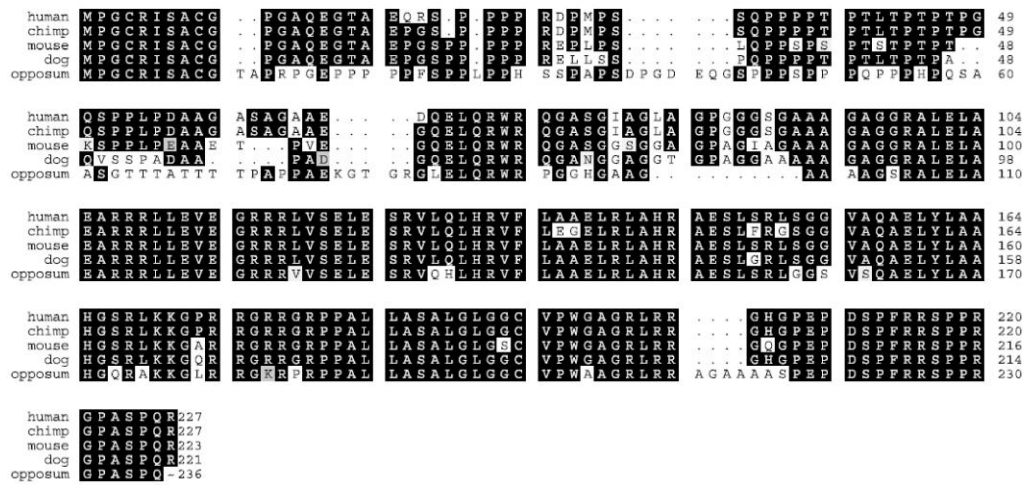
Phylogenetic tree analysis supports the existence of a single (never duplicated) mammalian ancestral gene for all *Trnp1* orthologs (Volpe et al., 2006). Volpe et al performed extensive search for *Trnp1* homologues in other sequenced vertebrate genomes and claimed that they did not reveal any homolog, thus the *Trnp1* gene seemed to have arisen exclusively in the mammalian lineage (Volpe et al., 2006). Moreover, protein sequence analysis did not convincingly reveal any known protein motif or domain. However, two regions of low structural complexity can be identified and are present in all mammalian orthologs: a proline rich region (P²⁰-P⁵⁴ in the murine protein) and a glycine/alanine rich region (G⁷²-G⁹⁴ in the murine protein) (Volpe et al., 2006).

Western blot analysis of HEK cells overexpressing a Trnp1-HA or Trnp1-Myc fusion protein revealed multiple heterogeneous bands extending from about 30 to 36 kDa that were suggested to be due to extensive posttranslational modification (Volpe et al., 2006). Immunocytochemical analysis of ectopically expressed Trnp1-Myc in C2C12 cells showed an exclusively nuclear localization of Trnp1 being excluded from defined nuclear spots strongly labeled by propidium iodide. This indicated that Trnp1 is not localizing to highly condensed chromatin. Nevertheless, Trnp1 was detectable in a highly insoluble nuclear fraction that also contained histones. The inclusion of the protein in a nuclear precipitate was suggested to reflect the association of Trnp1 with chromatin (Volpe et al., 2006). Treatment of nuclei with micrococcal endonuclease led to the release of histones to the nucleoplasm but did not affect the association of Trnp1 with the insoluble nuclear fraction (Volpe et al., 2006). However, combination of nuclease treatment with a 0.5M NaCl wash led to a partial release of Trnp1 from the insoluble fraction.

In order to functionally assess the role of Trnp1, Volpe et al. ectopically overexpressed the protein in MCF-7 cells (a breast carcinoma cell line that does not express Trnp1 endogenously). Trnp1 overexpression accelerated the cell cycle with significantly more cells residing in S-phase five days after transient transfection *in vitro* suggesting, that Trnp1 may be involved in cell proliferation. However, an endogenous role of Trnp1 *in vivo* remained elusive.

Introduction

A



B

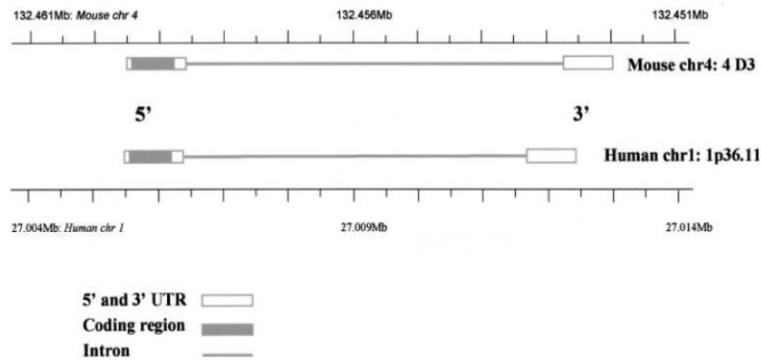


Figure 7: *Trnp1* is a highly conserved mammalian gene with a single protein coding exon
 (A) Multialignment of five mammalian *Trnp1* protein sequences: human protein gi: 61966741; mouse protein gi: 38078875; and chimpanzee, dog and cow protein models derived through sequence similarities to genome and expressed sequences of these three organisms. Amino acid identities are shown in black boxes, similarities in shades of gray. (B) Human and mouse *Trnp1* genes each produce an invariantly spliced approximately 1.7-kb two exon message from an approximately 7-kb nascent message. The entire coding region resides within the first exon of each message. Exons, introns and coding regions are diagrammed according to the provided key. Genome position is indicated by cytogenetic locus (4D3 for mouse and 1p36.11 for human) and by position of the chromosome's sequence axes (with provided scales). Illustration modified from Volpe et al. (2006).

3 Aim of this study

Heterogeneity amongst stem cells is crucial for developmental processes. In search of factors specifically expressed in subpopulations of radial glial cells during forebrain development of the murine brain, Pinto et al previously described a molecular screen of radial glial subsets (see Introduction 2.1.5). Amongst the factors highly expressed in directly neurogenic radial glial cells several genes with so far unknown *in vivo* function were identified. Trnp1 was chosen for further analysis, as the protein is highly conserved within the mammalian lineage and its nuclear localization *in vitro* (described by Volpe et al, 2006) proposed a possible function in stem cell regulation. As Trnp1 had so far not been described *in vivo* I set out to investigate the expression of Trnp1 during cerebral cortical development. Using gain- and los-of-function experiments *in vitro* and *in vivo* I then aimed at analyzing the role of Trnp1 in neurogenesis and its molecular mode of action.

4 Results

In order to search for regulators of radial glial fate in an unbiased manner, a gene expression analysis of apical progenitor cells has previously been performed (Pinto et al., 2008) (see Introduction 2.1.5). In this context, microarray data of radial glial cells with direct neurogenic potential were compared to such with indirect neurogenic potential (including the generation of basal, Tbr2-expressing progenitors). In order to identify molecular regulators promoting the generation of apical progenitors, candidate genes from the lineage of direct neurogenesis were selected. So far not a single molecular mechanism has been described to affect the formation of both outer radial glial cells (oRGs) and basal progenitors (BPs) at the same time; therefore another aim was to determine whether one may find co-regulators of basal progenitors and oRGs. One candidate for such a function was Trnp1, a nuclear protein previously described as TMF Regulated Nuclear Protein 1 (Volpe et al 2006 see 2.4) with unknown *in vivo* function. Trnp1 was chosen for further investigation, because the search for Trnp1 homologs in other species revealed its high degree of sequence conservation (with 90% sequence homology of the murine and the human protein) (Volpe et al., 2006). Trnp1 therefore represented an intriguing novel candidate for cerebral cortex evolution. Remarkably, the Trnp1 protein sequence does not carry any known motif or domain (Volpe et al., 2006) thereby possibly opening an avenue for a new class of proteins.

Trnp1 was first described in 2006 as TMF-regulated nuclear protein *in vitro* upon overexpression (Volpe et al., 2006). However, the existence of the endogenous protein at cellular level has never been shown before *in vivo*.

4.1 Generation of an antibody raised against Trnp1

Antibodies directed against Trnp1 are currently not commercially available. In order to be able to analyze the expression of endogenous Trnp1 an antibody had to be generated first.

4.1.1 Antibody recognition site

To raise an antibody specifically detecting Trnp1 protein, a unique region of the protein needed to be identified. To exclude possible reactions of the antibody with other proteins a region of the protein was chosen that carries no overlap with other proteins (with the help of Dr. Robert Blum). For this purpose Blastp database search was performed together with an accessibility prediction by Peptide Specialty Labs GmbH Heidelberg. Two possible protein regions were identified: Peptide 1 with the length of 19 amino acids (AETPVEGQELQRWRQGASG) and Peptide 2 with the length of 20 amino acids (PEPDSPFRRSPPRGPASPQR) (underlined sequences in Figure 8). Antibodies raised in guinea pig were ordered from Peptide Specialty Labs GmbH Heidelberg. For each peptide serum of the animal was collected after 3 and after 4 immunizations. Specificity and affinity for Trnp1 protein was subsequently tested (see 4.1.2). As the antibody raised against Peptide 1 turned out to be more specific and had a higher affinity for Trnp1 as compared to the antibody raised against Peptide 2 (data not shown) all the studies presented in this work are based on the antibody raised against Epitope1.

Human	MPGCRISACG	PGAQEGTAEQ	RS.PPPPRDP	MPS SQPPPT	PTLTPTPTPG
Mouse	MPGCRISACG	PGAQEGTAEF	GSPPPPPREP	LPSLQPPSPS	PTSTPTPT..
Rat	MPGCRISACG	PGAQEGTAEF	GSPPPPPREP	LPSLQPPSSS	PTSTPTST..
Human	QSPPLFDAAAG	ASAGAAEDQE	LQRWRQGASG	IAGLAGPG..	GGSGAAAGAG
Mouse	KSPPLFEAAE	T...PVEGOE	<u>LQRWRQGASG</u>	GSGGAGPA..	GIAGAAAGAG
Rat	QSPQLFEAAE	T...PVEGQE	<u>LQRWRQGASG</u>	GSGGASPAGI	GGAGAAAGAG
Human	GRALELAEAR	RRLLEVEGRR	RLVSELESRV	LQLHRVFLAA	ELRLAHRAES
Mouse	GRALELAEAR	RRLLEVEGRR	RLVSELESRV	LQLHRVFLAA	ELRLAHRAES
Rat	GRALELAEAR	RRLLEVEGRR	RLVSELESRV	LQLHRVFLAA	ELRLAHRAES
Human	LSRLSGGVAQ	AELYLAAHGS	RLKKGPRRGR	RGRPPALLAS	ALGLGGCVPW
Mouse	LSRLSGGVAQ	AELYLAAHGS	RLKKGARRGR	RGRPPALLAS	ALGLGSCVPW
Rat	LSRLSGGVAQ	AELYLAAHGS	RLKKGARRGR	RGRPPALLAS	ALGLGSCVPW
Human	GAGRLRRGHG	PEPDSPFRRS	<u>PPRGPASPQR</u>		
Mouse	GAGRLRRQGQ	<u>PEPDSPFRRS</u>	<u>PPRGPASPQR</u>		
Rat	APQASTLWVW	TDFCI P RL L W	I P RLQEDF Q D		

Figure 8: Antibody Epitopes

Sequence Homology of the human, murine and rat version of Trnp1. Regions being conserved in all of the three species are indicated in turquoise, regions conserved in two of the three species are indicated in yellow. The two protein regions of the murine protein against which the different antibodies were raised are underlined in red. Peptide 1: aa 57 – aa 75. Peptide 2: aa204 - aa223 of the murine sequence. Note the differences in the protein sequence of human and mouse Trnp1 within the region of Peptide 1 – suggesting that this antibody may not be able to detect the human version of Trnp1.

4.1.2 Test of antibody specificity

To test the specificity of the generated antibody, a vector for the expression of a Trnp1-GFP fusion protein was cloned (encoding for the murine version of Trnp1). Through GFP-fusion and transient expression of Trnp1-GFP in HEK293 cells by transfection, the localization of the Protein was readily visible in living cell cultures. In agreement with previous analysis by Volpe and colleagues (Volpe et al., 2006), Trnp1 was found to be localized exclusively to the nucleus. Immunocytochemistry with the generated antibody confirmed the nuclear localization of Trnp1 and showed a co-localization with the GFP signal in all cases (Figure 9A to D). In addition, Trnp1 was only detectable in transfected cells, suggesting that the Trnp1 antibody does either not detect the endogenous version of Trnp1 (as HEK cells are human and the antibody recognition site carries strong differences in the human and murine version of Trnp1 – see Figure 8 Peptide 1) or that Trnp1 is not expressed in HEK cells. This observation confirmed the specificity of the antibody for the overexpressed murine protein. Western blotting further confirmed the specific recognition of Trnp1 with three to four distinct bands with a size ranging from 24kDa to 32kDa and no detectable signal in untransfected HEK cells (Figure 9E). Compared to the theoretically expected molecular weight of Trnp1 of 23,09kDa, the molecular weight of Trnp1 expressed in HEK cells is larger - possibly due to posttranslational modifications. This observation is supported by the work of Volpe et al. that also proposed Trnp1 to be posttranslationally modified. In addition, the serum of the pre-immunized guinea pig was used for immunohistochemistry and for western blotting as a control. In both cases no signal was detectable in Trnp1 transfected HEK cells (data not shown).

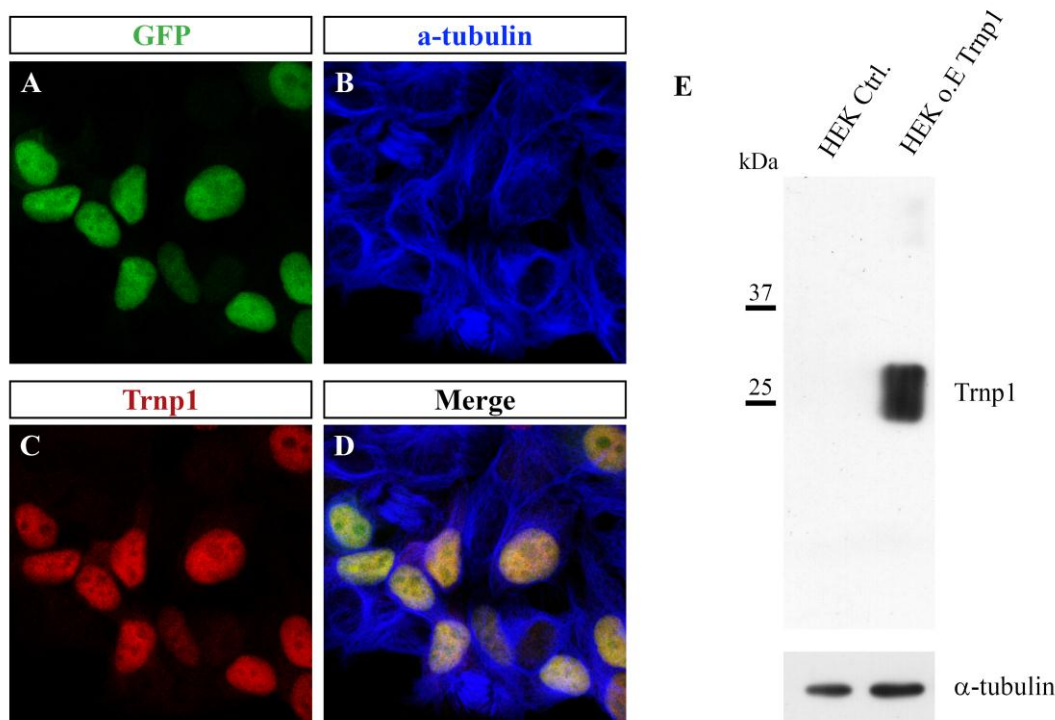


Figure 9: Analysis of Trnp1 localization and antibody specificity

(A-D) Immunocytochemistry of HEK293 cells transiently transfected with peGFP-*Trnp1*-N3 to express a Trnp1-GFP fusion protein. Cells were fixed 48h post transfection. Localization of the fusion protein was visualized by GFP staining (A). To visualize the cytoplasm of the cells staining for α -tubulin was performed (B). Trnp1 expression was directly visualized with the antibody generated against Trnp1 (Peptide 1) (C). Merge confirmed the specificity of the Trnp1 antibody and showed that the protein is exclusively expressed in the nucleus (D). Note that only transfected cells showed Trnp1 expression three days after transfection. Single optical sections are shown. (E) Western blot of HEK cells transfected with pCMV-*Trnp1* for overexpression of Trnp1. Note that no signal can be detected in untransfected HEK cells.

To further test possible non-specific signals in immunostaining, an antibody-antigen competition experiment was performed. For this purpose different concentrations of the 19-amino acid (epitope) peptide against which the antibody was raised were incubated together with the antibody. This antibody-peptide mixture was then used (Figure 10) for staining of HEK cells transfected with pCMV-*Trnp1*. The peptide was able to compete with the detected signal in a concentration dependent manner, thereby further showing that the antibody successfully recognizes Trnp1.

After characterization of the *in vivo* expression of Trnp1, the same experiment was later on also carried out on brain sections with a similar reduction of the signal upon antibody-antigen competition (data not shown).

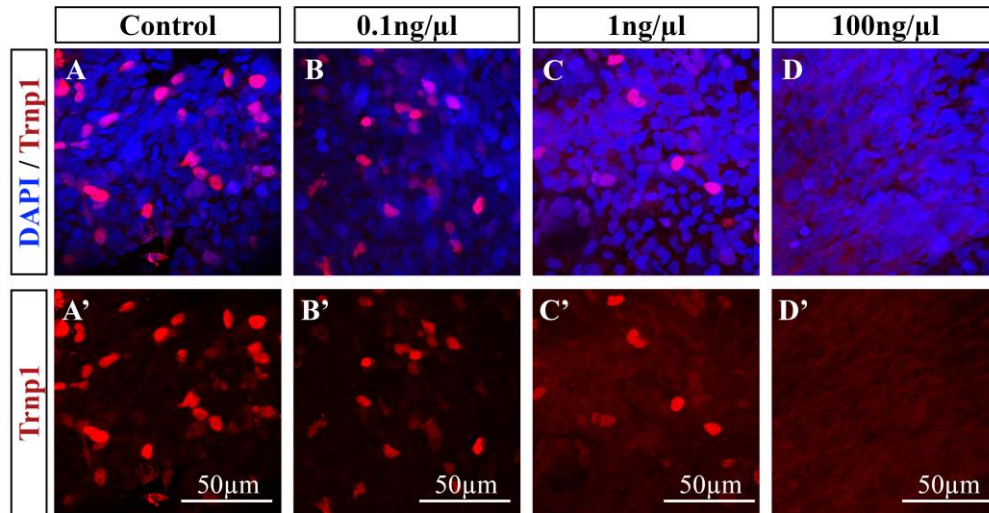


Figure 10: Test of antibody specificity – antibody antigen competition experiment

(A-D') Immunocytochemistry of HEK cells transfected with pCMV-*Trnp1*. Cells were fixed three days after transfection and stained with Trnp1 antibody pre-incubated with different concentrations (as indicated) of the peptide the antibody was raised against. Note that higher concentrations of the peptide were able to compete with the signal of immunocytochemistry.

4.2 Expression analysis of Trnp1 during murine telencephalic development

4.2.1 Analysis of Trnp1 expression during forebrain development

In order to get insights into the possible role of Trnp1 during brain development, expression of Trnp1 protein needed to be determined at the cellular level.

For this purpose, a detailed expression analysis was carried out at different developmental stages of the murine forebrain. Trnp1 was exclusively localized to the nucleus at all developmental stages analyzed confirming the localization of the protein found upon overexpression *in vitro*. Specifically, at embryonic day 12 (E12) Trnp1 was expressed in virtually all apical progenitors (Figure 11A and A'). At mid neurogenesis, Trnp1 was expressed in a subpopulation of apical progenitors lining the ventricle and in newborn neurons (Figure 11B and B'). Interestingly, Trnp1 immunoreactivity in the progenitor layer

at the ventricle underwent a significant decline during forebrain development with virtually all progenitors being Trnp1 positive at E12 to no detectable immunoreactivity at E18, the end of neurogenesis (Figure 11A to D'). This indicates that gliogenic radial glia lining the ventricle at later stages of telencephalic development (i.e. E18) do not express Trnp1. Conversely, the signal in neurons of the cortical plate persisted a little longer and faded within the first postnatal week (Figure 11E to F'), suggesting another role of Trnp1 in newborn neurons.

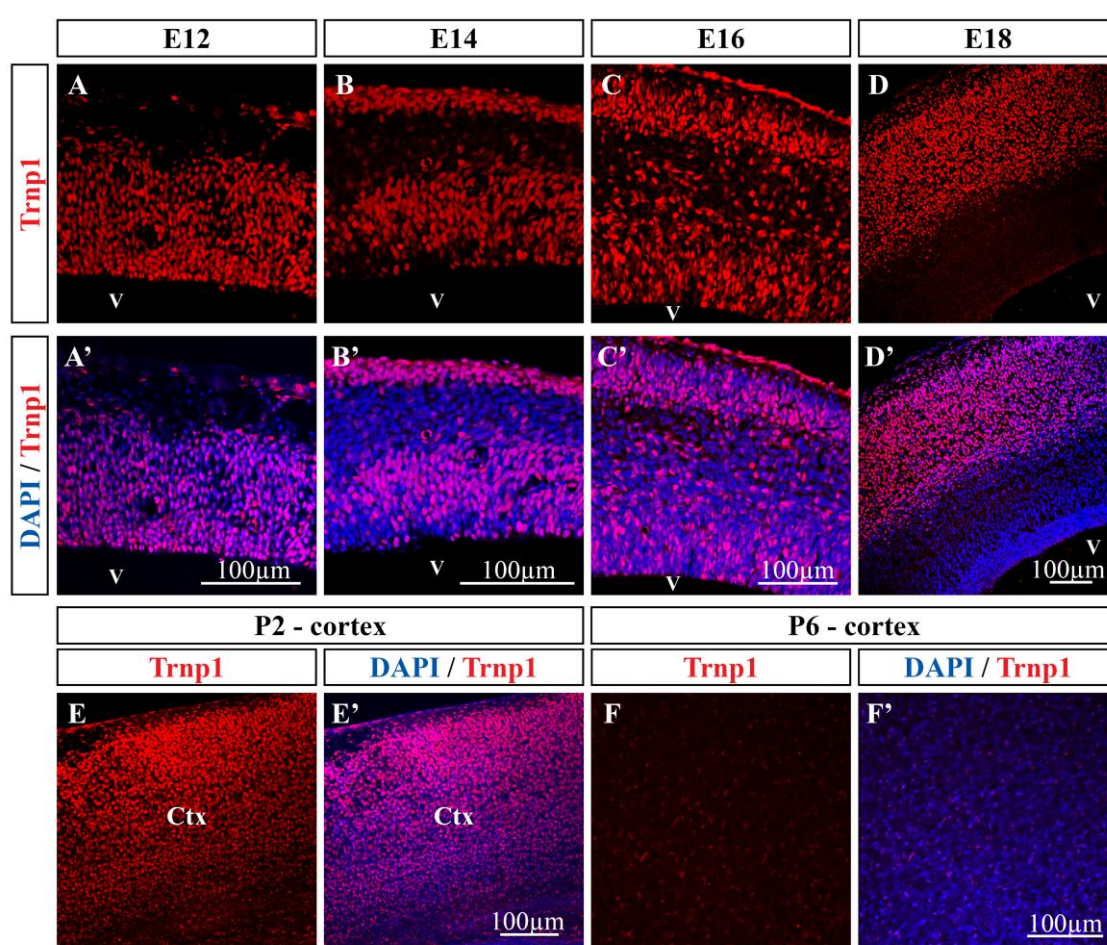


Figure 11: Expression analysis of Trnp1 protein at different stages of forebrain development
 (A-D') Micrographs of coronal sections of the developing cerebral cortex at different developmental stages (E12-E18) labeled for Trnp1 and DAPI. Note that Trnp1 is expressed in apical progenitors close to the ventricle and in the cortical plate. (E-F') Coronal sections of postnatal stages of murine development (Postnatal day 2 and 6 (P2 and P6)) were labeled for Trnp1 and DAPI. Note that Trnp1 expression in the postnatal cerebral cortex declines at postnatal stages. Single optical sections are shown. Ctx, cortex; V: ventricle.

4.2.2 Detailed expression analysis at mid-neurogenesis

To determine the identity of the progenitor subtype expressing *Trnp1* at mid-neurogenesis (E14), immunohistochemical staining for the progenitor specific markers *RC2*, *Pax6* (both labeling apical neural stem cells) and *Tbr2* (expressed in basal neural progenitors) was performed. Double staining with anti-*Trnp1* antibody revealed that *Trnp1* is expressed in a subpopulation of *Pax6* positive apical progenitors (radial glial cells) while hardly any *Tbr2* positive basal progenitor showed *Trnp1* expression (Figure 12A to C'). Double staining with the neuronal transcription factor *Tbr1* confirmed the neuronal identity of *Trnp1* positive cells within the cortical plate (Figure 12D and D'). Taken together, its expression pattern suggested a role of *Trnp1* in the regulation of different subsets of radial glial cells during cortical neurogenesis.

As *Trnp1* was not only found to be expressed in the dorsal but also in the ventral part of the telencephalon (Figure 12E and E') the ventral progenitor specific transcription factor (TF) *Mash1* (also called *Ascl1*) was utilized for further analysis. A mouse line expressing nuclear GFP under the *Mash1* promoter (Leung et al., 2007) was used to stain for GFP (labeling *Mash1* expressing progenitor cells in the ventral telencephalon) and *Trnp1*. *Trnp1* was expressed in all *Mash1*-driven, GFP expressing cells. However, *Trnp1* is also expressed in apical, *Mash1* negative progenitors lining the ventricle of the ganglionic eminence (GE) - indicating that *Trnp1* expression precedes the expression of *Mash1* in ventral neuronal development (Figure 12F and F').

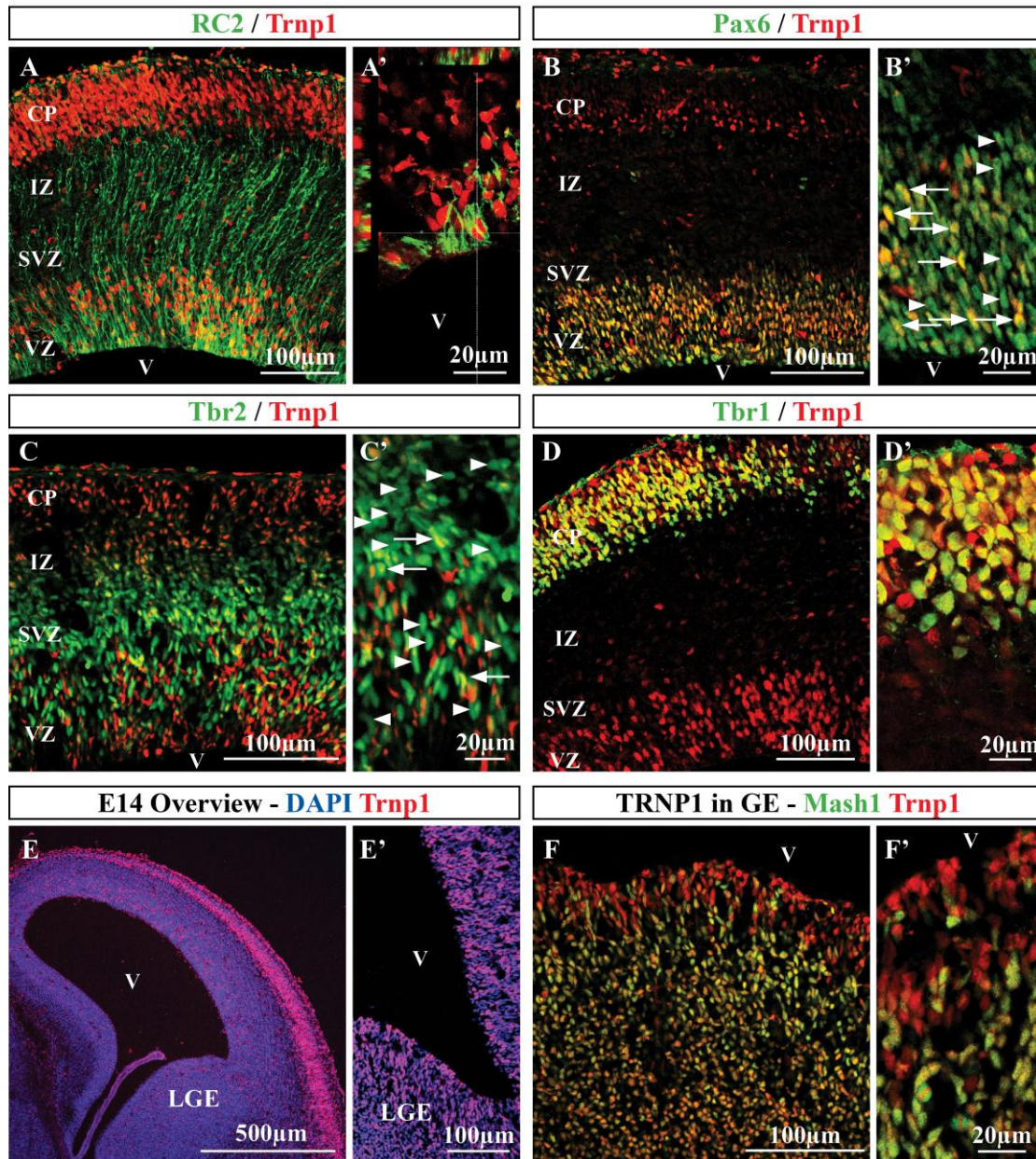


Figure 12: Trnp1 is expressed in a subset of radial glial cells and in newborn neurons

(A-F') Micrographs depicting immunolabeled coronal sections of the developing cerebral cortex at E14 (confocal, single optical sections are depicted). Co-expression analysis of Trnp1 together with the radial glial specific antibody RC2 (A-A'), the radial glial transcription factor (TF) Pax6 (B and B'), the basal progenitor TF Tbr2 (C and C') and the neuronal TF Tbr1 (D and D'). Note that Trnp1 is expressed in a subpopulation of Pax6 positive apical progenitors and that most of the Tbr2 positive basal progenitors do not express Trnp1. Arrows indicate double positive cells, arrowheads indicate Pax6+ or Tbr2+ cells that do not express Trnp1. (E-E') Overview of Trnp1 expression at E14. Note that Trnp1 is also expressed in ventral regions of the developing forebrain including the ganglionic eminence. (F-F') Coronal section of a transgenic embryo expressing GFP under the Mash1 promoter. Labeling for GFP and Trnp1 shows that virtually all Mash1 positive cells co-express Trnp1. Note that Trnp1 is also expressed in apical progenitors in the GE that are negative for Mash1. VZ: ventricular zone; SVZ: subventricular zone; IZ: intermediate zone; CP: cortical plate; LGE, lateral ganglionic eminence; V, ventricle; Scale bars as indicated.

4.2.3 Expression analysis of *Trnp1* in the adult murine brain

Neurogenesis is known to persist in the adult brain in two neurogenic niches – the subependymal zone (SEZ) of the lateral ventricle (from where newborn neurons migrate via the rostral migratory stream (RMS) to the olfactory bulb (OB)) and the subgranular zone of the dentate gyrus (Kriegstein and Alvarez-Buylla, 2009; see also Introduction 2.3). Given that expression of *Trnp1* was also observed in progenitors of the GE during development (see 4.2.2) together with the fact that adult neural stem cells of the SEZ originate from these progenitors, the next question was whether *Trnp1* protein might persist in regions of adult neurogenesis. Indeed, immunohistochemistry revealed that *Trnp1* is not expressed ubiquitously in the adult brain but rather specifically in the neurogenic SEZ, the RMS and the OB (Figure 13 and Figure 14).

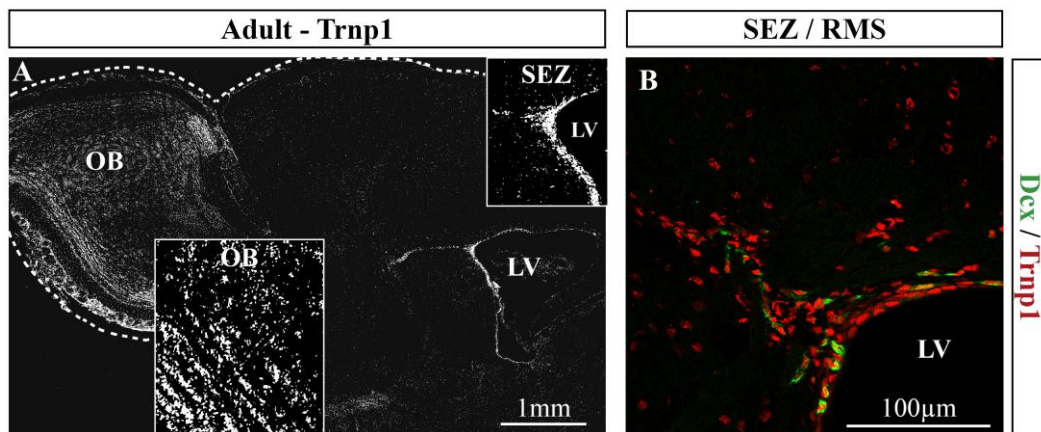


Figure 13: Overview of *Trnp1* expression in the adult murine brain

(A-B) *Trnp1* expression analyzed on sagittal sections of the adult murine brain. (A) Overview of *Trnp1* expression in the adult brain. Reconstruction of a sagittal section using Zeiss LSM710 “ZEN-tilescan”. Note that *Trnp1* is expressed selectively in the SEZ lining the LV, in the RMS and in the OB. (B) Higher Magnification of the SEZ/RMS labeled for *Trnp1* and doublecortin (Dcx). Confocal single optical section is shown. Note that Dcx positive neuroblasts do express *Trnp1*. OB, olfactory bulb; SEZ, subependymal zone; LV, lateral ventricle. Scale bars: 1mm (A) and 100µm (B).

Intriguingly, cells in the subgranular zone of the dentate gyrus (the other well known neurogenic niche in the adult brain) did not express *Trnp1* (Figure 14B). Double staining for the pyrimidine analogue Bromodeoxyuridine (BrdU) (applied one hour before sacrifice, thereby labeling fast proliferating cells) or doublecortin (Dcx) (labeling neuroblasts) together with *Trnp1* revealed its expression in all BrdU positive, fast proliferating cells

within the SEZ and in virtually all neuroblasts of the SEZ, RMS and OB (Figure 14C and D). Taken together, the expression pattern of *Trnp1* during development and in the adult brain suggested a functional role of *Trnp1* in neurogenesis.

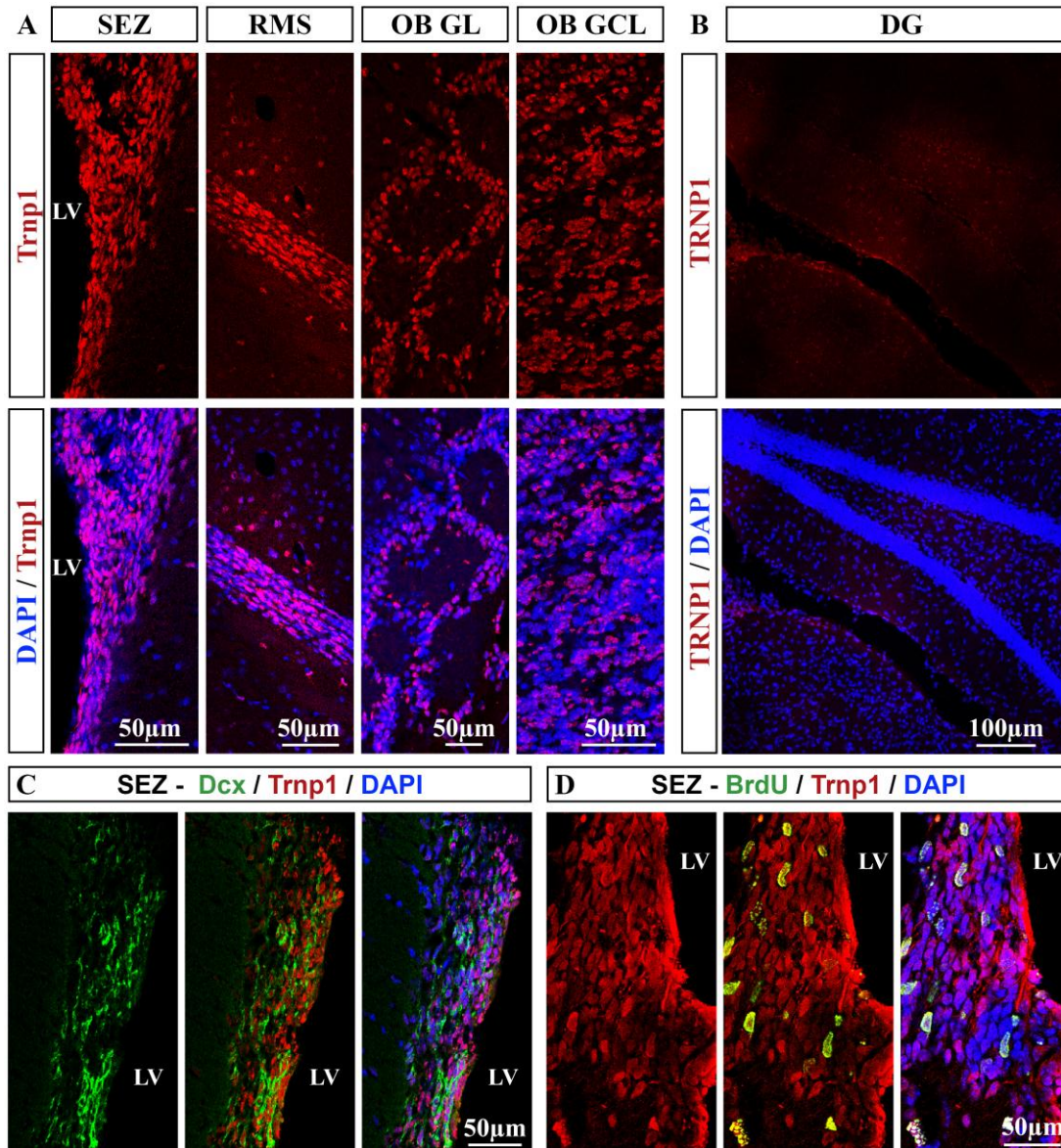


Figure 14: *Trnp1* expression in adult neurogenic niches of the mouse brain

(A-D) Sagittal sections of the adult murine brain were labeled for *Trnp1*, DAPI and *Dcx* or BrdU (single optical sections are shown). (A) *Trnp1* expression in the SEZ, RMS and OB. (B) *Trnp1* expression in the dentate gyrus. Note that *Trnp1* is not expressed in progenitors of the subgranular zone. (C) *Trnp1* and *Dcx* co-labeling in the SEZ. Note that *Dcx* positive neuroblasts do express *Trnp1*. (D) *Trnp1* and BrdU (BrdU treatment 1h prior to sacrifice) co-labeling in the SEZ. Note that all transit amplifying (BrdU positive) progenitors do express *Trnp1*. LV: lateral ventricle; scale bars as indicated.

4.3 Investigating the functional role of *Trnp1* *in vitro*

The above described expression pattern suggested a potential role of *Trnp1* in the regulation of neurogenic stem or progenitor cells. Therefore, the aim of this study was to determine the function of *Trnp1* in neurogenesis by gain and loss of function approaches.

4.3.1 Generation of a retroviral construct for forced expression of *Trnp1*

In order to overexpress *Trnp1*, its cDNA was cloned into a retroviral vector containing the chicken beta actin (CAG) promoter driving *Trnp1* expression together with GFP as a reporter linked by an internal ribosomal entry site (IRES) (Heinrich et al., 2011; see Figure 15A). Co-expression of GFP and *Trnp1* was confirmed by immunostaining of transfected HEK cells (data not shown). Furthermore, a retrovirus for overexpression of *Trnp1* was produced and tested for expression of *Trnp1* and GFP in HEK293 cells (Figure 15B and B') and dissociated cells from the cerebral cortex of E14 embryos (Figure 15C to C'') seven days post transduction. All infected cells showed co-expression of *Trnp1* and GFP.

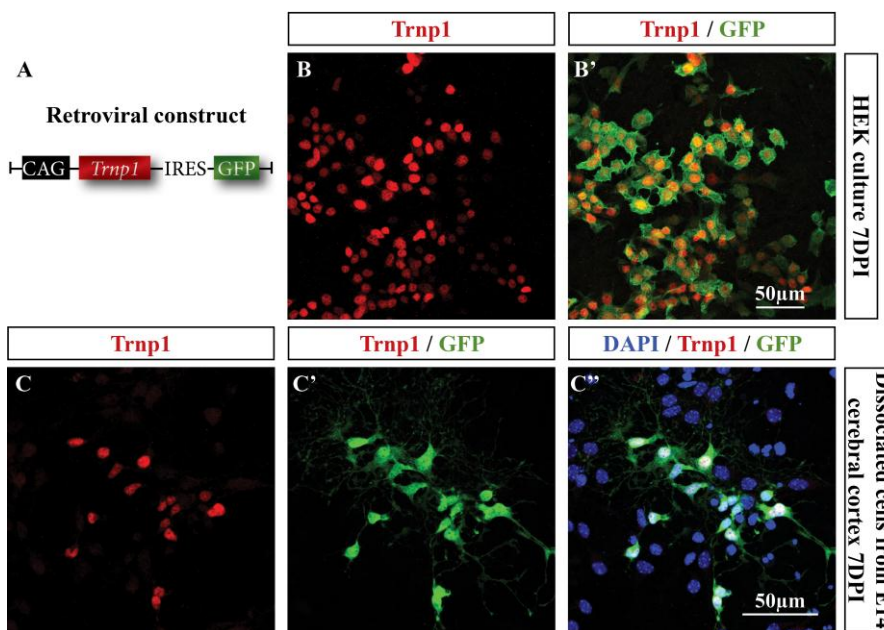


Figure 15: Generation of a retroviral vector for forced expression of *Trnp1*

(A) *Trnp1* cDNA lacking the 3'-UTR was cloned into a retroviral expression vector with the CAG promoter driving the transcription of *Trnp1*-IRES-GFP mRNA. GFP and *Trnp1* are thus translated from the same mRNA produced from pCAG-*Trnp1*-GFP. (B) HEK cells were transduced with viral particles containing pCAG-*Trnp1*-GFP and tested

for *Trnp1* expression seven days post infection. Labeling for *Trnp1* and GFP is shown. Note that each cell expressing GFP also expresses *Trnp1*. (C) Dissociated cells from the cerebral cortex of E14 mouse embryos were infected with the same virus for overexpression of *Trnp1*. Reliable co-expression of *Trnp1* and GFP in infected cells was tested by immunostaining seven days post infection. CAG, chicken beta actin promoter; IRES, internal ribosomal entry site; DPI, days post infection.

4.3.2 Overexpression of *Trnp1* increases proliferation of neurogenic progenitors in vitro

The above-described viral vector was utilized to overexpress *Trnp1*. By using less than 25 viral particles per well (in a 24 well plate) a clear separation of single clones was ensured. Each clone represents the progeny of initially one single infected cell (note that retroviruses do not integrate into non-dividing cells) (Williams et al., 1991; Haubst et al., 2004; Costa et al., 2008). Interestingly, overexpression of *Trnp1* led to a dramatic increase in clone size seven days post transduction at clonal density. Clones transduced with *Trnp1* virus contained more than double the number of cells compared to such infected with the control virus (Figure 16).

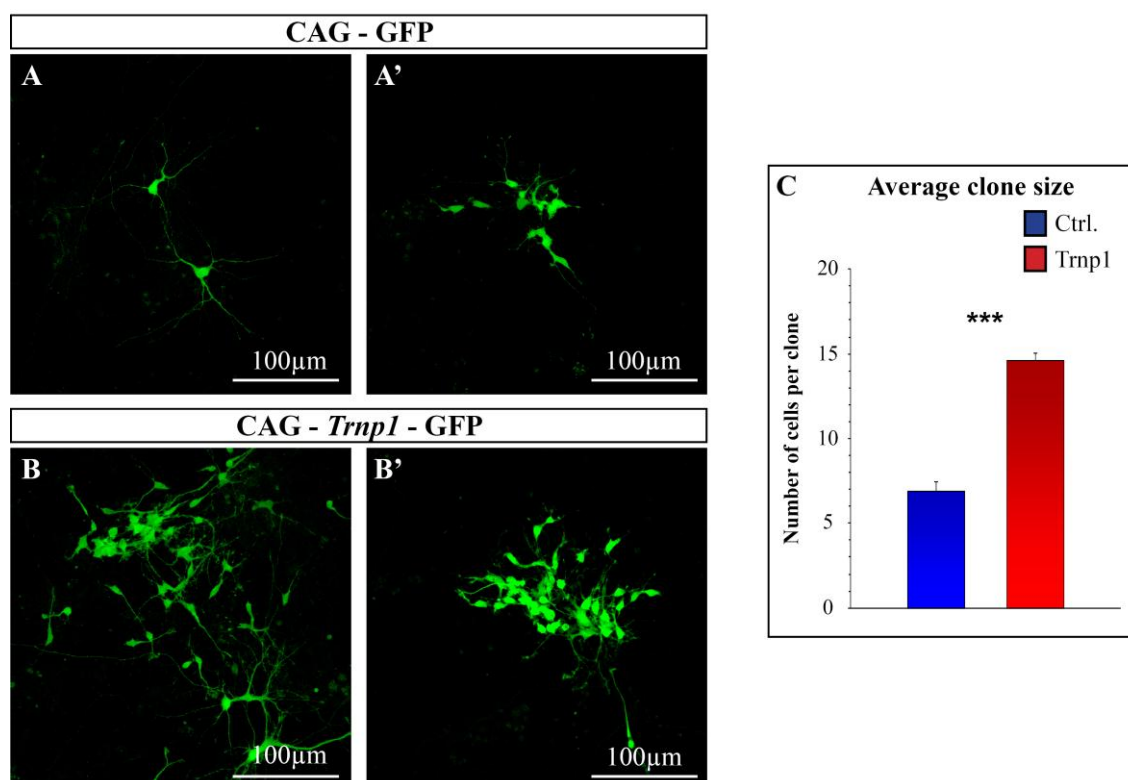


Figure 16: Forced expression of *Trnp1* in dissociated cells from the embryonic cerebral cortex dramatically increases clone size

Representative images of dissociated cell cultures of the embryonic cerebral cortex at E14 infected with either CAG-GFP control (A-A') or CAG-*Trnp1*-GFP virus (B-B'). Cells were infected with a low number of viral particles and analyzed seven days post infection. Note that the clones transduced with CAG-*Trnp1*-GFP virus are bigger than clones transduced with control virus. (C) Quantification of the average size of clones expressing either GFP control or *Trnp1*. Data are shown as mean +/- SEM, n=4 (independent experiments); ***p<0.001. Blue bars: control virus, red bars: *Trnp1* virus. Statistical significance tested using students t-test.

The observed strong increase in clone size suggested a profound increase in proliferation, reduced cell death or alterations in the mode of cell division as possible effects of *Trnp1* overexpression. To elucidate these possibilities, live imaging of transduced cells was performed. For that purpose dissociated cell cultures of the embryonic cerebral cortex at E14 were transduced with *Trnp1* or control virus respectively. Imaging was started one day post transduction and cells were imaged for the next six days. Remarkably, *Trnp1* overexpression led to a strong increase of proliferation rate and promoted self renewal of stem cells (see Figure 17). Specifically, *Trnp1* increased cell cycle reentry and led to sustained self renewal of proliferating stem cells (Figure 17D and E). However, it is important to mention, that the effect of *Trnp1* overexpression was so strong, that tracking of cell divisions and following single cells turned out to be impossible in most of the cases some days after transduction (see Figure 17B first lineage tree). Therefore Figure 17 represents only the “trackable” proportion of clones. Nevertheless, the strong increase of proliferation and continued self-renewal of proliferating cells was clearly shown by this experiment.

Results

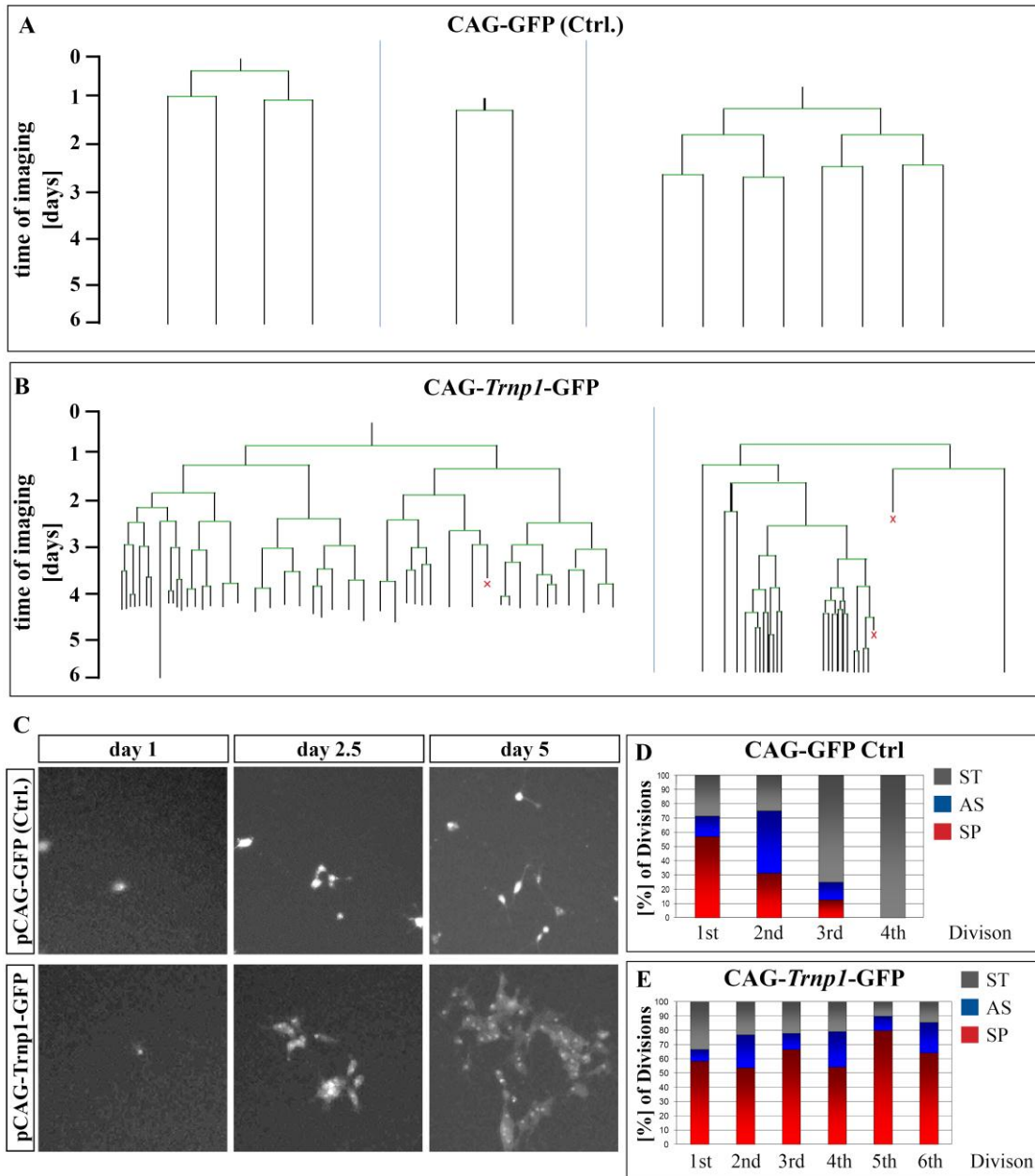


Figure 17: Live imaging of dissociated cells from the developing cerebral cortex overexpressing Trnp1
Dissociated cells from the developing cerebral cortex at E14 were transduced either with CAG control virus or with Trnp1 virus. (A and B) Lineage tree analysis of single cells infected with either control (A) or Trnp1 virus (B) - representative trees are depicted (time lapse images for analysis were taken every five minutes over a period of six days). Horizontal lines represent cell divisions; vertical lines represent single cells over time. Red cross indicates cell death. Time axis in days is shown on the left side. Note that in many cases of Trnp1 overexpression tracking of single cells was impossible after several days. (C) Time lapse analysis of representative clones for control and Trnp1 transduced cells. Images over time of one single clone derived from initially one single cell are shown for both control and Trnp1 transduced cells. Note the persistent self renewal of progenitors through symmetric progenitor divisions upon Trnp1 transduction. (D and E) Quantification of the mode of cell division of control (D) and Trnp1 (E) transduced cells. ST: symmetric terminal divisions (none of the daughter cells divided anymore); AS: asymmetric divisions (one daughter cell divided further, the other did not proliferate anymore) SP: symmetric progenitor divisions (both daughter cells underwent another round of proliferation). n = 14 clones each, from two independent experiments.

As during cortical neurogenesis *Trnp1* was expressed in only a subset of radial glial cells (Figure 12) the next question addressed was whether neurogenic progenitors are affected by sustained *Trnp1* expression. To determine possible changes in cell fate, the different types of generated clones were examined. Dissociated cells from the mouse embryonic cerebral cortex typically form three different types of clones seven days post infection with a control virus:

1. Purely non-neuronal clones (consisting only of glia or undifferentiated progenitors)
2. Purely neuronal clones (consisting only of neurons)
3. Mixed, neural stem cell clones (generating a mixed neuronal and glial / progenitor progeny).

Immunostaining for the neuron specific protein β III-tubulin and progenitor and glia antigens such as Nestin and GFAP allowed the classification accordingly as mixed (stem cell) clones (comprising both β III-tubulin positive (+) cells and β III-tubulin negative (-) cells), purely neuronal clones (all GFP+ cells were also β III-tubulin+) and purely non-neuronal clones (no GFP+ cell was β III-tubulin+).

Forced *Trnp1* expression significantly increased the percentage of mixed (stem cell) clones at the expense of purely neuronal clones (Figure 18A to C). Interestingly, the proportion of non-neuronal clones was not affected. This suggests that high levels of *Trnp1* do not simply suppress the generation of neurons per se (otherwise one would expect more purely non-neuronal clones). High levels of *Trnp1* rather increase the self-renewal of neural stem cells still allowing neurogenesis to occur at the same time (leading to more mixed clones, some of which would otherwise terminally differentiate into neurons generating a purely neuronal clone). This interpretation was further corroborated by analysis of the size of the different clone types. Quantification revealed a selective size increase of mixed clones while the clone size of restricted, purely glial and purely neuronal clones was not affected (Figure 18D). Furthermore, co-immunolabeling for GFAP or PDGFR α (labeling oligodendrocytes) showed that *Trnp1* overexpression still allowed the generation of different cell lineages (Figure 18E and F). Taken together this analysis suggested an effect of *Trnp1* levels on cell fate. Forced *Trnp1* expression promoted neural stem cell self-

Results

renewal and inhibited symmetric terminal divisions that would give rise to neurons only (as described previously: Costa et al., 2008; Asami et al., 2011).

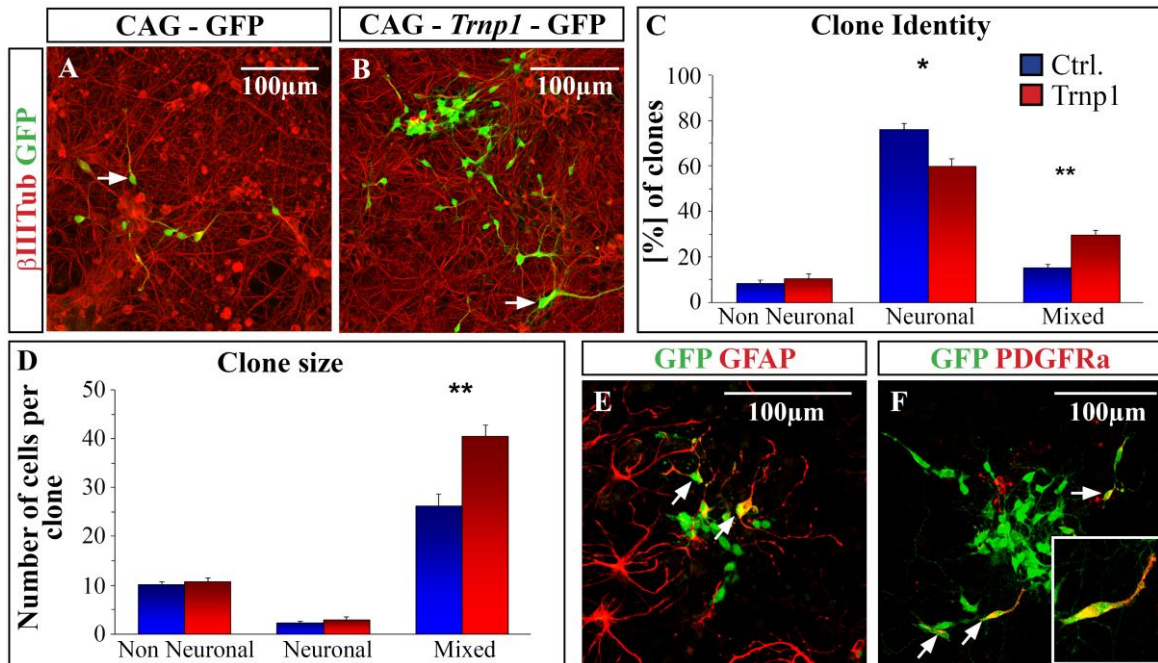


Figure 18: Forced expression of *Trnp1* increases self renewal of neurogenic progenitors

(A and B) Representative micrographs of dissociated cell cultures of the embryonic cerebral cortex at E14 transduced with a low titer of either CAG-IRES-GFP control virus (A) or CAG-*Trnp1*-IRES-GFP virus (B) immunostained for GFP and β III-tubulin seven days post transduction. Arrows indicate examples of double positive cells. (C) Quantification of the percentage of purely non-neuronal, purely neuronal or mixed clones seven days post transduction. Note that *Trnp1* overexpression specifically increases the self-renewal of neurogenic progenitors thereby increasing the percentage of mixed clones. (D) Quantifications of the number of cells per clone within the different clone types. *Trnp1* overexpression specifically affects the clone size of mixed clones. (E-F) Infected clones were immunostained for *Trnp1* and GFAP (E) or PDGFR α (F). Note that overexpression of *Trnp1* still allowed production of different cell lineages such as glial (GFAP) and oligodendrocytic cells (PDGFR α). Data are shown as mean \pm SEM, n=4 (independent experiments); *p<0.05, **p<0.01, ***p<0.001. Blue bars: control virus, red bars: *Trnp1* virus. Statistical significance was tested using students t-test.

4.4 Functional analysis of *Trnp1* *in vivo*

Analysis of *Trnp1* overexpression *in vitro* raised the question to which extent forced *Trnp1* expression may also promote proliferation or expansion of radial glial cells *in vivo*. On the other hand, another question was how knock down of the endogenous protein would affect neurogenesis. In utero electroporation at mid neurogenesis has previously been shown to specifically target radial glial cells and not basal progenitors (Stancik et al., 2010). Therefore, utilizing this technique allowed analyzing the function of *Trnp1* on radial glial cells and their fate during forebrain development *in vivo*.

4.4.1 Forced expression of *Trnp1* *in vivo* by in utero electroporation

4.4.1.1 Forced expression of *Trnp1* *in vivo* increases the number of apical progenitors and causes tangential expansion

To study the effect of forced *Trnp1* expression *in vivo*, pCAG-*Trnp1*-IRES-GFP or pCAG-IRES-GFP as a control were electroporated into the cerebral cortex of embryos at E13.5. The brains of electroporated embryos were examined 3 days later at E16.5. *Trnp1* overexpression led to a clear overall increase in the number of GFP immunoreactive cells with many cells still residing below the cortical plate in progenitor layers (Figure 19A to B'). Quantification of the distribution of electroporated cells – discriminating between cells still residing in the ventricular/subventricular zone (VZ/SVZ - harboring proliferative progenitors), cells found in the intermediate zone (IZ - mainly consisting of migrating neurons) and the cortical plate (CP) (consisting of newborn neurons) – confirmed a remarkably different distribution as compared to control electroporations. Upon forced *Trnp1* expression the majority of cells (56.6%) was found in the VZ/SVZ at the expense of migrating/newborn neurons in the IZ and CP (Figure 19C). Notably, in each experiment large numbers of weakly GFP positive cells were found in the VZ. The weak GFP expression is indicative of strong proliferation through which the cells typically dilute the protein and the GFP encoding plasmid (Figure 19B, note the number of weakly GFP positive cells close to the ventricular surface). Accordingly, a strong tangential expansion of GFP positive cells was observed upon overexpression of *Trnp1* as compared to control electroporated cells (Figure 18E-F'). Such tangential expansion is indicative of

proliferating apical progenitors that expand laterally, whereas basal progenitor proliferation is believed to lead to radial expansion.

To ensure, that Trnp1 is indeed overexpressed upon electroporation, immunostaining for Trnp1 was performed. A clear increase of Trnp1 immunostaining was detectable upon overexpression through in utero electroporation (Figure 19D and D'). In this context it should be mentioned that, upon overexpression, Trnp1 was detectable without any pretreatment of brain sections whereas endogenous protein levels were only detectable after pretreatment with hydrochloric acid. This suggests a strong interaction of the endogenous protein with an acidic partner (such as DNA) whereas binding partners may be saturated upon protein overexpression above a critical level, making Trnp1 detection easier.

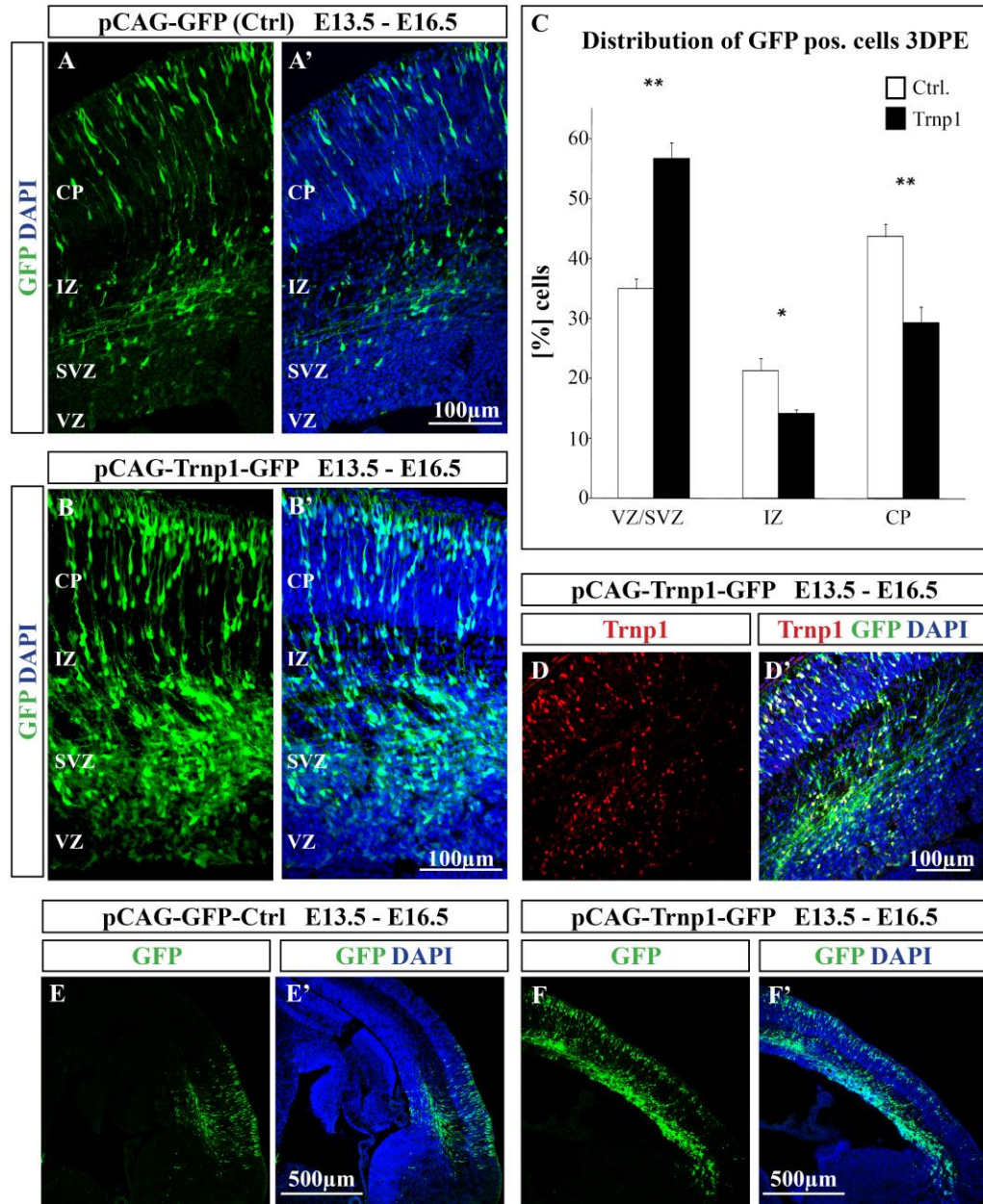


Figure 19: Forced expression of *Trnp1* *in vivo* increases cells residing within the progenitor area and causes tangential expansion

Embryonic cortices were electroporated at E13.5 with either pCAG-IRES-GFP control plasmid or pCAG-*Trnp1*-IRES-GFP plasmid and analyzed three days later. (A-B') DAPI and GFP labeling of coronal sections of embryonic brains electroporated with either control (A and A') or *Trnp1* (B and B') encoding plasmid. (C) Quantification of the cellular distribution of electroporated cells revealed a significant increase of cells residing in the proliferative VZ/SVZ with significantly less cells in the IZ and CP. (D-D') Analysis of *Trnp1* expression upon *Trnp1* overexpression by in utero electroporation. Note that the *Trnp1* immunostaining was carried out without HCl pre-treatment and the endogenous *Trnp1* protein is not detectable without pre-treatment. (E-F') Overview of the distribution of transfected cells three days after in utero electroporation of either pCAG-GFP control plasmid (E-E') or *Trnp1* expression plasmid (F-F'). Note the strong tangential expansion upon *Trnp1* overexpression. Data are shown as mean +/- SEM, n=5 embryos; *p<0.05, **p<0.01, statistical significance calculated using Mann Whitney U-Test. White bars represent control electroporated cells, black bars represent *Trnp1* overexpressing cells. Single optical sections are shown in (A-B' and D-D').

4.4.1.2 Forced expression of *Trnp1* *in vivo* increases self renewal of Pax6+ radial glial cells

The accumulation of cells residing in the VZ/SVZ and the observed tangential expansion raised the question to which extent this observation was due to postmitotic neurons that failed to migrate towards the cortical plate or whether these cells remained in the progenitor state and continued to proliferate. To address this issue, BrdU was injected intraperitoneally into electroporated animals one hour before sacrifice. As an analogue of the nucleoside thymidine, BrdU is being incorporated into newly synthesized DNA thereby labeling cells in S-phase when applied for one hour only. The proportion of proliferating cells of *Trnp1* or GFP electroporated embryos was analyzed based on their incorporation of BrdU. *Trnp1* overexpression led to a highly significant increase of cell proliferation by about threefold compared to control electroporated animals (Figure 20A, A' and C). Given the endogenous expression of *Trnp1* in only a subset of radial glial cells and its increase of progenitor clones *in vitro*, *Trnp1* might have an effect on apical versus basal progenitor equilibrium. Therefore, the number of apical (Pax6+) and basal (Tbr2+) progenitors was quantified three days after *Trnp1* electroporation. *Trnp1* overexpression provoked a strong increase in Pax6+ radial glial cells as compared to control electroporated embryos (Figure 20B, B' and D). These results showed that *Trnp1* expression leads to the maintenance of proliferating radial glial cells and thereby significantly amplifies the pool of apical progenitors. Interestingly, conversely to the increase in apical progenitor cells high levels of *Trnp1* significantly inhibited the generation of Tbr2+ basal progenitors to less than 50% of the control (Figure 20E). The reduced proportion of basal progenitors may also explain the decrease in neurons found within the intermediate zone and the cortical plate. Thus, high levels of *Trnp1* increase the maintenance and proliferation of Pax6+ apical progenitors and reduce the generation of Tbr2+ basal progenitors *in vivo*. This finding is consistent with the higher expression levels of *Trnp1* in radial glia that do not generate Tbr2+ basal progenitors (Pinto et al., 2008) and with the above described results *in vitro* of *Trnp1* promoting self-renewal of neural stem cells (see 4.3.2).

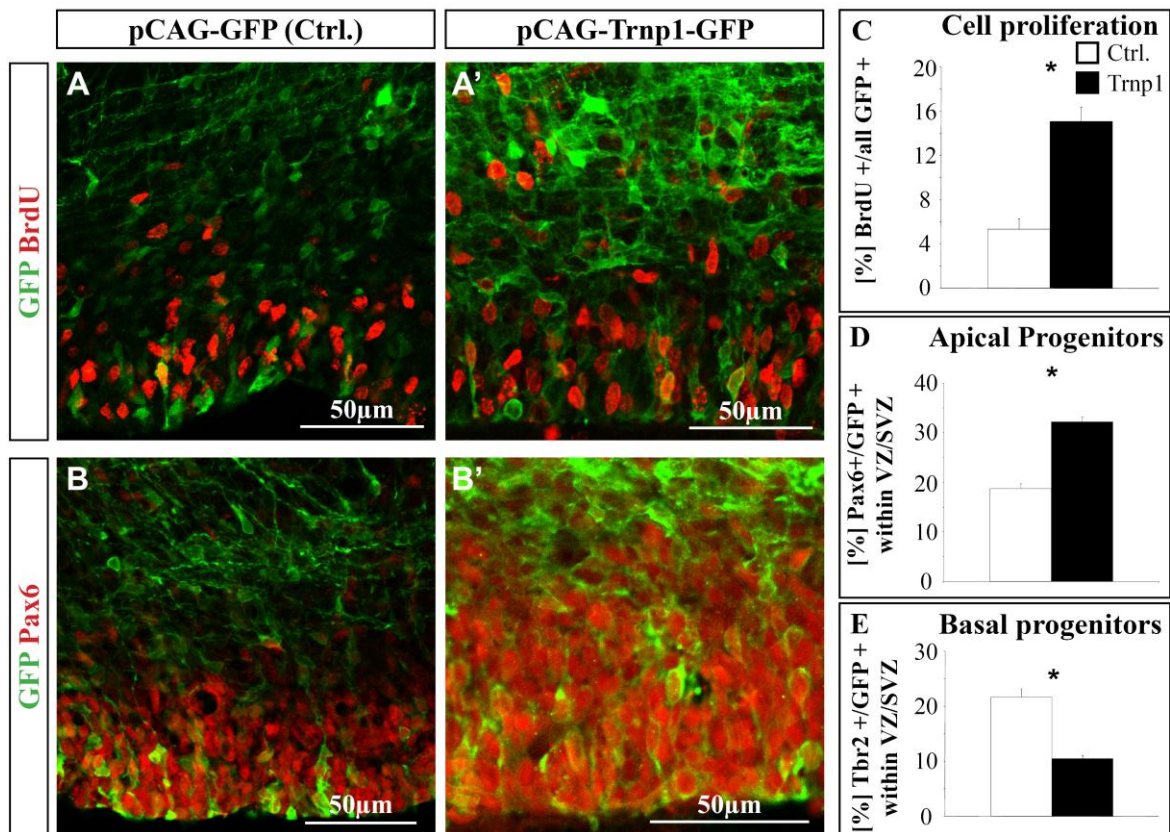


Figure 20: Proliferation analysis and characterization of radial glial fate upon forced *Trnp1* expression
 Embryonic cortices were electroporated at E13.5 with either pCAG-IRES-GFP control plasmid or pCAG-*Trnp1*-IRES-GFP plasmid for the overexpression of *Trnp1* and analyzed three days later. (A-B') Co-Immunostaining of GFP together with BrdU (A and A') or Pax6 (B' and B') of electroporated cortices. Single optical sections are shown. (C) Quantification of proliferating cells (BrdU+/GFP+) revealed a strong increase in proliferation (BrdU treatment one hour prior to sacrifice). (D and E) Analysis of the number of Pax6 (D) and Tbr2 (E) positive cells within the proliferative VZ/SVZ. Note that the proportion of Pax6 positive apical progenitors is significantly increased upon *Trnp1* overexpression, whereas the proportion of Tbr2 positive basal progenitors is decreased. Data are shown as mean +/- SEM, n=4; *p<0.05, **p<0.01, Mann Whitney U-Test. White bars represent control electroporated cells, black bars represent *Trnp1* overexpressing cells.

4.4.2 Knock down of *Trnp1* in vivo by in utero electroporation

As forced expression of *Trnp1* resulted in an increase of apical progenitors, the next question was whether *Trnp1* is not only sufficient for the increase of radial glia proliferation but is also necessary for the self-renewal of these neural stem cells. In order to determine to which extent loss of *Trnp1* may result in an opposing effect as compared to overexpression, short hairpin RNAs were created targeting *Trnp1* mRNA.

4.4.2.1 Generation of short hairpin RNAs for the knock down of *Trnp1*

Three of initially five designed short hairpin RNAs (shRNAs) targeting the 3'-UTR of *Trnp1* mRNA were generated. In order to reduce possible off-target effects, the shRNA target sequences were designed with the help of BlockIT (Invitrogen) and Oligoengine software. In addition, Blast search was used to confirm specificity of the sequences. ShRNAs were cloned into pSUPER.GFP vector (Figure 21A) as this vector has the advantage of expressing the shRNA (controlled by the H1 promoter) and GFP (controlled by the PGK promoter) from the same plasmid. The knock down efficiency of the different shRNAs was tested using western blotting (Figure 21B) and immunostaining (Figure 21C). To test the efficiency of RNA interference, HEK cells were co-transfected with a plasmid encoding full length *Trnp1* mRNA (pCMV-*Trnp1*) plus the pSUPER.GFP-shRNA vector or the empty pSUPER.GFP vector as a control. Cells were collected 48 hours later and western blotting was performed. Two out of three generated shRNAs showed significant reduction of protein signal in western blot analysis. ShRNA#4 had only marginal effects on *Trnp1* protein expression, whereas shRNA#1 resulted in a strong knock down of the protein and shRNA#5 was able to reduce the protein to almost un-detectable levels (see Figure 21B). These results were confirmed in three independent experiments. In order to exclude off-target effects of the shRNAs, one approach is to rescue the knock down effect of the gene of interest by simultaneously re-expressing a resistant form of it. Thereby off-targets of the used shRNA can be excluded, as only the gene of interest is re-expressed. Towards this end, the shRNA was tested with an shRNA resistant form of the *Trnp1* sequence (i.e. *Trnp1* coding sequence lacking the 3'-UTR which is the target of all the shRNAs). The shRNAs described above were not able to reduce the signal of the shRNA resistant form of *Trnp1* (Figure 21B'). Thus the *Trnp1* version lacking its 3'-UTR could be subsequently used for rescue experiments (see 4.4.2.5. "Rescue of *Trnp1* knock down"). To further test the efficiency of the generated shRNAs to reduce endogenous *Trnp1* levels, immunocytochemistry was performed. In this context, dissociated cells from the cerebral cortex of E12 embryos were infected with a lentivirus encoding for the shRNA plus GFP or GFP only as a control. A strong reduction of *Trnp1* protein levels was observed five days post infection (Figure 21C).

In summary, two of three generated shRNAs were very effective in reducing *Trnp1* protein levels. Both shRNAs (shRNA#1 and shRNA#5) were therefore subsequently used for in utero electroporation and analysis of the effect of *Trnp1* knock down *in vivo*.

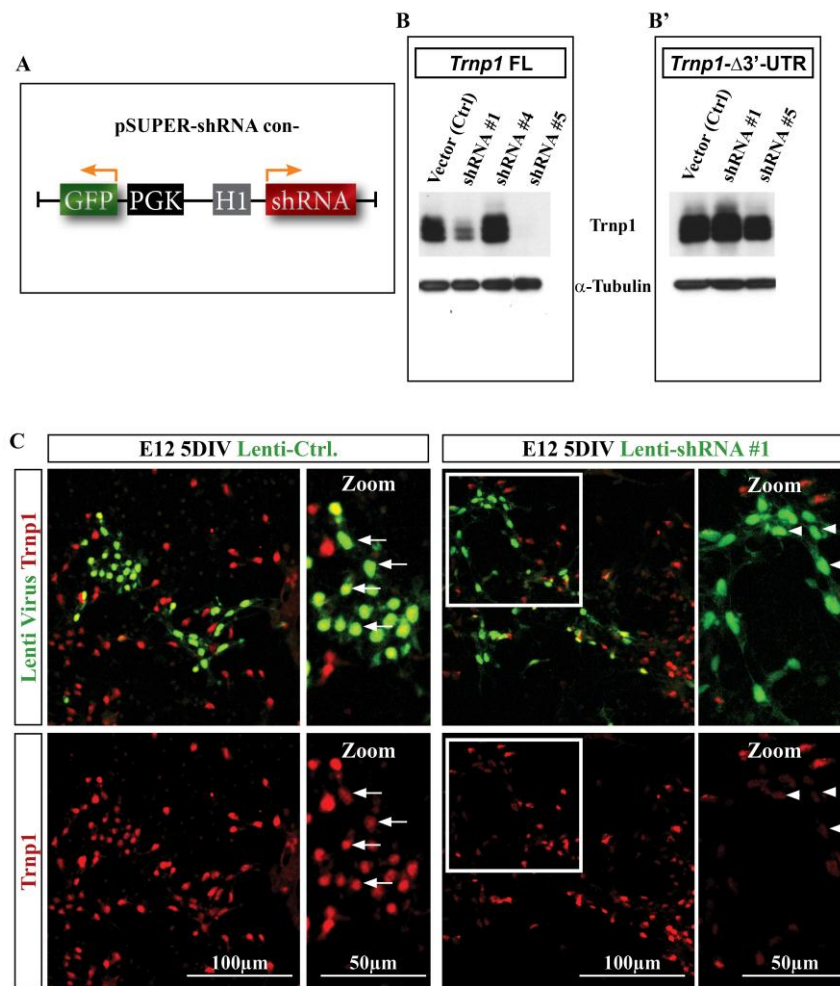


Figure 21: Generation and test of shRNAs targeting *Trnp1*

(A) Three different shRNAs (each targeting the 3'-UTR of *Trnp1*) were cloned into pSUPER.GFP. ShRNA expression is driven by H1 promoter, GFP expression is driven by the PGK promoter from the same plasmid. (B) Test of knock down efficiency of these shRNAs. HEK293 cells were co-transfected with pCMV-*Trnp1* and pSUPER.GFP-shRNA plasmids or the empty pSUPER.GFP as a vector control. Note that shRNA#1 and #5 led to significant knock down of *Trnp1*, whereas #4 was not effective in reducing *Trnp1* levels. (B') Test of a resistant version of *Trnp1* lacking the shRNA targeted 3'-UTR. HEK 293 cells were co-transfected with pCAG-*Trnp1*-GFP (*Trnp1*Δ3'-UTR) and pSUPER.GFP

shRNA plasmids or the empty pSUPER.GFP as a vector control. Note that neither shRNA#1 nor #5 were able to down regulate the resistant (Δ3'-UTR) *Trnp1* version. (C) ShRNAs were also sub-cloned into a lentiviral vector (pLVTHM) and viral particles were used to transduce dissociated cells from the embryonic cerebral cortex (at day 12) in order to test successful down regulation of endogenous *Trnp1*. As a control the same GFP-only expressing lentivirus was used. Five days post transduction immunostaining for *Trnp1* and GFP was performed. Note that the shRNA#1 was able to significantly down regulate endogenous *Trnp1* levels. Arrows indicate GFP positive, *Trnp1* positive cells, arrowheads indicate GFP positive cells with down-regulated *Trnp1* expression.

4.4.2.2 Knock down of Trnp1 *in vivo* leads to radial expansion of the developing forebrain

In order to test the effects of down regulation of Trnp1 *in vivo*, embryos were electroporated at E13.5 and analyzed three days later at E16.5. Knock down of Trnp1 consistently led to a very strong and obvious radial expansion of the developing cortex in the electroporated region compared to the non-electroporated hemisphere and to control electroporations (Figure 22A to B'; compare A' with B' – note the white bar indicating the radial length of the control cortex and compare it to the radial expansion of the cortex upon knockdown). Surprisingly, the proportion of cells residing in the VZ/SVZ was not altered. However, knock down of Trnp1 by electroporation of pSUPER.GFP-shRNA#5 at E13.5 resulted in a consistently altered distribution of GFP+ cells at E16.5. In pronounced contrast to the overexpression of Trnp1, knock down of the protein resulted in a significant increase in the proportion of cells within the cortical plate three days after electroporation (Figure 22C).

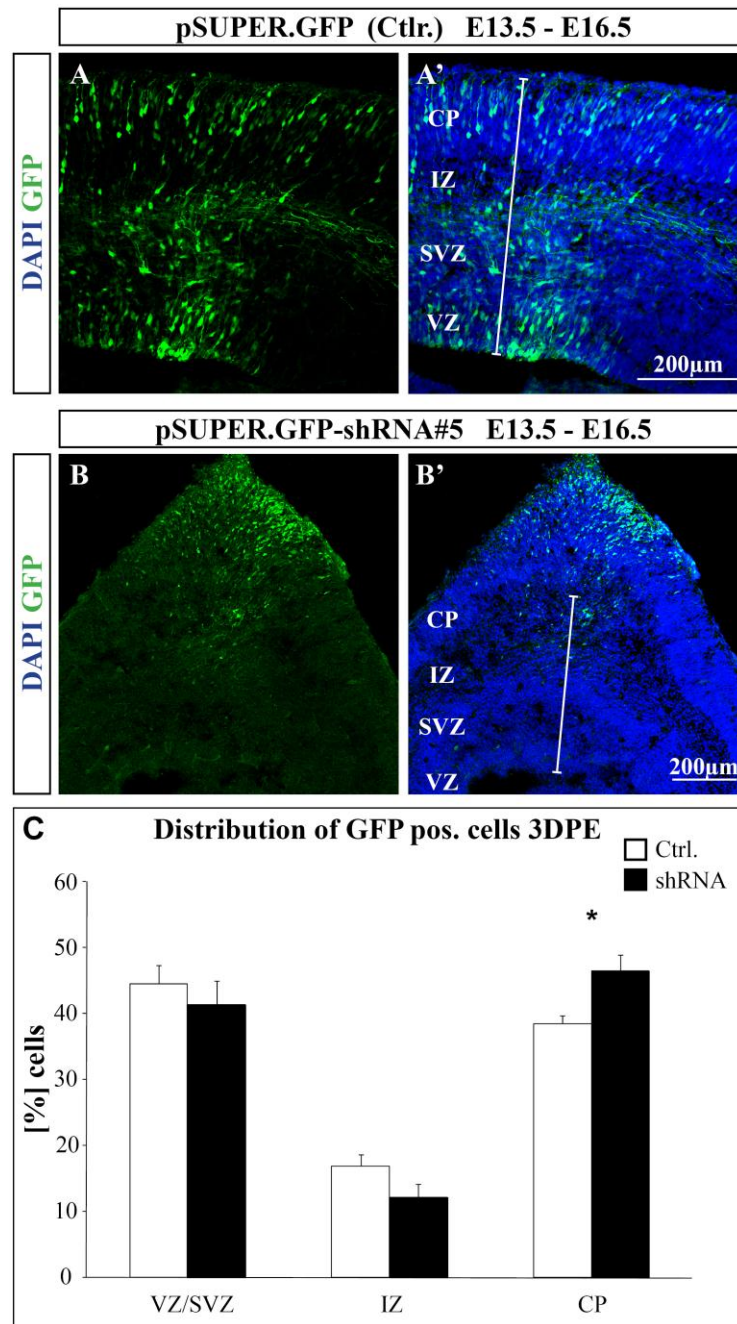


Figure 22 Knock down of *Trnp1* *in vivo* results in strong radial expansion of the developing cortex

Embryonic cortices were electroporated at E13.5 with either pSUPER.GFP control (A-A') or pSUPER.GFP-shRNA (B-B') plasmid for the knock down of *Trnp1* and analyzed three days later. (A-B') Images of GFP and DAPI labeled coronal sections of electroporated brains. Note the strong radial expansion of shRNA electroporated cortices. The white bar (in A' and B') represents the radial length of the control electroporated cortex. (C) Quantification of the localization of GFP+ cells in shRNA electroporated brains (black bars) compared to control electroporated brains (white bars). Data are shown as mean \pm SEM; n=5 embryos; *p<0.05, Mann Whitney U-Test.

4.4.2.3 Knock down of *Trnp1* increases the number of basal progenitors

As down regulation of *Trnp1* did not alter the proportion of cells residing within the proliferative VZ/SVZ, overall proliferation was analyzed next. For this purpose, BrdU was injected intraperitoneally into electroporated animals one hour before sacrifice. Surprisingly, co-immunostaining for BrdU and GFP revealed, that the overall proportion of proliferating BrdU⁺/GFP⁺ cells was not altered as compared to control electroporations (Figure 23E). Thus *Trnp1* is able to increase proliferation but it is not necessary to maintain proliferation overall. However, quantification of the proportion of basal progenitors revealed that the number of Tbr2⁺ basal progenitors was significantly increased when levels of *Trnp1* were reduced in radial glia (Figure 23A to D). Remarkably, immunostaining for Tbr2 clearly showed an atypically increased band of basal progenitors within the shRNA electroporated region (Figure 23C). A diffuse expansion of Tbr2⁺ cells towards very basal regions of the SVZ with concomitant expansion of the SVZ was observed (see Figure 22C) resembling the situation observed in larger brains where an expanded diffuse Tbr2⁺ band has recently been described (Martínez-Cerdeño et al., 2012).

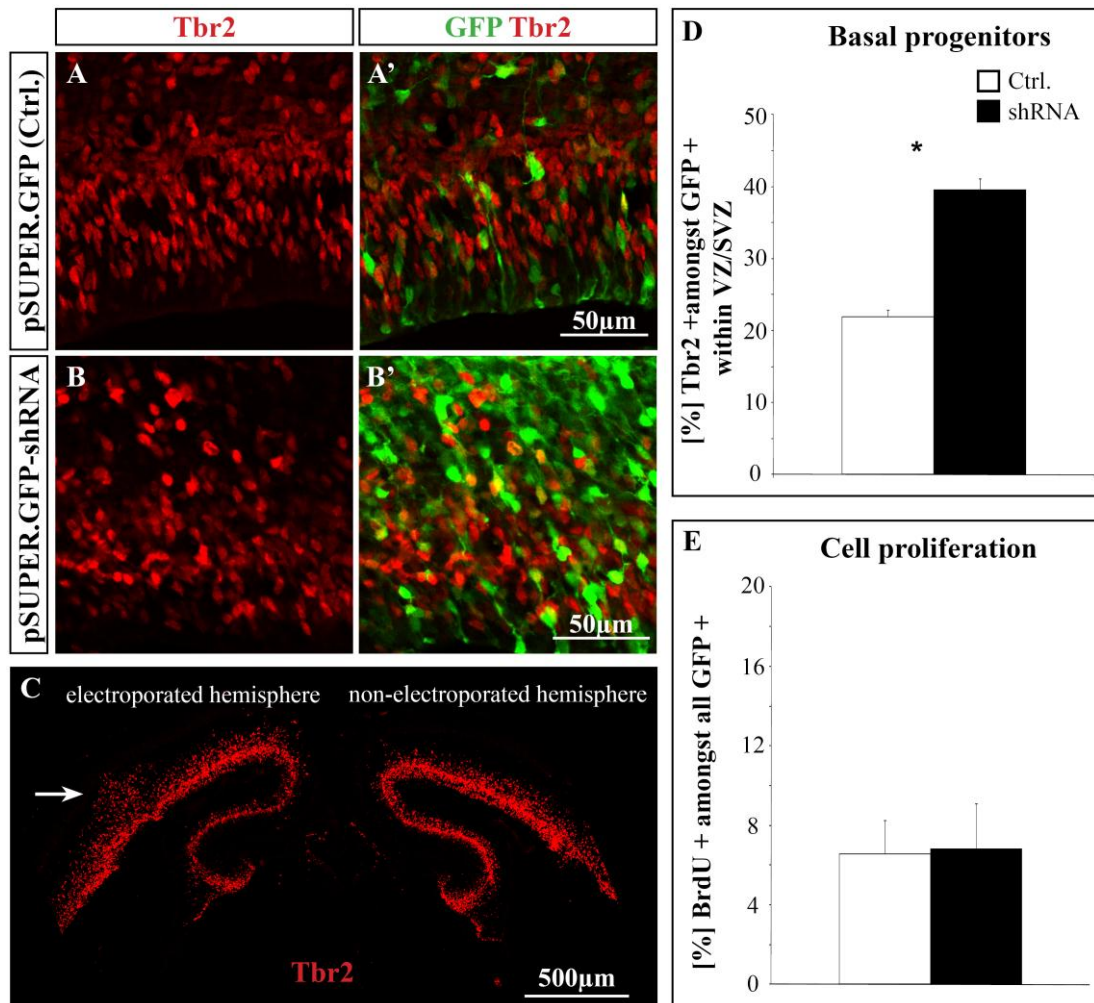


Figure 23: Loss of Trnp1 provokes generation of Tbr2+ basal progenitors

Coronal section of embryonic brains electroporated at E13.5 with either pSUPER.GFP control plasmid or pSUPER.GFP-shRNA#5 plasmid and analyzed three days post electroporation. (A-B') Images of control or shRNA electroporated cortices immunostained with GFP and Tbr2. Single optical sections are depicted. (C) Reconstruction of a coronal section of an shRNA electroporated cerebral cortex immunolabeled for Tbr2. Note that the knock down of Trnp1 led to a strong increase of Tbr2 positive basal progenitors at the electroporation site (indicated by an arrow) with a resulting diffuse band of Tbr2+ cells that is usually not seen in control electroporated sections or in the non-electroporated hemisphere. (D-E) Quantifications of the number of basal progenitors (D) and cell proliferation (E) in shRNA electroporated brains (black bars) compared to control electroporated brains (white bars). Data are shown as mean \pm SEM; n=4 for basal progenitor and n=3 for cell proliferation analysis; *p<0.05, Mann Whitney U-Test.

4.4.2.4 Knock down of *Trnp1* at mid neurogenesis induces an increase of oRGs and folding of the cortical plate

Previous studies of neocortical development showed that besides radial glia and basal progenitors another subtype of progenitor exists in the developing brain. This type of cells, the so-called basal- or outer radial glial cells (bRGs or oRGs) are implicated in expansion of the cerebral cortex (Fietz et al., 2010; Hansen et al., 2010; Reillo et al., 2011; Shitamukai et al., 2011; Wang et al., 2011). While basal progenitors lack Pax6 expression, oRGs are characterized by the expression of Pax6, the location of their nucleus in the outer (basal) area of the SVZ and the presence of a basally anchoring process with the absence of an apical process. Given the strong radial expansion of the region electroporated with shRNA against *Trnp1* it was conceivable that *Trnp1* knock down not only leads to increased abundance of basal progenitors but may also increase the number of outer radial glial cells.

To address this possibility, sections of shRNA electroporated brains and control brains were immunostained with Pax6 and GFP antibodies. Remarkably, after knocking down *Trnp1* many Pax6⁺ cells were found to be located in the outer area of the SVZ (Figure 24A to A''). These cells were clearly separated from the VZ where Pax6⁺ cells are normally located. Consistent with an oRG identity, these cells lacked an apical process but still possessed a long basal process (Figure 24C to C') thereby clearly distinguishing them from VZ radial glia and SVZ basal progenitors. Quantification further confirmed the significant increase of Pax6⁺ cells within the outer SVZ by more than threefold in the electroporated regions as compared to the unelectroporated hemisphere of the same embryo (Figure 24D). Remarkably, only one third of these cells are Tbr2 negative in control conditions, whereas about two third were Pax6⁺ but Tbr2 negative upon *Trnp1* knock down (Figure 24E) resembling a drastic increase of oRGs upon down regulation of *Trnp1*.

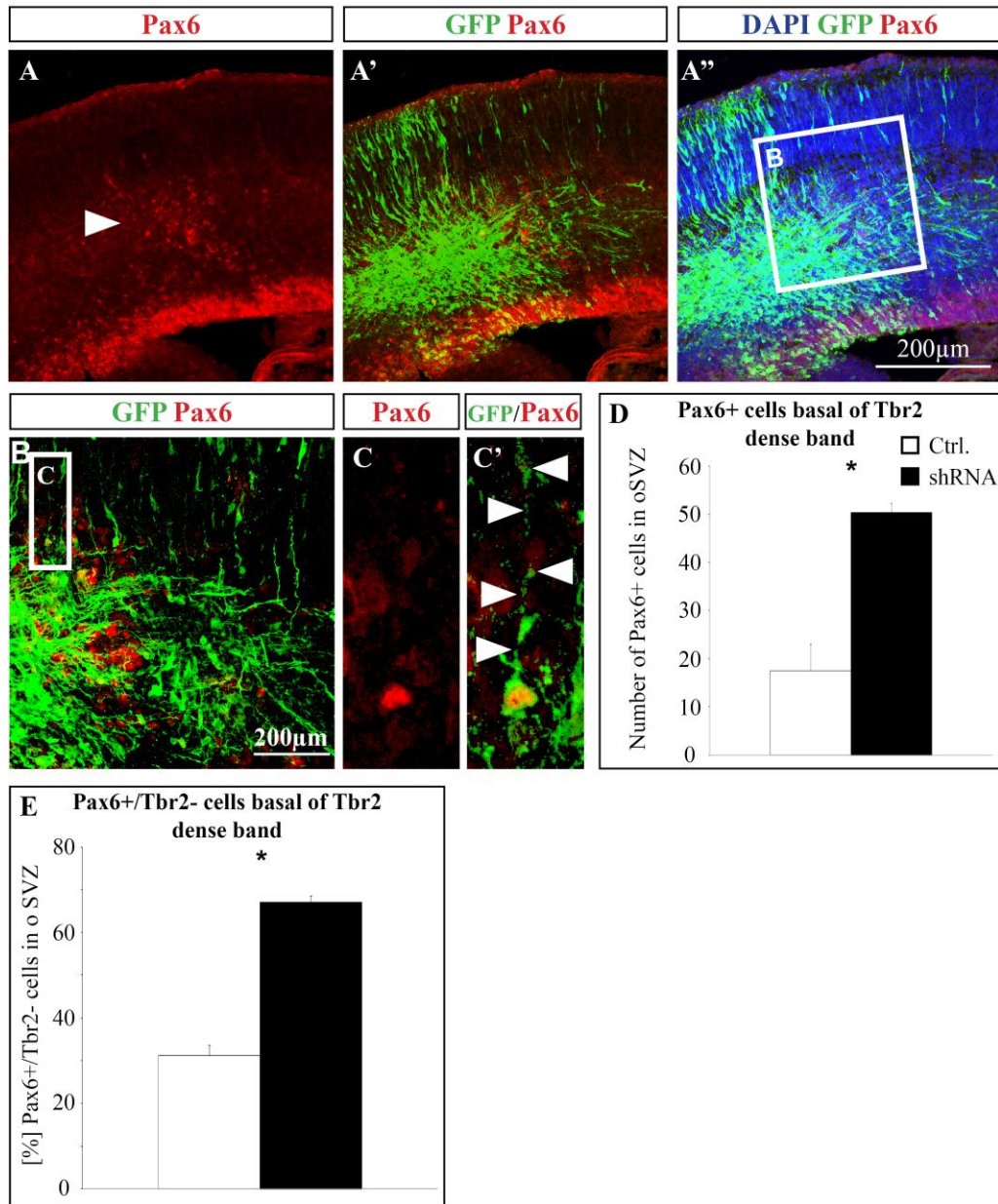


Figure 24: Loss of Trnp1 increases the number of outer radial glial cells

Knock down of Trnp1 through shRNA electroporation at E13.5 and analysis at E16.5 not only increased the number of Tbr2+ basal progenitors, but also lead to an increase of Pax6 positive outer radial glial cells. (A-A'') Coronal section of an shRNA electroporated cortex labeled with Pax6, GFP and DAPI. Note the number of Pax6 positive cells residing far outside the ventricular zone indicated by an arrowhead in A. (B) Higher magnification of the area indicated by a square in A''. (C and C') Example of a Pax6+ cell residing in a very basal region of the SVZ (square in B) possessing only a basal but no apical process. (D) Quantification of the number of Pax6+ cells at the site of electroporation residing in basal SVZ areas. (E) Quantification of the percentage of Pax6+/Tbr2- cells amongst basal Pax6+ cells counted in (D). Note that upon loss of Trnp1 significantly more Pax6+ cells in basal SVZ regions were detected (D), with two third of them being Tbr2 negative (E). Data are shown as mean +/- SEM; n=3 embryos; *p<0.05, Mann Whitney U-Test.

One very interesting feature observed upon loss of *Trnp1* was the either simple outward directed radial expansion of the neocortex (see Figure 22A to B') or alternatively an expansion that resulted in folding of the neocortex (Figure 25A to B'). In this context, in 4 out of 10 shRNA electroporated embryos not only expansion but also folding of the neocortex was observed (Figure 25A to B'). This observation together with the increase in oRGs is consistent with previous reports on oRGs implicated in expansion and folding of the cortex (Lui et al., 2011 for review; Reillo et al., 2011). To examine the morphology of radial glia in these folded regions, shRNA electroporated brains were examined by staining with the radial glia specific antibody RC2 (Figure 25C). Interestingly, radial fibers diverged as they entered the cortical plate resembling a fanned array that has been described in larger brains (see Lui et al., 2011). Figure 26 shows more examples of different expanded brains upon *Trnp1* shRNA electroporation and compares non-electroporated hemispheres to electroporated hemispheres of the same section.

Altogether, down regulation of *Trnp1* leads to cortical expansion in a dual mode. First, low levels of *Trnp1* induce the generation of basal progenitors thereby increasing the total number of neurons. Second, radial glia with low levels of *Trnp1* are also capable of generating outer radial glial cells lacking a ventricular apical process thereby leading to regional expansion in another way resembling cortical folding of gyrencephalic brains (see Model Figure 38).

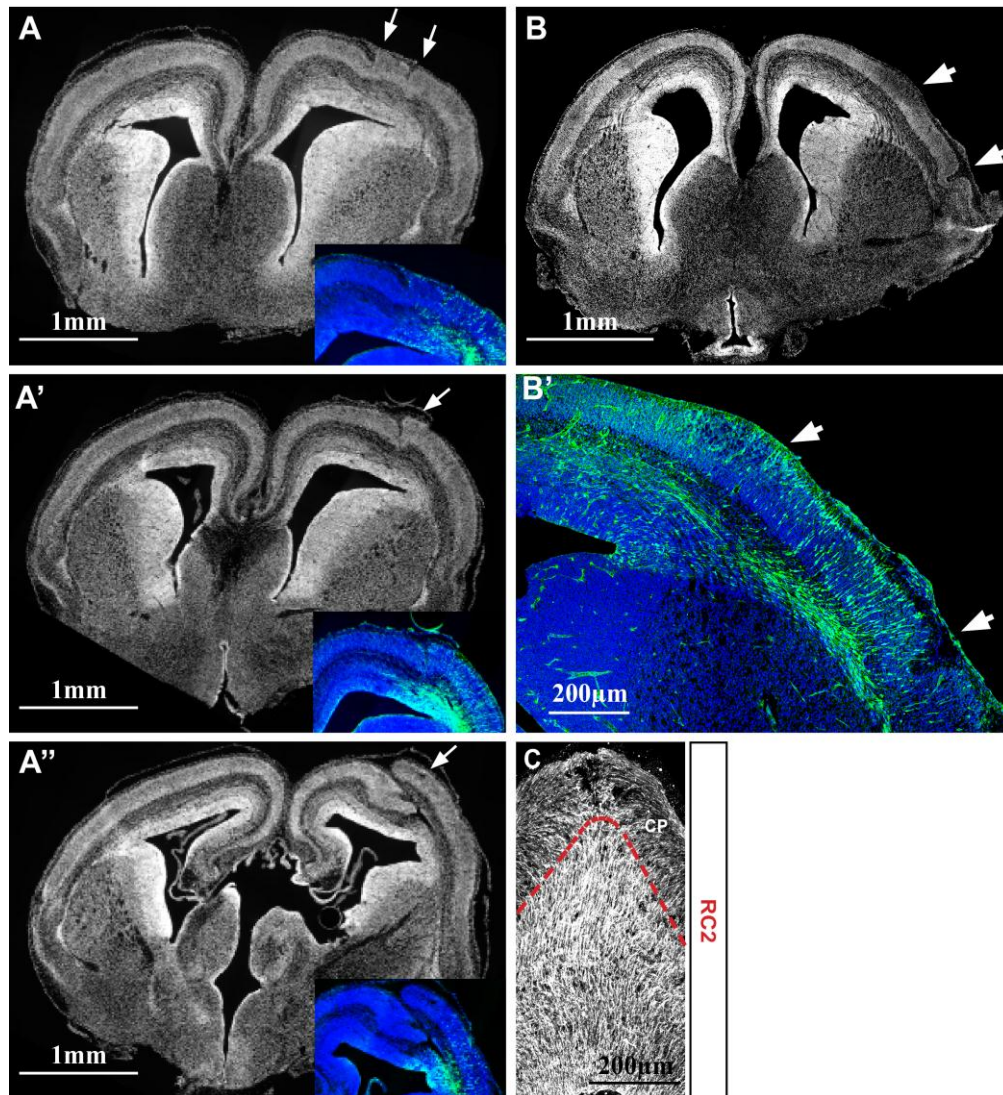


Figure 25: Loss of *Trnp1* induces folding of the murine developing neocortex

(A-A'') Series of rostral to caudal images of an example of a *Trnp1* shRNA electroporated brain. Note the folds that developed at the site of electroporation and how the folding develops from two independent folds rostrally (A) to one big fold caudally (A'-A''). (B-B') DAPI and GFP labeling of a different brain electroporated with shRNA targeting *Trnp1*. Note the radial expansion and folding of the cortex in a more lateral region (indicated by two arrows). (C) Staining of radial glial fibers (RC2) in an shRNA electroporated, radially expanded brain (image is a reconstruction out of 2 single confocal images). Note the divergence of radial fibers as they enter the cortical plate forming a fanned array. (A-B' are reconstructions of a coronal section using Zeiss or Nikon fluorescence imaging software)

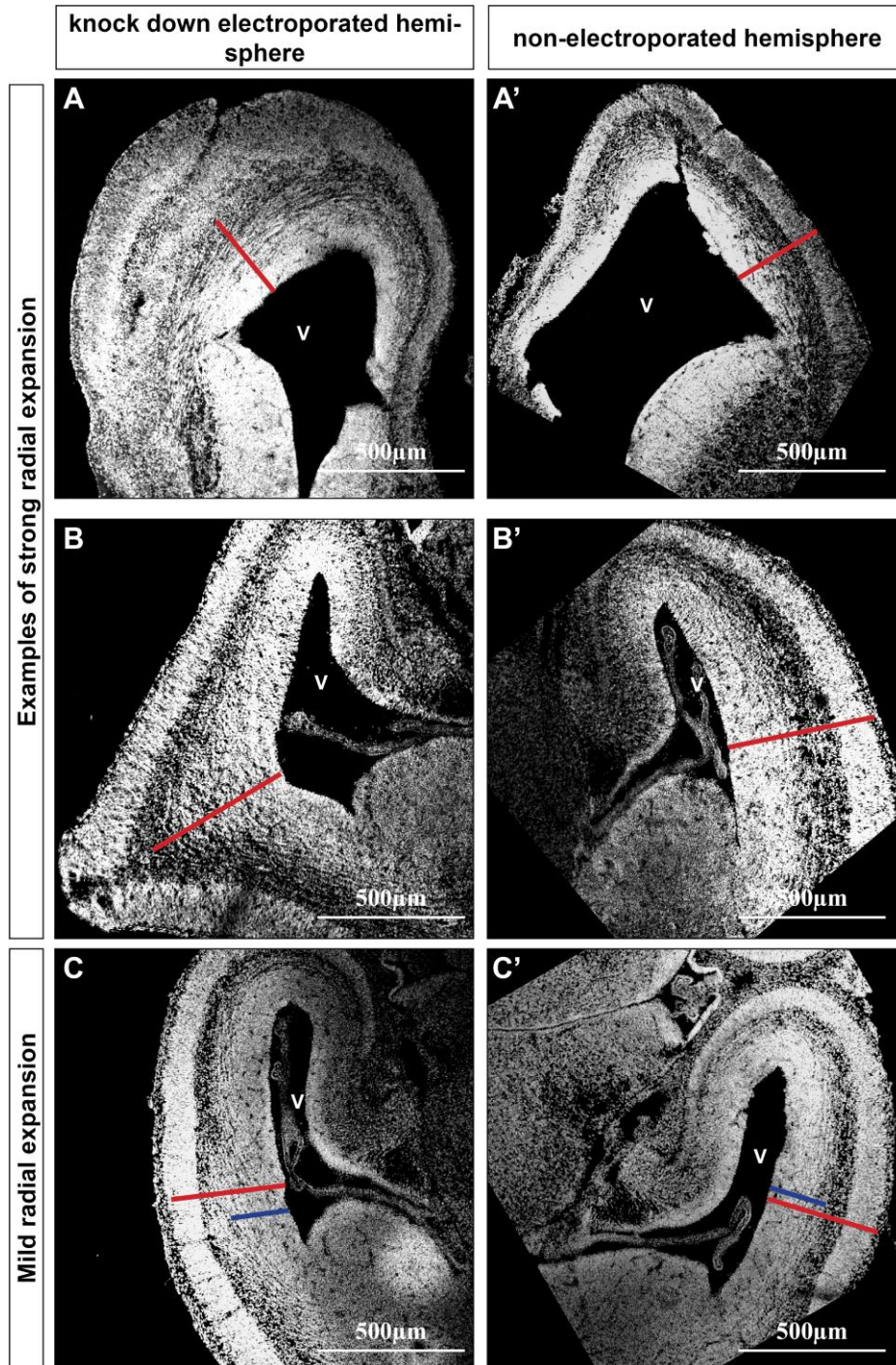


Figure 26: Different Examples of radially expanded /folded forebrains

(A-C') DAPI labeled examples of coronal sections of embryonic brains electroporated with pSUPER.GFP-shRNA to down regulate *Trnp1*. A, B and C show the electroporated hemispheres, A', B' and C' show the non-electroporated hemispheres of the same (!) sections. Red bars indicate the radial length and blue bars the ventricular zone size of the non-electroporated side. Bars are shown to compare with the size-increase of the electroporated side. Note the dramatic radial expansion in examples with strong expansion (A-B') and the milder expansion as seen in some examples (C, C'), which still show a strong increase of the DAPI dense ventricular zone (blue bars).

4.4.2.5 Rescue of *Trnp1* knock down

Utilizing one particular shRNA may additionally result in down regulation of genes other than the one targeted (such side actions are called off-target effects). However, use of another, second shRNA reduces the likelihood that both result in down regulation of the same off-targets. Therefore, to exclude possible off-target effects of the used shRNA#5, the second shRNA (shRNA#1) targeting a different region within the 3'-UTR of *Trnp1* mRNA was used for in utero electroporation. Knock down of *Trnp1* with this second shRNA resulted in similar effects as observed with shRNA#5 ultimately leading to cortical expansion. Comparable to shRNA#5 knock down of *Trnp1* through shRNA#1 increased the number of *Tbr2*⁺ basal progenitors and provoked folding of the cerebral cortex (see Figure 27A-D). However, despite an increase of the number of cells residing in the cortical plate, shRNA#1 did not reach the significance level as obtained by shRNA#5 (Figure 27C). This may possibly be due to the slightly lower knock down efficiency of shRNA#1 as compared to shRNA#5 (see Figure 21B). However, as both shRNAs led to radial expansion and increase in *Tbr2*⁺ basal progenitors, the next question was whether this effect can be rescued through expression of a knock down resistant form of *Trnp1*. As a further test of specificity, the shRNA-resistant form of *Trnp1* (lacking the targeted 3'-UTR of *Trnp1*, which was tested before for shRNA resistance – see Figure 21B') was simultaneously expressed to test its ability to preclude the increased generation of *Tbr2*⁺ basal progenitors observed upon down regulation of *Trnp1*. Consistent with a key role of *Trnp1* in regulating basal progenitor generation, co-electroporation of shRNA against endogenous *Trnp1* mRNA together with the shRNA resistant *Trnp1* cDNA was able to rescue the effect on basal progenitors to a level comparable to the control situation (Figure 27E to F). In addition, radial expansion of the cortex was precluded by simultaneous expression of the shRNA and the resistant *Trnp1* in the rescue experiment. Altogether, these data showed, that the effects of *Trnp1* knock down described in this work are specifically due to a loss of *Trnp1* function and are not a result of secondary, off target effects. Thus these results further support the previously described impact of basal progenitors and oRGs on expansion of the neocortex. Furthermore, these data suggest that

Trnp1 expression levels play a pivotal role in regulating the generation of these progenitor types.

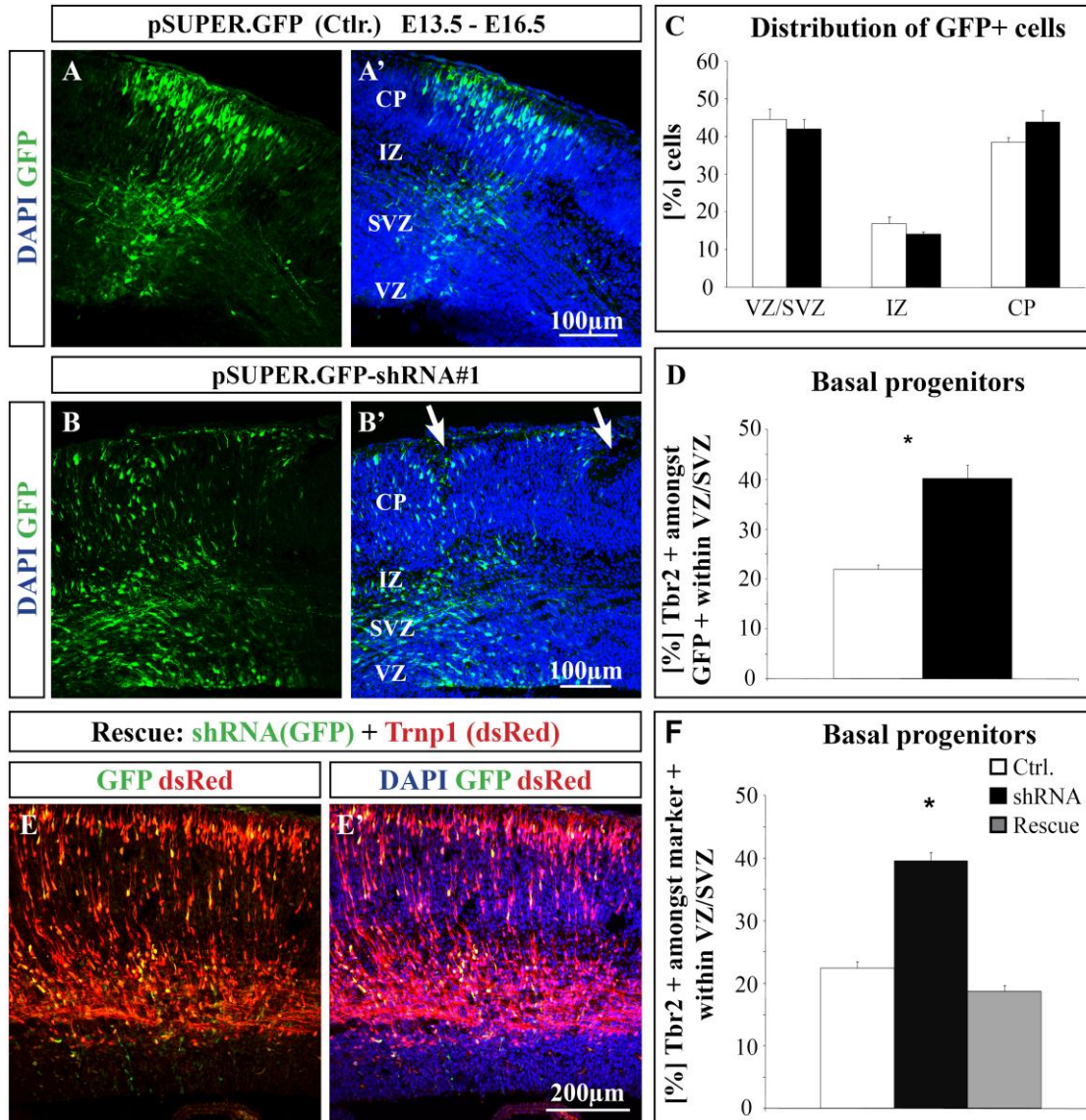


Figure 27: Confirming the specificity- and rescue of *Trnp1* knock down

(A-B'). Coronal sections of embryonic cortices labeled with GFP and DAPI. Embryos were electroporated either with pSUPER.GFP control plasmid (A-A') or pSUPER.GFP-shRNA#1 (B-B') at E13.5 and analyzed at E16.5. Distribution of cells was analyzed (C) and the number of basal progenitors was characterized using *Tbr2* immunolabeling (D). Note that use of shRNA#1 - a second, independent shRNA against *Trnp1* - resulted in a similar effect on basal progenitors with significantly more basal progenitors upon knock down of *Trnp1* in radial glia. (E-E') Rescue experiment of *Trnp1* knock down by simultaneously expressing the shRNA directed against endogenous *Trnp1* together with an shRNA resistant version of *Trnp1*. Coronal sections of embryonic cerebral cortices co-electroporated with pSUPER.GFP-shRNA#5 and pCAG-*Trnp1*($\Delta 3'$ -UTR)-dsRed labeled for GFP, dsRed and DAPI. (F) Quantification of the number of basal progenitors upon rescue as compared to control- and the knock down situation. Data are shown as mean +/- SEM; n=3 embryos for shRNA#1 and n=5 embryos for rescue experiments; *p<0.05, Mann Whitney U-Test.

4.5 Molecular analysis of Trnp1

Given the functional importance of Trnp1 during brain development described above, unraveling its molecular function is of major interest. Trnp1 localizes to the nucleus and has been proposed by Volpe et al. (2006) to bind DNA. Its highly basic biochemical characteristics with a very high (calculated) isoelectric point of 11.43 (with 32 out of 223 amino acids being positively charged – arginines (29) and lysines (3)) suggests that Trnp1 may bind to DNA due to electrostatic interactions (see Introduction: 2.4). However, Trnp1 sequence analysis did not reveal any homology to known protein motifs or domains. Therefore predictions of its molecular function were primarily not possible. In addition, its highly basic characteristics make biochemical analysis very difficult as electrostatic interactions during the experimental procedure may lead to false-positive results.

4.5.1 *Trnp1 is tightly associated with DNA*

Trnp1 was found in a highly insoluble nuclear fraction upon overexpression *in vitro* (Volpe et al., 2006) and it was suggested that Trnp1 is bound to DNA (Volpe et al., 2006). However, *in vivo* DNA binding has never been shown before. As shown in Figure 28 (A and B) endogenous Trnp1 is distributed throughout the nucleus rather homogenously in euchromatin but not detectable in heterochromatin. To analyze the localization of Trnp1 during M-phase, sections of the mouse brain at embryonic day 12 (a highly proliferative stage during brain development) were immunolabeled with Trnp1 antibody and co-labeled with DAPI. Investigation of the ventricular surface allowed analyzing the localization of the protein during chromatin condensation as radial glial cells undergo M-phase including cytokinesis at the apical surface. Remarkably, Trnp1 was tightly associated with chromatin during mitosis, co-localizing with condensed chromosomes (see Figure 28C and D). Taken together these data suggest, that during G1, G2 and S-phase Trnp1 is localized to DNA regions of active transcription but not to highly compact, silenced regions of the genome, whereas Trnp1 is associated with condensed chromosomes during M-phase. However, further investigation of the molecular function of the protein needs to be done in order to

identify the reason for this characteristic behavior. Accordingly, its exact interaction partners remained to be identified.

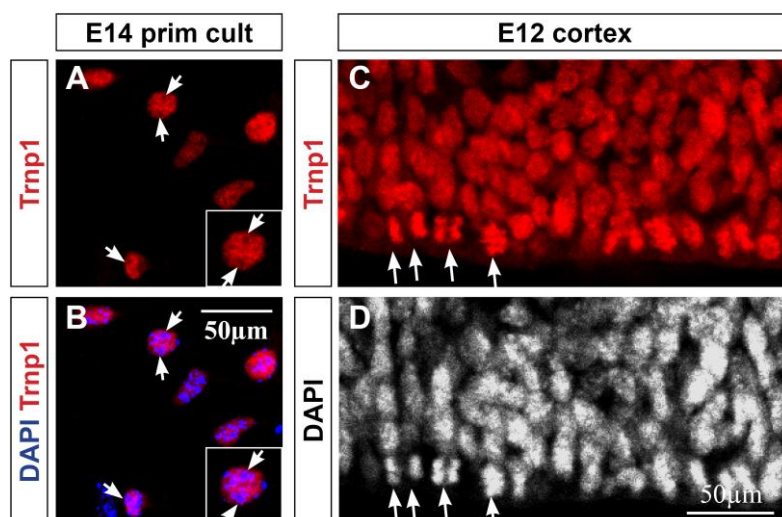


Figure 28: Trnp1 co-localizes with condensed chromatin during mitosis

(A-B) Dissociated cells from the embryonic cerebral cortex at E14 transduced with CAG-*Trnp1* virus. Immunostaining for Trnp1 and labeling for DAPI shows overexpressed Trnp1 localized in the nucleus but excluded in highly dense chromatin areas (areas of strong DAPI signal) - arrows indicate examples and one cell is shown as an example in a higher magnification. (C-D) Coronal sections of wild type E12 mouse embryos were labeled for Trnp1 and DAPI. Note the clear association of Trnp1 with condensed chromatin as seen in anaphase chromosomes indicated by arrows. Single optical confocal images are shown.

To determine possible interaction partners, first Trnp1 was examined using western blot analysis. In the adult olfactory bulb Trnp1 protein was clearly detectable and resembled the pattern seen in lysates of Trnp1 overexpressing HEK cells (Figure 29A). As immunohistochemical-staining did not reveal any Trnp1 expression in the cerebral cortex of the adult murine brain (see Figure 13), tissue from the adult cerebral cortex was used as a control. In agreement with these data, a specific Trnp1 band was only detectable in the OB but not in the cortex (Figure 29A). Surprisingly, tissue lysates from the developing cerebral cortex revealed multiple bands ranging from about 20kDa to more than 100kDa (when using regular RIPA buffer for tissue lysis) (see Figure 29B). Use of very high salt concentrations (1M NaCl) or DNase treatment improved the signal of Trnp1 from the E14 cerebral cortex (see Figure 29B). However, a clear identification of Trnp1 bands without background signals as compared to overexpression in HEK cells or compared to the adult OB was not possible using regular RIPA, high salt or DNase treatments. A characteristic

and highly reproducible pattern of bands with a wide range of molecular weight was detectable with all these lysis protocols. These bands may represent very strong complexes of Trnp1 with other proteins or may be due to protein-DNA interactions. In order to access the association of Trnp1 with DNA in a different way, E14 embryonic cortices were lysed with a different protocol to detect the endogenous protein upon acidic lysis - which is usually used for detection of very strong DNA binding proteins such as for example Histones or MeCP2 (protocol kindly provided by Dr. Raymond Poot, Erasmus MC, Rotterdam – see 6.2.3.1). Use of this acidic lysis protocol revealed Trnp1 in a highly insoluble pellet (Figure 29C). Histones released from DNA were detectable (strong background signal of the secondary antibody at 15kDa) in the soluble fraction (supernatant) upon acidic lysis showing that the lysis worked per se but was not able to solubilize Trnp1. Interestingly, Trnp1 was highly enriched in the insoluble fraction using this procedure. This shows that Trnp1 is tightly associated with DNA but is less soluble than Histones. Taken together, Trnp1 is tightly associated to DNA in stem cells during cortical development and release of the protein from an insoluble complex was very difficult. However, in the adult olfactory bulb (lacking progenitor or stem cells) release of the protein is easier and clear Trnp1 bands were observed with tissue lysis using RIPA buffer containing 0.5M NaCl. The characteristic pattern of signals seen in E14 lysates (similar to a ladder, see Figure 29B) was not visible in lysates from the OB. These data suggest a different way of association of Trnp1 with DNA and/or protein complexes in the adult OB (Trnp1 is expressed in neurons in the OB see Figure 14) as compared to the developing cortex (Trnp1 expressed in stem cells and newborn neurons see Figure 12).

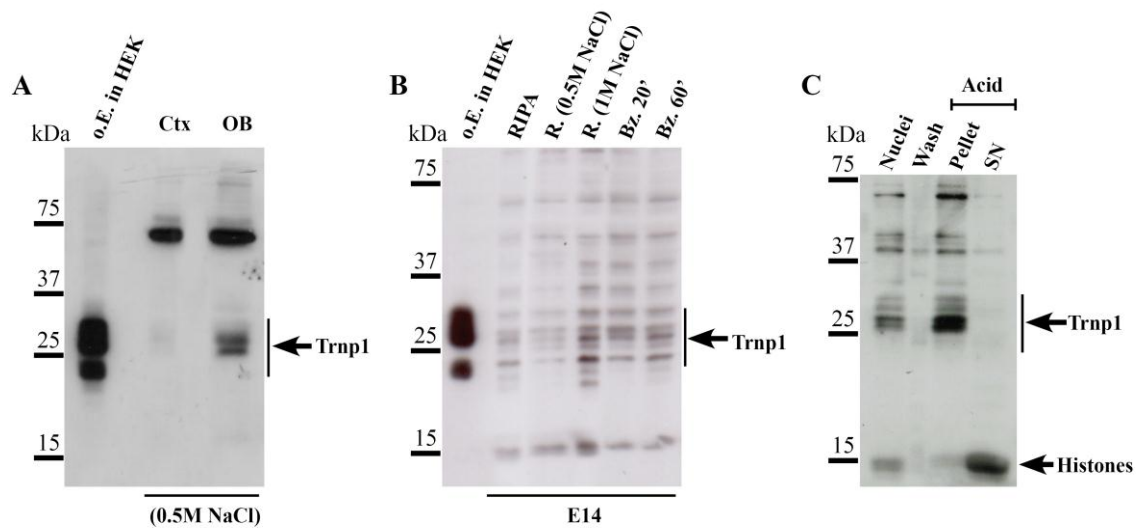


Figure 29: Endogenous Trnp1 in Western blot analysis

Tissue from the adult cerebral cortex and adult OB (A) or from the E14 cerebral cortex (B and C) was lysed using different lysis buffers and protocols. Protein lysates were subjected to SDS-PAGE and analyzed by western blotting using Trnp1 antibody. (A) Adult cerebral cortical tissue (Ctx) and adult OBs were lysed using RIPA buffer containing 0.5M NaCl. Note the clear Trnp1 signal in OB lysates but not from cortical lysates. As a positive control, lysates from HEK cells overexpressing Trnp1 was used (o.E. in HEK); (B) Cortices from E14 mouse embryos were lysed with RIPA buffer (R.) containing either 150mM NaCl, 0.5M NaCl or 1M NaCl respectively. Alternatively tissue was lysed with RIPA buffer and treated with Benzonase DNase (Bz.) for 20 or 60 minutes. (C) Nuclei from E14 cortices were isolated using HRSB buffer and acidic protein extraction. Nuclei, wash, pellet and supernatant of acidic extraction were subjected to western blot analysis using anti-Trnp1 antibody. Note that Trnp1 is mainly detectable in the insoluble fraction upon acidic treatment and that histones are detectable as a background signal of the secondary antibody in the acidic soluble fraction (SN). SN: supernatant.

4.5.2 Bioinformatic analysis of Trnp1 structure

Search for homology revealed no similarity of Trnp1 with any known motif or domain. The only distinguishable features are a proline rich region (P²⁰-P⁵⁴) and a glycine alanine rich region (G⁷²-G⁹⁴) (see also Introduction - 2.4). As endogenous Trnp1 was found to bind to DNA, crystallography of the protein would give further insights into its mode of interaction with DNA. For this purpose, in collaboration with the group of Prof. Dr. Patrick Cramer a first bioinformatical analysis of Trnp1 was carried out. In this context the Bioinformatic toolkit available online (<http://toolkit.tuebingen.mpg.de>) was used to further analyze the probability of characteristic secondary structure of the protein. The murine protein sequence of Trnp1 was used for bioinformatical analysis of native disordered regions (Figure 30A and B), analysis of regions of coiled coil structures (Figure 30C) and for PSIPRED analysis (a structure prediction method that incorporates two feed-forward

neural networks to perform an analysis of results obtained by the PSI-Blast homology search algorithm) (Figure 30D). Predictions of the secondary structure of Trnp1 revealed highly unstructured N- and C-terminal regions whereas the central part of the protein has a very high probability to form either one large helix stretch or multiple shorter helices that may then form a coiled coil structure (see Figure 30). These results finally dismissed seeking for crystallography of Trnp1 as it is impossible to analyze unstructured regions using this method. However, this analysis revealed characteristics of the Trnp1 protein structure: highly unstructured N- and C-terminal ends with a very structured central part.

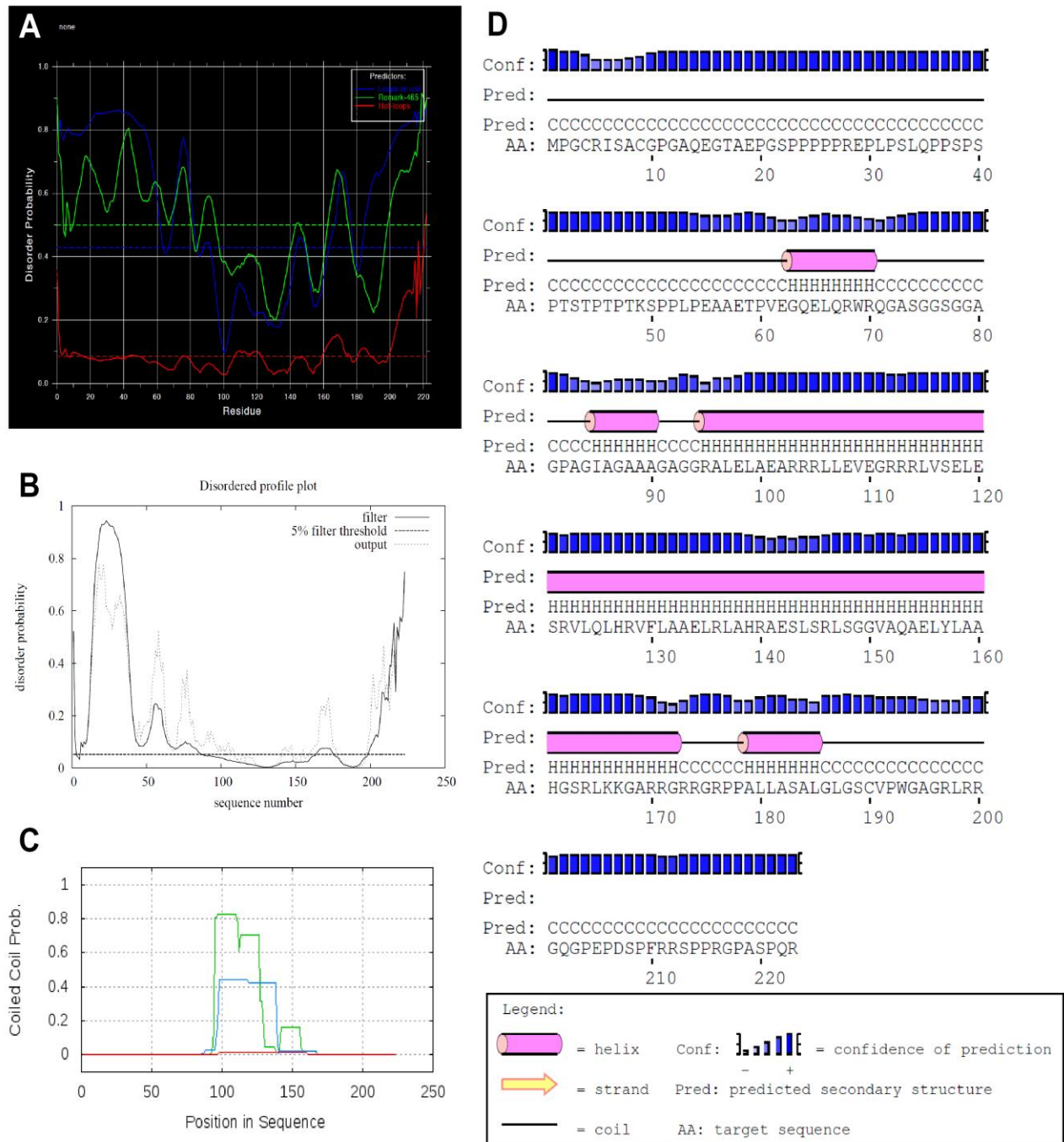


Figure 30: Bioinformatic analysis of the Trnp1 protein structure

(A-B) Disorder analysis of the Trnp1 protein structure. Values range from 0 to 1, 1 represents the highest value of disorder, 0 stands for highly ordered protein regions. (A) DisEMBL analysis of Trnp1 - protein disorder prediction based on neural networks. DisEMBL Predicts propensity for loops, hot loops and disordered regions. (B) DISOPRED analysis for protein disorder prediction. (C) PCoils analysis of the probability to adopt a coiled-coil structure. 1 represents the highest likelihood, 0 the lowermost likelihood to adopt a coiled coil structure. (D) PSIPRED analysis of the secondary structure of Trnp1. Analysis was carried out using “Bioinformatics toolkit” from the Max Planck Institute of Developmental Biology Tübingen. For details see: <http://toolkit.tuebingen.mpg.de>

4.5.3 Mass Spectrometry analysis to uncover direct binding partners of Trnp1

To find direct interaction partners of one protein of interest co-immunoprecipitation with subsequent mass spectrometry is a commonly used approach. For this purpose, the molecule of interest needs to be precipitated under mild conditions using an antibody raised against it. Every protein that is bound to the protein of interest will be co-immunoprecipitated and can be subsequently analyzed and identified through mass spectrometry.

In general to test for successful immunoprecipitation of a given protein two antibodies that were raised in different species against the same protein are used. With the first antibody the protein is being precipitated, the second antibody is then used for western blotting to test for enrichment of the protein. Unfortunately in the case of Trnp1 both generated antibodies were raised in guinea pig. As Trnp1 has a molecular weight of about 30kDa (correlating with the size of the light chains of immunoglobulins) test of successful immunoprecipitation was difficult. The light chain of the antibody used for immunoprecipitation would always be detected by the secondary (anti guinea pig) antibody used to detect Trnp1 in western blot analysis. In addition, the pattern observed in western blotting revealed several additional bands for Trnp1 – either due to strong complexes of Trnp1 or simply due to unspecific reactions of the antibody. Altogether these observations triggered the aim of a clean immunoprecipitation using a fusion protein of Trnp1 with commercially available antibodies. In this context the previously used Trnp1-GFP fusion construct was utilized to overexpress Trnp1 *in vitro* and precipitate the fusion construct together with its interaction partners.

Therefore, Trnp1-GFP was expressed in HEK cells, cells were lysed and pull down was performed using GFP-Trap®_A (ChromoTek) according to the manufacturer's protocol. Efficiency of the pull down was tested using western blotting (Figure 31). Co-precipitated samples were separated on coomassie gels and the different bands were excised and submitted for mass spectrometry analysis. However, using three independent biological replicates no protein was found to reproducibly interact with the Trnp1-GFP fusion construct (see Appendix 7.1). This may be due to the use of HEK cells, which do not express Trnp1 endogenously. Therefore, endogenous interaction partners may simply be

not expressed in HEK cells. Or, alternatively due to the use of a fusion protein of Trnp1 that may represent a non-functional version of Trnp1. To test this possibility I later transfected HEK cells with the Trnp1-GFP fusion construct and examined its ability to still interact with DNA (see 4.5.5).

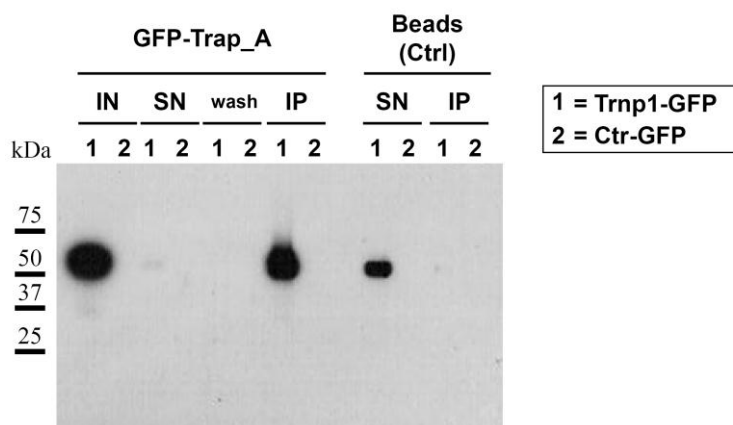


Figure 31: Pull down of Trnp1-GFP using GFP-Trap®_A

In order to test for specificity and efficiency of the pull down of Trnp1-GFP fusion construct by GFP-Trap®_A (Chromotek) the input (IN), supernatant (SN), wash and pull down (IP) was tested by western blotting using the anti-Trnp1 antibody. Note the high efficiency of the pull down with almost no residual protein left in the supernatant and wash after pull down. Using beads only (without the GFP trap coupled to them) as a control tested the specificity of the GFP-trap_A pull down.

4.5.4 FRAP experiment for Trnp1

Trnp1 was found to be tightly associated with condensed chromosomes during mitosis. One possibility to test the immobility of the protein due to its association to DNA was the use of Fluorescence Recovery After Photo bleaching (FRAP). FRAP is used to measure the speed of diffusion of a protein of interest which correlates with its mobility. The protein is fused to a fluorescent protein such as GFP. The fusion protein is then expressed *in vitro* and the fluorescing signal is being bleached using a short laser pulse. The time of recovery is then recorded and a correlation between the speed of signal recovery and immobility/mobility of the protein can be visualized. Fast recovery kinetics upon bleaching correlate with a high mobility of the protein. In case of a tightly associated protein lateral diffusion and fluorescence recovery is very difficult, as only few free molecules are

available to replace the bleached ones. Proteins tightly bound to cell compartments are therefore immobile and the signal will recover slowly as compared to such that are freely available or loosely attached and mobile (Schermelleh et al., 2005). All FRAP experiments in this study were carried out in the laboratory of Professor Dr. Heinrich Leonhardt with the help of Katrin Schneider. C2C12 or HeLa cells and alternatively also murine primary cortical cultures of embryonic day 14 were transfected with peGFP-Trnp1. FRAP experiments were then performed 48h later. Trnp1-GFP molecules were bleached in a small strip spanning half of the nucleus with 100% laser intensity and recovery was recorded with 20% laser intensity. Nuclei were imaged for 5 seconds before and 60 seconds after bleaching. Trnp1-GFP showed fast recovery of fluorescence with about 80% of signal recovery within 10 seconds after bleaching (Figure 32A). Compared to that, the vast majority of tightly DNA associated molecules such as Histones, DNA methyl transferases or other known DNA binding molecules is long term immobilized and exhibits little recovery after bleaching (Kanda et al., 1998; Kimura and Cook, 2001; Schermelleh et al., 2005; van den Boom et al., 2007). However, Trnp1-GFP showed slower recovery as compared to the GFP control. This may be due to the size differences in GFP only versus Trnp1-GFP (about twice as big as GFP) that also influence the speed of diffusion. As Trnp1-GFP showed such fast kinetics, the association of Trnp1-GFP with DNA was tested in time-lapse analysis. Live, time lapse analysis of Trnp1-GFP fusion protein showed a clear localization of Trnp1-GFP to the nucleus but surprisingly did not show Trnp1 localized to condensed chromosomes during M-phase (Figure 32B) as seen before *in vivo* (see Figure 28). Taken together, these data suggested that the fusion of Trnp1 with GFP may lead to conformational changes ultimately abolishing the endogenous function of the protein. Trnp1-GFP fusion protein therefore needed to be further tested for its DNA binding ability compared to full length Trnp1.

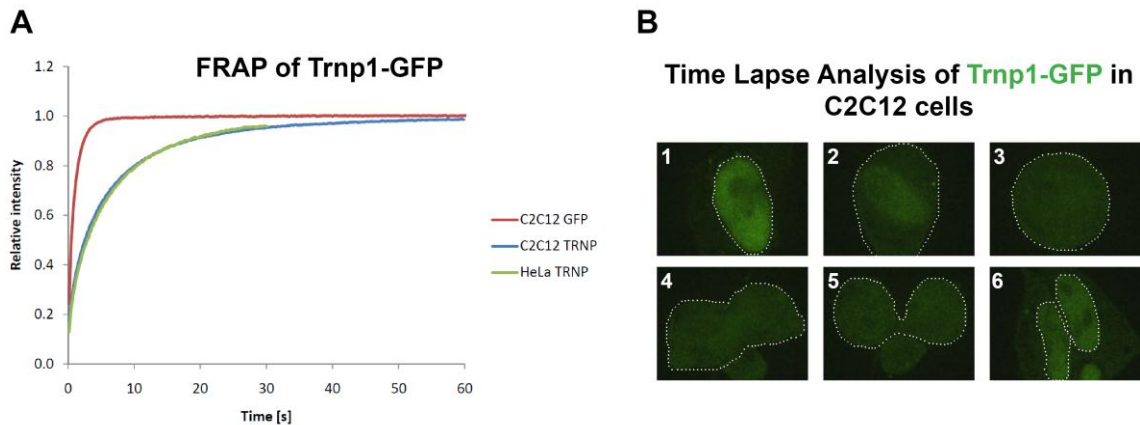


Figure 32: FRAP analysis of Trnp1-GFP fusion protein

(A) Fluorescence recovery after photo bleaching with either GFP as a control or Trnp1-GFP in C2C12 and HeLa cells. Relative intensity is shown depending on the time after bleaching. (B) Time-lapse analysis of Trnp1-GFP in C2C12 cells during the cell cycle. 1-6: subsequent time points of the same cell undergoing mitosis. Dashed lines indicate either nuclei (1 and 6) or cell bodies during mitosis. Note, that Trnp1-GFP is localized exclusively in the nucleus and dissolves completely in the whole cell body during M-phase (note that not clear association of Trnp1-GFP with DNA is visible).

4.5.5 C-terminal fusion of GFP to Trnp1 inhibits its DNA binding ability

Both the FRAP experiment and the Mass Spectrometry experiments revealed very unexpected results and time lapse imaging indicated that Trnp1-GFP fusion protein did not localize to chromosomes during M-phase anymore. Therefore, the next question was whether this was due to a non-functional GFP-Trnp1 fusion protein. In this context the C-terminal fusion of GFP to Trnp1 might inhibit its interaction with DNA or Trnp1-GFP was not able to bind its regular partners anymore (and one may be the consequence of the other). For a protein that is co-localizing with condensed chromosomes in anaphase one would expect very slow recovery kinetics in FRAP experiments. However the experiments with the Trnp1 fusion construct revealed fast kinetics indicating, that the fusion construct did not interact with the DNA in the same way as the endogenous protein did. To test this possibility with a higher sensitivity as compared to the previously performed live imaging immunocytochemistry was used. The co-localization of the fusion protein with DNA was compared to that of the endogenous, full-length protein (Figure 33A to A'' and B to B''). Consistent with the live imaging data, Trnp1-GFP fusion protein did not co-localize with

condensed chromosomes during M-phase anymore. The fusion protein clearly detached from DNA and was separated from condensed chromosomes identified by PH3 immunostaining and DAPI labeling (Figure 33C to C''). This result shows that Trnp1 association with DNA is abolished by C-terminal fusion of GFP and explains the fast kinetics found in FRAP experiments but may also be an explanation why no consistent interaction partners were found in mass spectrometry analysis. It is conceivable that Trnp1-GFP shows conformational changes and therefore does also no longer interact with the regular partners of Trnp1.

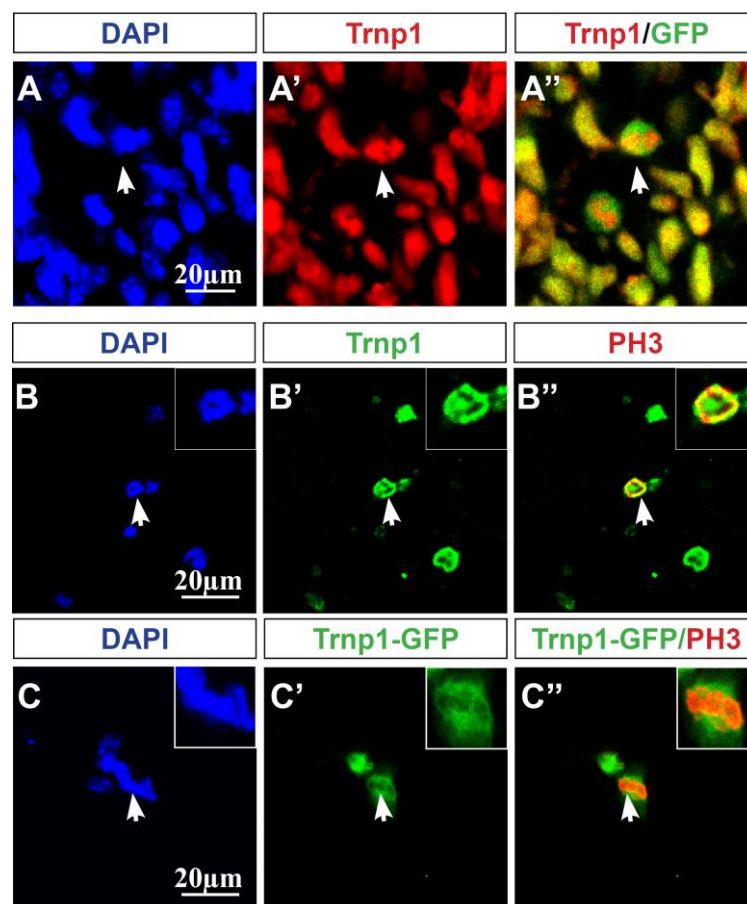


Figure 33: Trnp1-GFP fusion protein behaves differently as compared to the full-length protein

(A-A'') Example of endogenous Trnp1 expression and localization in the GE of an E14 murine brain. Coronal sections of a Mash1-GFP E14 brain (expressing a nuclear GFP version in Mash1 positive cells in the GE) were immunostained for Trnp1, GFP and labeled with DAPI. Arrows indicate condensed chromosomes of a cell during M-Phase. Note the clear association of Trnp1 with condensed chromosomes during anaphase. (B-C'') E14 primary culture either stained for endogenous Trnp1 and phosphohistone 3 (PH3) (B-B'') or transfected with a construct to express the Trnp1-GFP fusion protein stained for GFP and PH3 (C-C''). Cells were fixed three days post transfection, stained and co-labeled with DAPI. Arrows indicate an example of a cell during mitosis and intersects show a higher magnification of the same cell. Single optical sections are shown. Note the clear dissociation of Trnp1-GFP from condensed chromatin during M-Phase.

4.5.6 Analysis of direct regulation of gene expression through *Trnp1*

The tight association of *Trnp1* with DNA implicated a possible role in gene regulation. Furthermore, *Trnp1* overexpression and down regulation showed a strong effect on radial glial cell fate as analyzed by the radial glia and basal progenitor specific transcription factors Pax6 and *Tbr2*. One possible explanation would be that *Trnp1* may directly regulate expression of genes such as Pax6 target genes or of the basal progenitor TF *Tbr2*. Overexpression of *Trnp1* increased the number of Pax6 positive radial glia in the developing cortex. To elucidate a possible direct transcriptional activation of Pax6 target genes through *Trnp1*, a luciferase reporter assay in P19 cells was utilized. The pGL3-based promoter plasmids containing the Pax6 consensus binding site P6CON (binding site of the Pax6 paired domain) together with the retroviral *Trnp1* expression plasmid pCAG-*Trnp1*-IRES-GFP were used either alone or in combination with Pax6 to elucidate a possible activating function of *Trnp1* (i.e. a function as co-factor) on Pax6 target gene regulation. As a positive control Pax6 alone was used (Figure 34). However, no effect of *Trnp1* on activation of the P6CON promoter was observed, neither alone, nor in combination with Pax6.

On the other hand, *Trnp1* overexpression reduced the number of *Tbr2*⁺ basal progenitors, hence another possible scenario was that *Trnp1* acts as a transcriptional repressor of *Tbr2*. Therefore, the effect of *Trnp1* on *Tbr2* expression activated through Pax6 (a known *Tbr2* transcriptional activator (Sansom et al., 2009)) was tested in P19 cells. Cells were co transfected with the pGL3-based promoter plasmid containing the *Tbr2* promoter and the retroviral *Trnp1* expression construct pCAG-*Trnp1*-IRES-GFP in combination with a Pax6 expression construct. As a positive control Pax6 expression alone was used (Figure 34). While Pax6 alone activated the *Tbr2* promoter as previously described (Pinto et al., 2009), no repression of *Tbr2* activation was observed after co-expression of *Trnp1*. Taken together these data could not show any direct gene regulatory function of *Trnp1* on these promoters. However, the luciferase reporter assay may not contain the *Trnp1* binding sites and hence direct gene regulation through *Trnp1* may still occur for these or other target genes *in vivo*.

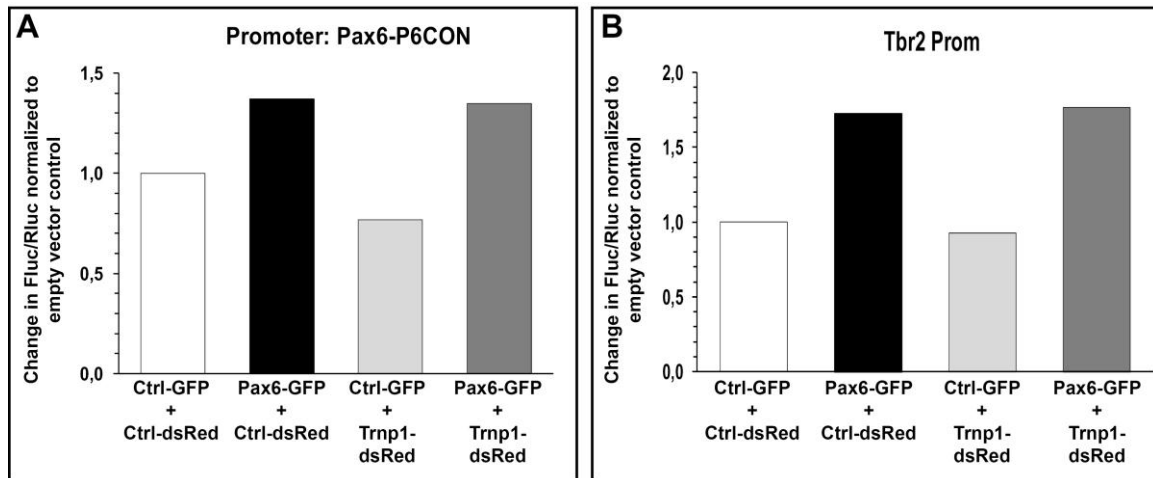


Figure 34: Luciferase Assays of Trnp1 on P6CON and Tbr2 promoter

(A-B) Histograms depicting the transcriptional activation of the Pax6 consensus site P6CON (A) and the Tbr2 promoter (B) through Pax6 alone, Trnp1 alone or both Pax6 and Trnp1 together. Transactivation was measured by reporter gene activation in luciferase assay in P19 cells. Absolute values were normalized to vector controls. Data are shown as mean values of different wells of one experiment.

4.5.7 Gene Expression analysis of gain and loss of Trnp1

In order to analyze the genes that are directly or indirectly regulated by overexpression or knock down of Trnp1, gene expression analysis after in utero electroporation was performed. For this purpose, embryos were electroporated at E13 with either pCAG-Trnp1-GFP (for forced expression of Trnp1), pSUPER.GFP-shRNA (for knock down of endogenous Trnp1) or pCAG-GFP control plasmid. Cerebral cortices were then dissected 22-24 hours post electroporation and GFP positive cells were separated from non-electroporated cells through fluorescence activated cell sorting (FACS) (Figure 35). As a control non-electroporated cortices were used to set the gates for forward- and sideward scatter (to select relevant and living cells and exclude debris), the gates for FSC-A and FSC-W (to exclude cellular aggregates such as doublets) and to set the gates for GFP sorting. RNA was immediately extracted from sorted cells and cDNA was produced for Microarray analysis. cDNA was hybridized on Affymetrix Gene ST 1.0 arrays (containing about 28.000 probe sets) and gene expression differences between GFP control, Trnp1 overexpression and knock down electroporated cells were determined. Genewise testing for differential expression was done employing the limma *t*-test and Benjamini-Hochberg multiple testing correction. Datasets were filtered for average expression levels > 50 in at

Results

least one group (overexpression, knock down or control) and for a linear ratio difference of > 1.5-fold between control and overexpression or control and knock down. To verify successful overexpression and knock down of *Trnp1* and as a first test of the performed microarray, the expression levels of *Trnp1* in the different probes were analyzed. Exon level analysis with two different probe sets (one in the non-coding exon 2 and one in the protein coding exon 1) were used and showed differences in *Trnp1* levels for control versus overexpression or knock down probes.

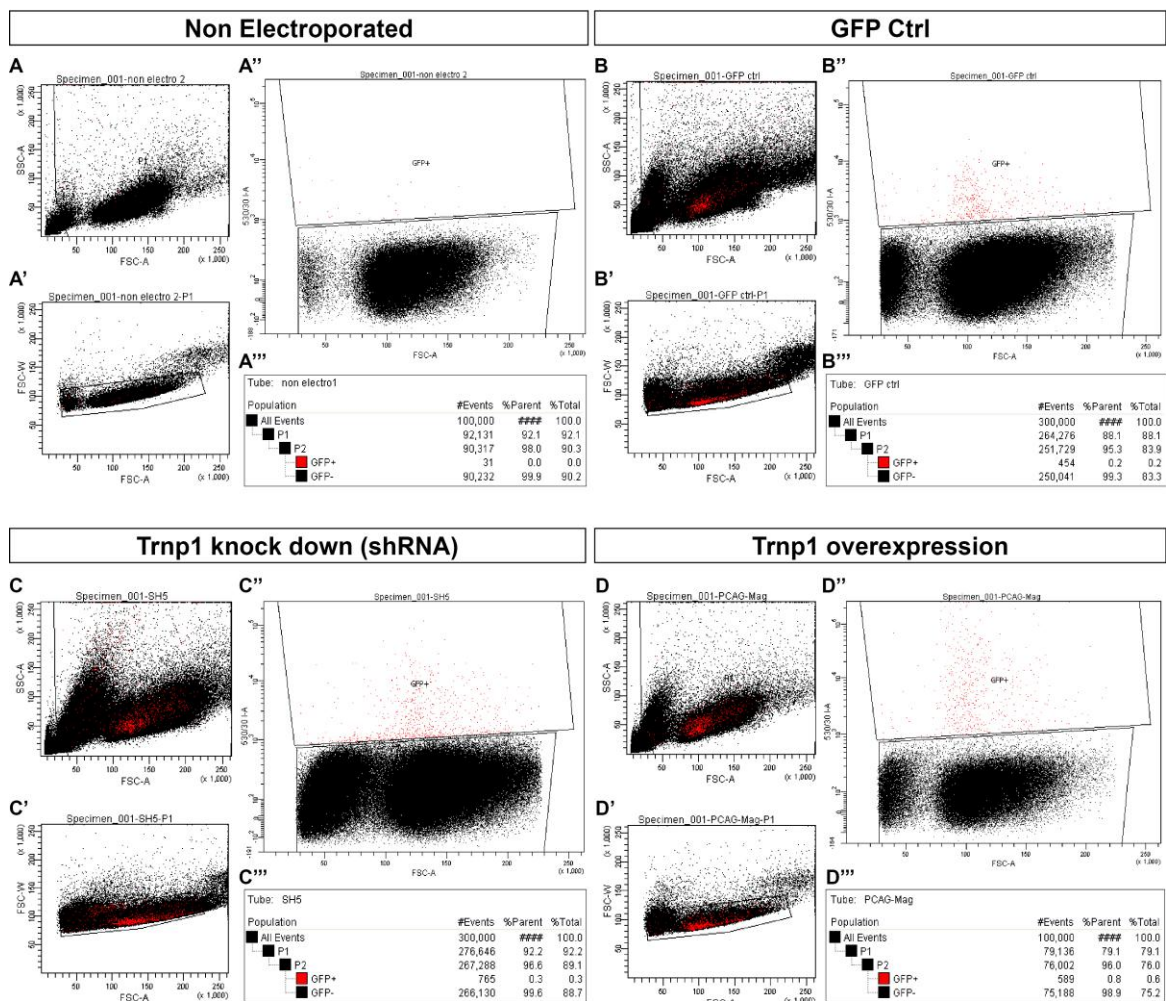


Figure 35: Sorting of GFP positive cells after in utero electroporation

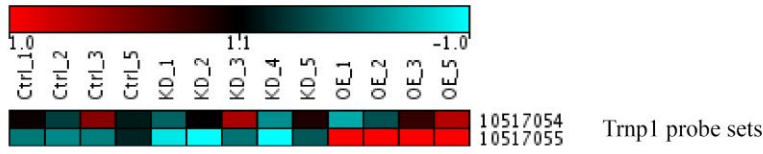
Cortices electroporated at E13 with either pCAG-GFP control plasmid (B-B'''), pSUPER.GFP/Neo-shRNA#5 for knock down of *Trnp1* (C-C''') or pCAG-*Trnp1*-GFP for *Trnp1* overexpression (D-D''') were dissected one day later at E14 and FACS sorted. As a control and to set the gates, dissociated cells from non-electroporated cortices were used (A-A'''). (A, B, C and D) Relevant and living cells were selected by setting forward (FSC-A) and sideward scatter (SSC-A). (A', B', C' and D') Cellular aggregates were excluded based on FSC-A and FSC-W. (A'', B'', C'' and D'') Gates for GFP sorting. (A''', B''', C''' and D''') Analysis of cell numbers and percentage of the sorted cells in the different gates. Graphs represent 100.000 (A and D) or 300.000 sorted cells (B and C). Red dots indicate GFP positive cells.

As overexpression was performed with a plasmid lacking the non-coding 3'-UTR of *Trnp1* detected by probe-set#1 (10517054: within the non-coding exon 2) this probe-set showed expectedly almost no differences in *Trnp1* expression versus control. Probe set#2 (10517055: within the protein coding exon 1) revealed strong differences in *Trnp1* levels with strong up-regulation in all four biological replicates of *Trnp1* overexpression compared to control (Figure 36 A). Additionally, both probe-set#1 and probe-set#2 showed successful down regulation of *Trnp1* mRNA in three of five biological replicates of shRNA electroporated *Trnp1* knock down. The other two probes (KD_3 and KD_5) showed only slight down regulation as compared to control and were therefore not used for subsequent gene expression analysis. Thus, four probes of *Trnp1* overexpression, three probes of *Trnp1* knock down and four probes of control GFP electroporation were used for transcriptome analysis.

In total 152 genes were found differentially expressed upon *Trnp1* down-regulation as compared to control probes (all meeting the criteria of an average expression > 50 , a p-value < 0.01 and fold changes of > 1.5) (Figure 36B; for a detailed table of genes and expression levels see Appendix 7.2.1). Upon overexpression of *Trnp1* 31 genes were found differentially expressed using the same criteria ($p < 0.01$, average expression > 50 and fold changes of > 1.5) (Figure 36C; for detailed list of the genes and their expression levels see Appendix 7.2.2). The genes with the strongest differences upon *Trnp1* overexpression were genes that are endogenously only expressed in the ventral part of the developing telencephalon such as *Dlx1*, *Dlx2*, *Dlx5*, *Dlx6*, *Gsx2* (5 out of the top 9 genes up regulated upon *Trnp1* overexpression). As progenitor cells in the ganglionic eminence show a stronger proliferative behaviour, the expression of these genes may correlate with the increased proliferative activity of radial glial cells observed upon overexpression of *Trnp1* in the cortex. Remarkably, genes differentially regulated upon loss of *Trnp1* function comprised bHLH transcription factors known to play a role in neural differentiation such as *Neurod1*, -2 and -6 but also several chromatin-remodelling factors such as *Chd7*, *Smarca5*, *Bmi1* and different histone variants. The reliability of the transcriptome analysis was confirmed by qPCR (Figure 36D).

Results

A

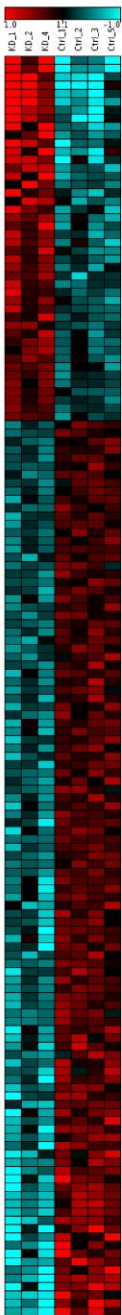


B

**KD (shRNA) -left 3 lanes
vs.
Ctrl (right 4 lanes)**

152 probe sets with raw p-values < 0.01 and ratios > 1.5x and average expression in at least one group > 50

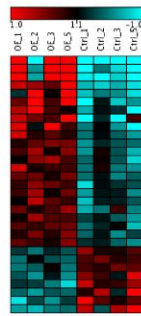
The gene with the highest significant change was *Neurod1*



C

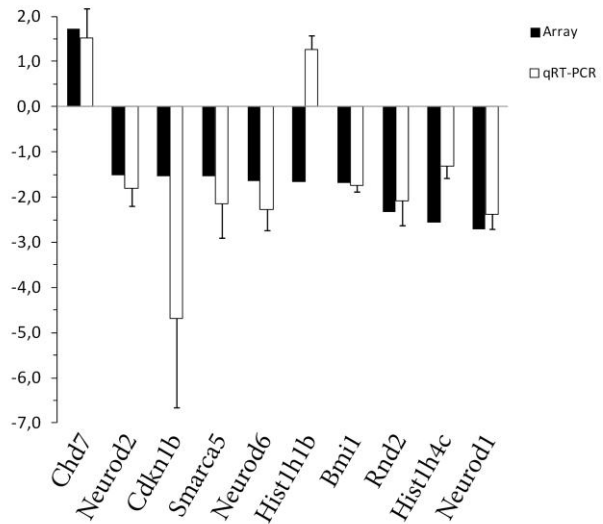
**Trnp1 o.E. -left 4 lanes
vs.
Ctrl (right 4 lanes)**

31 probe sets with raw p < 0.01 and ratio > 1.5x and average expression in at least one group > 50



D

qPCR validation of Microarray data shRNA



Genomatix GO term analysis showed that most of the differentially expressed genes upon knock down or overexpression of *Trnp1* are known to be directly or indirectly involved in transcriptional regulation (DNA binding, transcriptional repression or -activation, RNA metabolic processes, regulation of gene expression etc.) (Figure 37). Additionally, overall expression differences upon knock down contained more down regulated genes than such that were up regulated, whereas overexpression of *Trnp1* resulted in more up regulated genes than such that were down regulated (compare Figure 36B to C). Taken together these data suggest, that *Trnp1* is involved in gene regulation and, more specifically acts directly or indirectly in transcriptional activation. This is in agreement with the co-localisation of *Trnp1* with euchromatin (see Figure 28A and B).

Figure 36: Microarray Data

Transcriptome analysis of differentially expressed genes upon knock down and overexpression of *Trnp1* in the developing telencephalon. (A) Analysis of *Trnp1*-mRNA levels of knock down (KD), overexpression (OE) or control (Ctrl). Two different probe-sets were used for *Trnp1* expression analysis (10517054 within the 3'-UTR of *Trnp1* and 10517055 within the coding region of *Trnp1*). Note that as overexpression was performed with a construct lacking the 3'-UTR, only probe-set 10517055 can reliably be used for analysis of *Trnp1* levels. (B) Heatmap showing 152 genes differentially expressed upon *Trnp1* knock down as compared to control electroporated cells. Genes have an average expression > 50, p-value <0.01 and fold changes of >1.5. (C) Heatmaps showing 31 genes differentially expressed in *Trnp1* overexpression versus control. (C) Differentially expressed genes of *Trnp1* overexpression with p<0.01, average expression > 50 and ratio differences >1.5. Red indicates higher expression levels, green indicates lower expression levels. Genes are shown from up regulated (up) to down regulated. Note that more genes are overall down regulated upon *Trnp1* knock down and more are up regulated upon *Trnp1* overexpression. (D) qPCR analysis of several genes confirmed the validity of the shRNA microarray.

Results

A

Enriched GO terms knock down vs. Ctrl

GO-Term	P-value	# Genes (observed)	List of observed genes
DNA binding	3.75E-04	28	Nhlh1, Hist3h2a, Smarca5, Csd2, Neurod1, Nfe2l3, Nkrf, Irf5, Sap30, Neurod2, Rora, Hist1h2bm, Zfp422, Zfp518b, Zfp238, Chd7, Gtf2b, Atf2, Zbtb42, E4f1, Zfp639, Neurod6, Zfp30, Hist1h1b, Mef2d, Foxk2, Dedd2, Arrb1
transcription repressor activity	1.05E-03	9	Nkrf, Meg3, Zfp238, Zbtb42, Zfp639, Bhlhe22, Bmi1, Atxn1, Foxk2
gene expression	2.21E-05	50	Caprin2, Brms1, Nhlh1, Cdkn1b, Smarca5, Csd2, Neurod1, Nfe2l3, Ptdcd2, Mapk8, Zcchc12, Cdc101, Nkrf, Irf5, Pten, Sap30, Neurod2, Cbx8, Rora, Zfp422, Rrm3, Zfp518b, Zfp238, Ccnk, Chd7, Gtf2b, Atf2, Zbtb42, E4f1, Zfp639, Zfp27, Neurod6, 2810006K23Rik, Ecsit, Bhlhe22, Chmp1a, Bmi1, Zfp30, Lmo3, Mki2, Atxn1, Mef2d, Sf3b4, Tceal1, Pkia, Foxk2, Trnc6b, Ccdc8c, Dedd2, Arrb1
RNA metabolic process	5.17E-07	49	Caprin2, Brms1, Nhlh1, Cdkn1b, Smarca5, Csd2, Neurod1, Nfe2l3, Ptdcd2, Mapk8, Zcchc12, Cdc101, Nkrf, Irf5, Pten, Sap30, Neurod2, Cbx8, Rora, Zfp422, Rrm3, Zfp518b, Meg3, Zfp238, Ccnk, Chd7, Gtf2b, Atf2, Zbtb42, E4f1, Zfp639, Zfp27, Neurod6, Ecsit, Bhlhe22, Chmp1a, Bmi1, Zfp30, Lmo3, Mki2, Atxn1, Mef2d, Tceal1, Pkia, Foxk2, Trnc6b, Ccdc8c, Dedd2, Arrb1
regulation of gene expression	6.18E-08	48	Caprin2, Brms1, Nhlh1, Cdkn1b, Smarca5, Csd2, Neurod1, Nfe2l3, Ptdcd2, Mapk8, Zcchc12, Cdc101, Nkrf, Irf5, Pten, Sap30, Neurod2, Cbx8, Rora, Zfp422, Rrm3, Zfp518b, Zfp238, Ccnk, Chd7, Gtf2b, Atf2, Zbtb42, E4f1, Zfp639, Zfp27, Neurod6, Ecsit, Bhlhe22, Chmp1a, Bmi1, Zfp30, Lmo3, Mki2, Atxn1, Mef2d, Tceal1, Pkia, Foxk2, Trnc6b, Ccdc8c, Dedd2, Arrb1
regulation of transcription, DNA-dependent	1.76E-08	45	Caprin2, Brms1, Nhlh1, Cdkn1b, Smarca5, Csd2, Neurod1, Nfe2l3, Ptdcd2, Mapk8, Zcchc12, Cdc101, Nkrf, Irf5, Pten, Sap30, Neurod2, Cbx8, Rora, Zfp422, Rrm3, Zfp518b, Zfp238, Ccnk, Chd7, Gtf2b, Atf2, Zbtb42, E4f1, Zfp639, Zfp27, Neurod6, Ecsit, Bhlhe22, Chmp1a, Bmi1, Zfp30, Lmo3, Mki2, Atxn1, Mef2d, Tceal1, Pkia, Foxk2, Dedd2, Arrb1
regulation of neuron differentiation	3.14E-06	12	Caprin2, Cd24a, Neurod1, Chrb2, Pten, D0H4514, Ntn1, Bnip2, Plxna4, Robo2, Dguok, Nr1
regulation of neurogenesis	2.07E-05	12	Caprin2, Cd24a, Neurod1, Chrb2, Pten, D0H4514, Ntn1, Bnip2, Plxna4, Robo2, Dguok, Nr1
DNA packaging	8.76E-04	5	Hist3h2a, Smarca5, Hist1h2bm, Chmp1a, Hist1h1b
SEMAPHORIN	4.30E-04	5	Sema6a, Pten, Ntn1, Plxna4, Nr1
CYCLIN DEPENDENT KINASE INHIBITOR 2	2.85E-03	2	Cdkn1b, Pten
DUAL SPECIFICITY PHOSPHATASE	4.15E-03	4	Mapk8, Pten, Dusp14, Hspa1b
CYCLIN DEPENDENT KINASE	4.87E-03	8	Plk2, Cdkn1b, Cdkn22, Ccnk, Cdc37, Hist1h1b, Mef2d, Fam89b
DOPAMINE RECEPTOR	6.90E-03	3	Penk, Atxn1, Arrb1
TUMOR PROTEIN P53	9.69E-03	9	Irf5, Txnrd1, Nuak1, Hspa1a, Zmat3, Bmi1, Trp53inp1, Tceal1, Sesn1
p38 cascade (TGF-beta signaling(through TAK1))	6.86E-04	3	MAPK8, ATF2, MAP2K6
Toll-like receptor signaling pathway (through ECSIT, MEKK1, MKKs, JNK cascade) (Toll-like receptor signaling pathway (through ECSIT, MEKK1, MKKs, JNK cascade))	9.15E-04	3	ECSIT, MAPK8, MAP2K6
regulation of target gene expression by AP-1 (Toll-like receptor signaling pathway (through ECSIT, MEKK1, MKKs, p38 cascade))	1.05E-03	3	ECSIT, ATF2, MAP2K6
mapkinase signaling pathway	1.44E-03	4	MAPK8, ATF2, MEF2D, MAP2K6
p38 mapk signaling pathway	2.30E-03	3	ATF2, MEF2D, MAP2K6
angiotensin ii mediated activation of jnk pathway via pyk2 dependent signaling	3.30E-03	3	MAPK8, ATF2, MEF2D
toll-like receptor pathway	3.90E-03	3	ECSIT, MAPK8, MAP2K6
signal transduction through Il1r	4.21E-03	3	ECSIT, MAPK8, MAP2K6
CXCR3-mediated signaling events	4.21E-03	3	RICTOR, MAP2K6, ARRB1
the 41bb-dependent immune response	6.72E-03	2	ATF2, MAP2K6
the information processing pathway at the ifn beta enhancer	6.88E-03	3	IRF5, ATF2, GTF2B
il12 and stat4 dependent signaling pathway in th1 development	7.71E-03	2	MAPK8, MAP2K6
BMP2 signaling pathway(through TAK1) (BMP2 signaling(through TAK1))	7.71E-03	2	ATF2, MAP2K6

B

Enriched GO terms Overexpression vs. Ctrl

GO-Term	P-value	# Genes (observed)	List of observed genes
gene expression	8.47E-06	50	Rbm15, Hnf4g, Pes1, Csd2, Pop7, Zfp287, Dlx5, Ascl1, Gspt2, Sall1, Pim1, Dlx2, Nhlh2, Thrb, Foxn3, Foxo3, Zfp329, Thrap3, AW146020, Mtpap, Plp1, Mrpl18, Bmi1, Mynn, Sfmbt1, Mrps18c, Zfp451, Zfp110, Mrpl3, Dlx6, Rg9mtd1, Rnu7, Wnt10b, Ict1, Atf1, Meox1, Gmeb2, Med7, Dlx1, Hey2, Ppp1r15b, Qrs1, Mrpl20, Kdm5c, Meis1, Srsf3, Foxk2, Pdcd7, Yeats2, Gsx2
RNA metabolic process	3.11E-05	43	Rbm15, Hnf4g, Pes1, Csd2, Pop7, Zfp287, Dlx5, Ascl1, Sall1, Pim1, Papd5, Dlx2, Nhlh2, Thrb, Foxn3, Foxo3, Zfp329, Thrap3, AW146020, Mtpap, Bmi1, Mynn, Sfmbt1, Zfp451, Zfp110, Dlx6, Rg9mtd1, Rnu7, Wnt10b, Atf1, Meox1, Gmeb2, Med7, Dlx1, Hey2, Kdm5c, Meis1, Srsf3, Foxk2, Pdcd7, Yeats2, Gsx2, Meg3
regulation of gene expression	3.12E-04	37	Rbm15, Hnf4g, Csd2, Zfp287, Dlx5, Ascl1, Sall1, Pim1, Dlx2, Nhlh2, Thrb, Foxn3, Foxo3, Zfp329, Thrap3, AW146020, Mtpap, Bmi1, Mynn, Sfmbt1, Zfp451, Zfp110, Dlx6, Wnt10b, Atf1, Meox1, Gmeb2, Med7, Dlx1, Hey2, Ppp1r15b, Kdm5c, Meis1, Foxk2, Pdcd7, Yeats2, Gsx2
transcription, DNA-dependent	7.37E-05	36	Rbm15, Hnf4g, Csd2, Zfp287, Dlx5, Ascl1, Sall1, Pim1, Dlx2, Nhlh2, Thrb, Foxn3, Foxo3, Zfp329, Thrap3, AW146020, Mtpap, Bmi1, Mynn, Sfmbt1, Zfp451, Zfp110, Dlx6, Wnt10b, Atf1, Meox1, Gmeb2, Med7, Dlx1, Hey2, Kdm5c, Meis1, Foxk2, Pdcd7, Yeats2, Gsx2
regulation of developmental process	2.78E-03	17	Rbm15, Dlx5, Ascl1, Sall1, Pvr1, Luc7l, Dlx2, Thrb, Foxo3, Bmi1, Wnt10b, Atf1, Dlx1, Hey2, Abl1, Meis1, Bnip2
neurogenesis	2.16E-03	15	Dlx5, Ascl1, Sall1, Pvr1, Dlx2, Sema6a, Plp1, Atg7, Atf1, Epha7, Dlx1, Fscn2, Meis1, Bnip2, Gsx2
regulation of gene-specific transcription	1.12E-03	10	Rbm15, Ascl1, Dlx2, Foxn3, Foxo3, Wnt10b, Dlx1, Hey2, Foxk2, Yeats2
ubiquitin ligase complex	1.99E-03	5	Bre, Bmi1, Smurf2, Ercc8, Tnfrsf1
nuclear chromosome, telomeric region	9.72E-03	2	Pot1b, Pif1
DNA binding	3.06E-06	33	Hnf4g, Akap8l, Csd2, Zbp1, Zfp287, Dlx5, Ascl1, Sall1, Pot1b, Papd5, Dlx2, Nhlh2, Thrb, Recq4, Foxn3, Foxo3, Zfp329, AW146020, Pif1, Mynn, Zfp451, Zfp110, Dlx6, Atf1, Meox1, Gmeb2, Dlx1, Hey2, Rdm1, Kdm5c, Meis1, Foxk2, Gsx2
transcription regulator activity	1.02E-05	21	Hnf4g, Zfp287, Dlx5, Ascl1, Sall1, Dlx2, Nhlh2, Thrb, Foxn3, Foxo3, Thrap3, Bmi1, Dlx6, Meox1, Med7, Dlx1, Hey2, Foxk2, Yeats2, Gsx2, Meg3
structure-specific DNA binding	2.26E-04	8	Zbp1, Ascl1, Pot1b, Thrb, Recq4, Foxn3, Foxo3, Foxk2
specific transcriptional repressor activity	7.60E-03	4	Foxn3, Foxo3, Foxk2, Yeats2
HEDGEHOG	4.05E-04	7	Dlx5, Ascl1, Plp1, Bmi1, Rab23, Meox1, Gsx2
Enriched for downregulated genes:			
CYCLIN DEPENDENT KINASE INHIBITOR 1	3.57E-03	3	Pim1, Foxo3, Bmi1
Enriched for upregulated genes:			
HEDGEHOG	2.14E-03	5	Dlx5, Ascl1, Plp1, Rab23, Gsx2
EPHRIN	9.59E-03	3	Acp1, Epha7, Abl1

Figure 37 Genomatix GO term Analysis

GO term Analysis of genes differentially expressed upon knock down (A) or overexpression of Trnp1 (B) in the developing mouse cortex. Note that most of the differentially expressed genes are directly or indirectly involved in regulation of gene expression.

5 Discussion

5.1 Expression of Trnp1 in the murine brain

In this study, the expression pattern of Trnp1 during forebrain development was elucidated. For this purpose, two antibodies targeting different regions of the protein (size of each epitope 19-20 amino acids) were generated in guinea pig. One of the two generated antibodies was able to specifically and efficiently recognize Trnp1 upon overexpression and was also able to detect the endogenous protein in the developing murine brain by immunohistochemistry. The specificity of the antibody was tested using competition experiments *in vitro* and *in vivo*. Furthermore, specificity was demonstrated by the use of shRNAs for knock down of Trnp1 (see 4.4.2.1). In agreement with the previous description of Trnp1 by Volpe et al., Trnp1 protein was detectable as multiple bands upon overexpression in HEK293 cells. In this context, Trnp1 may be posttranslationally modified such as phosphorylated. Several Bioinformatic predictions of posttranslational modifications such as KinasePhos (<http://kinasephos.mbc.nctu.edu.tw>) or ELM (<http://elm.eu.org/>) suggest that Trnp1 is target of several kinases such as CDK, MAPK, PKA, PGC or PKG. Accordingly, endogenous Trnp1 protein was also detectable as multiple bands in the developing cortex as well as in the adult olfactory bulb suggesting that post translational modifications occur endogenously and may regulate Trnp1 function *in vivo* (see Figure 29).

In this study, Trnp1 was for the first time identified in brain tissue as a nuclear protein. This observation is in agreement with Volpe et al. that showed Trnp1 localizing to the nucleus upon overexpression in immortalized cell lines. Characterization of different cell types at different developmental stages revealed that Trnp1 is expressed in the developing murine forebrain in neural stem cells but also in newborn neurons. However, supporting its initial identification in directly neurogenic radial glial cells (Pinto et al., 2008), Trnp1 is absent in most basal progenitors and localizes to a subset of radial glial cells at mid neurogenesis in the developing cortex. Trnp1 was found in all Tbr1 expressing newborn neurons at E14 indicating that Trnp1 is re-expressed in neurons derived from basal progenitors. In cortical development Trnp1 is ON (expressed) in a subset of stem cells

(radial glial cells) and their direct neuronal progeny while it is OFF (not expressed) in the subset of RG generating basal progenitors (being responsible for the expansion of neuronal output) and ON again in newborn neurons.

In contrast to its expression in the developing cortex, *Trnp1* was detectable in both apical progenitors and in Mash1 positive basal progenitors in the ventral forebrain. Accordingly, in the adult SEZ (that is developmentally derived from the ventral part of the forebrain) *Trnp1* is expressed in GFAP positive stem cells but also in transit amplifying progenitors (TAPs) labeled by a short BrdU pulse. Similar to its expression in newborn neurons in the developing forebrain, the protein is also detectable in neuroblasts and in neurons in the olfactory bulb. However whether its expression in the OB is restricted to newborn neurons remains to be elucidated. In contrast to the SEZ, *Trnp1* is not detectable in neurons of the adult cortex and is also absent in the other well-known neurogenic niche of the adult murine brain, the dentate gyrus of the hippocampus. Previous reports showed differences of the progenitors in the DG as compared to the ones in the SEZ (see Ming and Song, 2005 for a review) and such differences may explain why *Trnp1* is restricted to the SEZ/RMS/OB neurogenic niche in the adult brain. In this context it needs to be mentioned, that Volpe et al showed quantitative PCR data of *Trnp1* of different adult tissues and claimed that *Trnp1* is present in adult whole brain extracts. Importantly, the Primers used contained a very high content of GC basepairs increasing the possibility of unspecific signals. In my work mRNA levels were not analyzed, but *Trnp1* protein was not detectable utilizing immunohistochemistry or western blotting in the adult murine cortex. However, in agreement with the obtained immunohistochemical data, *Trnp1* is clearly detectable in lysates from the OB as multiple distinct bands (comparable to overexpressed *Trnp1* in HEK cells). In contrast to that, Volpe et al. provided a western blot that shows one single very weak band in whole brain extracts which seems to be likely due to background signal of the used primary or secondary antibody, especially since the multiple distinct bands observed in the OB but also upon overexpression are lacking. Alternatively *Trnp1* may be expressed at very low levels in the cortex and the antibody used in this work was not able to detect these low levels. If this would be the case, the lack of multiple posttranslational modifications in the cortex may represent differently regulated *Trnp1* protein in the cortex as compared to the OB.

The observed expression pattern strongly suggested that Trnp1 is involved in regulation of neurogenesis and in early integration of newborn neurons. Supporting this hypothesis Trnp1 was found being expressed in neural stem cells at highly neurogenic stages of murine cortical development, but at the time of gliogenesis (late embryonic stages such as E18) the protein was absent in gliogenic progenitors.

In his Master thesis that Michael Metzger performed under my supervision in our laboratory, he showed that Trnp1 is not restricted to the central nervous system (Metzger, 2011). Trnp1 was detectable in proliferating cells throughout the developing mouse embryo in different tissues such as the developing heart, the eye and the spinal cord and was found in proliferating cells labeled by PH3 (Metzger, 2011). However, in strong contrast to the previously suggested function in proliferation (Volpe et al., 2006), overexpression of Trnp1 was not able to increase the proliferation rate in HEK cells (data not shown). Remarkably, Trnp1 protein was not detectable in highly proliferating cells such as HEK, NRK and embryonic stem (ES) cell derived neurogenic progenitors (data not shown for NRK and ES cells) thereby showing that Trnp1 is not necessary for proliferation. Additionally, Trnp1 was absent in gliogenic progenitors at late embryonic stages but highly expressed in post-mitotic neurons. Altogether these data questioned the exclusive function of Trnp1 in cell proliferation and suggested that it is additionally regulating the process of differentiation of newborn neurons.

In summary, Trnp1 is found in proliferating cells of multiple tissues in the developing mouse but strikingly not in all proliferating cells. Therefore, its expression in stem cells suggested a role in fate specification. As Trnp1 is additionally also expressed in newborn neurons of the developing and adult brain an important role in differentiation seemed also likely.

5.2 The function of Trnp1 in the developing forebrain

During development, radial glia comprise neurogenic, but at later stages also gliogenic progenitors (Kriegstein and Alvarez-Buylla, 2009). In addition, some radial glial cells give rise to the neural stem cells responsible for adult neurogenesis (Merkle et al., 2004; Kriegstein and Alvarez-Buylla, 2009). Yet little is known about the molecular

determinants that regulate radial glia self-renewal and expansion of the cortex. Using a new antibody raised against Trnp1 I was able to show its expression at protein level in neurogenic niches both during development and in the adult murine brain. The expression of Trnp1 in only a subpopulation of Pax6-positive radial glial cells at mid neurogenesis together with its initial identification in directly neurogenic radial glial cells suggested a specific regulatory role of Trnp1 in neurogenesis. Functional analysis presented in this work identified Trnp1 as a novel regulator of brain development and neocortical expansion. First, to directly examine Trnp1 function a retroviral vector was constructed to overexpress Trnp1. Forced expression in dissociated primary cell cultures derived from the cerebral cortex of E14 mouse embryos resulted in increased proliferation and self-renewal of neural stem cells. This finding was further corroborated with live imaging and single cell tracking which showed an impressive increase of symmetric progenitor division and sustained neurogenesis over a longer time. In utero electroporation to overexpress Trnp1 in the developing cerebral cortex revealed a significant increase of radial glia proliferation *in vivo* supporting the *in vitro* findings. In contrast, knock down experiments using short hairpin RNA strongly increased the number of BPs and neurons after three days *in vivo*. These data show, that high levels of Trnp1 lead to self-renewal of neurogenic radial glial cells, whereas low levels promote increased production of basal progenitors and neuronal output. This result is consistent with our initial identification of Trnp1 in the radial glial subset that does not generate basal progenitors during forebrain development (Pinto et al., 2008).

During brain evolution a remarkable increase in size of the cerebral cortex has occurred especially amongst mammals. One open key question is how expansion of this brain region is regulated at the molecular level and which mechanisms distinguish larger cerebral cortices from smaller ones. Gyrification seems to have developed a long time ago as a blueprint for today's mammalian brains (Reillo et al., 2011; Borrell and Reillo, 2012; Martínez-Cerdeño et al., 2012). Some species kept the ability to form cortical folds, whereas others lost this ability (Kriegstein et al., 2006; Borrell and Reillo, 2012; Kelava et al., 2012; Martínez-Cerdeño et al., 2012). This hypothesis provokes the question what distinguished that blueprint ancestor from other species, and what factors may have been responsible for such an evolution. In this context it is very tempting to think about factors

that may have developed such a function in the mammalian lineage and are involved in these processes. *Trnp1* was initially identified in a screen for directly neurogenic radial glial cells. This sub population is suggested to give rise to neurons directly and to self renew itself through asymmetric divisions (Miyata et al., 2001; Noctor et al., 2001; Haubensak et al., 2004; Noctor et al., 2004; Pinto and Götz, 2007; Stancik et al., 2010). Acute loss of *Trnp1* not only increased the number of BPs but also led to a dramatic local radial expansion of the cortex. This is consistent with previous studies suggesting basal progenitors as the main source of increased neuronal output and expansion (Haubensak et al., 2004; Miyata et al., 2004; Noctor et al., 2004; Kriegstein et al., 2006; Pontious et al., 2008; Sessa et al., 2008; 2010; Hevner and Haydar, 2012). Besides BPs outer radial glial cells (oRGs) lacking an apical process have recently been suggested to be a prerequisite of brain expansion and folding / gyrification of the cortex (Fietz et al., 2010; Hansen et al., 2010; Lui et al., 2011; Molnár, 2011; Reillo et al., 2011). Down regulation of *Trnp1* was able to increase the number of such outer radial glial cells in the murine brain. The striking folding of the brain upon *Trnp1* knockdown strongly supported this observation and is likely a consequence of both the increase in BP and oRG numbers. In summary, loss of *Trnp1* was able to acutely reproduce several hallmarks of larger brain development: 1) strong radial expansion, 2) diverging radial fibers forming a fanned array as has been described for gyrencephalic brains (Smart and McSherry, 1986a; 1986b; Lui et al., 2011; Reillo et al., 2011), 3) increased numbers of oRGs that have been suggested to be a characteristic of larger brains (Fietz et al., 2010; Hansen et al., 2010; Reillo et al., 2011; Wang et al., 2011; Borrell and Reillo, 2012; Martínez-Cerdeño et al., 2012), 4) increased proportion of *Tbr2*⁺ basal progenitors. Additionally, a strong increase of the DAPI dense SVZ region in combination with a diffuse *Tbr2*⁺ band was found upon down regulation of *Trnp1*. These observations are indicative of an increased SVZ and somewhat reminiscent of the diffuse band of BPs present in the oSVZ of higher mammalian brains (Martínez-Cerdeño et al., 2012). Altogether, these data suggest that *Trnp1* represents a molecular switch that needs to be expressed or “ON” in progenitors in order to increase the progenitor pool and lead to a tangential (lateral) expansion. Accordingly, at the time of strong lateral expansion of forebrain development (i.e. in neuroepithelial cells) *Trnp1* is expressed in virtually all progenitors. Later, when the time for increased neuronal

production has come Trnp1 is acutely down regulated in subsets of radial glia to initiate abventricular amplification by basal progenitors and oRGs that then together increase the number of neurons and their guidance structures resulting in radial expansion (see model Figure 38). Therefore, Trnp1 controls progenitor pool expansion and subsequently neuronal expansion. In this context, the timing of Trnp1 down regulation may determine the extent of radial expansion. Acute loss of Trnp1 immediately increases neuronal output at the expense of remaining apical radial glial cells. Hence, acute loss of Trnp1 will presumably lead to an acute radial expansion. This suggests, that regulation of Trnp1 expression may be involved in radial expansion and gyrification to accommodate the additional neuron numbers in larger brains. The process of oRG generation in the murine brain is endogenously very inefficient and slow as oRGs are found only sparsely (Shitamukai et al., 2011; Wang et al., 2011). The level of Trnp1 seems to play a critical role in this process and knock down of Trnp1 released the inhibition of oRG production. The loss of apical radial glia upon Trnp1 down regulation seems to be compensated by the increase in oRG numbers that have been shown to have a higher proliferation coefficient than BPs (Lui et al., 2011).

In summary, using both clonal analysis *in vitro* and in utero electroporation *in vivo* Trnp1 was found to be a master regulator of radial glial fate. So far, Trnp1 represents the first factor identified to regulate the generation of both oRGs and BPs at the same time. In strong contrast to Volpe et al, Trnp1 was not simply increasing proliferation but it does rather represent a crucial regulator of cellular fate and neurogenesis. Additionally, Trnp1 also represents the first factor capable to generate folding in an otherwise lissencephalic brain recapitulating all the hallmarks of higher mammalian gyrencephalic brain development. In this context, it should be mentioned that a transgenic mouse line expressing a stabilized form of beta catenin has previously been reported to show folding of the neocortex (Chenn and Walsh, 2002). However, in strong contrast to the observed local expansion and folding upon Trnp1 knock down, the beta catenin induced folding did not resemble folding of higher mammalian gyrencephalic brain, but rather represents a secondary folding due to lateral expansion of the progenitor pool. Importantly, the folding observed by Chenn et al. included folding and expansion of the ventricular surface and did not fulfill characteristics of radial expansion. In contrast, down-regulation of Trnp1

resulted in a local radial expansion and folding of the cortical plate without increasing the ventricular surface thereby reflecting the situation in gyrencephalic brains. Together with the above mentioned characteristics such as the appearance of oRG cells, timed and local manipulation of *Trnp1* was able to recapitulate central features of gyrencephalic brains.

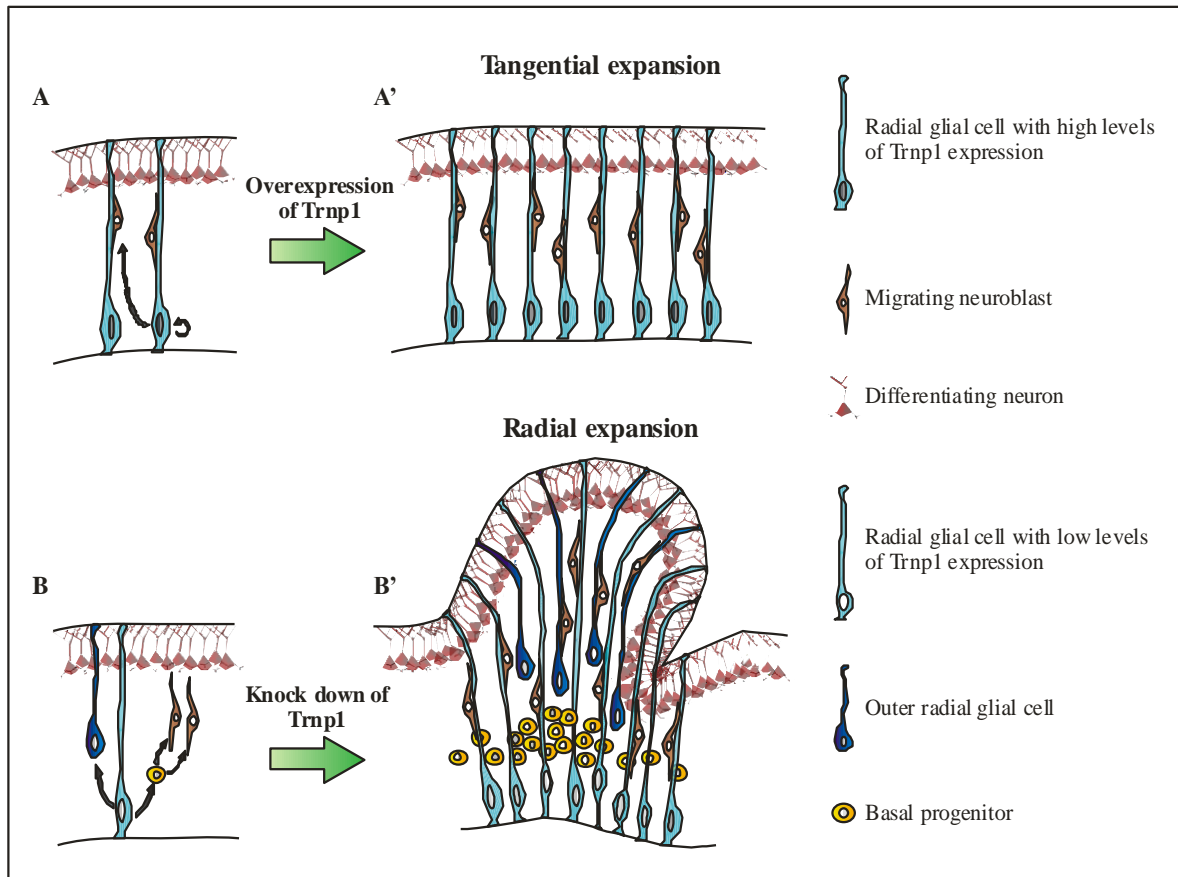


Figure 38: Model of *Trnp1* action during mammalian cortical brain development

Illustration of the mode of *Trnp1* action in neural stem cells during cerebral cortical development. (A) High levels of *Trnp1* in radial glial cells lead to proliferation and self renewal of radial glia with either symmetric divisions to generate two radial glial cells or asymmetric division allowing direct neurogenesis to occur at the same time. (A') High levels of *Trnp1* enlarge the pool of stem cells leading to tangential expansion. (B) In contrast to that, low levels of *Trnp1* lead to the generation of basal progenitor cells that subsequently amplify the neuronal output. At the same time, low levels of *Trnp1* also provoke generation of outer radial glia (oRG) that lost their apical process and serve to amplify the neuronal output but also are essential for folding of an expanding cortex. (B') Both the high number of basal progenitors and the generation of oRGs together lead to a radial expansion of the cortex and ultimately result in folding of the brain as naturally occurring in higher mammalian species.

5.3 The role of Trnp1 in neurogenesis and its potential in reprogramming

Trnp1 is an important regulator of direct versus indirect neurogenesis and generation of different progenitor sub-classes. Regarding the direct role of Trnp1 in neurogenesis, I also identified Trnp1 to be expressed at protein level upon reprogramming of postnatal astrocytes into neurons (data not shown). It has previously been shown that astrocytes from the postnatal cerebral cortex (postnatal day 7) can be directly converted into functional neurons by forced expression of Ngn2 or Mash1/Dlx2 (Berninger et al., 2007; Heinrich et al., 2010). Trnp1 was induced and detectable in reprogrammed cells generated both from Ngn2 and Mash1 transduced astrocytes 14 days after infection only in reprogrammed cells, i.e. in neurons (data not shown). Along this line, using chromatin immunoprecipitation our collaborator Francois Guillemot was able to detect Ngn2 as well as Mash1 to bind very closely to the proposed promoter region of Trnp1. This suggested that Ngn2 and Mash1 might directly regulate Trnp1 activity. Altogether, Trnp1 seems to have an additional role in newborn neurons, which is emphasized by its endogenous expression in newborn neurons during cortical development. During his master thesis under my supervision Michael Metzger was able to show that Trnp1 is an important survival factor for newborn neurons in their early days. *In vitro* time-lapse analysis of loss of Trnp1 function in newborn neurons of dissociated cells from the developing cerebral cortex (at E12) identified Trnp1 as a promoter of survival in newborn neurons (Metzger, 2011). Therefore, in addition to its role in neural stem cells, Trnp1 may represent a crucial factor for neuronal survival in their early days.

5.4 TRNP1 in human brain development

5.4.1 TRNP1 expression in the developing human brain

Down regulation of Trnp1 resulted in increased numbers of BPs and oRGs with a “fanned array” expansion of the cortex, which ultimately led to folding and pseudo-gyrification of the otherwise lissencephalic murine brain. These observations initiated the hypothesis that

Trnp1 may be an important regulator of higher mammalian brain development. It has been suggested, that gyri and sulci in gyrencephalic brains form due to differences in progenitor expansions (Smart and McSherry, 1986a; 1986b; Kriegstein et al., 2006). In this scenario local differences of Trnp1 expression levels could regulate differential expansion in folded brains. To address this question, our collaborator Victor Borell was investigating *TRNP1* expression in the human developing brain. *In situ* mRNA analysis demonstrated the expression of *TRNP1* in the developing human brain. Remarkably, *TRNP1* is expressed in a similar manner in the human brain as it is in the murine brain with high levels of *TRNP1* in the ventricular zone and in newborn neurons in the cortical plate, but rather low levels in the subventricular zone where the basal progenitors and outer radial glial cells are located in the human brain. However, in strong contrast to the murine brain local differences of *TRNP1* expression within the VZ were clearly detectable in the human brain. Supporting the role of TRNP1 in cortical expansion, low levels of *TRNP1* in the VZ were associated with a rather expanded cortical area, whereas high levels of *TRNP1* in the VZ correlated with less neurons in the CP. This expression pattern is intriguing in regard to my observation in the murine brain *in vivo* where manipulation of the protein resulted in differences of radial glial cell fate with high levels of Trnp1 leading to self renewal of RGs and tangential expansion, whereas low levels of Trnp1 provoked amplification of neuronal output and radial expansion through production of basal progenitors and outer radial glial cells. The local differences of *TRNP1* expression in the VZ of the human brain may therefore be causative for folding and differential expansion of different regions within the human brain resulting in its gyrencephaly. This is in agreement with previously suggested models in which a locally enlarged oSVZ correlated with increased expansion (Smart and McSherry, 1986a; 1986b; Kriegstein et al., 2006; Martínez-Cerdeño et al., 2012).

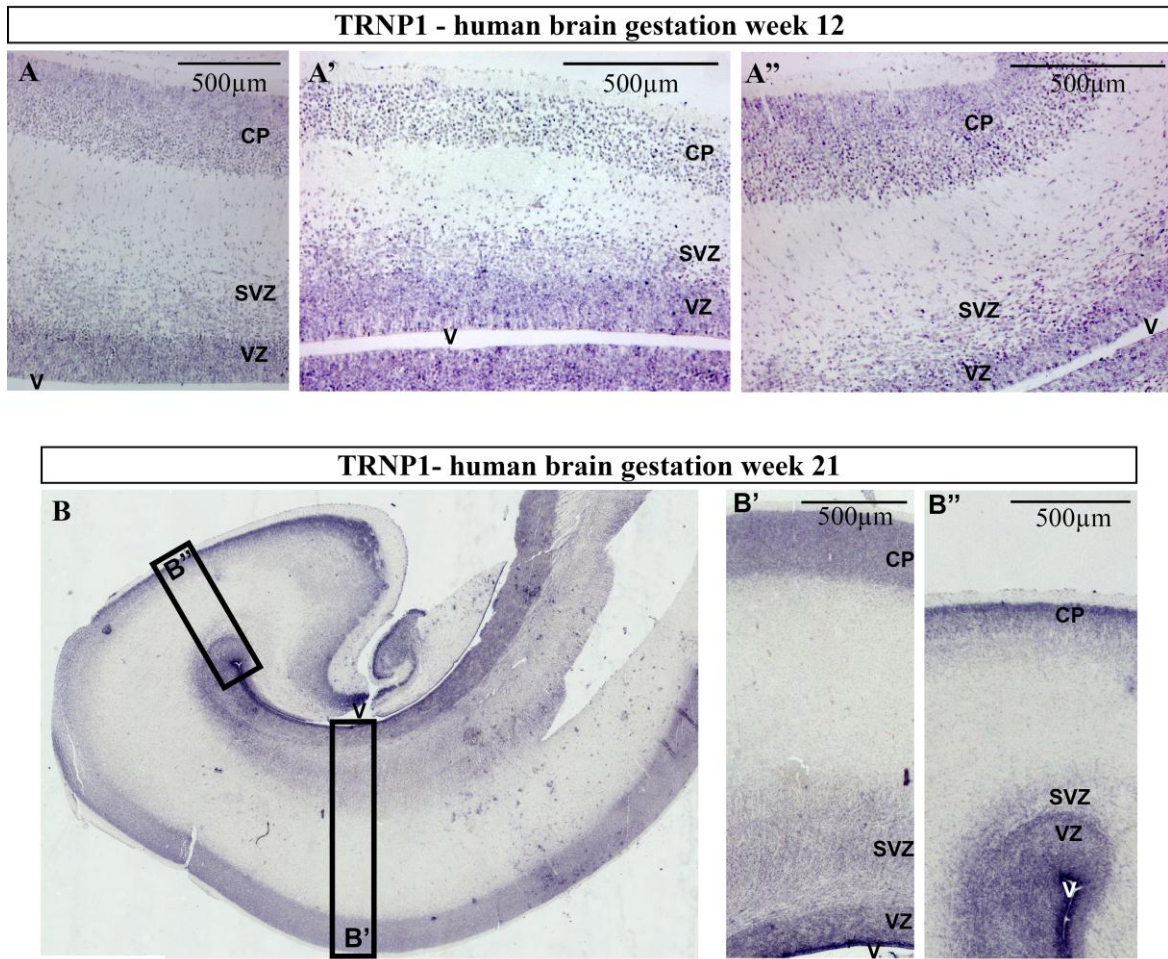


Figure 39: *TRNP1* expression in the developing human brain

In situ analysis of *TRNP1* transcript expression in the human brain. Embryonic brain sections of gestation week 12 and 21 were hybridized with *TRNP1* antisense probe. (A-A'') *In situ* hybridization on embryonic sections of gestation week 12. (B-B'') *In situ* hybridization on embryonic sections of gestation week 21. Note the differential expression of *TRNP1* in the VZ of different areas with high levels of *TRNP1* in the VZ correlating with low numbers of neurons in the CP of the same region and low-level expression of *TRNP1* in the VZ correlating with increased numbers of neurons in the CP.

5.4.2 Investigation of a possible association of *TRNP1* with human diseases

The presence of *TRNP1* in the human brain emphasized the significance of the findings of this work and also led to the question whether *TRNP1* may also be disease associated. Especially diseases with developmental neurogenesis defects such as lissencephaly or mental retardations could be possibly caused by genetic mutations of *TRNP1*. Online search using well established databases such as the genetic association database (<http://geneticassociationdb.nih.gov/>) the human gene mutation database (<http://www.hgmd.cf.ac.uk>) for human disease cases associated with deletions or mutations

of *TRNP1* did not reveal a single case of *TRNP1* affected individuals. However, personal internet search revealed one case of a genomic duplication including *TRNP1*. This particular case carries a duplication comprising 763 kilobases of chromosome 1p36.11 including a duplication of *TRNP1* (position: chr. 1 26716140 - 27480136; see Figure 40). Other than this genetic duplication no genetic abnormalities were found using 244k-Oligonucleotide Array (Agilent) and the duplication does not represent a known Polymorphism. The above female patient is now six years old and was diagnosed with Rett syndrome. The typical “washing movements” initially gave a first hint towards the syndrome causative for her disability. In contrast to this patient that carries a duplication on chromosome 1, Rett syndrome is typically an X-chromosomal dominantly inherited disease. Male fetuses with the disorder rarely survive to term. The main genetic background of Rett syndrome is mutations in the gene *MeCP2* that is encoded on the X-chromosome. Loss of function mutations in *MeCP2* can arise sporadically or within the germ line and are associated with 75% of Rett cases (Hoffbuhr et al., 2001; 2002). However, in less than 10% of Rett cases, mutations in the genes *CDKL5* or *FOXP1* (involved in control of proliferation of apical progenitors in forebrain development (Manuel et al., 2011)) have also been found to cause the syndrome (Tao et al., 2004; Weaving et al., 2004; 2005; Chen et al., 2010). Today, Rett syndrome is still diagnosed by clinical observation, and in some very rare cases, no known mutated gene can be found. These clinical observations prompt the hypothesis that *Trnp1* might be directly or indirectly associated with *MeCP2* thereby causing a similar phenotype as *MeCP2* mutations. It is conceivable, that *Trnp1* may represent a downstream target, a co-factor or a competitor of *MeCP2* and further investigations need to be performed in order to elucidate this association. The duplicated chromosomal region of course also includes other genes and an effect of the combined action of more than only one gene that is duplicated is possible. Nevertheless, the importance of *Trnp1* during cortical development together with the severe syndrome observed in a case of chromosomal duplication in humans indicates, that *Trnp1* may also play a central role in development of the human brain.

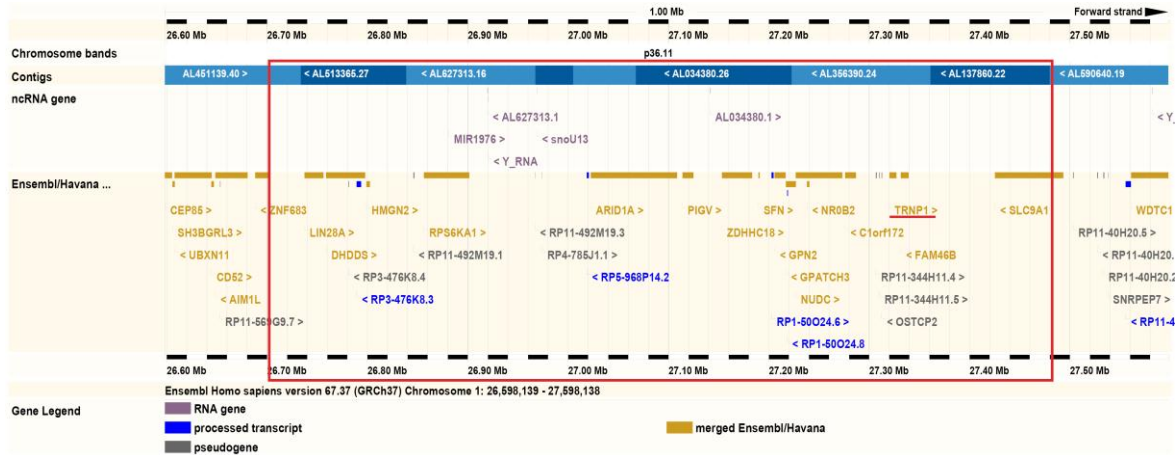


Figure 40: Chromosomal duplication of a girl presented with Rett syndrome

Graphical representation of human chromosome 1 - region 1p36.11. The region between 26 598 139 and 27 598 138 is depicted. The region duplicated in the female patient with Rett syndrome is marked with a red square. Genes are labeled as indicated. The *TRNP1* gene is underlined in red.

Additionally two cases of chromosomal abnormalities in a region similar to the mentioned case (also comprising the *TRNP1* gene locus) have recently been reported on the DECIPHER homepage (<https://decipher.sanger.ac.uk>). Both patients showed mental retardation. One female patient carries a deletion comprising 1.97 megabases (chr. 1 27237958 - 29205507) with 38 genes affected (including *TRNP1*). The other diseased case, a male patient with unknown age has two chromosomal regions affected: a deletion on chromosome 6 comprising 1.11 megabases (chr.6 169786414 - 170892243) with 10 genes affected and a duplication on chromosome 1 comprising 580 kilobases (chr. 1 27190888 – 27773330) with 17 genes (including *TRNP1*) affected. Remarkably, the overlap of all the three cases comprises a very small region of only 242 kilobases on chromosome 1 including only 6 genes: *NUDC*, *NR0B2*, *C1orf172*, *TRNP1*, *FAM46B* and *SLC9A1* (27237958 – 27480136). Additionally, the latter patient also presented with lissencephaly (possibly due to increased *TRNP1*-levels as only timed loss of the protein was able to induce radial expansion and folding of the otherwise lissencephalic murine brain). However, in the latter case another gene known to play a central role in neurogenesis was affected: *DLL1* (deletion on chr. 6).

While some hypotheses emerge in regard to the cellular and possibly disease associated function of *Trnp1*, it is important to also understand how it may exert its fascinating roles at the molecular level.

5.5 The Molecular function of Trnp1

5.5.1 Biochemical characteristics of Trnp1

Trnp1 is a highly basic protein with many positively charged amino acids at physiological pH. Extensive posttranslational modifications have been suggested for Trnp1 (Volpe et al., 2006) and may regulate its endogenous function. Trnp1 has been identified as a chromatin component in this work. Given the absolute lack of any known molecular motif within the protein sequence, Trnp1 may be part of a new, so far unrecognized class of nuclear proteins. Especially its highly basic biochemical character in combination with the high abundance of arginine residues within the protein sequence, a proline rich region at the N-terminus and an alanine/glycine rich region seem to be very special features of Trnp1. In addition, as shown in 4.5.2, Trnp1 is highly unstructured at its N- and C-terminal ends, but carries a highly structured central part. This structural characteristics together with the abundance of many basic amino acids is somewhat similar to the reported structure of linker histones such as H1 (Li, 1975; Happel and Doenecke, 2009). A comparison of both protein sequences shows that they both concentrate their positive charges at the C-terminal half of the protein (see Figure 41). A possible similarity with linker histones was tested by use of a typical linker histone lysis protocol (following a suggestion of Prof. Dr. Axel Imhof). Cells were lysed with perchloric acid (HClO₄) and linker histones and high mobility group proteins were specifically released from DNA. However, this method of lysis was not able to release Trnp1 from an insoluble fraction. Accordingly, when using another protocol for protein extraction typically used for strongly DNA associated proteins, Trnp1 was being concentrated but remarkably not in the soluble fraction but rather in the insoluble fraction. Indicating that Trnp1 is even more insoluble than for example proteins binding methylated DNA such as MeCP2 (Raymond Poot, unpublished data) or even core histones which are released into the soluble fraction using this protocol. Further molecular analysis will shed light on the way Trnp1 executes its function on the molecular level. The tight association of Trnp1 with DNA suggests that Trnp1 may act as chromatin-associated factor possibly involved in regulation similar to epigenetic factors or chromatin remodeling factors. The functional importance observed *in vitro* and *in vivo* suggests that Trnp1 may represent a master regulator of diverse cellular activities such as has also been reported for

chromatin remodeling or epigenetic factors (Kouzarides, 2007; Li et al., 2007; Ho and Crabtree, 2010)

A TRNP1

MPGCRRISACG PGAQEGTAEP GSPPPPPREP LPSLQPPSPS PTSTPTPTKS PPLPEAAETP
 VEGQELQRWR QGASGGSGGA GPAGIAGAAA GAGGRALELA EARRRLLEVE GRRRLVSELE
SRVLQLHRVF LAAELRLAHR AESLSRLSGG VAQAELYLAA HGSRLKKGAR RGRRGRPPAL
 LASALGLGSC VPWGAGRLRR GQGPEPDSPF RRSPRGPAS PQR

B Linker Histone H1.1

MSETAPVAQA ASTATEKPAA AKKTKKPAKA AAPRKKPAGP SVSELIVQAV SSSKERSGVS
 LAALKKSLAA AGYDVEKNNS RIKLGLKSLV NKGTLVQTKG TGAAGSFKLN KKAESKAITT
KVSVKAKASG AAKKPKKTAG AAAKKTVKTP KKPKKPAVSK KTSKSPKKPK VVKAKVAKS
 PAKAKAVKPK ASKAKVTKPK TPAKPKKAAP KKK

Figure 41: Comparison of Trnp1 to linker histone H1.1

Protein sequence comparison of Trnp1 and linker histone H1.1. Positively charged amino acids are labeled in red and underlined. Note the high abundance of positively charged amino acids in both proteins with the difference, that Trnp1 carries mainly arginines I and H1.1 carries mainly Lysines (K) possibly indicating differential regulation through posttranslational processing. Also note that the distribution of positively charged amino acids is strongly shifted towards the C-terminal half of both proteins.

5.5.2 The regulatory function of Trnp1 on gene expression

The tight association of Trnp1 with DNA (together with the dramatic phenotype observed upon loss of Trnp1 function) suggested that Trnp1 may be involved in regulation of gene expression during neural development. In order to identify differences of gene expression upon gain and loss of Trnp1 function, a transcriptome analysis was performed. To ensure identification of early, primary and not secondary responding genes upon gain- and loss of function, gene expression analysis of cells electroporated with either overexpression plasmid, Trnp1-shRNA plasmid or control GFP was performed one day post electroporation. Moreover, analysis of such an early time point after manipulation avoided artifacts due to changes in cellular composition (differences of progenitor composition

were observed after 3 days with more RG upon forced expression of *Trnp1* and more BP upon knock down of *Trnp1*). The observation that more genes were up regulated upon gain of *Trnp1* function, whereas more genes were down regulated upon loss of *Trnp1* function led to the conclusion that *Trnp1* activates expression of specific genes, which is in agreement with its co-localisation with euchromatin. Gene ontology analysis of the significantly regulated genes revealed a high proportion of genes involved in direct or indirect gene regulation (chromatin remodelling factors, transcription factors, nucleosome associated proteins and epigenetic factors). Forced expression revealed interesting candidates as *Trnp1* targets such as *Dlx1*, *Dlx2*, *Dlx5*, *Dlx6* and *Gsx2*. These genes are endogenously expressed in the developing ganglionic eminence but not in the developing cortex. In this context ventral forebrain progenitors have been reported to be characterized by higher proliferation rates as compared to dorsal progenitors. It is of interest to mention that *Dlx5* was shown to increase proliferation in tumor cells through activation of *Myc* (Xu and Testa, 2009). Increased self-renewal and proliferation observed upon forced *Trnp1* expression might be explained with an alteration of progenitor characteristics towards ventralized gene expression.

In contrast, knock down of *Trnp1* mainly showed down-regulation of genes. Amongst them important regulators of chromatin state such as *Bmi1*, *Smarca5*, *Chd7* or *Nuak1* but also genes important for neuronal differentiation such as *Neurod1*, *Neurod2*, *Neurod6* and *Rnd2*. Differences in differentiation-associated genes can be explained by the inhibition of direct neurogenesis from radial glial cells upon knock down of *Trnp1* with RGs generating more BPs and oRGs cells instead of directly generating postmitotic neurons. In summary, gene expression analysis showed that *Trnp1* has a severe impact on gene expression already 24 hours after initiating alterations in its own expression level. These data suggested that *Trnp1* is involved in regulation of gene expression either directly or indirectly (possibly by changing the chromatin state).

5.5.3 Similarities of *Trnp1* with other known proteins

Proteins with sequence characteristics similar to *Trnp1* and tight association with DNA comprise well-known factors such as UTF1 (Undifferentiated embryonic cell Transcription

Factor 1) or MeCP2 (Methyl CpG binding protein 2). UTF1 is expressed in embryonic stem cells and has been reported to act as a transcriptional repressor (Okuda et al., 1998; Fukushima et al., 1999; van den Boom et al., 2007). Additionally, UTF1 has also been shown to act as a co-activator of transcription and to interact with the basal transcription factor TFIID (Fukushima et al., 1998; Okuda et al., 1998). UTF1 was also suggested to play a role in proliferation and in teratoma formation of ES cells (Nishimoto et al., 1999; 2005). Similar to the observed characteristics of Trnp1, UTF1 was shown to be tightly associated with chromatin (van den Boom et al., 2007). This study also showed by FRAP analysis that UTF1 has a dynamic behavior similar to core histones. Remarkably, just like Trnp1 UTF1 has a high isoelectric point (10.46) with 34 out of 339 amino acids being arginines (see Figure 42) and a coiled coil domain (in the case of UTF1 a typical leucine zipper motif) (Okuda et al., 1998; van den Boom et al., 2007). Recently, the functional importance of UTF1 was shown in direct reprogramming as it highly increased the efficiency to generate induced pluripotent cells (iPS) from fibroblasts up to 100-fold (Zhao et al., 2008). This suggested that UTF1 facilitates the formation of a chromatin structure, which is supporting pluripotency. In this context it has also been shown, that UTF1 directly interacts with core histones and leads to chromatin condensation of target regions thereby acting as a repressor of gene expression (Kooistra et al., 2009; 2010). However, although UTF1 is found globally associated with chromatin during Meta- Ana- and Telophase (van den Boom et al., 2007), it was shown that UTF1-bound regions were significantly enriched on chromosomes 11, 17 and Y (Kooistra et al., 2010). Additionally, UTF1 is able to alter the chromatin state and thereby also influence gene expression indirectly (Kooistra et al., 2010).

A TRNP1

MPGCRISACG PGAQEGTAEP GSPPPPPREP LPSLQPPSPS PTSTPTPTKS PPLPEAAETP
 VEGQELQRWR QGASGGSGGA GPAGIAGAAA GAGGRALELA EARRRLLLEVE GRRRLVSELE
SRVLQLHRVF LAAELRLAHR AESLSRLSGG VAQAELYLAA HGSRLKKGAR RGRRRGPPAL
 LASALGLGSC VPWGAGRLRR GQGPEPDSPF RRSPPRGPAS PQR

B UTF1

MLLRPRRLPA FSPSPASPD AELRSAGDVP VTTSDAFATS GGMAEPGSPK APVSPDSAQR
 TPWSARETEL LLGTTLLQPAM WRSLLLDRRQ TLPTYRRVSA ALARQQVRRT PAQCRRRYKF
LKDKLRDSQG QPSGPFNDQI RQLMGLLGDD GPPRVRRRST GPGRPQRRGR SLSALAPAP
 APVEQEAELP LAAENDEPAP ALRFSSTTK SAGAHRITSS PPLTSTDITLP PEPGHTFESS
 PTPTPDHDVE TPNEPPGLSQ GRASSPQVAP QSLNTALLQT LTHLGDISTV LGPLRDQLST
 LNQHVEHLRG SFDQTVSLAV GFILGSAASE RGILGDLRQ

Figure 42: Comparison of Trnp1 and UTF1 protein

Protein sequence comparison of Trnp1 and UTF1. Positively charged amino acids are labeled in red and underlined. Note the high abundance of positively charged amino acids in both proteins with the common abundance of arginines (R). Also note that the distribution of positively charged amino acids is strongly shifted towards one half of both proteins.

Another tightly DNA associated protein with a highly basic pI of 9.5 is MeCP2 which binds to methyl-CpG (methylated DNA) base pairs (Lewis et al., 1992; Meehan et al., 1992). MeCP2 is a well-investigated protein and mutations in *MeCP2* are known to cause Rett syndrome (Carter and Segal, 2001; Hoffbuhr et al., 2001; 2002; Luikenhuis et al., 2004; Weaving et al., 2005; Villard, 2007; Marchetto et al., 2010; Liroy et al., 2011; Babbio et al., 2012; Goffin et al., 2012) a human neurodevelopmental disorder that can lead to cognitive impairment, autistic features, motor disabilities, seizures and anxiety (Chahrour and Zoghbi, 2007) as described above (see 5.4.2 - Investigation of a possible association of TRNP1 with human diseases). In vertebrates methylated DNA is associated with transcriptional repression and inactive chromatin (Meehan et al., 1992). In this context, MeCP2 has been shown to inhibit transcription from both methylated and non-methylated

DNA and to contribute to the long-term repression and nuclease resistance of methyl-CpG (Meehan et al., 1992). MeCP2 has been shown to be essential for embryonic development (Tate et al., 1996) and correlates with the function of DNA methyl-transferase (Li et al., 1992). Additionally, it has been shown that MeCP2 is able to displace Histone H1 from preassembled chromatin containing methyl CpG (Nan et al., 1997). However, the exact molecular mode of action still remains partially elusive. MeCP2 is regulated through phosphorylation (Zhou et al., 2006; Murgatroyd et al., 2009; Deng et al., 2010) and recently it has been suggested, that the protein acts as a histone-like factor regulating genome-wide response of chromatin to neuronal activity (Cohen et al., 2011) rather than being a sequence specific transcriptional repressor of specific genes.

The presented data in this work showed, that *Trnp1* - just like MeCP2 and UTF1 – is tightly bound to DNA and regulates expression of specific genes. Therefore it is conceivable, that *Trnp1* may act as a chromatin remodeler similar to UTF1 or MeCP2 thereby exerting its functional effects during neural development. However, further experiments are necessary to test this possibility.

5.5.4 A possible role of *Trnp1* in regulation of chromatin state

It has been previously shown, that stem cells have a chromatin structure, DNA methylation pattern and nuclear organization that is different from differentiated somatic cells (Mayer et al., 2005; Boyer et al., 2006a; Kobayakawa et al., 2007; Mikkelsen et al., 2007; Chen and Daley, 2008; Meissner et al., 2008; Gaspar-Maia et al., 2009; Lim et al., 2009; Sun et al., 2011; Yellajoshyula et al., 2011; Zhou et al., 2011; Armstrong, 2012). Additionally, alterations in chromatin structure are able to change cellular fate and to influence differentiation of stem cells into different cell types (Lin and Dent, 2006; Graf and Stadtfeld, 2008; Lim et al., 2009; Yellajoshyula et al., 2011; Hung et al., 2012). The control of such chromatin alterations is important to regulate amplification of stem cells versus their differentiation. Furthermore, heterogeneity plays a central role and is a hallmark in both embryonic and adult stem cells (Graf and Stadtfeld, 2008). In this context, for neural stem cells it has been previously suggested that there are subtypes of radial glia: some that mainly regenerate themselves and produce neurons directly and others that

generate basal progenitors (which in turn are prone to generate neurons) to amplify the neuronal output (Miyata et al., 2001; Noctor et al., 2001; 2004; Pinto and Götz, 2007; Stancik et al., 2010).

Epigenetic processes have previously been suggested to be involved in control of stem cell proliferation versus differentiation (Bibikova et al., 2008; Eilertsen et al., 2008; Sasaki and Matsui, 2008; Sauvageau and Sauvageau, 2010; Ben-David and Benvenisty, 2011; Cedar and Bergman, 2011; Su et al., 2011). In this context, several reports showed that differentiation-genes in ES cells are silenced by Polycomb Group (PcG) complexes (Azuara et al., 2006; Bernstein et al., 2006; Bracken et al., 2006; Lee et al., 2006; Loh et al., 2006; Boyer et al., 2006b). As another example, the NuRD (nucleosome remodeling and disruption) complex is necessary for lineage commitment of ES cells showing that nucleosome remodeling is crucial in this process (Kaji et al., 2006).

Analysis of genome-wide association was able to show that transcription factors occupy less than a few percent of their consensus target sites (Carr and Biggin, 1999; Iyer et al., 2001; Yang et al., 2006; Joseph et al., 2010; Kaplan et al., 2011). Recently, it has been suggested that there are three different levels of transcription factor dependent gene regulation: DNA-binding site recognition, chromatin accessibility (controlled by epigenetic modifications) and co-factor availability in different cell-types (Fong et al., 2012). Therefore, accessibility of distinct target sites is of key importance for regulation of gene expression. So-called pioneer transcription factors are the first ones in a cascade of events establishing competence for gene expression ultimately leading to determination of cell fate (Zaret and Carroll, 2011). These pioneer transcription factors initiate the sequential binding of a series of factors by independently accessing the first target sites and reducing the number of co-factors needed (Carroll et al., 2006; Eeckhoutte et al., 2006; Zaret and Carroll, 2011). In addition these factors can actively open up local chromatin and thus make it competent for further transcription factor binding (Xu et al., 2009; Zaret and Carroll, 2011).

Trnp1 may act similar to UTF1 as a chromatin associated protein involved in gene expression but also in alteration of chromatin structure at the same time (Okuda et al., 1998; van den Boom et al., 2007; Kooistra et al., 2009). Upon down regulation of Trnp1 most regulated genes were down regulated whereas upon forced Trnp1 expression most

affected genes were up regulated. This suggested an activating rather than a repressing role of Trnp1 on gene expression. It is therefore conceivable that Trnp1 represents a pioneer factor initiating transcription directly but also concomitantly leading to changes in chromatin state (see also the genes affected upon down regulation of Trnp1 7.2.1) thereby influencing gene expression indirectly through other factors as well.

To further investigate the tight association of Trnp1 with chromatin, fluorescence recovery after photo bleaching was performed. However, fusion of GFP to the C-terminal end of Trnp1 inhibited its association with chromatin. FRAP experiments therefore were not able to show the strong interaction of Trnp1 with DNA. Trnp1-GFP exhibited much faster recovery rates than reported for core histones that are tightly associated with DNA and show slow recovery rates in FRAP experiments (Kanda et al., 1998; Kimura and Cook, 2001). However, Trnp1-GFP still showed much slower recovery rates as compared to GFP only. It has previously been suggested for Oct4-GFP (which recovered still faster as compared to Trnp1-GFP) that it is residing in a high molecular weight complex and therefore kinetics would be slower than expected for the size of the protein itself (van den Boom et al., 2007). The same may apply to Trnp1-GFP (although the protein does not interact anymore with DNA) as interactions with other protein complexes cannot be excluded (especially as Trnp1 has been reported to be endogenously expressed at low levels in the cell line used in this experiment (Volpe et al., 2006)). Additionally, as Trnp1 shows a highly predictable coiled coil domain, it may also interact with itself to form oligomers and therefore exhibit slower kinetics than GFP alone.

Towards an identification of Trnp1 interacting proteins, mass spectrometry analysis was performed. However, use of Trnp1-GFP for pull down in HEK cells showed no reproducible binding partner of Trnp1. This fusion construct later turned out to preclude chromatin association of Trnp1 during mitosis and it may therefore also inhibit interaction with binding partners. However, as HEK cells do not endogenously express Trnp1, it is also possible, that the natural binding partners of Trnp1 are not expressed in HEK cells. Thus use of a cell line that shows endogenous expression of Trnp1 may help to identify naturally Trnp1 associated proteins in the future.

The exact molecular mode of Trnp1 action remains partially unidentified and needs further investigation. Lacking any known DNA binding domain or protein motif, Trnp1 may represent the first member of a new class of molecules.

In summary, this work showed a key functional role of Trnp1 during mammalian forebrain development, which was further emphasized by its intriguing expression pattern in the developing human brain. Trnp1 regulates tangential versus radial expansion of the cerebral cortex and is able to control folding of the developing brain. Thus this work identified an entirely novel, previously unrecognized DNA associated protein as a molecular switch in neural stem cells.

6 Material and Methods

6.1 Materials

6.1.1 Buffers and Solutions

6.1.1.1 10x PBS

Material: 1.4 M NaCl
 27 mM KCl
 83 mM Na₂HPO₄
 15 mM KH₂PO₄
 pH 6.8

For 5 l of 10x PBS 400g NaCl, 10g KCl, 73,66g Na₂HPO₄ x 2H₂O and 10g KH₂PO₄ were dissolved in ddH₂O and the pH value was adjusted to 6.8. The buffer was autoclaved. After dilution of 1:10 this resulted in 1x PBS with a pH-value of 7.4

6.1.1.2 4 % PFA (from initially a 20% PFA Stock)

Material for 20% stock (2 l): 400 g PFA
 134 g Na₂HPO₄
 1600 ml ddH₂O
 add 32% NaOH until PFA was completely dissolved

The mixture was stirred on a heater at 60 °C under the hood until the solution cleared (approximately 30 min). After the solution cooled down on ice the pH-value was adjusted with HCl to 7.4. Then the solution was filled up to 2 l with ddH₂O. Finally the solution was filtered (0.22 µm) and aliquotted in 50 ml falcon tubes. This 20 % stock solution was then stored at -20 °C and diluted 1:5 for fixation of tissue or cells with 4 % PFA.

6.1.1.3 50x TAE-buffer

Material: 2 M Tris acetate
 50 mM EDTA
 Adjust pH 8.0 with HCl

For 1l of 50x TAE-buffer 242 g Tris Base, 57.1 ml acetic acid and 37,2 g Na₂EDTA x 2H₂O were dissolved in ddH₂O, pH 8.0 was adjusted with HCl.

6.1.1.4 10x SDS running-buffer

Material: 0.25 M TRIS-base
 1.92 M Glycine
 1 % SDS

For 1l 10 x Elektrophoresis buffer 30.3 g TRISbase, 144 g Glycine and 10 g SDS were dissolved in ddH₂O pH was adjusted to 8.45 and finally the volume was adjusted to 1l with ddH₂O.

6.1.1.5 Separation Gel buffer for SDS Gels

1.5 M TRIS
pH 8.8

For 500 ml of separation gel buffer 90.86 g of TRIZMA base was dissolved in 300 ml ddH₂O. pH was adjusted to 8.8 with HCl. Subsequently volume was adjusted to 500 ml with ddH₂O.

6.1.1.6 Stacking Gel buffer for SDS Gels

0.5 M TRIS
pH 6.8

For 500 ml of stacking gel buffer 30.29 g of TRIZMA base was dissolved in 300 ml ddH₂O. pH was adjusted to 6.8 with HCl. Subsequently volume was adjusted to 500 ml with ddH₂O.

6.1.1.7 Transfer-buffer (wet blot)

Material: 0.025 M Tris-base
 0.192 M Glycine
 0.1 % SDS
 20 % v/v Methanol

For 1l of transfer-buffer 100 ml of 10x SDS running buffer were mixed with 200 ml Methanol and 700 ml ddH₂O.

6.1.1.8 Lysis Buffers for Cell/Tissue Lysis

RIPA Buffer

50 mM Tris-HCl pH 8.0
150 mM NaCl
1 % DOC (Sodium Deoxycholate)
1 % NP-40
0.1 % / 1 % SDS (for cells / for tissue)

HRSB-0.5% NP40 buffer:

20 mM Hepes pH 7.6,
3 mM MgCl₂,
10 mM NaCl,
0.5 % NP40

HRSB +1.2M Sucrose:

HRSB + 41 gr/100 ml Sucrose

Extraction-EDTA buffer:

10 mM Hepes pH 7.6,
150 mM NaCl,
1 mM EDTA,
10 % glycerol,
add 1 mM DTT

To each buffer protease inhibitors were added before use (Complete Protease Inhibitor cocktail Roche®)

6.1.2 Cell lines

Bacterial strains: *E.coli* TOP10 (Invitrogen)
E.coli Dh5alpha (Invitrogen)
E.coli DB3.1 (ccdB resistant, Invitrogen)

Eucaryotic cell lines: HEK 293 cells (kind gift of Dr. Alex Lepier)
NRK (kind gift of Dr. Robert Blum)
P19 carcinoma cells (kind gift of Dr. Francois Guillemot)
C2C12 (Dr. Heinrich Leonhard)
HeLa (Dr. Heinrich Leonhard)

6.1.3 Antibodies

6.1.3.1 Primary antibodies

Antigen	Host	WB	IC	IH	Supplier
RC2	Mouse (IgM)	-	-	1:200	Kind gift of P. Leprince
Pax6	rabbit	-	-	1:500	Millipore
Pax6	Mouse (IgG1)	-	-	1:50	Dev. Hybridoma Bank
Tbr2	rabbit	-	-	1:500	Abcam
Tbr1	Rabbit		1:400	1:200	Abcam
dsRed/RFP	Rat	-	1:500	1:500	Chromotek
GFAP	Rabbit	-	1:2.000	1:500	Dako Cytomation
β III-Tubulin	Mouse (IgG2b)	-	1:500	-	Sigma Aldrich
α -Tubulin	Mouse (IgG1)	1:5.000	-	-	Sigma
γ -Tubulin	Mouse (IgG1)	1:5.000	-	-	Sigma
Mash1	Mouse (IgG1)	-	-	1:200	Dev. Hybridoma Bank
GFP	Chicken	-	1:1.000	1:500	Aves Labs
Trnp1	Guinea Pig	1:2.000	1:500	1:100	Self made

Nestin	Mouse (IgG1)	-	1:20	1:10	Dev Hybridoma Bank
BrdU	Rat (IgG2a)	-	-	1:500	Abcam
Dcx	Rabbit	-	1:2.000	1:1.000	Abcam
PDGFRα	Rat	-	1:200	1:200	BD Bioscience

WB: dilution used for Western blotting, IC: dilution used for Immunocytochemistry (cells *in vitro*), IH: dilution used for Immunohistochemistry (cells in tissue sections).

Nuclei were visualized with 4',6-Diamidino-2-Phenylindole, Dihydrochloride (DAPI) (0,02mg/ml inddH₂O)

6.1.3.2 Secondary antibodies

Immunocytochemistry and Immunohistochemistry was performed with the appropriate species- or subclass-specific secondary antibodies conjugated to either AlexaFluor 488 (1:500 Invitrogen), CyTM2, CyTM3, CyTM5 (1:500, Jackson ImmunoResearch), FITC (fluorescence isothiocyanate; 1:500, Jackson ImmunoResearch) or TRITC (tetramethyl rhodamine isothiocyanate; 1:500, Jackson ImmunoResearch). For Enhanced Chemical Luminescence (ECL) detection after Western blotting, appropriate Horseradish-Peroxidase (HRP) coupled anti-guinea pig (Abcam – ab6771-1), anti-mouse (Dako), anti-rabbit (GE Healthcare – Na934VS) or anti-rat (DAKO) antibodies were used in a 1:5.000-10.000 dilution.

6.1.4 Oligonucleotides

Primer name	Sequence (5'→3')	Description
shRNA#1 Top Strand	5'-GATCCCC ACTCTGCATTGCTTCCCATACACTGT TCAAGAGACAGTGTATGGGAAGCAATGCAGAGTT TTTTA -3'	shRNA target sequence (sense/antisense) Loop sequence Overhangs forming BglIII / HindIII restriction sites
shRNA#1 Bottom Strand	5'-AGCTTAAAAA ACTCTGCATTGCTTCCCATACAC TGTCTCTTGAA CAGTGTATGGGAAGCAATGCAGA GTGGG -3'	
shRNA#4 Top Strand	5'-GATCCCC GCAGAAAGGCAAGCCACTTCTTTC AAGAGAAGAAGTGGCTTGCCTTTCTGCTTTTTA -3'	
shRNA#4 Bottom Strand	5'-AGCTTAAAAA GCAGAAAGGCAAGCCACTTCT TCTCTTGAAAGAAGTGGCTTGCCTTTCTGCGGG -3'	
shRNA#5 Top Strand	5'-GATCCCC GATGGACGGCGTCATCTACTTC AAGAGAGTAGATGACGCCGTCCATCTTTTTA -3'	

shRNA#5 Bottom Strand	5'-AGCTTAAAAA GATGGACGGCGTCATCTACTCT CTTGAAGTAGATGACGCCGTCCATCGGG-3'	
----------------------------------	--	--

Overhangs used for cloning into pSUPER are according to the manufacturer's protocol.

6.1.5 Plasmids

Plasmid	Source
pCMV-Sport6-<i>Trnp1</i>	RZPD
pCMV-Sport6-<i>Trnp1</i>-Δpoly-A	Personally cloned
pENTR1A	Invitrogen/Life Technologies
pENTR1A-<i>Trnp1</i>	Personally cloned
pENTR4-<i>Trnp1</i>	Personally cloned (not used in this study)
pCAG-GFP-DEST/ pCAG-dsRed-DEST (with Gateway cassette)	Kind gift of Dr. Paolo Malatesta
pCAG-<i>Trnp1</i>-GFP	Personally cloned
pCAG-<i>Trnp1</i>-dsRed	Personally cloned
pSUPER	Oligoengine
pSUPER-shRNA#1	Personally cloned
pSUPER-shRNA#4	Personally cloned
pSUPER-shRNA#5	Personally cloned
pSUPER.GFP/Neo	Oligoengine
pSUPER.GFP/Neo-shRNA#1	Personally cloned
pSUPER.GFP/Neo-shRNA#4	Personally cloned
pSUPER.GFP/Neo-shRNA#5	Personally cloned
pLVTHM	King gift of Dr. Alex Lepier
pLVTHM –shRNA#1	Personally cloned
pLVTHM –shRNA#4	Personally cloned
pLVTHM –shRNA#5	Personally cloned
peGFP-<i>Trnp1</i>-N3	Kind gift of Dr. Robert Blum
pCAG-GS	King gift of Dr. Alex Lepier

pMXIG-IRES-GFP	(Nosaka et al., 1999)
pRenilla-TK	Promega
pGL3-P6CON	Kind gift of Dr. Anastasia Stoykova
pGL3-Tbr2	Kind gift of Dr. Jovica Ninkovic

Personally cloned plasmids: I cloned these plasmids during this study using standard molecular biology methods. Detailed Information about cloning procedure is described under 6.2.2. Plasmid maps (electronic – VectorNTI / .gb files) with relevant sequence information are available electronically in the lab and are also stored by Dr. Alex Lepier.

6.2 Methods

6.2.1 DNA Methods

6.2.1.1 Ethanol precipitation of DNA

Solutions: 3 M Sodium acetate pH 5.2

100 % Ethanol

70 % Ethanol

TE-buffer (pH 8.0): 10 mM Tris/Hcl pH 8.0

1 mM EDTA pH 8.0

1/10 Vol. of 3 M Sodium acetate, pH 5.2 and 2.5 Vol. 100 % Ethanol (-20 °C) was added to the DNA sample, mixed well, and incubated for 30 min at -20 °C. The precipitated DNA was centrifuged for 20 min at 4 °C/13.000 rpm, washed with ice cold 70 % Ethanol, and centrifuged for 5 min at 4 °C/13.000 rpm. The supernatant was removed, and the precipitated DNA was air-dried and diluted in TE-buffer or H₂O.

Regular Plasmid Maxi preparations of DNA were precipitated according to this protocol after isopropanol precipitation.

6.2.1.2 PCR

DNA was amplified by PCR using *Taq*, *Pfu*, or *High Fidelity Taq/Pwo* (Roche), as appropriate. Specific sense and antisense oligonucleotide primers flanking the desired target sequence were used.

A typical PCR reaction was prepared as follows:

10-100 ng	DNA template
1 µl	Polymerase (1 U)
5 µl	10x reaction buffer
1 µl	10 mM dNTP (Desoxy-Nucleotide-Triphosphate)-Mix: (dATP, dTTP, dGTP, dCTP)
2 µl	sense-Primer, 10 pM
2 µl	anti-sense-Primer, 10 pM
ad 50 µl	H₂O

PCR parameters were adjusted to the appropriate conditions. Generally, 25-35 cycles were used for amplification.

6.2.1.3 Colony PCR

Colony PCR allows screening of a large number of transformed *E. coli* colonies for positive clones before isolation from small-scale cultures of these cells.

Colonies were picked with a sterile toothpick and dipped three times in 25 µl dd H₂O. To break the cell walls and release plasmid DNA, the mixture was boiled at 95 °C for 5 min prior to the PCR. *Taq*-Polymerase, dNTPs, MgCl₂, and buffer were added, together with specific primers for the transformed plasmid. The PCR products were analyzed on an agarose gel.

In parallel, small scale liquid cultures were inoculated with the colonies for isolation of plasmid DNA, and incubated on a shaker at 37 °C in LB-medium containing the appropriate antibiotic for selection.

6.2.1.4 Restriction digestion of DNA

A typical reaction was prepared as follows:

1 µg	DNA plasmid
2 µl	10x reaction buffer (NEB)
0.5 – 1.0 µl	Restriction enzyme (5-10 U) (NEB)
ad 20 µl	H₂O

The reaction was incubated at the appropriate temperature (generally 37 °C) for 1-2 h. Alternatively, for highly efficient enzymes and for cloning analysis incubation time was shortened. Cleavage efficiency was investigated by gel electrophoresis.

6.2.1.5 Analysis of DNA-fragments on agarose gels (Meyers et al., 1976)

Solutions :	1x TAE buffer :	40 mM Tris-acetate 1 mM EDTA pH 8.0
	Ethidiumbromide stock:	10 mg/ml (use 1:10.000)
	6x DNA sample buffer:	0.25 % (w/v) Bromophenol-blue

60 % Glycerol (w/v)

0.1 mM EDTA pH 8.0

Depending on the size of the DNA fragments of interest, appropriate 0.8-2 % (w/v) Agarose gels were used for separation. The Agarose was dissolved in 1x TAE buffer by boiling in a microwave oven. Ethidiumbromide was added to a final concentration of 1 µg/ml, and the solution was poured into a gel chamber. Samples supplemented with DNA sample buffer and (for comparison) a 1 kb DNA ladder were loaded, and electrophoresis was performed at 100-200 V. After separation, the gels were photographed and pictures were printed.

For gel extraction DNA fragments were cut out under UV light (254 nm) and transferred into an Eppendorf tube. To purify DNA fragments from agarose, the QIAquick gel extraction kit (Qiagen) was used according to the manufacturer's protocol. The DNA was eluted in 30 µl H₂O pH 8.4.

6.2.1.6 Ligation

A typical ligation reaction was prepared as follows:

300 ng	DNA insert fragment
30 ng	DNA vector fragment
2 µl	5x T4-DNA-Ligase buffer (Invitrogen)
1 µl	T4-DNA-Ligase (Invitrogen)
ad 10 µl	H₂O

Insert DNA was generally used in a 5-10 fold excess of vector DNA. The ligation reaction was incubated for 2-3 h at 25°C or overnight at 16°C.

Alternatively, the Quick-Ligation-kit (NEB) was used according to the manufacturer's protocol. The ligation reaction was then incubated for 15-30 min at room temperature.

6.2.1.7 Preparation of bacterial agar plates (Sambrook et al., 1989)

Solutions: LB-(Luria-Bertani) Medium: 0.5 % (w/v) NaCl
1 % (w/v) Bacto-Tryptone

0.5 % (w/v) yeast extract

20 mM Tris/HCl pH 7.5

The pH value was adjusted to 7.0 with NaOH.

2x YT-Medium:

1 % (w/v) NaCl

1.6 % (w/v) Bacto-Tryptone

1 % (w/v) yeast extract

20 mM Tris/HCl pH 7.5

The pH value was adjusted to 7.0 with NaOH.

Ampicillin stock (100 mg/ml): use 1:1.000

Kanamycin stock (50 mg/ml): use 1:1.000

Material: Bacto-agar

For agar plates, 7.5 g bacto-agar was added to 500 ml LB or 2x YT medium, and autoclaved. After cooling to 60 °C, the appropriate antibiotic was added to a final concentration of 100 µg/ml for Ampicillin or 50 µg/ml for Kanamycin, respectively. The liquid medium was poured into 10 cm culture dishes and allowed to cool to room temperature. The agar plates were stored upside down at 4 °C and covered from light.

6.2.1.8 Generation of chemo-competent *E.coli* (modified CaCl₂-method)

Solutions:

TfbI: 30 mM Kac (1,47 g for 500 ml of TfbI)

100 mM RbCl (6,05 g for 500 ml of TfbI)

10 mM CaCl₂ x 2H₂O(0.74 g for 500 ml of TfbI)

15 % Glycerine (75 ml for 500 ml of TfbI)

adjust pH to 6 with HCl

50 mM MnCl₂ x 4H₂O(4.95 g for 500 ml of TfbI)

adjust pH to 5.8. Solution was sterile filtered.

TfbII: 10 mM MOPS (0.21 g for 100 ml of TfbII)

75 mM CaCl₂ x 2H₂O(1.10 g for 100 ml of TfbII)

10 mM RbCl (0.12 g for 100 ml of TfbII)

15 % Glycerine (15 ml for 100 ml of TfbII)
adjust pH to 6.5. Solution was sterile filtered

A single colony (*E. coli* TOP10) was inoculated into 2 ml LB-medium and incubated for 6 h at 37 °C under vigorous shaking. Afterwards 500 µl were inoculated into 500 ml LB-medium and incubated at 37 °C for 90min to 2.5h under vigorous shaking (w/o antibiotics). Solutions TfbI and TfbII were pre-cooled on ice. Bacteria were grown at 37 °C until an OD₆₀₀ ~0.3 was reached. Cells were then cooled down for 5 min on ice and pelleted at 3000 g for 1min at 4°C. The following steps were carried out at 4 °C with pre-cooled materials and solutions. Cell pellet was resuspended in 20 ml TfbI and kept on ice for 5 min before another centrifugation step for 1 min at 3000 g (4°C). Cells were subsequently resuspended in 1 ml TfbII and incubated on ice for 15 min. Chemocompetent cells were then transferred as 100µl aliquots in eppendorf tubes (pre-cooled) and shock-frozen in liquid nitrogen. Competent TOP10 cells were stored at -80 °C.

Cells were checked for competence by transformation of 100 µl competent cells with 10, 1, 0.1, 001 or 0.001 ng of pUC-18. Competence was >10⁶ (i.e. colonies per 1 µg of transformed vector).

Alternatively commercially available competent *E.coli* TOP10 cells (Invitrogen) were used for transformation.

6.2.1.9 Transformation of chemo-competent *E.coli*

Material: LB-medium
 Chemo-competent *E.coli*
 Bacterial agar plates

Chemo-competent cells were treated according to (Hanahan, 1983). Cells were thawed on ice, DNA (5-200 ng) was added to a 100 µl cell aliquot and incubated for 20 min on ice. Cells were heat-shocked for 60-120 s at 42 °C, and cooled on ice for 2 min. 900 µl LB medium were added and cells were incubated for 30-60 min at 37 °C on a roller shaker. Afterwards, different aliquots were plated on bacterial agar plates (50-500 µl) and incubated overnight at 37 °C.

6.2.1.10 Small scale DNA-preparation (MiniPrep)

For small scale DNA preparation (1-5 μg DNA), a single colony was inoculated into 2-3 ml LB medium supplemented with the appropriate antibiotic, and incubated overnight (or at least 8 hours) at 37 °C under vigorous shaking. The Qiagen MiniPrep Kit was used.

Small scale liquid cultures (1-2 ml) were transferred into an Eppendorf tube and centrifuged at 6.000 rpm for 5 min. Cells were resuspended in 250 μl P1-buffer and further processed according to the manufacturer's protocol. Finally plasmid-identity was confirmed by restriction digestion and analysis on agarose gels.

6.2.1.11 Large scale DNA-preparation (MaxiPrep)

For large scale DNA preparation (200-500 μg DNA), a 200 μl aliquot of a 2 ml pre-culture was inoculated into 200 ml LB-medium supplemented with the appropriate antibiotic, and incubated overnight (max. 16 h) at 37 °C under vigorous shaking. The Qiagen MaxiPrep kit, or the PureLink HiPure Plasmid MaxiPrep kit (Invitrogen) were used.

The liquid cell culture was centrifuged for 10 min at 6.000 rpm/4 °C. Cells were further processed according to the manufacturer's protocol. The DNA precipitated with isopropanol was dissolved in 500 μl H₂O and precipitated again with Ethanol as described (see "Ethanol Precipitation of DNA"). After centrifugation, the precipitated DNA was washed with 70 % Ethanol once and centrifuged for 5 min at 13.000 rpm. The DNA pellet was air-dried and dissolved in TE-buffer or H₂O.

6.2.1.12 Sequencing of DNA

Cloned plasmids were sequenced by MWG Eurofins, Martinsried, München.

6.2.2 Plasmids and Cloning of Constructs

6.2.2.1 Cloning of pCAG-*Trnp1*-GFP/dsRed

The coding region of *Trnp1* was subcloned into Gateway® (Invitrogen/Life Technologies) forms of pCAG-GFP or pCAG-dsRed (pCAG Destination vectors were kindly provided by Dr. Paolo Malatesta). To do so *Trnp1* coding sequence was first subcloned from pCMV-Sport6-*Trnp1* (RZPD) into pENTR1A and then cloned into the corresponding pCAG

vectors through Gateway LR-reactions. As in pCAG-GFP/dsRed the coding sequence of the gene of interest is connected through an internal ribosomal entry site to the coding sequence of GFP/dsRed ultimately generating one single mRNA holding both sequences and a poly-A signal at the end of the full mRNA, removal of the intrinsic poly-A signal of the gene of interest is necessary. Therefore, the poly-A signal and parts of the 3'-UTR were first removed from the initial pCMV-Sport6-Trnp1 expression clone by BamHI/XbaI digestion, reblunting and relegation. Subsequently, *Trnp1* cDNA was subcloned into pENTR1A via EcoRI/XhoI and *Trnp1* cDNA was then recombined into the pCAG destination vectors using Gateway® LR-reaction(Invitrogen/Life Technologies).

6.2.2.2 Cloning of pSUPER-shRNA constructs

For knock down of *Trnp1* three different shRNAs were created (target sequences were designed with the help of BlockIT (Invitrogen) and Oligoengine software). The following shRNAs were cloned into pSUPER according to the manufacturer's protocol (Oligoengine):

shRNA#1: 5'-ACTCTGCATTGCTTCCCATACTG-3';

shRNA#4: 5'-GCAGAAAGGCAAGCCACTTCT-3' and

shRNA#5: 5'-GATGGACGGCGTCATCTAC-3'.

According to the manufacturer's protocol (Oligoengine) pSUPER was digested with BglIII/HindIII and the plasmid fragment was cleaned up by agarose gel extraction. Annealed oligos were subsequently ligated into BglIII/HindIII digested pSUPER.

Note: Each of the shRNAs targets different regions within the 3'-UTR of *Trnp1*. Note that these shRNAs are able to knock down endogenous, full length *Trnp1* mRNA but that the target sequences are not contained in the retroviral pCAG-Trnp1-GFP/dsRed vectors (see above).

6.2.2.3 Cloning of pLVTHM-shRNA constructs

The three shRNAs were subcloned from the corresponding pSUPER construct into the lentiviral pLVTHM plasmid. For that purpose, ClaI/EcoRI excised fragments (including H1-Promoter plus the shRNA) from pSUPER were purified using agarose gel extraction and ligated with the ClaI/EcoRI digested backbone fragment of pLVTHM.

6.2.2.4 Cloning of pSUPER.GFP/Neo-shRNA constructs

For in vivo analysis all shRNAs used in this study were subcloned into pSUPER.GFP/Neo. The advantage of using this construct is the simultaneous expression of GFP from the same construct. ShRNAs were subcloned from the corresponding pSUPER construct into the pSUPER.GFP/Neo plasmid through EcoRI/XhoI excision of the shRNA fragments (including H1-Promoter plus the shRNA) from pSUPER (fragments were purified using agarose gel extraction) and ligation with the EcoRI/XhoI digested backbone fragment of pSUPER.GFP/Neo.

Note: As each of the shRNAs used in this study target different regions within the 3'-UTR of *Trnp1* which is not contained in the pCAG-Trnp1-GFP/dsRed vector (see above), pCAG-Trnp1-dsRed was also usable to rescue the knock down effect of shRNAs.

All constructs were verified by fully sequencing the insert before use in experiments. The constructs are all depicted in “9 – Plasmid maps”. For in vivo applications plasmids were produced under endotoxin free conditions (Qiagen EndoFree Plasmid Maxi Kit). Alternatively DNA purified from CsCl gradients was used.

6.2.3 Biochemical Protein Methods

6.2.3.1 Cell / Tissue Lysis

Cells or tissues were generally pelleted by centrifugation and shock frozen in liquid nitrogen and stored at - 80 °C until tissue Lysis.

RIPA buffer Lysis:

Generally cells or tissues were lysed using RIPA buffer (see 6.1.1.8) with the addition of complete protease inhibitor cocktail (Roche). Alternatively higher salt concentrations ranging from 300mM to 1M NaCl were used to release proteins bound to DNA. Other alterations also included the addition of EtBr (25 µg/µl end concentration) to release DNA bound proteins. An adequate amount of RIPA buffer was added to the cells / tissue (e.g.

100µl of RIPA to 2 E14 cortices or 150µl per 35mm dish of cultured cells) and homogenized by pipetting up and down with a 200 µl tip. The homogenates were sonicated in order to open nuclei and shear DNA (5 sec at 10 % power). Samples were centrifuged at 14.000rpm, 4°C for 30min to remove cellular debris and DNA. Supernatant was collected and protein concentration was measured using the BCA method.

Acidic extraction of DNA associated molecules using HRSB buffers:

Nuclei were first prepared by re-suspending the cellular pellet in 3 volumes of HRSB – 0.5 % NP40 (see 6.1.1.8). The mixture was kept for 10 minutes on ice and then homogenized by pipetting up and down 10 times with a 200 µl pipette tip. Nuclei suspension was pipetted on top of a 1 ml HRSB-Sucrose (see 6.1.1.8) and centrifuged for 5 min at 2400 g at 4 °C. Sedimented nuclei were reconstituted in 10 pellet volumes Extraction – EDTA buffer and kept on ice for 10 minutes followed by a centrifugation step at 3000 g at 4 °C. Supernatant was kept and labeled as washing fraction. For acidic extraction, the pellet was resuspended in 10 pellet volumes (or more) ice-cold 0.4 M HCl and kept on ice for 1 h. Samples were vortexed every 15 min during the 1 h incubation time. Samples were centrifuged for 10 min at 13 000 rpm and supernatant (acid supernatant containing most of DNA bound molecules) was collected. 8 volumes of acetone were added to the pellet, mixed and then stored at -20 °C overnight. The next day, acetone pellets were centrifuged at 4600 rpm for 10 min at 4 °C and pellets were washed with 0.5 ml acetone (-20°C), spun at 4600 rpm for 5 min. The pellet was dried and resuspended in 100 µl SDS loading buffer. Nuclei, washing fraction, acidic supernatant and acidic pellet were separated by SDS PAGE and western blotting was performed to detect the protein of interest.

Samples were generally resuspended in Laemmli buffer and boiled for 5 min at 95 °C and cooled down on ice prior to SDS PAGE. In general 5-30 µg of total protein were loaded per lane on an SDS gel.

6.2.3.2 Perchloric Acid Extraction

Perchloric acid extraction is used to extract highly basic proteins such as linker Histone H1 or high mobility group proteins (HMGs) according to the protocol described by (Lindner et al., 1998; Talasz et al., 2002). HEK cells transfected with peGFP Trnp1-GFP-N3 (to express Trnp1-GFP fusion protein) were pelleted and the pellet was resuspended in 3 pellet volumes of 6.6 % (w/v) HClO₄ (e.g. for a pellet of the size of 40 µl, 120 µl of 6.6 % HClO₄ were added) to reach an end concentration of roughly 5 % HClO₄. Eppendorf tubes were then rotated for 1 – 1.5 h at 4 °C. The insoluble material was then pelleted at 21 000 rcf for 5 min at 4 °C and the supernatant was subsequently dialyzed against 0.1 M acetic acid containing 1 mM DTT for 2 x 1 h at 4°C and 1 x overnight. at 4°C. The samples were filled up to a volume of 500 µl with 20 mM Tris, 1 mM DTT, pH 6.8 and then frozen at -80 °C (for minimum 30 minutes) and material was lyophilized overnight. For lyophilization (a.k.a freeze drying) the lids of the eppendorf tubes were covered with holes in order to make lyophilization possible. The pellet was then reconstituted in 50 – 100 µl (depending on size of the pellet) of 20 mM Tris, 1 mM DTT, pH 6.8. Coomassie Gels or western blotting was then performed to test for Trnp1 extraction.

6.2.3.3 SDS-Polyacrylamide gel electrophoresis (SDS-PAGE) (Tris-Glycine)

Tris-Glycine gels were prepared according to (Laemmli, 1970).

Solutions: 30 % (w/v) Acrylamide/Bis Solution (BioRad)
20 % (w/v) SDS (Sodium dodecylsulfate)
10 % (w/v) APS (Ammoniumperoxodisulfate)
TEMED

Buffers: separation gel buffer: 1.5 M Tris/HCl, pH 8.8
Stacking gel buffer: 0.5 M Tris/HCl, pH 6.8
1x running buffer: 25 mM Tris-base, 192 mM Glycine, 0.1 % SDS

Separating gel:

Gel Percentage	Acrylamide [ml]	2 M Tris, pH 8.8 [ml]	20 % SDS [μl]	ddH ₂ O [ml]	10 % APS [μl]	TEMED [μl]	Final volume [ml]
8 %	4.05	3.75	75	7.05	75	15	15
10 %	4.95	3.75	75	6.15	75	7.5	15
12%	6	3.75	75	5.1	75	7.5	15
14%	7.05	3.75	75	4.05	75	7.5	15

Stacking gel:

Acrylamide [ml]	1 M Tris, pH 6.8 [ml]	20 % SDS [μl]	ddH ₂ O [ml]	10 % APS [μl]	TEMED [μl]	Final volume [ml]
0.975	1.875	37.5	4.575	37.5	7.5	7.5

SDS PAGE was performed using the vertical Mini-PROTEAN 3 cell System (BIO-RAD 165-3301). Gels were polymerized with the corresponding gel casting system. After pouring the separation gel isopropanol was added on top as a thin layer in order to assure a defined boundary layer. As soon as the separating gel was polymerized (approximately 45min-1 h) isopropanol was removed and the remaining space washed with ddH₂O to remove remaining isopropanol residues. The stacking gel was poured and a comb pushed in the gel. After 30min protein samples could be loaded and electrophoresis was performed in 1x running buffer at 80V first (about 15 minutes to allow slow running through the stacking gel) and then at 150-200V when probes reached the separation gel.

6.2.3.4 Western blot (wet blot)

Transfer-buffer: 192 mM Glycine,
 25 mM Tris-Base,
 20 % Methanol

Following SDS-PAGE, the gel was equilibrated in transfer-buffer for 5 min. Whatman-sheets and a nitrocellulose or PVDF membrane were cut to the size of the gel and soaked in transfer-buffer. The gel and the membrane were sandwiched between soaked pieces of sponge pads, Whatman paper, and perforated plastic plates as follows:

Anode (+)
Sponge pad
3 Whatman-sheets
Nitrocellulose/PVDF
SDS gel
3 Whatman-sheets
Sponge pad
Cathode (-)

The transfer was performed in a blotting tank (Biorad) for 1h at 100V. Alternatively Gels were run overnight at 4°C 30V constant.

6.2.3.5 Western blot detection

Buffers: PBST: 1xPBS, 0.05% Tween20
10x TBST (Tris buffered saline Tween): 1M Tris/HCl
1.5 M NaCl
TBST: 1xTBS, 0.05 % Tween 20
Detection Kit: ECL-Kit (GE Healthcare)

After western blot transfer of the proteins to the nitrocellulose/PVDF membrane, nonspecific binding was blocked by incubation of the membrane for 1 h in 5 % (w/v) skimmed milk in TBST or PBST. The primary antibody was diluted in 5 % (w/v) skimmed milk in TBST or PBST to an appropriate concentration and the blot was incubated for 2-4 h at room temperature or alternatively overnight at 4 °C. Afterwards the membrane was briefly rinsed twice with TBST or PBST, and further incubated two times in TBST or PBST for 10 min. The appropriate secondary antibody (directed against the species of the primary antibody) conjugated to horseradish-peroxidase (HRP, dilution 1:10.000 in TBST or PBST) was incubated for 1 h at room temperature. The membrane was again rinsed

(twice with TBST or PBST) and washed two times in TBST or PBST for 10 min. The protein of interest was detected by enhanced chemical luminescence (ECL) utilizing the reaction of Luminol and H₂O₂, which is catalyzed by HRP. For this purpose, the membrane was incubated with the ECL reagent (GE Healthcare) and the chemiluminescence signal was visualized by exposure of Hyperfilm ECL (Amersham) films.

6.2.3.6 Reprobing of western blot membranes (stripping)

Stripping-buffer: 62.5 mM Tris/HCl pH 6.7
 100 mM β-Mercaptoethanol
 2 % SDS

For reprobing the membrane with different antibodies, the previously applied antibodies had to be removed first. For this purpose, stripping-buffer was preheated to 80 °C. The membrane was incubated in 100-200 ml preheated stripping-buffer on a horizontal shaker until room temperature was reached (30-45 min). The membrane was further washed several times in TBST (3-5 times). The blot was again blocked in TBST/5 % (w/v) skimmed milk for 1 h, and a new primary antibody could be applied as described.

6.2.3.7 Coomassie staining

Coomassie staining solution: 0.1 % (w/v) Coomassie Brilliant Blue R-250
 45 % (v/v) Methanol
 45 % (v/v) dd H₂O
 10 % (v/v) Acetic acid

Destaining/fixation solution: 30 % (v/v) Methanol
 60 % (v/v) dd H₂O
 10 % (v/v) Acetic acid

After SDS-PAGE, the gel was incubated with Coomassie-staining solution on a horizontal shaker for 30 min. Afterwards, the gel was washed several times with destaining solution on a horizontal shaker, until the nonspecific Coomassie background had been removed. The gel was rehydrated in ddH₂O for 1-3 h. Two sheets of Whatman-paper were soaked

with ddH₂O and the gel was put on top of the Whatman-papers and covered with sealing film.

Alternatively Colloidal Blue Staining Kit (Invitrogen/Life Technologies, Cat no. LC6025) was used according to the manufacturer's protocol.

6.2.3.8 Mass Spectrometry

For Mass Spectrometry protein probes were separated using SDS PAGE. Proteins on gels were fixed for 2h by incubation in a solution of 10 % acetic acid, 50 % methanol. Gels were then stained using colloidal blue staining kit and protein bands were excised and submitted to mass spectrometry. To avoid contamination of the samples with human proteins, the whole procedure was carried out with pharmaceutical water and with full coverage of all body parts (such as wearing a coat, gloves, a mask, glasses). Band excision was carried out under a laminar flow. Mass spectrometry was carried out by the "Zentrallabor für Proteinanalytik" (ZfP) at the LMU München.

6.2.4 *Trnp1* Antibody generation

Antibody recognition sites were selected as described in 4.1.1. Two different epitopes of Trnp1 were used to order antibodies generated by "Peptide Specialty Labs GmbH Heidelberg". Epitope1 consisting of 19 amino acids: AETPVEGQELQRWRQGASG and Epitope2 consisting of 20 amino acids: PEPDSPFRRSPPRGASPQR. Antibodies were raised in guinea pig. For each immunization serum of the animal was collected after 3 and after 4 immunizations (immunizations were carried out every other week). Specificity and affinity for Trnp1 protein were subsequently tested.

6.2.5 *Cell- and Tissue-Culture Methods*

6.2.5.1 Preparation of Coverslips coated with PDL

Cover glasses were first washed in acetone and further boiled for 30 minutes in ethanol containing 0.7% HCl. Cover slips were washed twice in 100% ethanol thereafter and dried

at room temperature. Subsequently cover glasses were sterilized through autoclaving for 2h at 180°C. One sterilized cover slip was added to each well of a 24 well plate and moistened with PBS. PBS was replaced by 1% poly-D-lysine (PDL) in PBS and glasses were incubated for at least 2h at 37°C. Afterwards cover slips were washed three to four times with autoclaved Millipore water. Plates were dried for 2h under a laminar flow and then stored at 4°C until use (usually within several days).

6.2.5.2 Cultivation of HEK cells

Culture medium: DMEM (Dulbecco's Modified Eagles Medium)
 10 % FCS
 1 % Penicillin/Streptomycin

The cells were cultivated at 37 °C and 5 % CO₂ in T-75 flasks. Cells were passaged with Trypsin-EDTA at 80% confluency. For passaging, cells were washed with sterile 1x PBS once, and trypsinized with 1.5 ml of Trypsin-EDTA for 3-5 min at 37 °C. The detached cells were re-suspended in 4.5 ml fresh growth medium until a single cell suspension was present. Aliquots (1/20-1/3) of the resuspended cells were plated on flasks containing 10-15ml ml fresh medium and equally distributed by gentle shaking.

6.2.5.3 Freezing of cells for long term storage

Freezing medium: 10 % (v/v) DMSO in growth medium
 20 % FCS and w/o antibiotics

Cells at 70-80 % confluency were used for freezing. HEK cells from a T-75 flask were trypsinized as described and transferred into 15 ml tubes with 10 ml of fresh medium. The cells were pelleted at 300g for 5 min and resuspended in 3-4.5 ml freezing medium. 1.5 ml aliquots were transferred into cryovials (Nunc). The vials were directly incubated in a cryobox (Nunc) containing Isopropanol at -80 °C overnight, and afterwards transferred into a liquid nitrogen tank.

6.2.5.4 Thawing cells

Cells frozen in liquid nitrogen were quickly thawed at 37 °C in a water bath. Cells were then transferred into a T-75 flask with 15 ml of fresh medium and equally distributed by gentle shaking. The medium was replaced the next day to remove residual DMSO.

6.2.5.5 Dissociated cell cultures of the embryonic cerebral cortex

Timed pregnant mice (E12 or E14) were anesthetized with CO₂ and sacrificed by cervical dislocation. Embryos were isolated by caesarian sections and immediately placed into ice cold Hanks balanced salt medium (HBSS) supplemented with 10 mM HEPES. Cortices were dissected from embryos (telencephalic hemispheres were separated and the ganglionic eminence, the hippocampal anlage, the olfactory bulbs and the meninges were removed) and pooled in ice cold HBSS containing 10 mM HEPES and spun down at 1200 rpm for 5 minutes. After addition of Dulbecco's modified Eagle medium (DMEM) containing 10% fetal calf serum (FCS) tissue was dissociated with a fire polished, filtered Pasteur pipette. Cells were again centrifuged at 1200 rpm for 5 minutes and resuspended in fresh medium (DMEM, 10% FCS). Cells were counted using a "Neubauer" microscope counting chamber and primary cortical cultures were plated on PDL coated coverslips at a density of $2,5 \times 10^5$ cells/well (in 100 µl volume per coverslip). 2 h later 400 µl medium was added and- if needed – cells were infected with a low titer (<25 particles) of virus. Medium changes and fixation after 7 days *in vitro* were performed as described previously (Heins, 2001; Costa et al., 2007; Asami et al., 2011). A clear separation of clones – each derived from a single cell could be achieved as described previously (Williams et al., 1991; Haubst et al., 2004; Costa et al., 2007) by using a low number of viral particles (<25 clones per well).

6.2.5.6 Transient transfection of cells with Lipofectamine

Cells were plated on 6 well dishes at 30-40 % confluency the day before transfection in 4 ml total volume. Prior transfection, growth medium was collected and replaced with OptiMEM. Cells were transfected with Lipofectamine2000 (Invitrogen) according to the manufacturer's protocol. 0.5 µg of plasmid DNA was used per well in a 12 well dish. Alternatively, 1,5-2 µg of plasmid DNA was used per well of a 6 well dish.

2-4 hours later, OptiMEM was replaced by conditioned medium (collected prior to transfection). Reporter expression was generally visible 12-16 h later.

6.2.5.7 Retroviral production

For Virus production all viral construct were purified using a caesium chloride density gradient centrifugation. Using this method ensures separation of supercoiled DNA from linear and open circular DNA. Viral production was performed with technical support by Simone Bauer, Ines Mühlhahn, Dr. Alexandra Lepier or Detlef Franzen.. Replication incompetent MLV based, VSV-G pseudo typed retroviruses of the different pCAG constructs (see above) were produced in GPG-293 packaging cells (Ory et al., 1996) as described previously (Tashiro et al., 2006; Heinrich et al., 2011). Packaging cells were transfected with the viral plasmids (pCAG constructs) and incubated in packaging medium for production. Viral particles in supernatant were collected after 48 h (first harvest) and 72 h (second harvest). Viral particles were filtered and estimation of the titer was performed as previously described (Hack et al., 2005) resulting in a typical titer of 5×10^7 /ml.

6.2.5.8 Time-lapse video microscopy

Live imaging of dissociated cultures from the embryonic cerebral cortex at E14 was performed (Costa et al., 2008; Eilken et al., 2009) with a cell observer (Zeiss) at a constant temperature of 37°C and 8 % CO₂. Phase contrast images were acquired every 5 minutes for 6-8 days using a 20x phase contrast objective (Zeiss) and an AxioCamHRm camera with a self-written VBA module remote controlling Zeiss AxioVision 4.7 software (Rieger and Schroeder, 2009). Single-cell tracking was performed using a self-written computer program (TTT) (Rieger and Schroeder, 2009). Movies were assembled using Image J 1.42q (National Institute of Health, USA) software with 3 frames per second.

6.2.5.9 Dual Luciferase reporter Assay

Transcriptional activity of Trnp1 on selected promoters was tested by luciferase reporter assay. The assays were performed in multipotent P19 teratocarcinoma cells that can easily be differentiated into neurons (by exposure to retinoic acid) thereby representing a cell line

with neurogenic potential. Cells were cultured in DMEMGlutaMAX, 10%FCS, Pen/Strep media and 20 h prior to transfection P19 cells were plated at a density of 8×10^5 cells per well (24 well plate) in media without antibiotics. Co-transfections of 1 μ g expression plasmid, 1 μ g of the promoter construct (driving firefly (*Photinus pyralis*) luciferase) and 0.1 μ g of Renilla-TK luciferase plasmid (Promega) (for control of transfection efficiency) was performed in medium w/o serum using Lipofectamine2000 (Invitrogen) according to the manufacturer's protocol. 4 hours after transfection, medium was changed and 48 hours later cell extracts were prepared for luciferase activity measurement with a luminometer (Berthold Centro LB 960) according to the manufacturer's instruction protocol (Promega). Relative light units were normalized to Renilla luciferase activity and then to control transduced cells.

As promoter constructs, the pGL3-based promoter plasmids containing the Tbr2 promoter or the Pax6 consensus sites P6CON (PD-binding site) were used. As expression plasmids, the retroviral vector constructs, expressing Trnp1 and Pax6 under the CAG promoter were used.

6.2.5.10 Fluorescence recovery after photo bleaching (FRAP)

In order to determine the strength of DNA-Protein interaction fluorescence recovery after photo bleaching (FRAP) is a commonly used technique. In this context FRAP is used to measure the speed of diffusion of one protein which correlates with the mobility of the same. The protein of interest is fused to a fluorescing protein such as GFP. The fusion protein is expressed *in vitro* and the fluorescent signal is bleached using a short laser pulse. The time of recovery is then recorded and a correlation between the speed of signal recovery and immobility/mobility of the protein can be visualized. Proteins tightly bound to cell compartments are immobile and thus will be slow in diffusion and recovery of the signal in the area that was bleached. The signal will recover slowly as compared to such that are freely available or loosely attached and mobile (Schermele et al., 2005). All FRAP experiments in this study were carried out in the laboratory of Professor Dr. Heinrich Leonhardt with the help of Katrin Schneider.

To express Trnp1 fused to GFP, C2C12 or HeLa cells and alternatively also murine primary cortical culture of embryonic day 14 were transfected with peGFP-Trnp1 with

Lipofectamine2000 as described (6.2.5.6). FRAP Experiments were then performed 48h later. Time lapse analysis was performed under 5% CO₂ atmosphere at 37°C with a spinning disc microscope (PerkinElmer, Ultra View Vox). The upper or left part of the nuclei were bleached with 100% laser intensity of the 488nm laser. Recovery was recorded with 20% laser intensity. Nuclei were imaged for 5 seconds before and 60 seconds after bleaching.

6.2.6 *In vivo* Methods

6.2.6.1 Animals

C57BL/6J wild-type mice were bred in the animal facility of the Helmholtz-Zentrum München and the day of the vaginal plug was considered embryonic day (E) 0. The day of birth is considered postnatal (P) day 0. Animals were kept in a 12h day-night cycle. All experimental procedures were performed in accordance with guidelines of the European Union and the government of upper Bavaria.

6.2.6.2 Anesthesia

For perfusion animals were anesthetized by intraperitoneal injection of Ketamine (Ketamine hydrochloride 100 µg per gram of bodyweight) and Rompun (Xylazinehydrochloride, 20 µg per g of bodyweight). For in utero operations mice were anaesthetized by intra-peritoneal (i.p.) injection of a solution containing Fentanyl (0.05 mg/kg), Midazolam (5 mg/kg) and Medetomidine (0.5 mg/kg) (Btm license number: 4518395). Anesthesia was terminated by subcutaneous injection of a solution containing Buprenorphine (0.1 mg/kg), Atipamezol (2.5 mg/kg), Flumazenil (0.5 mg/kg).

6.2.6.3 In utero Electroporations

Animals were operated as approved by the Government of Upper Bavaria under licence number 55.2-1-54-2531-144/07 and number 55.2-1-54-2532-79/11. E13.5 timed pregnant mice were anaesthetized as described above. In utero electroporations were done as described before (Saito, 2006). Briefly, the abdomen of the animal was depilated using common depilation cream. Uterine horns were exposed through caesarian section. Sterile,

pre-warmed saline (Ringer solution) was repeatedly applied during the operation to keep intestines moist. Animals were kept on a heating blanket during the whole process of operation. Plasmids (endotoxin free (!) DNA) were mixed with Fast Green (2.5 mg/ μ l, Sigma) and 1 μ l (at a concentration of 1 μ g/ μ l) was injected into the lateral ventricle by use of a glass capillary (self made with a micropipette puller) under illumination of the uterine horns by a halogen cold light. DNA was electroporated into the telencephalon with four pulses of 38 mV and 100 ms. After electroporation, the uterine horns were carefully repositioned into the abdominal cavity, which was then filled with pre-warmed saline. The abdominal wall was then sewn closed by surgical sutures with medical sewing equipment. Anesthesia was terminated as described above and animals were monitored.

One to three days later, animals were injected with BrdU intraperitoneally (if needed – depending on the experiment) and sacrificed one hour later. Animals were anesthetized with CO₂ and sacrificed by cervical dislocation. Embryos were dissected and brains were either fixed as described below (6.2.6.5) or used for FACS sorting.

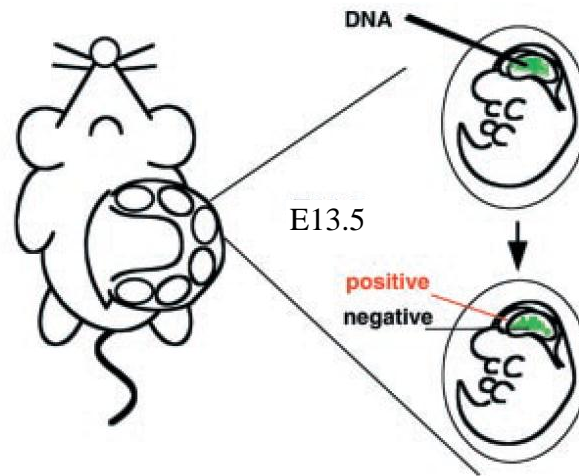


Figure 43 Schematic drawing of in utero electroporation
Adopted from Shimogori and Grove (2001)

6.2.6.4 BrdU administration

In order to label proliferating cells in S-phase 5-bromo-2'-deoxyuridine (BrdU, dissolved in saline) was injected intraperitoneally (5 mg per 100 g bodyweight). As a thymidine analogue BrdU is incorporated into newly synthesized DNA during S-phase thereby labeling proliferating cells. BrdU was administered one hour prior to sacrifice – thereby labeling acutely proliferating cells in S-phase at this time.

6.2.6.5 Fixation and Sectioning of Mouse Brains

Embryonic brains were fixed for 1,5-6 h (E10/E12: 1,5 h; E14: 2 h; E16/E16,5: 4 h; E18: 6 h) in 4 % Paraformaldehyde (PFA) (in PBS) with gentle rotation at 4 °C. Adult animals were perfused and brains were post fixed overnight in 4 %PFA (in PBS). Brains were then cryoprotected in 30 % sucrose (in PBS) overnight, embedded in tissue-tek and frozen on dry ice. Brains were stored at -20 °C until they were cryosectioned (12-30µm).

6.2.7 Immuno labeling

Cell cultures were fixed in 4 % PFA for 15 minutes and washed with PBS. For immuno labeling, sections of fixed brains (see above) or fixed cell cultures on coverslips were

blocked with 2 %BSA, 0.5 % Triton-X100 (in PBS) for 1 h prior to staining. Primary antibodies were applied in blocking solution overnight at 4 °C (cryosections) or for 2 h at room temperature (for coverslips). Sections or coverslips were washed at least three times in PBS, 0,1 % Triton-X100. Fluorescent secondary antibodies were applied according to the manufacturer's protocols (Jackson or Molecular Probes) for 2 h at RT. Following secondary antibody incubation the sections or coverslips were again washed at least three times with PBS, 0,1 % Triton-X100. To visualize nuclei, sections or cover glasses were incubated for 10 minutes in 0.1 µg/ml DAPI (4',6-Diamidin-2-phenylindol, Sigma). Sections were mounted in Aqua Polymount (Polyscience). Stainings were analyzed using Zeiss (LSM710) or Leica (SP5) confocal laser-scanning microscopes or, alternatively Zeiss AxioImager.M2 for fluorescence images.

Several Primary antibodies required one of the following specific pre-treatments to retrieve the antigen:

HCL pre-treatment: sections were pretreated with 2 N HCl for 30 min and subsequently neutralized with sodium-tetraborate (0.1 M Na₂B₄O₇, pH: 8,5) for 2 x 15 minutes prior to primary antibody incubation. This pre-treatment was especially necessary for Trnp1 and BrdU antibodies.

Citrate-buffer pre-treatment: Coverslips were boiled for 30 sec and sections for 8 min in 0.01 M sodium citrate (pH6) at 700 V in a microwave. This pre-treatment was necessary for Pax6 antibody (mIgG1 – Developmental Hybridoma Bank).

After pre-treatment, sections were washed extensively with PBS prior to incubation with the primary antibody. If co-labelling with two different primary antibodies required no pre-treatment for one antibody but pre-treatment for the other antibody, staining without pre-treatment was performed first. Antibody-antigen complexes were then post-fixed with 4 % PFA (in PBS) for 30 min at RT followed by several washing steps before pre-treatment was applied for the second primary antibody.

6.2.8 Fluorescence Activated Cell Sorting

To identify genes responding to overexpression or knock down of *Trnp1*, cortices from E14 embryos electroporated one day earlier (at E13 with either *Trnp1* overexpressing plasmid, shRNA plasmid or control plasmid) were dissected removing the ganglionic eminence, olfactory bulb and the hippocampal anlage as well as the meninges. Cortical cells were enzymatically dissociated using 0.05 % Trypsin/EDTA for 15 min at 37 °C with subsequent resuspension of cells in DMEM containing 10 % fetal calf serum (FCS) to stop the enzymatic reaction and a fire polished Pasteur pipette (pre-incubated in DMEM/FCS to coat the glass) was used to mechanically dissociate the cells. The cells were finally resuspended in PBS and GFP positive cells were isolated using the FACSariaIII (BD Bioscience) system at purity mode and a flow rate lower than 1200 cells per second for high purity. Forward- and sideward scatter were adjusted to exclude cell debris and include only GFP positive cells (endogenous GFP expression without staining using the 488nm laser) of interest. Gating for GFP fluorescent cells was set using WT cortical cells from non-electroporated embryos. To enhance efficiency of RNA extraction and RNA quality cells were directly sorted into RLT (QIAGEN®) buffer.

6.2.9 Microarray Analysis

RNA was isolated from FACS sorted GFP positive cells (from embryonic day 14 embryos – 4 different litters per condition, cells from different embryos were pooled per litter) (see 6.2.8) using the Rneasy Micro kit (Qiagen) or Rneasy Mini kit (Qiagen) according to the manufacturer's instructions including digestion of remaining genomic DNA. For microarray analysis RNA concentration and quality was measured using the Agilent 2100 Bioanalyzer. The Agilent software assigns a specific quality number to the RNA sample based on its electrophoretic profile. This RNA Integrity Number (RIN) ranges from 1 (reflecting totally degraded RNA) to 10 (reflecting completely intact RNA). For microarray analysis only high quality RNA (RIN > 7) is used. RIN values of the used samples ranged from 8.0 to 10.

For each microarray 0.5 – 2 ng of RNA per experiment was first amplified using the „Ovation Pico WTA System V2“ kit in combination with the Encore Biotin Module (Nugen). Then, 2.1 µg of amplified cDNA was hybridized to Affymetrix Gene ST 1.0

arrays (containing about 28.000 probe sets) according to the manufacturer's instructions. Expression console software (Affymetrix) was used for quality control and to obtain annotated normalized RMA gene-level data (standard settings including sketch-quantile normalization). The statistical analysis of the microarray data was performed by utilizing the statistical programming environment R (Team, 2005) implemented in CARMAweb (Rainer et al., 2006). Genewise testing for differential expression was done employing the limma *t*-test and Benjamini-Hochberg multiple testing correction (FDR < 10%). Datasets were filtered for average expression > 50 in at least one group (overexpression, knock down or WT) and for linear ratios > 1.5 x (o.e. / WT or kd / WT). Heatmaps were generated with CARMAweb. GO term and pathway enrichment analyses were done with GePS software (Genomatix, Germany) or Ingenuity Pathway software and significant terms ($p < 0.05$) were determined.

6.2.10 Data Analysis

Quantifications of cellular distributions after in utero electroporation were carried out on single optical sections (confocal microscopy). For each electroporated brain, sections of different rostral to caudal regions were used representing the full electroporated region. Each brain slice was analyzed in a 200 μ m radial stripe for GFP+ cell distribution, BrdU, Pax6 and Tbr2 percentage or numbers. For oRG quantifications, Pax6+ cells outside of the Tbr2+ dense cellular band (typically more than 200 μ m away from apical surface) were quantified. Quantifications are given as the mean \pm SEM. For the overexpression analysis (pCAG-GFP vs. pCAG-Trnp1-GFP) more than 4000 cells were quantified from 5 different embryos (from 3-4 different litters) for each control and overexpression. For the knock down analysis (pSUPER.GFP/Neo vs. pSUPER.GFP/Neo-shRNA) more than 3500 cells were quantified from 5 different embryos (from 2-4 different litters) for each control, knock down and rescue experiments.

For the *in-vitro* clonal analysis, clone size and clone composition of each clone was determined and the mean was calculated per experiment (5 coverslips per experiment, with less than 25 clones each) from 4 independent experiments.

Statistical significance was tested using nonparametric Mann-Whitney U-Test (also called Wilcoxon rank-sum test or Mann–Whitney–Wilcoxon (MWW) test) in the case of *in vivo* studies (in utero electroporations) and Students t-test in the case of *in vitro* studies. P-values less than 0.05 were considered significant.

7 Appendix

7.1 Mass Spectrometry Data

Mass spectrometry analysis showing top 100 proteins found with Trnp1-GFP pull down. Note that only proteins marked in yellow were reproducibly found in three independent replicates. All the other proteins were found in only one or two out of three replicates.

Accession	MW [kDa]	Description	GFP Average	GFP-Trnp1 Average	Trnp1/GFP	Log2 (Trnp1/GFP)
Q6NT89	23,5	TMF-regulated nuclear protein 1 OS=Homo sapiens GN=TRNP1	1,000E0	3,263E8	3,263E8	28,28
Q80Z11	23,1	TMF-regulated nuclear protein 1 OS=Mus musculus GN=Trnp1	1,000E0	2,672E8	2,672E8	27,99
gi225007648	114,6	ribonucleases P/MRP protein subunit POP1 [Homo sapiens]	1,000E0	7,441E7	7,441E7	26,15
Q76LN2	67,9	NADH-ubiquinone oxidoreductase chain 5 OS=Rousettus amplexicaudatus GN=MT-ND5	1,000E0	3,221E7	3,221E7	24,94
P34812	19,7	Allophycocyanin subunit B18 OS=Aglaothamnion neglectum GN=apcF	1,000E0	8,372E6	8,372E6	23,00
P31689	44,8	DnaJ homolog subfamily A member 1 OS=Homo sapiens GN=DNAJA1	1,000E0	8,065E6	8,065E6	22,94
P61026	22,5	Ras-related protein Rab-10 OS=Homo sapiens GN=RAB10	1,000E0	7,707E6	7,707E6	22,88
Q9Y3F4	38,4	Serine-threonine kinase receptor-associated protein OS=Homo sapiens GN=STRAP	1,000E0	7,206E6	7,206E6	22,78
P20674	16,8	Cytochrome c oxidase subunit 5A, mitochondrial OS=Homo sapiens GN=COX5A	1,000E0	7,165E6	7,165E6	22,77
Q96HS1	32,0	Serine/threonine-protein phosphatase PGAM5, mitochondrial OS=Homo sapiens	1,000E0	6,653E6	6,653E6	22,67
gi4506457	36,9	reticulocalbin-2 precursor [Homo sapiens]	1,000E0	6,027E6	6,027E6	22,52
P32007	32,9	ADP/ATP translocase 3 OS=Bos taurus GN=SLC25A6	1,000E0	5,475E6	5,475E6	22,38
gi30424655	23,4	ras-related protein Rab-6B [Mus musculus]	1,000E0	5,331E6	5,331E6	22,35
Q9Y230	51,1	RuvB-like 2 OS=Homo sapiens GN=RUVBL2	1,000E0	4,904E6	4,904E6	22,23
P48047	23,3	ATP synthase subunit O, mitochondrial OS=Homo sapiens GN=ATP5O	1,000E0	4,672E6	4,672E6	22,16
P31948	62,6	Stress-induced-phosphoprotein 1 OS=Homo sapiens GN=STIP1	1,000E0	4,532E6	4,532E6	22,11
O60884	45,7	DnaJ homolog subfamily A member 2 OS=Homo sapiens GN=DNAJA2	1,000E0	4,520E6	4,520E6	22,11
gi18390323	23,9	ras-related protein Rab-14 [Mus musculus]	1,000E0	4,506E6	4,506E6	22,10
gi83305924	39,6	Mitochondrial import inner membrane translocase subunit TIM50	1,000E0	3,808E6	3,808E6	21,86

Appendix

O95721	29,0	Synaptosomal-associated protein 29 OS=Homo sapiens GN=SNAP29	1,000E0	3,569E6	3,569E6	21,77
A6H767	45,3	Nucleosome assembly protein 1-like 1 OS=Bos taurus GN=NAP1L1	1,000E0	3,479E6	3,479E6	21,73
Q86YZ3	282,2	Hornerin OS=Homo sapiens GN=HRNR	1,000E0	3,380E6	3,380E6	21,69
Q96EY1	52,5	DnaJ homolog subfamily A member 3, mitochondrial OS=Homo sapiens GN=DNAJA3	1,000E0	3,291E6	3,291E6	21,65
Q9BVK6	27,3	Transmembrane emp24 domain-containing protein 9 OS=Homo sapiens GN=TMED9	1,000E0	3,252E6	3,252E6	21,63
Q53GQ0	34,3	Estradiol 17-beta-dehydrogenase 12 OS=Homo sapiens GN=HSD17B12	1,000E0	3,233E6	3,233E6	21,62
P36542	33,0	ATP synthase subunit gamma, mitochondrial OS=Homo sapiens GN=ATP5C1	1,000E0	3,163E6	3,163E6	21,59
Q9Y265	50,2	RuvB-like 1 OS=Homo sapiens GN=RUVBL1	1,000E0	3,067E6	3,067E6	21,55
O75534	88,8	Cold shock domain-containing protein E1 OS=Homo sapiens GN=CSDE1	1,000E0	2,273E6	2,273E6	21,12
O00161	23,3	Synaptosomal-associated protein 23 OS=Homo sapiens GN=SNAP23	1,000E0	2,253E6	2,253E6	21,10
O75190	36,1	DnaJ homolog subfamily B member 6 OS=Homo sapiens GN=DNAJB6	1,000E0	2,233E6	2,233E6	21,09
P62854	13,0	40S ribosomal protein S26 OS=Homo sapiens GN=RPS26	1,000E0	2,225E6	2,225E6	21,09
gi6755448	24,7	vesicle-trafficking protein SEC22b [Mus musculus]	1,000E0	2,109E6	2,109E6	21,01
P50402	29,0	Emerin OS=Homo sapiens GN=EMD	1,000E0	2,053E6	2,053E6	20,97
O43169	16,3	Cytochrome b5 type B OS=Homo sapiens GN=CYB5B	1,000E0	1,831E6	1,831E6	20,80
gi169164514	9,7	PREDICTED: barrier-to-autointegration factor-like [Homo sapiens]	1,000E0	1,814E6	1,814E6	20,79
Q86211	17,8	60S ribosomal protein L24 OS=Bos taurus GN=RPL24	1,000E0	1,812E6	1,812E6	20,79
P27708	242,8	CAD protein OS=Homo sapiens GN=CAD	1,000E0	1,732E6	1,732E6	20,72
P32322	33,3	Pyrroline-5-carboxylate reductase 1, mitochondrial OS=Homo sapiens GN=PYCR1	1,000E0	1,708E6	1,708E6	20,70
Q3MJ13	123,3	WD repeat-containing protein 72 OS=Homo sapiens GN=WDR72	1,000E0	1,667E6	1,667E6	20,67
O95816	23,8	BAG family molecular chaperone regulator 2 OS=Homo sapiens GN=BAG2	1,000E0	1,655E6	1,655E6	20,66
gi4759300	11,3	vesicle-associated membrane protein 3 [Homo sapiens]	1,000E0	1,569E6	1,569E6	20,58
Q9HCN8	23,6	Stromal cell-derived factor 2-like protein 1 OS=Homo sapiens GN=SDF2L1	1,000E0	1,563E6	1,563E6	20,58
P61019	23,5	Ras-related protein Rab-2A OS=Homo sapiens GN=RAB2A	1,000E0	1,553E6	1,553E6	20,57
P51149	23,5	Ras-related protein Rab-7a OS=Homo sapiens GN=RAB7A	1,000E0	1,513E6	1,513E6	20,53
O95831	66,9	Apoptosis-inducing factor 1, mitochondrial OS=Homo sapiens GN=AIFM1	1,000E0	1,469E6	1,469E6	20,49
gi288558822	34,1	Cyclin-dependent kinase 1; Short=CDK1	1,000E0	1,433E6	1,433E6	20,45
Q9Y3D0	17,7	UPF0195 protein FAM96B OS=Homo sapiens GN=FAM96B	1,000E0	1,339E6	1,339E6	20,35

Appendix

O14654	133,7	Insulin receptor substrate 4 OS=Homo sapiens GN=IRS4	1,000E0	1,316E6	1,316E6	20,33
P62873	37,4	Guanine nucleotide-binding protein subunit beta-1 OS=Homo sapiens GN=GNB1	1,000E0	1,269E6	1,269E6	20,28
O95292	27,2	Vesicle-associated membrane protein-associated protein B/C OS=Homo sapiens GN=VAPB	1,000E0	1,258E6	1,258E6	20,26
O15173	23,8	Membrane-associated progesterone receptor component 2 OS=Homo sapiens GN=PGRMC2	1,000E0	1,232E6	1,232E6	20,23
P51148	23,5	Ras-related protein Rab-5C OS=Homo sapiens GN=RAB5C	1,000E0	1,225E6	1,225E6	20,22
gi5453559	18,5	ATP synthase subunit d, mitochondrial isoform a [Homo sapiens]	1,000E0	1,149E6	1,149E6	20,13
P51970	20,1	NADH dehydrogenase 1 alpha subcomplex subunit 8 OS=Homo sapiens GN=NDUFA8	1,000E0	1,128E6	1,128E6	20,11
Q56JX8	17,2	40S ribosomal protein S13 OS=Bos taurus GN=RPS13	1,000E0	1,060E6	1,060E6	20,02
O14579	34,5	Coatomer subunit epsilon OS=Homo sapiens GN=COPE	1,000E0	1,042E6	1,042E6	19,99
P53597	36,2	Succinyl-CoA ligase subunit alpha, mitochondrial OS=Homo sapiens GN=SUCLG1	1,000E0	9,798E5	9,798E5	19,90
P09211	23,3	Glutathione S-transferase P OS=Homo sapiens GN=GSTP1	1,000E0	9,477E5	9,477E5	19,85
gi32454741	46,4	serpin H1 precursor [Homo sapiens]	1,000E0	9,242E5	9,242E5	19,82
Q0MQG6	30,1	NADH dehydrogenase iron-sulfur protein 3, mitochondrial OS=Pongo abelii GN=NDUFS3	1,000E0	9,128E5	9,128E5	19,80
O24111	17,1	40S ribosomal protein S5 (Fragment) OS=Nicotiana plumbaginifolia GN=RPS5	1,000E0	8,865E5	8,865E5	19,76
Q9BSD7	20,7	Nucleoside-triphosphatase C1orf57 OS=Homo sapiens GN=C1orf57	1,000E0	8,499E5	8,499E5	19,70
P17844	69,1	Probable ATP-dependent RNA helicase DDX5 OS=Homo sapiens GN=DDX5	1,000E0	8,105E5	8,105E5	19,63
P54920	33,2	Alpha-soluble NSF attachment protein OS=Homo sapiens GN=NAPA	1,000E0	8,037E5	8,037E5	19,62
A6H769	22,1	40S ribosomal protein S7 OS=Bos taurus GN=RPS7	1,000E0	7,819E5	7,819E5	19,58
P62701	29,6	40S ribosomal protein S4, X isoform OS=Homo sapiens GN=RPS4X	1,000E0	7,707E5	7,707E5	19,56
P00387	34,2	NADH-cytochrome b5 reductase 3 OS=Homo sapiens GN=CYB5R3	1,000E0	7,612E5	7,612E5	19,54
O14625	10,4	C-X-C motif chemokine 11 OS=Homo sapiens GN=CXCL11	1,000E0	7,267E5	7,267E5	19,47
Q9NTJ3	147,1	Structural maintenance of chromosomes protein 4 OS=Homo sapiens GN=SMC4	1,000E0	7,175E5	7,175E5	19,45
P49721	22,8	Proteasome subunit beta type-2 OS=Homo sapiens GN=PSMB2	1,000E0	6,902E5	6,902E5	19,40
Q13257	23,5	Mitotic spindle assembly checkpoint protein MAD2A OS=Homo sapiens GN=MAD2L1	1,000E0	6,886E5	6,886E5	19,39
Q15293	38,9	Reticulocalbin-1 OS=Homo sapiens GN=RCN1	1,000E0	6,775E5	6,775E5	19,37

Appendix

Q53H96	28,6	Pyrroline-5-carboxylate reductase 3 OS=Homo sapiens GN=PYCRL	1,000E0	6,754E5	6,754E5	19,37
Q8WUK0	22,8	Protein-tyrosine phosphatase mitochondrial 1 OS=Homo sapiens GN=PTPMT1	1,000E0	6,034E5	6,034E5	19,20
P40616	20,4	ADP-ribosylation factor-like protein 1 OS=Homo sapiens GN=ARL1	1,000E0	5,972E5	5,972E5	19,19
Q16099	107,2	Glutamate receptor, ionotropic kainate 4 OS=Homo sapiens GN=GRIK4	1,000E0	5,825E5	5,825E5	19,15
Q16637	31,8	Survival motor neuron protein OS=Homo sapiens GN=SMN1	1,000E0	5,575E5	5,575E5	19,09
P57088	28,0	Transmembrane protein 33 OS=Homo sapiens GN=TMEM33	1,000E0	5,542E5	5,542E5	19,08
O00483	9,4	NADH dehydrogenase 1 alpha subcomplex subunit 4 OS=Homo sapiens GN=NDUFA4	1,000E0	5,529E5	5,529E5	19,08
P29692	31,1	Elongation factor 1-delta OS=Homo sapiens GN=EEF1D	1,000E0	5,389E5	5,389E5	19,04
P21670	29,5	Proteasome subunit alpha type-4 OS=Rattus norvegicus GN=Psma4	1,000E0	5,154E5	5,154E5	18,98
P15880	31,3	40S ribosomal protein S2 OS=Homo sapiens GN=RPS2	1,000E0	5,127E5	5,127E5	18,97
O14980	123,3	Exportin-1 OS=Homo sapiens GN=XPO1	1,000E0	5,063E5	5,063E5	18,95
Q13409	71,4	Cytoplasmic dynein 1 intermediate chain 2 OS=Homo sapiens GN=DYNC1I2	1,000E0	4,948E5	4,948E5	18,92
O43819	29,8	Protein SCO2 homolog, mitochondrial OS=Homo sapiens GN=SCO2	1,000E0	4,847E5	4,847E5	18,89
gi51038269	31,1	complement inhibitory receptor [Homo sapiens]	1,000E0	4,825E5	4,825E5	18,88
gi8655683	36,1	hypothetical protein [Homo sapiens]	1,000E0	4,812E5	4,812E5	18,88
gi119590124	9,0	cornichon homolog 4 (Drosophila), isoform CRA_b [Homo sapiens]	1,000E0	4,770E5	4,770E5	18,86
Q15363	22,7	Transmembrane emp24 domain-containing protein 2 OS=Homo sapiens GN=TMED2	1,000E0	4,758E5	4,758E5	18,86
A6NIZ1	20,9	Ras-related protein Rap-1b-like protein OS=Homo sapiens	1,000E0	4,715E5	4,715E5	18,85
Q96C36	33,6	Pyrroline-5-carboxylate reductase 2 OS=Homo sapiens GN=PYCR2	1,000E0	4,714E5	4,714E5	18,85
Q9QZP1	30,4	Survival of motor neuron protein-interacting protein 1 OS=Rattus norvegicus GN=Sip1	1,000E0	4,687E5	4,687E5	18,84
O43592	109,9	Exportin-T OS=Homo sapiens GN=XPOT	1,000E0	4,497E5	4,497E5	18,78
Q12904	34,3	Aminoacyl tRNA synthetase complex-interacting multifunctional protein 1 GN=AIMP1	1,000E0	4,001E5	4,001E5	18,61
Q8N5K1	15,3	CDGSH iron sulfur domain-containing protein 2 OS=Homo sapiens GN=CISD2	1,000E0	3,946E5	3,946E5	18,59
P09543	47,5	2',3'-cyclic-nucleotide 3'-phosphodiesterase OS=Homo sapiens GN=CNP	1,000E0	3,937E5	3,937E5	18,59
O00165	31,6	HCLS1-associated protein X-1 OS=Homo sapiens GN=HAX1	1,000E0	3,933E5	3,933E5	18,59

Appendix

Q04898	11,6	Putative uncharacterized protein YMR321C OS= <i>Saccharomyces cerevisiae</i> GN=YMR321C	1,000E0	3,792E5	3,792E5	18,53
P52434	17,1	DNA-directed RNA polymerases I, II, and III subunit RPABC3 OS= <i>Homo sapiens</i> GN=POLR2H	1,000E0	3,759E5	3,759E5	18,52
Q5RFC2	64,9	Melanoma-associated antigen D2 OS= <i>Pongo abelii</i> GN=MAGED2	1,000E0	3,704E5	3,704E5	18,50

7.2 Transcriptome Analysis

7.2.1 *Trnp1* knock down versus control GFP electroporation (152 genes)

Transcriptome analysis of *Trnp1* knock-down (shRNA#5) electroporated cells versus control (GFP) electroporated embryonic cortical cells 24 hours post electroporation. 152 genes fulfilled the criteria of $p < 0.01$, a fold change ration of > 1.5 and average expression > 50 . Expression levels upon *Trnp1* overexpression are shown for comparison.

Probeset	Gene symbol or ID	Ratios ($p < 0.01$, ratio $> 1.5x$ Av > 50)	KD	OE	Ctrl	KD vs Ctrl	OE vs Ctrl	KD vs OE
Up regulated genes								
10584580	Snord14e	4,62	817	387	177	4,62	2,19	2,11
10398326	Meg3	4,54	982	349	217	4,54	1,61	2,81
10444589	Hspa1b	4,11	310	102	75	4,11	1,35	3,05
10366951	Ndufa4l2	3,85	90	22	23	3,85	0,93	4,15
10450369	Hspa1a	3,69	248	80	67	3,69	1,19	3,11
10582376	Fam38a	3,28	50	18	15	3,28	1,17	2,81
10450367	Hspa1b	2,72	285	111	105	2,72	1,06	2,57
10427095	Tenc1	2,71	51	20	19	2,71	1,05	2,60
10450365	ENSMUST00000082728	2,69	1071	630	397	2,69	1,58	1,70
10372324	Syt1	2,37	52	25	22	2,37	1,14	2,07
10407126	Plk2	2,37	388	159	164	2,37	0,97	2,43
10384885	Spnb2	2,29	388	180	169	2,29	1,07	2,15
10458843	Sema6a	2,24	171	138	76	2,24	1,80	1,25
10382360	D11Wsu47e	2,24	66	44	29	2,24	1,50	1,50
10487595	ENSMUST00000083123	2,12	58	33	27	2,12	1,20	1,77
10506781	2010305A19Rik	1,94	56	37	29	1,94	1,29	1,51
10524882	Wsb2	1,93	307	228	159	1,93	1,43	1,35
10491621	4932438A13Rik	1,93	63	27	32	1,93	0,84	2,29
10455967	2610318N02Rik	1,92	224	174	117	1,92	1,48	1,29
10443120	Ggnbp1	1,90	226	171	119	1,90	1,44	1,32
10422892	2410089E03Rik	1,89	117	83	62	1,89	1,34	1,41
10427862	Cdh6	1,86	155	149	84	1,86	1,78	1,05
10394805	2410018L13Rik	1,85	75	57	40	1,85	1,42	1,31
10581013	Cdh11	1,80	111	77	62	1,80	1,24	1,45
10399671	Hpcal1	1,78	72	52	41	1,78	1,27	1,40
10596281	Dnajc13	1,74	115	73	66	1,74	1,11	1,57
10433633	Mkl2	1,73	59	40	34	1,73	1,19	1,45
10365302	A230046K03Rik	1,72	201	123	117	1,72	1,05	1,64

Appendix

10503184	Chd7	1,72	280	214	163	1,72	1,31	1,31
10548940	Lmo3	1,71	175	120	102	1,71	1,17	1,46
10345704	ENSMUST00000083695	1,69	128	74	76	1,69	0,98	1,72
10508228	Zmym6	1,68	76	52	46	1,68	1,15	1,46
10355534	Tns1	1,68	108	67	65	1,68	1,04	1,61
10569494	Tnfrsf22	1,66	56	39	34	1,66	1,16	1,43
10394833	ENSMUST00000085626	1,66	52	43	31	1,66	1,36	1,22
10425623	Csdc2	1,64	78	77	47	1,64	1,63	1,01
10425799	Rnu12	1,63	89	88	55	1,63	1,60	1,02
10515688	Szt2	1,60	221	158	138	1,60	1,14	1,40
10448563	E4f1	1,58	94	74	60	1,58	1,24	1,28
10437852	4921513D23Rik	1,56	328	237	210	1,56	1,13	1,38
10422781	Rictor	1,56	85	62	54	1,56	1,13	1,37
10366409	Zfc3h1	1,54	135	94	88	1,54	1,07	1,44
10478854	Slc9a8	1,54	156	117	101	1,54	1,15	1,33
10493189	Mef2d	1,53	63	53	41	1,53	1,28	1,19
Down regulated genes								
10478401	Ttpal	0,66	37	45	56	0,66	0,80	0,83
10560983	Dedd2	0,66	37	45	56	0,66	0,80	0,83
10390618	Neurod2	0,66	387	541	584	0,66	0,93	0,72
10556658	9030624J02Rik	0,66	140	195	211	0,66	0,92	0,72
10376444	Hist3h2bb-ps	0,66	775	1041	1173	0,66	0,89	0,74
10448030	GENSCAN00000033295	0,66	70	107	106	0,66	1,01	0,65
10571567	Sorbs2	0,66	317	437	479	0,66	0,91	0,72
10433691	Ntan1	0,66	101	134	153	0,66	0,88	0,75
10447120	Tmem178	0,66	284	426	433	0,66	0,98	0,67
10384555	Aftph	0,66	162	227	247	0,66	0,92	0,72
10478962	2010011I20Rik	0,66	289	455	440	0,66	1,03	0,63
10542317	Cdkn1b	0,65	686	1069	1051	0,65	1,02	0,64
10376455	Hist3h2a	0,65	654	943	1004	0,65	0,94	0,69
10369779	Ado	0,65	54	69	83	0,65	0,84	0,78
10536429	Tmem106b	0,65	113	120	174	0,65	0,69	0,94
10582474	Chmp1a	0,65	52	83	80	0,65	1,04	0,62
10352548	Slc30a10	0,65	298	420	460	0,65	0,91	0,71
10510176	Smarca5	0,65	86	134	133	0,65	1,01	0,64
10553501	Slc17a6	0,64	198	314	307	0,64	1,03	0,63
10490950	Bhlhe22	0,64	50	72	78	0,64	0,93	0,69
10369989	Ddt	0,64	265	348	415	0,64	0,84	0,76
10478374	Gdap1l1	0,64	132	221	207	0,64	1,07	0,60
10545697	Dguok	0,63	44	60	69	0,63	0,87	0,73
10476401	Plcb1	0,63	114	160	180	0,63	0,89	0,71
10419073	Tspan14	0,63	169	173	268	0,63	0,65	0,98
10573048	Anapc10	0,63	43	58	69	0,63	0,85	0,74
10352092	Zfp238	0,62	606	822	970	0,62	0,85	0,74

Appendix

10430748	Rangap1	0,62	134	264	215	0,62	1,23	0,51
10399465	Fam84a	0,62	62	95	99	0,62	0,95	0,65
10474867	ENSMUST00000121613	0,62	103	154	165	0,62	0,93	0,67
10398195	Ccnk	0,62	268	378	432	0,62	0,87	0,71
10370914	Fam108a	0,62	77	114	124	0,62	0,92	0,67
10376459	ENSMUST00000116301	0,62	106	166	171	0,62	0,97	0,64
10460517	Brms1	0,62	35	53	57	0,62	0,93	0,66
10383012	Pgs1	0,62	47	76	76	0,62	1,00	0,62
10543802	Plxna4	0,62	256	377	414	0,62	0,91	0,68
10376603	Drg2	0,62	171	265	277	0,62	0,96	0,65
10591472	Cdc37	0,62	215	339	350	0,62	0,97	0,64
10388042	6330403K07Rik	0,62	625	1068	1016	0,62	1,05	0,59
10578763	Sap30	0,61	246	390	401	0,61	0,97	0,63
10597833	Sec22c	0,61	32	57	52	0,61	1,09	0,56
10439695	Tagln3	0,61	435	772	712	0,61	1,08	0,56
10544936	Neurod6	0,61	1373	1974	2255	0,61	0,88	0,70
10604053	Nkrf	0,61	78	128	129	0,61	1,00	0,61
10497673	Zmat3	0,60	71	85	118	0,60	0,71	0,85
10604100	Ndufa1	0,60	318	592	527	0,60	1,12	0,54
10538394	Plekha8	0,60	44	59	74	0,60	0,80	0,76
10483737	Atf2	0,60	219	345	364	0,60	0,95	0,63
10434758	St6gal1	0,60	110	181	183	0,60	0,99	0,61
10408081	Hist1h1b	0,60	1774	2944	2967	0,60	0,99	0,60
10576335	Def8	0,60	39	46	66	0,60	0,69	0,87
10524310	Ttc28	0,59	511	771	862	0,59	0,89	0,66
10391454	Vat1	0,59	202	289	342	0,59	0,85	0,70
10486166	Ccdc32	0,59	130	225	219	0,59	1,03	0,58
10469514	Bmi1	0,59	161	210	273	0,59	0,77	0,77
10388520	Glod4	0,59	79	108	135	0,59	0,80	0,73
10464586	Gstp2	0,59	244	341	417	0,59	0,82	0,72
10494288	Golph3l	0,59	126	211	215	0,59	0,98	0,60
10529305	Tmem129	0,59	62	99	106	0,59	0,93	0,63
10437205	Pcp4	0,58	378	507	647	0,58	0,78	0,75
10360202	Nhlh1	0,58	421	601	722	0,58	0,83	0,70
10572757	Rab8a	0,58	221	382	380	0,58	1,00	0,58
10465209	Mtvr2	0,58	361	591	621	0,58	0,95	0,61
10503259	Trp53inp1	0,58	245	359	422	0,58	0,85	0,68
10410370	Zfp71-rs1	0,58	46	75	79	0,58	0,94	0,61
10547173	Zfp422	0,58	69	103	120	0,58	0,86	0,67
10535184	Psmg3	0,57	71	136	125	0,57	1,09	0,52
10411508	Ptcd2	0,57	67	141	117	0,57	1,20	0,48
10591517	Cdkn2d	0,57	116	178	203	0,57	0,87	0,65
10548857	Hist4h4	0,57	219	399	387	0,57	1,03	0,55
10382300	Map2k6	0,56	125	204	221	0,56	0,92	0,61

Appendix

10591726	Ecsit	0,56	58	78	103	0,56	0,76	0,74
10550597	Fbxo46	0,56	106	129	189	0,56	0,68	0,82
10529708	Zfp518b	0,56	123	203	220	0,56	0,92	0,61
10410341	Zfp87	0,55	83	139	151	0,55	0,92	0,60
10459604	4933403F05Rik	0,55	50	77	91	0,55	0,84	0,65
10579341	Mpv17l2	0,55	294	437	540	0,55	0,81	0,67
10469046	Phyh	0,55	85	83	156	0,55	0,53	1,03
10577999	Unc5d	0,54	70	99	132	0,54	0,76	0,71
10511498	Plekhf2	0,54	127	224	238	0,54	0,94	0,57
10408200	Hist1h4f	0,53	467	764	877	0,53	0,87	0,61
10558029	Sec23ip	0,53	118	178	224	0,53	0,80	0,66
10427991	Trio	0,53	50	107	94	0,53	1,13	0,46
10488589	Fam110a	0,52	216	375	420	0,52	0,89	0,58
10531610	Rasgef1b	0,51	228	406	443	0,51	0,92	0,56
10496621	Gtf2b	0,51	161	287	316	0,51	0,91	0,56
10430593	Josd1	0,51	127	245	250	0,51	0,98	0,52
10608656	NM_024475.3	0,50	53	101	106	0,50	0,96	0,53
10397882	Chga	0,49	112	180	229	0,49	0,79	0,62
10440344	Robo2	0,49	187	320	384	0,49	0,83	0,58
10568553	Chst15	0,48	81	145	171	0,48	0,85	0,56
10601878	Tceal1	0,46	71	134	154	0,46	0,87	0,53
10378024	Mis12	0,45	71	180	156	0,45	1,16	0,39
10574096	Ap3s1	0,44	384	865	867	0,44	1,00	0,44
10604230	Ap3s1	0,44	398	863	901	0,44	0,96	0,46
10455542	Ap3s1	0,44	374	861	856	0,44	1,01	0,43
10361055	Vash2	0,43	49	87	114	0,43	0,76	0,57
10381416	Rnd2	0,43	139	244	321	0,43	0,76	0,57
10499643	Chrn2	0,43	44	95	103	0,43	0,93	0,46
10567999	Ccdc101	0,43	29	64	69	0,43	0,93	0,46
10473349	Ypel4	0,42	102	118	245	0,42	0,48	0,86
10408225	Hist1h4c	0,39	359	907	925	0,39	0,98	0,40
10576639	Nrp1	0,38	110	235	290	0,38	0,81	0,47
10484276	Neurod1	0,37	167	429	448	0,37	0,96	0,39
10389238	Dusp14	0,36	137	322	377	0,36	0,86	0,43
10422052	Commd6	0,32	81	168	256	0,32	0,66	0,48
10371379	Nuak1	0,31	110	315	351	0,31	0,90	0,35
10453555	2610044O15Rik	0,30	22	45	73	0,30	0,62	0,49

7.2.2 *Trnp1* overexpression vs. control GFP electroporation (31 genes)

Transcriptome analysis of embryonic cortical cells electroporated for overexpression of *Trnp1* compared to cells electroporated with GFP control. 31 genes fulfilled the criteria of $p < 0.01$, average expression levels of > 50 and fold change ratios of > 1.5 . Expression levels upon *Trnp1* knock down are shown for comparison.

Probeset	Gene symbol or ID	Ratios ($p < 0.01$, ratio > 1.5 , Av > 50)	KD	OE	Ctrl	KD vs Ctrl	OE vs Ctrl	KD vs OE
Up-regulated genes								
10543058	Dlx5	8,61	182	221	26	7,11	8,61	0,83
10472809	Dlx1	5,42	156	143	26	5,94	5,42	1,10
10483626	Dlx2	4,94	148	169	34	4,31	4,94	0,87
10601612	Atrn	3,09	27	60	19	1,38	3,09	0,45
10556611	ENSMUST00000083940	2,88	44	60	21	2,10	2,88	0,73
10396466	1700086L19Rik	2,65	43	58	22	1,98	2,65	0,75
10584580	Snord14e	2,19	817	387	177	4,62	2,19	2,11
10360832	1700056E22Rik	2,18	81	101	46	1,75	2,18	0,80
10357948	Ppp1r12b	2,17	101	126	58	1,74	2,17	0,80
10384504	Meis1	1,71	52	62	36	1,44	1,71	0,84
10381462	Rdm1	1,70	54	79	46	1,16	1,70	0,68
10539220	AW146020	1,69	48	59	35	1,40	1,69	0,83
10451860	Pot1b	1,69	76	107	63	1,20	1,69	0,71
10565570	4632434I11Rik	1,64	47	70	43	1,11	1,64	0,68
10425623	Csdc2	1,63	78	77	47	1,64	1,63	1,01
10543118	Glcci1	1,62	226	262	161	1,40	1,62	0,86
10398326	Meg3	1,61	982	349	217	4,54	1,61	2,81
10586416	Pif1	1,60	50	69	43	1,16	1,60	0,72
10382508	Ict1	1,60	193	327	205	0,94	1,60	0,59
10458767	Trim36	1,59	64	75	47	1,37	1,59	0,86
10443459	Srsf3	1,58	245	385	243	1,01	1,58	0,64
10599719	Slc9a6	1,57	55	51	32	1,71	1,57	1,09
10490653	Gmeb2	1,55	78	107	69	1,13	1,55	0,73
Down-regulated genes								
10460085	Cndp2	0,66	102	77	116	0,88	0,66	1,33
10452030	Plin3	0,66	40	38	58	0,70	0,66	1,06
10419073	Tspan14	0,65	169	173	268	0,63	0,65	0,98
10521907	1810013D10Rik	0,56	63	60	107	0,59	0,56	1,04
10469046	Phyh	0,53	85	83	156	0,55	0,53	1,03
10445338	Enpp5	0,51	107	50	97	1,09	0,51	2,13
10473349	Ypel4	0,48	102	118	245	0,42	0,48	0,86
10444068	Tapbp	0,43	71	49	115	0,62	0,43	1,44

7.3 Abbreviations

Amino acids		
A	Ala	Alanine
R	Arg	Arginine
N	Asn	Asparagine
D	Asp	Aspartate
C	Cys	Cysteine
Q	Gln	Glutamine
E	Glu	Glutamate
G	Gly	Glycine
H	His	Histidine
I	Ile	Isoleucine
L	Leu	Leucine
K	Lys	Lysine
M	Met	Methionine
F	Phe	Phenylalanine
P	Pro	Proline
S	Ser	Serine
T	Thr	Threonine
W	Trp	Tryptophan
Y	Tyr	Tyrosine
V	Val	Valine

Nucleobases	
A	Adenine
C	Thymine
G	Guanine
T	Cytosine
U	Uracil

Appendix

General Abbreviations	
%	Percent
°C	Degrees Celsius
3'-UTR	3'-UnTranslated Region
5'-UTR	5'-UnTranslated Region
aa	amino acid
APS	Amonium PerSulfate
bHLH	Basic Helix Loop Helix
bp	base pair
BP	Basal Progenitors
BrdU	5-Bromo-2'-deoxyUridine
bRG	basal Radial Glia (also called oRG)
BSA	Bovine Serum Albumine
cDNA	complementary DeoxyriboNucleic Acid
CNS	Central Nervous System
CP	Cortical Plate
Ctx	Cortex
DAPI	4',6-DiAmidin-2-PhenylIndol
Dcx	Doublecortin
dd	double distilled (ultrapure)
DG	Dentate Gyrus
Dlx	Distal less homeobox
DMEM	Dulbecco's Modified Eagle Medium

DNA	DeoxyriboNucleic Acid
dNTP	deoxyriboNucleoside TriPhoshate
ds	double stranded (DNA/RNA)
<i>E.coli</i>	Escherichia coli
FACS	Fluorescence Activated Cell Sorting
FCS	Fetal Calf Serum
FRAP	Fluorescence Recovery after Photobleaching
g	grams
GABA	Gamma-Amino Butyric Acid
GCL	Granule Cell Layer
GE	Ganglionic Eminence
GFAP	Glial Fibrillary Acidic Protein
GFP	Green Fluorescent Protein
GL	Glomerular Layer
h	hours
HBSS	Hank's Balanced Salt Solution
HCl	Hydrochloric acid
HEPES	4-(2-Hydroxyethyl)-1-piperazineethanesulfonic acid
HRP	HorseRadish Peroxidase
IgG/IgM	Immunoglobuline G/M
INM	Interkinetic Nuclear Migration
IRES	Internal Ribosomal Entry Site

Appendix

ISH	In Situ Hybridization
IZ	Intermediate Zone
kb	kilobase
kDa	kiloDalton
kg	kilograms
LB	Luria-Bertani medium
LGE	Lateral Ganglionic Eminence
Mash1	Mammalian achaete scute homologue 1
MGE	Medial Ganglionic Eminence
min	minute
ng	nanograms
Ngn2	Neurogenine 2
NP-40	Nonidet P-40
o.N.	Over Night
OB	Olfactory Bulb
oRG	outer Radial Glia (also called bRG)
PAGE	PolyAcrylamide Gel Electrophoresis
Pax6	Paired box gene 6
PBS	Phosphate Buffered Saline
PCR	Polymerase Chain Reaction
PDGFRα	Platelet Derived Growth Factor Receptor α
PDL	Poly-D-lysine
PFA	ParaFormAldehyde

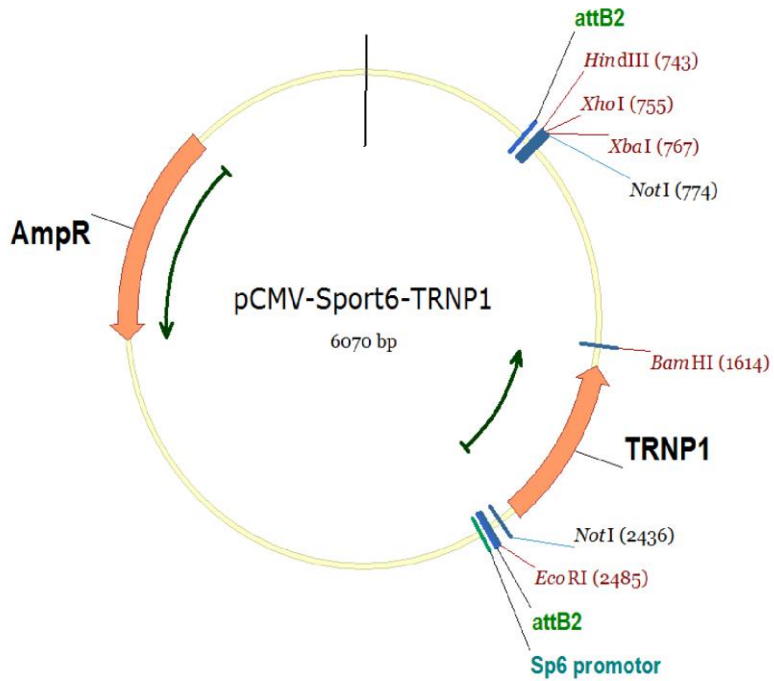
PH3	Phospho-Histone 3
RC2	Radial glial Cell marker 2
RG	Radial Glia
RMS	Rostral Migratory Stream
RNA	RiboNucleic Acid
rpm	revolutions per minute
RT	Room Temperature
s	seconds
SDM	Standard Deviation 142ft he Mean
SDS	Sodium DodecylSulfate
SEM	Standard Error of the Mean
SEZ	SubEpendymal Zone
SGZ	SubGranular Zone
shRNA	Short hairpin RNA
ss	single stranded (DNA/RNA)
SVZ	Subventricular Zone
TAE	Tris Acetate EDTA buffer
TAP	Transit Amplifying Precursor
TBR1/2	T-Box tRanscription factor 1/2
TBS	Tris Buffered Saline
TBST	Tris Buffered Saline with Tween 20
TE	Tris-EDTA buffer
TEMED	N, N, N', N'-TetraMethyl-EthylenDiamine

Appendix

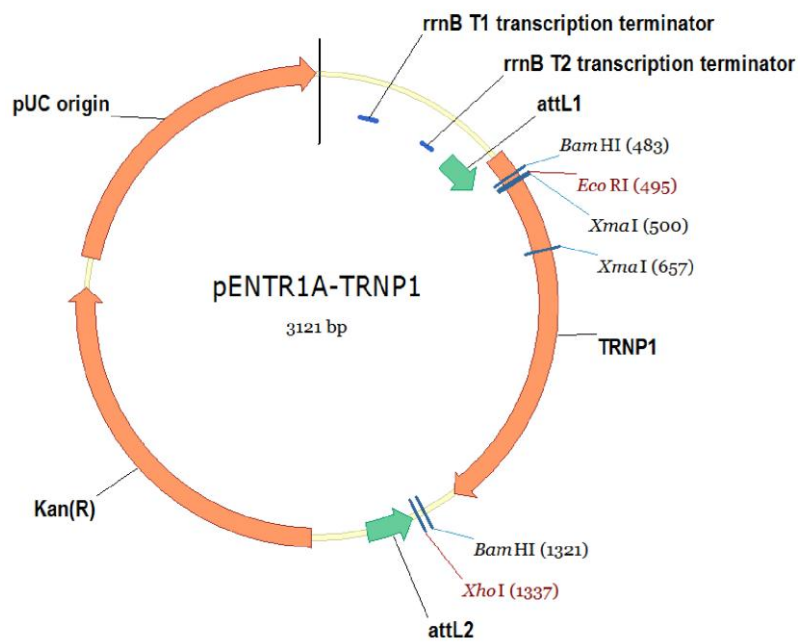
Tris	Tris-(Hydroxymethyl)-aminomethane
Trnp1	TMF regulated nuclear protein 1
Tween 20	polyoxyethylensorbitan-monolaurate
U	enzyme units
UV	UltraViolet light
V	Volts
v/v	volume per volume
VZ	Ventricular Zone
w/o	without
w/v	weight per volume
wt	wild type
µg	Microgram(s)
µl	Microlitre(s)

8 Plasmid maps

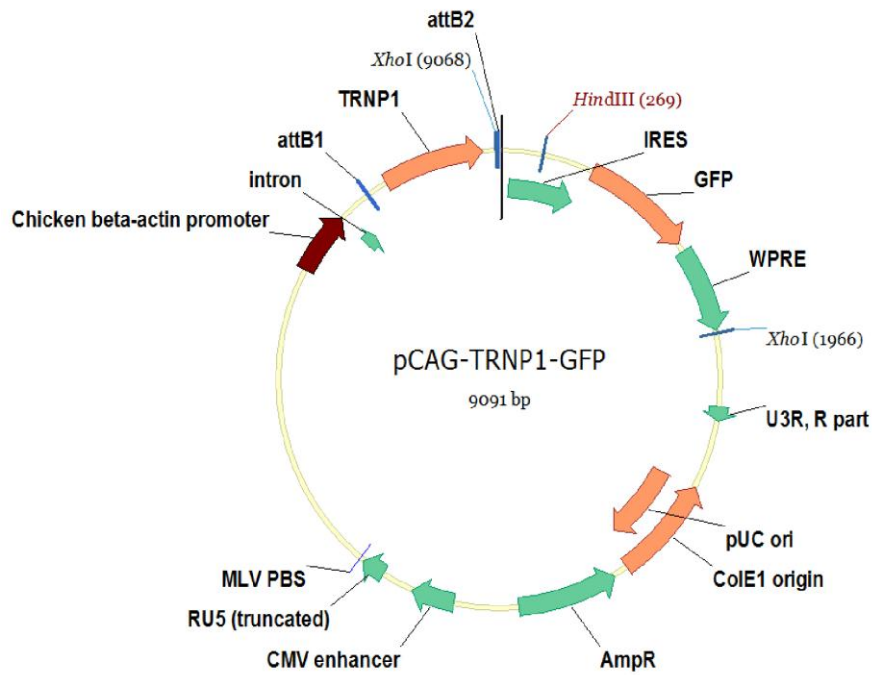
8.1 pCMV-Sport6-Trnp1



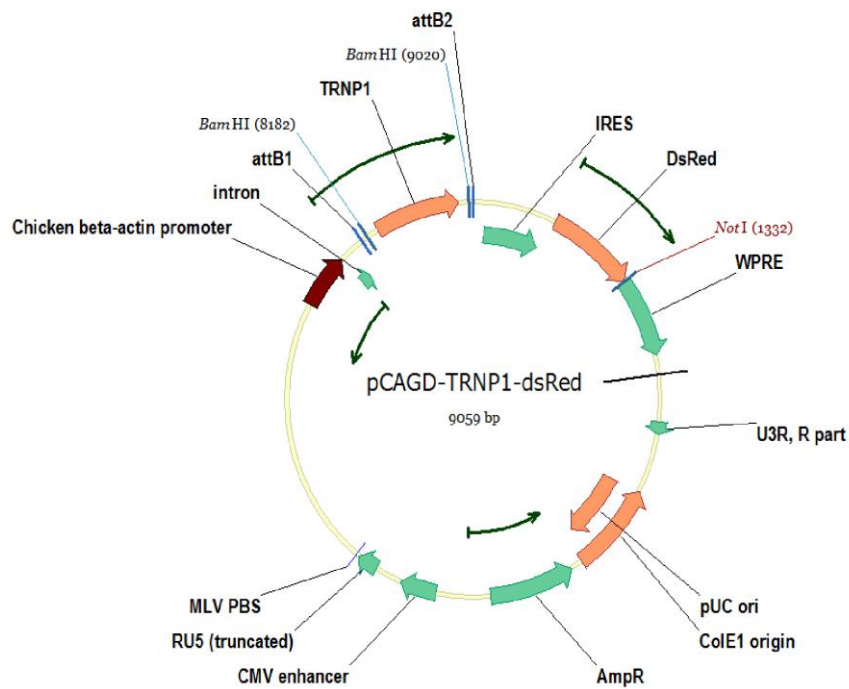
8.2 pENTR1A-Trnp1



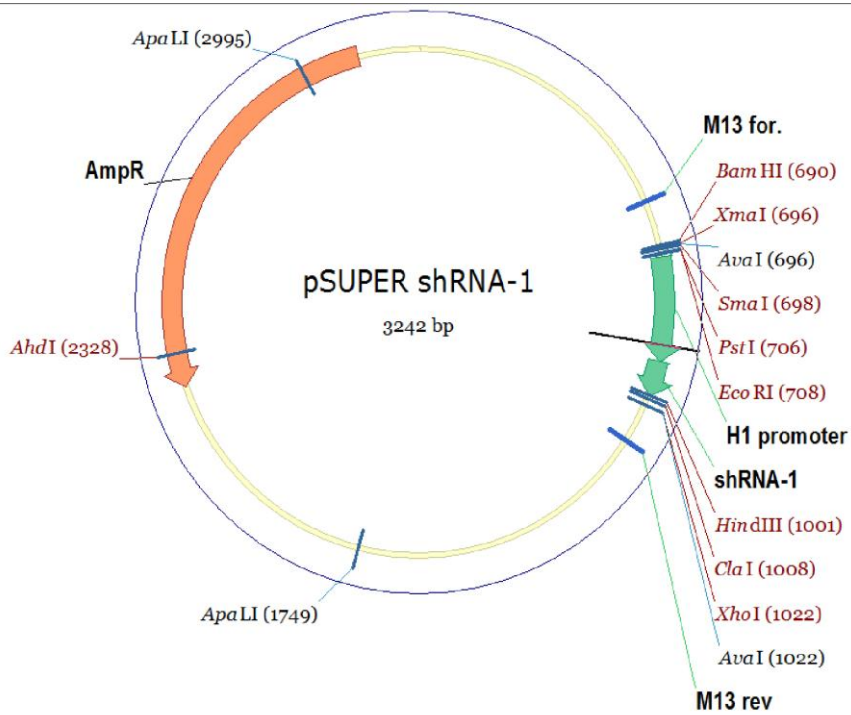
8.3 pCAG-Trnp1-GFP



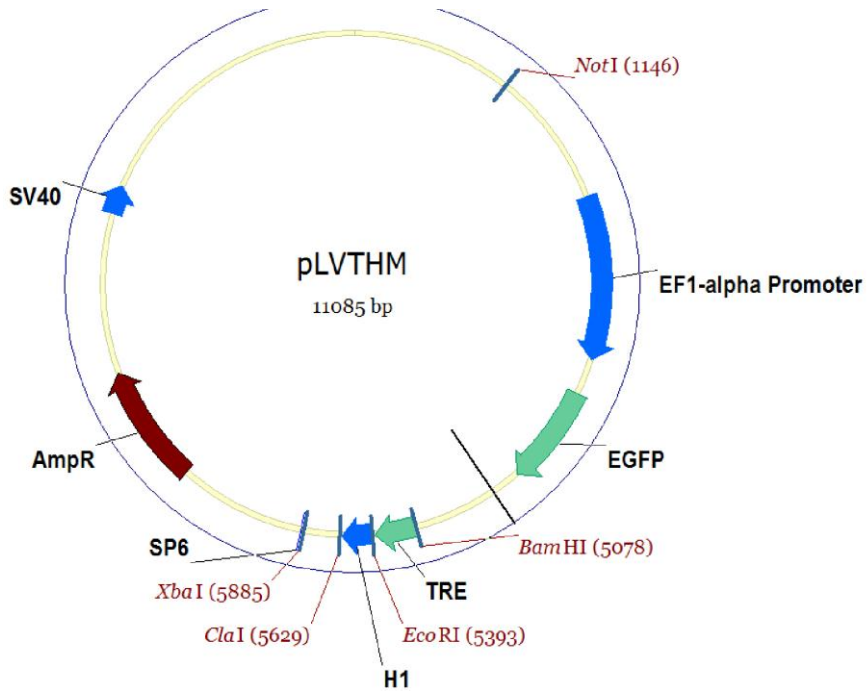
8.4 pCAG-*Trnp1*-dsRed



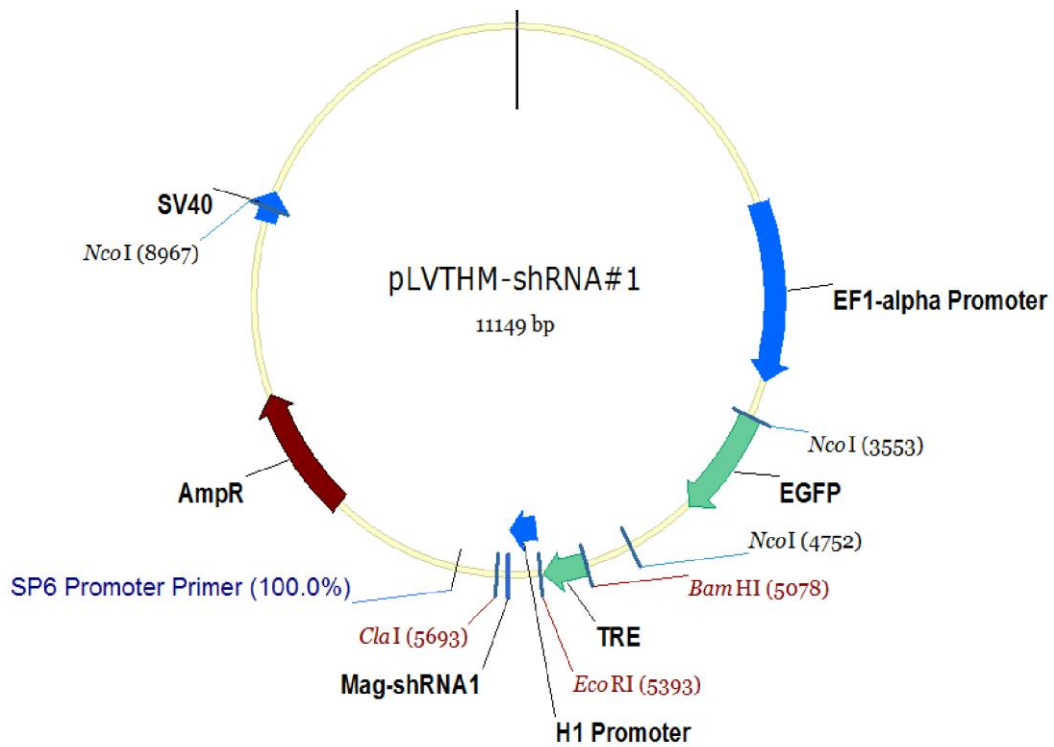
8.5 pSUPER-shRNA



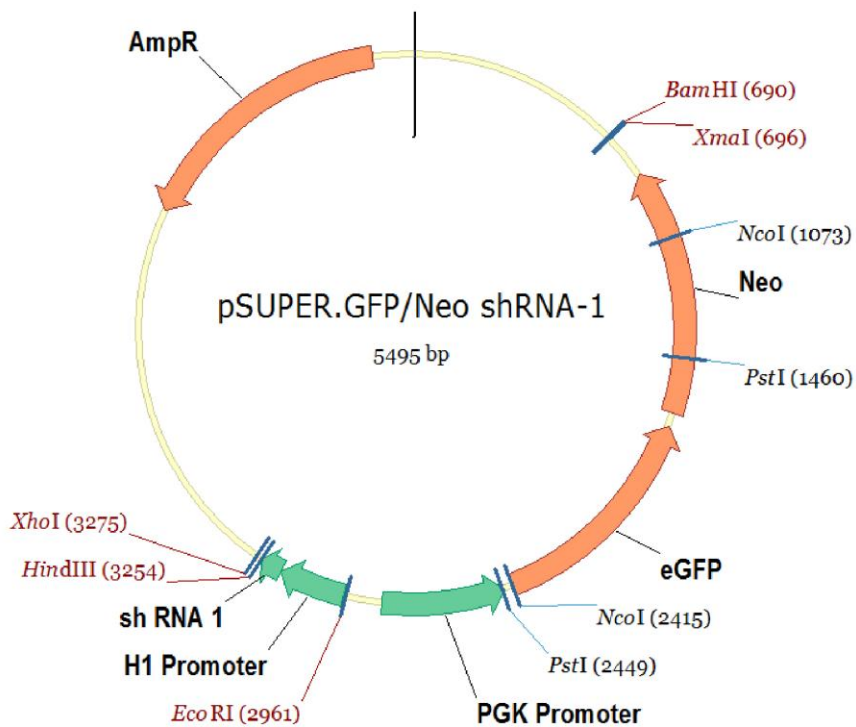
8.6 pLVTHM



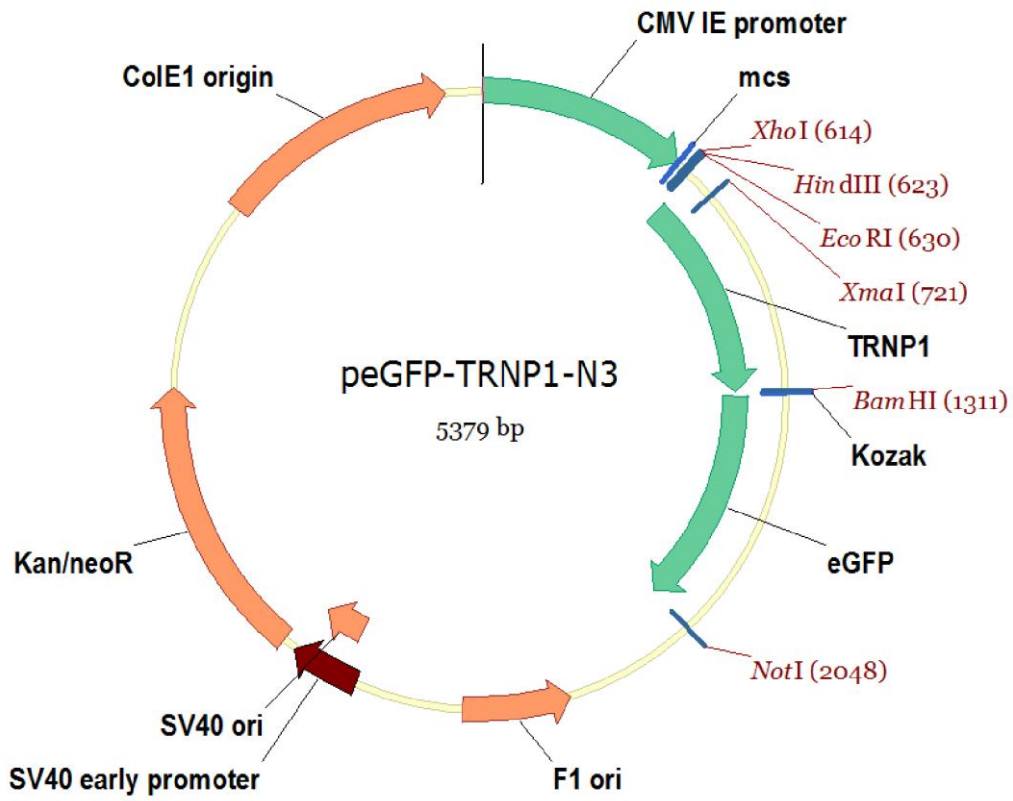
8.7 pLVTHM-shRNA



8.8 pSUPER.GFP/Neo-shRNA



8.9 peGFP-Trnp1-N3



9 References

- Altman J (1963) Autoradiographic investigation of cell proliferation in the brains of rats and cats. *Anat Rec* 145:573–591.
- Altman J (1969) Autoradiographic and histological studies of postnatal neurogenesis. IV. Cell proliferation and migration in the anterior forebrain, with special reference to persisting neurogenesis in the olfactory bulb. *J Comp Neurol* 137:433–457.
- Altman J, Bayer SA (1990) Mosaic organization of the hippocampal neuroepithelium and the multiple germinal sources of dentate granule cells. *J Comp Neurol* 301:325–342.
- Altman J, Das GD (1965) Autoradiographic and histological evidence of postnatal hippocampal neurogenesis in rats. *J Comp Neurol* 124:319–335.
- Altman J, Das GD (1966) Autoradiographic and histological studies of postnatal neurogenesis. I. A longitudinal investigation of the kinetics, migration and transformation of cells incorporating tritiated thymidine in neonate rats, with special reference to postnatal neurogenesis in some brain regions. *J Comp Neurol* 126:337–389.
- Alvarez-Buylla A, Lim DA (2004) For the long run: maintaining germinal niches in the adult brain. *Neuron* 41:683–686.
- Alvarez-Buylla A, Theelen M, Nottebohm F (1988) Mapping of radial glia and of a new cell type in adult canary brain. *J Neurosci* 8:2707–2712.
- Alvarez-Buylla A, Theelen M, Nottebohm F (1990) Proliferation “hot spots” in adult avian ventricular zone reveal radial cell division. *Neuron* 5:101–109.
- Armstrong L (2012) Epigenetic control of embryonic stem cell differentiation. *Stem Cell Rev* 8:67–77.
- Arnold SJ, Huang G-J, Cheung AFP, Era T, Nishikawa S-I, Bikoff EK, Molnár Z, Robertson EJ, Groszer M (2008) The T-box transcription factor Eomes/Tbr2 regulates neurogenesis in the cortical subventricular zone. *Genes & Development* 22:2479–2484.
- Asami M, Pilz GA, Ninkovic J, Godinho L, Schroeder T, Huttner WB, Götz M (2011) The role of Pax6 in regulating the orientation and mode of cell division of progenitors in the mouse cerebral cortex. *Development* 138:5067–5078 Available at: <http://eutils.ncbi.nlm.nih.gov/entrez/eutils/elink.fcgi?dbfrom=pubmed&id=22031545&retmode=ref&cmd=prlinks>.

References

- Azuara V, Perry P, Sauer S, Spivakov M, Jørgensen HF, John RM, Gouti M, Casanova M, Warnes G, Merckenschlager M, Fisher AG (2006) Chromatin signatures of pluripotent cell lines. *Nat Cell Biol* 8:532–538.
- Baala L, Briault S, Etchevers HC, Laumonnier F, Natiq A, Amiel J, Boddaert N, Picard C, Sbiti A, Asermouh A, Attié-Bitach T, Encha-Razavi F, Munnich A, Sefiani A, Lyonnet S (2007) Homozygous silencing of T-box transcription factor EOMES leads to microcephaly with polymicrogyria and corpus callosum agenesis. *Nat Genet* 39:454–456.
- Babbio F, Castiglioni I, Cassina C, Gariboldi MB, Pistore C, Magnani E, Badaracco G, Monti E, Bonapace IM (2012) Knock-down of methyl CpG-binding protein 2 (MeCP2) causes alterations in cell proliferation and nuclear lamins expression in mammalian cells. *BMC Cell Biol* 13:19.
- Bayer SA, Altman J, Russo RJ, Dai XF, Simmons JA (1991) Cell migration in the rat embryonic neocortex. *J Comp Neurol* 307:499–516.
- Bayer SA, Yackel JW, Puri PS (1982) Neurons in the rat dentate gyrus granular layer substantially increase during juvenile and adult life. *Science* 216:890–892.
- Behrens J, Jerchow BA, Würtele M, Grimm J, Asbrand C, Wirtz R, Köhl M, Wedlich D, Birchmeier W (1998) Functional interaction of an axin homolog, conductin, with beta-catenin, APC, and GSK3beta. *Science* 280:596–599.
- Ben-David U, Benvenisty N (2011) The tumorigenicity of human embryonic and induced pluripotent stem cells. *Nat Rev Cancer* 11:268–277.
- Bentivoglio M, Mazzarello P (1999) The history of radial glia. *Brain Res Bull* 49:305–315.
- Berninger B, Costa MR, Koch U, Schroeder T, Sutor B, Grothe B, Götz M, (2007) Functional Properties of Neurons Derived from In Vitro Reprogrammed Postnatal Astroglia. *Journal of Neuroscience* 27:8654–8664.
- Bernstein BE, Mikkelsen TS, Xie X, Kamal M, Huebert DJ, Cuff J, Fry B, Meissner A, Wernig M, Plath K, Jaenisch R, Wagschal A, Feil R, Schreiber SL, Lander ES (2006) A bivalent chromatin structure marks key developmental genes in embryonic stem cells. *Cell* 125:315–326.
- Bibikova M, Laurent LC, Ren B, Loring JF, Fan J-B (2008) Unraveling epigenetic regulation in embryonic stem cells. *Cell Stem Cell* 2:123–134.
- Blum R, Heinrich C, Sanchez R, Lepier A, Gundelfinger ED, Berninger B, Götz M (2011) Neuronal network formation from reprogrammed early postnatal rat cortical glial cells. *Cerebral Cortex* 21:413–424.

References

- Borrell V, Reillo I (2012) Emerging roles of neural stem cells in cerebral cortex development and evolution Bartlett PF, Berninger B, eds. *Dev Neurobiol* 72:955–971.
- Boyer LA, Mathur D, Jaenisch R (2006a) Molecular control of pluripotency. *Curr Opin Genet Dev* 16:455–462.
- Boyer LA, Plath K, Zeitlinger J, Brambrink T, Medeiros LA, Lee TI, Levine SS, Wernig M, Tajonar A, Ray MK, Bell GW, Otte AP, Vidal M, Gifford DK, Young RA, Jaenisch R (2006b) Polycomb complexes repress developmental regulators in murine embryonic stem cells. *Nature* 441:349–353.
- Bracken AP, Dietrich N, Pasini D, Hansen KH, Helin K (2006) Genome-wide mapping of Polycomb target genes unravels their roles in cell fate transitions. *Genes & Development* 20:1123–1136.
- Bulfone A, Martinez S, Marigo V, Campanella M, Basile A, Quaderi N, Gattuso C, Rubenstein JL, Ballabio A (1999) Expression pattern of the *Tbr2* (Eomesodermin) gene during mouse and chick brain development. *Mech Dev* 84:133–138.
- Bultje RS, Castaneda-Castellanos DR, Jan LY, Jan Y-N, Kriegstein AR, Shi S-H (2009) Mammalian *Par3* Regulates Progenitor Cell Asymmetric Division via Notch Signaling in the Developing Neocortex. *Neuron* 63:189–202.
- Cadigan KM, Liu YI (2006) Wnt signaling: complexity at the surface. *J Cell Sci* 119:395–402.
- Cajal SRY (1928) *Ramon y Cajal: Degeneration and Regeneration of the nervous system.* Oxford University Press.
- Calegari F, Haubensak W, Haffner C, Huttner WB (2005) Selective Lengthening of the Cell Cycle in the Neurogenic Subpopulation of Neural Progenitor Cells during Mouse Brain Development. *Journal of Neuroscience* 25:6533–6538.
- Calegari F, Huttner WB (2003) An inhibition of cyclin-dependent kinases that lengthens, but does not arrest, neuroepithelial cell cycle induces premature neurogenesis. *J Cell Sci* 116:4947–4955.
- Cameron HA, Woolley CS, McEwen BS, Gould E (1993) Differentiation of newly born neurons and glia in the dentate gyrus of the adult rat. *Neuroscience* 56:337–344.
- Campbell K, Götz M (2002) Radial glia: multi-purpose cells for vertebrate brain development. *Trends in Neurosciences* 25:235–238.
- Cappello S, Attardo A, Wu X, Iwasato T, Itohara S, Wilsch-Bräuninger M, Eilken HM, Rieger MA, Schroeder TT, Huttner WB, Brakebusch C, Götz M (2006) The Rho-GTPase *cdc42* regulates neural progenitor fate at the apical surface. *Nature Neuroscience* 9:1099–1107.

References

- Carr A, Biggin MD (1999) A comparison of in vivo and in vitro DNA-binding specificities suggests a new model for homeoprotein DNA binding in *Drosophila* embryos. *The EMBO Journal* 18:1598–1608.
- Carroll JS, Meyer CA, Song J, Li W, Geistlinger TR, Eeckhoute J, Brodsky AS, Keeton EK, Fertuck KC, Hall GF, Wang Q, Bekiranov S, Sementchenko V, Fox EA, Silver PA, Gingeras TR, Liu XS, Brown M (2006) Genome-wide analysis of estrogen receptor binding sites. *Nat Genet* 38:1289–1297.
- Carter AR, Segal RA (2001) Rett syndrome model suggests MECP2 gives neurons the quiet they need to think. *Nature Neuroscience* 4:342–343.
- Casanova MF, Trippe J (2006) Regulatory mechanisms of cortical laminar development. *Brain Research Reviews* 51:72–84.
- Cedar H, Bergman Y (2011) Epigenetics of haematopoietic cell development. *Nat Rev Immunol* 11:478–488.
- Chahrouh M, Zoghbi HY (2007) The story of Rett syndrome: from clinic to neurobiology. *Neuron* 56:422–437.
- Chapouton P, Gärtner A, Götz M (1999) The role of Pax6 in restricting cell migration between developing cortex and basal ganglia. *Development* 126:5569–5579.
- Chen L, Daley GQ (2008) Molecular basis of pluripotency. *Hum Mol Genet* 17:R23–R27.
- Chen Q, Zhu Y-C, Yu J, Miao S, Zheng J, Xu L, Zhou Y, Li D, Zhang C, Tao J, Xiong Z-Q (2010) CDKL5, a protein associated with rett syndrome, regulates neuronal morphogenesis via Rac1 signaling. *Journal of Neuroscience* 30:12777–12786.
- Chenn A, Walsh CA (2002) Regulation of cerebral cortical size by control of cell cycle exit in neural precursors. *Science* 297:365–369.
- Chenn A, Walsh CA (2003) Increased neuronal production, enlarged forebrains and cytoarchitectural distortions in beta-catenin overexpressing transgenic mice. *Cereb Cortex* 13:599–606.
- Cheung AFP, Kondo S, Abdel-Mannan O, Chodroff RA, Sirey TM, Bluy LE, Webber N, DeProto J, Karlen SJ, Krubitzer L, Stolp HB, Saunders NR, Molnar Z (2010) The Subventricular Zone Is the Developmental Milestone of a 6-Layered Neocortex: Comparisons in Metatherian and Eutherian Mammals. *Cerebral Cortex* 20:1071–1081.
- Cho S-H, Cepko CL (2006) Wnt2b/beta-catenin-mediated canonical Wnt signaling determines the peripheral fates of the chick eye. *Development* 133:3167–3177.

References

- Cohen S, Gabel HW, Hemberg M, Hutchinson AN, Sadacca LA, Ebert DH, Harmin DA, Greenberg RS, Verdine VK, Zhou Z, Wetsel WC, West AE, Greenberg ME (2011) Genome-wide activity-dependent MeCP2 phosphorylation regulates nervous system development and function. *Neuron* 72:72–85.
- Costa MR, Wen G, Lepier A, Schroeder T, Götz M (2008) Par-complex proteins promote proliferative progenitor divisions in the developing mouse cerebral cortex. *Development* 135:11–22.
- Deng JV, Rodriguiz RM, Hutchinson AN, Kim I-H, Wetsel WC, West AE (2010) MeCP2 in the nucleus accumbens contributes to neural and behavioral responses to psychostimulants. *Nature Neuroscience* 13:1128–1136.
- Doetsch F, Caille I, Lim DA, García-Verdugo JM, Alvarez-Buylla A (1999) Subventricular zone astrocytes are neural stem cells in the adult mammalian brain. *Cell* 97:703–716.
- Eckenhoff MF, Rakic P (1984) Radial organization of the hippocampal dentate gyrus: a Golgi, ultrastructural, and immunocytochemical analysis in the developing rhesus monkey. *J Comp Neurol* 223:1–21.
- Eeckhoute J, Carroll JS, Geistlinger TR, Torres-Arzayus MI, Brown M (2006) A cell-type-specific transcriptional network required for estrogen regulation of cyclin D1 and cell cycle progression in breast cancer. *Genes & Development* 20:2513–2526.
- Eilertsen KJ, Floyd Z, Gimble JM (2008) The epigenetics of adult (somatic) stem cells. *Crit Rev Eukaryot Gene Expr* 18:189–206.
- Eilken HM, Nishikawa S-I, Schroeder T (2009) Continuous single-cell imaging of blood generation from haemogenic endothelium. *Nature* 457:896–900.
- Englund C (2005) Pax6, Tbr2, and Tbr1 Are Expressed Sequentially by Radial Glia, Intermediate Progenitor Cells, and Postmitotic Neurons in Developing Neocortex. *Journal of Neuroscience* 25:247–251.
- Faedo A, Ficara F, Ghiani M, Aiuti A, Rubenstein JLR, Bulfone A (2002) Developmental expression of the T-box transcription factor T-bet/Tbx21 during mouse embryogenesis. *Mech Dev* 116:157–160.
- Farkas LM, Huttner WB (2008) The cell biology of neural stem and progenitor cells and its significance for their proliferation versus differentiation during mammalian brain development. *Curr Opin Cell Biol* 20:707–715.
- Fietz SA, Huttner WB (2010) Cortical progenitor expansion, self-renewal and neurogenesis—a polarized perspective. *Curr Opin Neurobiol*:1–13.

References

- Fietz SA, Kelava I, Vogt J, Wilsch-Bräuninger M, Stenzel D, Fish JL, Corbeil D, Riehn A, Distler W, Nitsch R, Huttner WB (2010) OSVZ progenitors of human and ferret neocortex are epithelial-like and expand by integrin signaling. *Nature Publishing Group* 13:690–699.
- Fode C, Ma Q, Casarosa S, Ang SL, Anderson DJ, Guillemot F (2000) A role for neural determination genes in specifying the dorsoventral identity of telencephalic neurons. *Genes & Development* 14:67–80.
- Fong AP, Yao Z, Zhong JW, Cao Y, Ruzzo WL, Gentleman RC, Tapscott SJ (2012) Genetic and Epigenetic Determinants of Neurogenesis and Myogenesis. *Developmental Cell* 22:721–735.
- Franco SJ, Gil-Sanz C, Martinez-Garay I, Espinosa A, Harkins-Perry SR, Ramos C, Müller U (2012) Fate-restricted neural progenitors in the mammalian cerebral cortex. *Science* 337:746–749.
- Frank CL, Tsai L-H (2009) Alternative Functions of Core Cell Cycle Regulators in Neuronal Migration, Neuronal Maturation, and Synaptic Plasticity. *Neuron* 62:312–326.
- Fujita (1962) Kinetics of cellular proliferation. *Experimental Cell Research* 28:52–60.
- Fukuchi-Shimogori T (2001) Neocortex Patterning by the Secreted Signaling Molecule FGF8. *Science* 294:1071–1074.
- Fukushima A, Nishimoto M, Okuda A, Muramatsu M (1999) Carboxy-terminally truncated form of a coactivator UTF1 stimulates transcription from a variety of gene promoters through the TATA Box. *Biochemical and Biophysical Research Communications* 258:519–523.
- Fukushima A, Okuda A, Nishimoto M, Seki N, Hori TA, Muramatsu M (1998) Characterization of functional domains of an embryonic stem cell coactivator UTF1 which are conserved and essential for potentiation of ATF-2 activity. *J Biol Chem* 273:25840–25849.
- Gal JS, Morozov YM, Ayoub AE, Chatterjee M, Rakic P, Haydar TF (2006) Molecular and morphological heterogeneity of neural precursors in the mouse neocortical proliferative zones. *Journal of Neuroscience* 26:1045–1056.
- Galceran J, Hsu SC, Grosschedl R (2001) Rescue of a Wnt mutation by an activated form of LEF-1: regulation of maintenance but not initiation of Brachyury expression. *Proc Natl Acad Sci USA* 98:8668–8673.

References

- Gaspar-Maia A, Alajem A, Polesso F, Sridharan R, Mason MJ, Heidersbach A, Ramalho-Santos J, McManus MT, Plath K, Meshorer E, Ramalho-Santos M (2009) Chd1 regulates open chromatin and pluripotency of embryonic stem cells. *Nature* 460:863–868.
- Goffin D, Allen M, Zhang L, Amorim M, Wang I-TJ, Reyes A-RS, Mercado-Berton A, Ong C, Cohen S, Hu L, Blendy JA, Carlson GC, Siegel SJ, Greenberg ME, Zhou Z (2012) Rett syndrome mutation MeCP2 T158A disrupts DNA binding, protein stability and ERP responses. *Nature Publishing Group* 15:274–283.
- Goh ELK, Ma D, Ming G-L, Song H (2003) Adult neural stem cells and repair of the adult central nervous system. *J Hematother Stem Cell Res* 12:671–679.
- Götz M, Barde Y-A (2005) Radial glial cells defined and major intermediates between embryonic stem cells and CNS neurons. *Neuron* 46:369–372.
- Götz M, Hartfuss E, Malatesta P (2002) Radial glial cells as neuronal precursors: a new perspective on the correlation of morphology and lineage restriction in the developing cerebral cortex of mice. *Brain Res Bull* 57:777–788.
- Götz M, Huttner WB (2005) The cell biology of neurogenesis. *Nat Rev Mol Cell Biol* 6:777–788.
- Götz M, Stoykova A, Gruss P (1998) Pax6 controls radial glia differentiation in the cerebral cortex. *Neuron* 21:1031–1044.
- Graf T, Stadtfeld M (2008) Heterogeneity of embryonic and adult stem cells. *Cell Stem Cell* 3:480–483.
- Gratzner HG (1982) Monoclonal antibody to 5-bromo- and 5-iododeoxyuridine: A new reagent for detection of DNA replication. *Science* 218:474–475.
- Gross CG (2000) Neurogenesis in the adult brain: death of a dogma. *Nat Rev Neurosci* 1:67–73.
- Gulacsi AA, Anderson SA (2008) Beta-catenin-mediated Wnt signaling regulates neurogenesis in the ventral telencephalon. *Nature Publishing Group* 11:1383–1391.
- Hack MA, Saghatelian A, de Chevigny A, Pfeifer A, Ashery-Padan R, Lledo P-M, Götz M (2005) Neuronal fate determinants of adult olfactory bulb neurogenesis. *Nature Neuroscience*.
- Hanahan D (1983) Studies on transformation of *Escherichia coli* with plasmids. *J Mol Biol* 166:557–580.
- Hansen DV, Lui JH, Parker PRL, Kriegstein AR (2010) Neurogenic radial glia in the outer subventricular zone of human neocortex. *Nature* 464:554–561.

References

- Happel N, Doenecke D (2009) Histone H1 and its isoforms: contribution to chromatin structure and function. *Gene* 431:1–12.
- Hatakeyama J, Bessho Y, Katoh K, Ookawara S, Fujioka M, Guillemot F, Kageyama R (2004) Hes genes regulate size, shape and histogenesis of the nervous system by control of the timing of neural stem cell differentiation. *Development* 131:5539–5550.
- Haubensak W, Attardo A, Denk W, Huttner WB (2004) Neurons arise in the basal neuroepithelium of the early mammalian telencephalon: a major site of neurogenesis. *Proc Natl Acad Sci USA* 101:3196–3201.
- Haubst N, Berger J, Radjendirane V, Graw J, Favor J, Saunders GF, Stoykova A, Götz M (2004) Molecular dissection of Pax6 function: the specific roles of the paired domain and homeodomain in brain development. *Development* 131:6131–6140.
- Hayes NL, Nowakowski RS (2000) Exploiting the dynamics of S-phase tracers in developing brain: interkinetic nuclear migration for cells entering versus leaving the S-phase. *Dev Neurosci* 22:44–55.
- Heinrich C, Blum R, Gascón S, Masserdotti G, Tripathi P, Sanchez R, Tiedt S, Schroeder T, Götz M, Berninger B (2010) Directing astroglia from the cerebral cortex into subtype specific functional neurons. *Plos Biol* 8:e1000373.
- Heinrich C, Gascón S, Masserdotti G, Lepier A, Sanchez R, Simon-Ebert T, Schroeder T, Götz M, Berninger B (2011) Generation of subtype-specific neurons from postnatal astroglia of the mouse cerebral cortex. *Nat Protoc* 6:214–228 Available at: <http://eutils.ncbi.nlm.nih.gov/entrez/eutils/elink.fcgi?dbfrom=pubmed&id=21293461&retmode=ref&cmd=prlinks>.
- Heins N (2001) Emx2 Promotes Symmetric Cell Divisions and a Multipotential Fate in Precursors from the Cerebral Cortex. *Molecular and Cellular Neuroscience* 18:485–502.
- Heins N, Malatesta P, Cecconi F, Nakafuku M, Tucker KL, Hack MA, Chapouton P, Barde Y-A, Götz M (2002) Glial cells generate neurons: the role of the transcription factor Pax6. *Nature Neuroscience* 5:308–315.
- Heng JI-T, Nguyen L, Castro DS, Zimmer C, Wildner H, Armant O, Skowronska-Krawczyk D, Bedogni F, Matter J-M, Hevner R, Guillemot F (2008) Neurogenin 2 controls cortical neuron migration through regulation of Rnd2. *Nature* 455:114–118.
- Hevner RF, Haydar TF (2012) The (Not Necessarily) Convolved Role of Basal Radial Glia in Cortical Neurogenesis. *Cerebral Cortex* 22:465–468.
- Ho L, Crabtree GR (2010) Chromatin remodelling during development. *Nature* 463:474–484.

References

- Hoffbuhr K, Devaney JM, LaFleur B, Sirianni N, Scacheri C, Giron J, Schuette J, Innis J, Marino M, Philippart M, Narayanan V, Umansky R, Kronn D, Hoffman EP, Naidu S (2001) MeCP2 mutations in children with and without the phenotype of Rett syndrome. *Neurology* 56:1486–1495.
- Hoffbuhr KC, Moses LM, Jerdonek MA, Naidu S, Hoffman EP (2002) Associations between MeCP2 mutations, X-chromosome inactivation, and phenotype. *Ment Retard Dev Disabil Res Rev* 8:99–105.
- Huelsken J, Vogel R, Erdmann B, Cotsarelis G, Birchmeier W (2001) beta-Catenin controls hair follicle morphogenesis and stem cell differentiation in the skin. *Cell* 105:533–545.
- Hung H, Kohnken R, Svaren J (2012) The nucleosome remodeling and deacetylase chromatin remodeling (NuRD) complex is required for peripheral nerve myelination. *Journal of Neuroscience* 32:1517–1527.
- Iyer VR, Horak CE, Scafe CS, Botstein D, Snyder M, Brown PO (2001) Genomic binding sites of the yeast cell-cycle transcription factors SBF and MBF. *Nature* 409:533–538.
- Johansson PA, Cappello S, Götz M (2010) Stem cells niches during development - lessons from the cerebral cortex. *Curr Opin Neurobiol* 20:400–407.
- Joseph R, Orlov YL, Huss M, Sun W, Kong SL, Ukil L, Pan YF, Li G, Lim M, Thomsen JS, Ruan Y, Clarke ND, Prabhakar S, Cheung E, Liu ET (2010) Integrative model of genomic factors for determining binding site selection by estrogen receptor- α . *Mol Syst Biol* 6:456.
- Kaji K, Caballero IM, MacLeod R, Nichols J, Wilson VA, Hendrich B (2006) The NuRD component Mbd3 is required for pluripotency of embryonic stem cells. *Nat Cell Biol* 8:285–292.
- Kanda T, Sullivan KF, Wahl GM (1998) Histone-GFP fusion protein enables sensitive analysis of chromosome dynamics in living mammalian cells. *Curr Biol* 8:377–385.
- Kaplan MS, Bell DH (1983) Neuronal proliferation in the 9-month-old rodent-radioautographic study of granule cells in the hippocampus. *Exp Brain Res* 52:1–5.
- Kaplan MS, Bell DH (1984) Mitotic neuroblasts in the 9-day-old and 11-month-old rodent hippocampus. *J Neurosci* 4:1429–1441.
- Kaplan MS, Hinds JW (1977) Neurogenesis in the adult rat: electron microscopic analysis of light radioautographs. *Science* 197:1092–1094.

References

- Kaplan T, Li X-Y, Sabo PJ, Thomas S, Stamatoyannopoulos JA, Biggin MD, Eisen MB (2011) Quantitative models of the mechanisms that control genome-wide patterns of transcription factor binding during early *Drosophila* development. *PLoS Genet* 7:e1001290.
- Kelava I, Reillo I, Murayama AY, Kalinka AT, Stenzel D, Tomancak P, Matsuzaki F, Lebrand C, Sasaki E, Schwamborn JC, Okano H, Huttner WB, Borrell V (2012) Abundant Occurrence of Basal Radial Glia in the Subventricular Zone of Embryonic Neocortex of a Lissencephalic Primate, the Common Marmoset *Callithrix jacchus*. *Cerebral Cortex* 22:469–481.
- Kempermann G, Gage FH (1999) New nerve cells for the adult brain. *Sci Am* 280:48–53.
- Kimura H, Cook PR (2001) Kinetics of core histones in living human cells: little exchange of H3 and H4 and some rapid exchange of H2B. *J Cell Biol* 153:1341–1353.
- Kobayakawa S, Miike K, Nakao M, Abe K (2007) Dynamic changes in the epigenomic state and nuclear organization of differentiating mouse embryonic stem cells. *Genes Cells* 12:447–460.
- Kooistra SM, Thummer RP, Eggen BJJ (2009) Characterization of human UTF1, a chromatin-associated protein with repressor activity expressed in pluripotent cells. *Stem Cell Res* 2:211–218.
- Kooistra SM, van den Boom V, Thummer RP, Johannes F, Wardenaar R, Tesson BM, Veenhoff LM, Fusetti F, O'Neill LP, Turner BM, de Haan G, Eggen BJJ (2010) Undifferentiated embryonic cell transcription factor 1 regulates ESC chromatin organization and gene expression. *Stem Cells* 28:1703–1714.
- Kouzarides T (2007) Chromatin modifications and their function. *Cell* 128:693–705.
- Kriegstein A, Alvarez-Buylla A (2009) The Glial Nature of Embryonic and Adult Neural Stem Cells. *Annu Rev Neurosci* 32:149–184.
- Kriegstein A, Noctor S, Martínez-Cerdeño V (2006) Patterns of neural stem and progenitor cell division may underlie evolutionary cortical expansion. *Nat Rev Neurosci* 7:883–890.
- Kriegstein AR, Götz M (2003) Radial glia diversity: A matter of cell fate. *Glia* 43:37–43.
- Kuhn HG, Dickinson-Anson H, Gage FH (1996) Neurogenesis in the dentate gyrus of the adult rat: age-related decrease of neuronal progenitor proliferation. *J Neurosci* 16:2027–2033.
- Laemmli UK (1970) Cleavage of structural proteins during the assembly of the head of bacteriophage T4. *Nature* 227:680–685.

References

- Lange C, Huttner WB, Calegari F (2009) Cdk4/CyclinD1 Overexpression in Neural Stem Cells Shortens G1, Delays Neurogenesis, and Promotes the Generation and Expansion of Basal Progenitors. *Cell Stem Cell* 5:320–331.
- Lee TI et al. (2006) Control of developmental regulators by Polycomb in human embryonic stem cells. *Cell* 125:301–313.
- Leung CT, Coulombe PA, Reed RR (2007) Contribution of olfactory neural stem cells to tissue maintenance and regeneration. *Nature Neuroscience* 10:720–726.
- Lewis JD, Meehan RR, Henzel WJ, Maurer-Fogy I, Jeppesen P, Klein F, Bird A (1992) Purification, sequence, and cellular localization of a novel chromosomal protein that binds to methylated DNA. *Cell* 69:905–914.
- Li B, Carey M, Workman JL (2007) The role of chromatin during transcription. *Cell* 128:707–719.
- Li E, Bestor TH, Jaenisch R (1992) Targeted mutation of the DNA methyltransferase gene results in embryonic lethality. *Cell* 69:915–926.
- Li HJ (1975) A model for chromatin structure. *Nucleic Acids Res* 2:1275–1289.
- Lie DC, Song H, Colamarino SA, Ming G-L, Gage FH (2004) Neurogenesis in the adult brain: new strategies for central nervous system diseases. *Annu Rev Pharmacol Toxicol* 44:399–421.
- Lim DA, Huang Y-C, Swigut T, Mirick AL, Garcia-Verdugo JM, Wysocka J, Ernst P, Alvarez-Buylla A (2009) Chromatin remodelling factor Mll1 is essential for neurogenesis from postnatal neural stem cells. *Nature* 458:529–533.
- Lin W, Dent SYR (2006) Functions of histone-modifying enzymes in development. *Curr Opin Genet Dev* 16:137–142.
- Lindner H, Sarg B, Hoertnagl B, Helliger W (1998) The microheterogeneity of the mammalian H1(0) histone. Evidence for an age-dependent deamidation. *J Biol Chem* 273:13324–13330.
- Lindvall O, Kokaia Z, Martinez-Serrano A (2004) Stem cell therapy for human neurodegenerative disorders-how to make it work. *Nat Med* 10 Suppl:S42–S50.
- Lioy DT, Garg SK, Monaghan CE, Raber J, Foust KD, Kaspar BK, Hirrlinger PG, Kirchhoff F, Bissonnette JM, Ballas N, Mandel G (2011) A role for glia in the progression of Rett's syndrome. *Nature* 475:497–500.
- Loh Y-H et al. (2006) The Oct4 and Nanog transcription network regulates pluripotency in mouse embryonic stem cells. *Nat Genet* 38:431–440.

References

- Lu QR, Sun T, Zhu Z, Ma N, Garcia M, Stiles CD, Rowitch DH (2002) Common developmental requirement for Olig function indicates a motor neuron/oligodendrocyte connection. *Cell* 109:75–86.
- Lui JH, Hansen DV, Kriegstein AR (2011) Development and Evolution of the Human Neocortex. *Cell* 146:18–36.
- Luikenhuis S, Giacometti E, Beard CF, Jaenisch R (2004) Expression of MeCP2 in postmitotic neurons rescues Rett syndrome in mice. *Proc Natl Acad Sci USA* 101:6033–6038.
- Lukaszewicz A, Savatier P, Cortay V, Giroud P, Huissoud C, Berland M, Kennedy H, Dehay C (2005) G1 phase regulation, area-specific cell cycle control, and cytoarchitectonics in the primate cortex. *Neuron* 47:353–364.
- Ma DK, Bonaguidi MA, Ming G-L, Song H (2009) Adult neural stem cells in the mammalian central nervous system. *Cell Res* 19:672–682.
- Malatesta P, Appolloni I, Calzolari F (2007) Radial glia and neural stem cells. *Cell Tissue Res* 331:165–178.
- Malatesta P, Hack MA, Hartfuss E, Kettenmann H, Klinkert W, Kirchhoff F, Götz M (2003) Neuronal or glial progeny: regional differences in radial glia fate. *Neuron* 37:751–764.
- Malatesta P, Hartfuss E, Götz M (2000) Isolation of radial glial cells by fluorescent-activated cell sorting reveals a neuronal lineage. *Development* 127:5253–5263
Available at:
<http://eutils.ncbi.nlm.nih.gov/entrez/eutils/elink.fcgi?dbfrom=pubmed&id=11076748&retmode=ref&cmd=prlinks>.
- Manuel MN, Ben Martynoga, Molinek MD, Quinn JC, Kroemmer C, Mason JO, Price DJ (2011) The transcription factor Foxg1 regulates telencephalic progenitor proliferation cell autonomously, in part by controlling Pax6 expression levels. *Neural Development* 6:9.
- Marchetto MCN, Carromeu C, Acab A, Yu D, Yeo GW, Mu Y, Chen G, Gage FH, Muotri AR (2010) A Model for Neural Development and Treatment of Rett Syndrome Using Human Induced Pluripotent Stem Cells. *Cell* 143:527–539.
- Marín O, Rubenstein JL (2001) A long, remarkable journey: tangential migration in the telencephalon. *Nat Rev Neurosci* 2:780–790.
- Marín O, Rubenstein JLR (2003) Cell Migration in the Forebrain. *Annu Rev Neurosci* 26:441–483.

- Marín O, Valiente M, Ge X, Tsai L-H (2010) Guiding neuronal cell migrations. *Cold Spring Harb Perspect Biol* 2:a001834.
- Martínez-Cerdeño V, Cunningham CL, Camacho J, Antczak JL, Prakash AN, Cziep ME, Walker AI, Noctor SC (2012) Comparative Analysis of the Subventricular Zone in Rat, Ferret and Macaque: Evidence for an Outer Subventricular Zone in Rodents Nelson B, ed. *PLoS ONE* 7:e30178.
- Mayer R, Brero A, Hase von J, Schroeder T, Cremer T, Dietzel S (2005) Common themes and cell type specific variations of higher order chromatin arrangements in the mouse. *BMC Cell Biol* 6:44.
- Meehan RR, Lewis JD, Bird AP (1992) Characterization of MeCP2, a vertebrate DNA binding protein with affinity for methylated DNA. *Nucleic Acids Res* 20:5085–5092.
- Meissner A, Mikkelsen TS, Gu H, Wernig M, Hanna J, Sivachenko A, Zhang X, Bernstein BE, Nusbaum C, Jaffe DB, Gnirke A, Jaenisch R, Lander ES (2008) Genome-scale DNA methylation maps of pluripotent and differentiated cells. *Nature* 454:766–770.
- Merkle FT, Tramontin AD, Garcia-Verdugo JM, Alvarez-Buylla A (2004) Radial glia give rise to adult neural stem cells in the subventricular zone. *Proc Natl Acad Sci USA* 101:17528–17532.
- Metzger M (2011) Characterisation of a novel nuclear protein involved in murine cerebral cortical development. Master Thesis Technical University Munich:1–65.
- Meyers JA, Sanchez D, Elwell LP, Falkow S (1976) Simple agarose gel electrophoretic method for the identification and characterization of plasmid deoxyribonucleic acid. *J Bacteriol* 127:1529–1537.
- Michaelidis TM, Lie DC (2008) Wnt signaling and neural stem cells: caught in the Wnt web. *Cell Tissue Res* 331:193–210.
- Mikkelsen TS et al. (2007) Genome-wide maps of chromatin state in pluripotent and lineage-committed cells. *Nature* 448:553–560.
- Ming G-L, Song H (2005) Adult neurogenesis in the mammalian central nervous system. *Annu Rev Neurosci* 28:223–250.
- Mirzadeh Z, Merkle FT, Soriano-Navarro M, Garcia-Verdugo JM, Alvarez-Buylla A (2008) Neural Stem Cells Confer Unique Pinwheel Architecture to the Ventricular Surface in Neurogenic Regions of the Adult Brain. *Cell Stem Cell* 3:265–278.
- Miyata T, Kawaguchi A, Okano H, Ogawa M (2001) Asymmetric inheritance of radial glial fibers by cortical neurons. *Neuron* 31:727–741.

References

- Miyata T, Kawaguchi A, Saito K, Kawano M, Muto T, Ogawa M (2004) Asymmetric production of surface-dividing and non-surface-dividing cortical progenitor cells. *Development* 131:3133–3145.
- Molnár Z (2011) Evolution of Cerebral Cortical Development. *Brain Behav Evol* 78:94–107.
- Molnár Z, Kennedy H (2007) Comparative aspects of cerebral cortical development 2006. *Eur J Neurosci*:1–26.
- Molyneaux BJ, Arlotta P, Menezes JRL, Macklis JD (2007) Neuronal subtype specification in the cerebral cortex. *Nat Rev Neurosci* 8:427–437.
- Morin X, Jaouen F, Durbec P (2007) Control of planar divisions by the G-protein regulator LGN maintains progenitors in the chick neuroepithelium. *Nature Neuroscience* 10:1440–1448.
- Murgatroyd C, Patchev AV, Wu Y, Micale V, Bockmühl Y, Fischer D, Holsboer F, Wotjak CT, Almeida OFX, Spengler D (2009) Dynamic DNA methylation programs persistent adverse effects of early-life stress. *Nature Neuroscience* 12:1559–1566.
- Nan X, Campoy FJ, Bird A (1997) MeCP2 is a transcriptional repressor with abundant binding sites in genomic chromatin. *Cell* 88:471–481.
- Nieto M, Schuurmans C, Britz O, Guillemot F (2001) Neural bHLH genes control the neuronal versus glial fate decision in cortical progenitors. *Neuron* 29:401–413.
- Nishimoto M, Fukushima A, Okuda A, Muramatsu M (1999) The gene for the embryonic stem cell coactivator UTF1 carries a regulatory element which selectively interacts with a complex composed of Oct-3/4 and Sox-2. *Molecular and Cellular Biology* 19:5453–5465.
- Nishimoto M, Miyagi S, Yamagishi T, Sakaguchi T, Niwa H, Muramatsu M, Okuda A (2005) Oct-3/4 maintains the proliferative embryonic stem cell state via specific binding to a variant octamer sequence in the regulatory region of the UTF1 locus. *Molecular and Cellular Biology* 25:5084–5094.
- Noctor SC, Flint AC, Weissman TA, Dammerman RS, Kriegstein AR (2001) Neurons derived from radial glial cells establish radial units in neocortex. *Nature* 409:714–720.
- Noctor SC, Martínez-Cerdeño V, Ivic L, Kriegstein AR (2004) Cortical neurons arise in symmetric and asymmetric division zones and migrate through specific phases. *Nature Neuroscience* 7:136–144.
- Noctor SC, Martínez-Cerdeño V, Kriegstein AR (2008) Distinct behaviors of neural stem and progenitor cells underlie cortical neurogenesis. *J Comp Neurol* 508:28–44.

References

- Nosaka T, Kawashima T, Misawa K, Ikuta K, Mui AL, Kitamura T (1999) STAT5 as a molecular regulator of proliferation, differentiation and apoptosis in hematopoietic cells. *The EMBO Journal* 18:4754–4765.
- Nóbrega-Pereira S, Marín O (2009) Transcriptional control of neuronal migration in the developing mouse brain. *Cerebral Cortex* 19 Suppl 1:i107–i113.
- Okuda A, Fukushima A, Nishimoto M, Orimo A, Yamagishi T, Nabeshima Y, Kuro-o M, Nabeshima YI, Boon K, Keaveney M, Stunnenberg HG, Muramatsu M (1998) UTF1, a novel transcriptional coactivator expressed in pluripotent embryonic stem cells and extra-embryonic cells. *The EMBO Journal* 17:2019–2032.
- Ory DS, Neugeboren BA, Mulligan RC (1996) A stable human-derived packaging cell line for production of high titer retrovirus/vesicular stomatitis virus G pseudotypes. *Proc Natl Acad Sci USA* 93:11400–11406.
- Pacary E, Heng J, Azzarelli R, Riou P, Castro D, Lebel-Potter M, Parras C, Bell DM, Ridley AJ, Parsons M, Guillemot F (2011) Proneural Transcription Factors Regulate Different Steps of Cortical Neuron Migration through Rnd-Mediated Inhibition of RhoA Signaling. *Neuron* 69:1069–1084.
- Parent JM (2003) Injury-induced neurogenesis in the adult mammalian brain. *Neuroscientist* 9:261–272.
- Petryniak MA, Potter GB, Rowitch DH, Rubenstein JLR (2007) Dlx1 and Dlx2 control neuronal versus oligodendroglial cell fate acquisition in the developing forebrain. *Neuron* 55:417–433.
- Pinto L (2008) Molecular mechanisms regulating neurogenesis in the developing mouse cerebral cortex. PhD Thesis:1–190.
- Pinto L, Drechsel D, Schmid M-T, Ninkovic J, Irmeler M, Brill MS, Restani L, Gianfranceschi L, Cerri C, Weber SN, Tarabykin V, Baer K, Guillemot F, Beckers J, Zecevic N, Dehay C, Caleo M, Schorle H, Götz M (2009) AP2 γ regulates basal progenitor fate in a region- and layer-specific manner in the developing cortex. *Nature Neuroscience*:1–11.
- Pinto L, Götz M (2007) Radial glial cell heterogeneity—The source of diverse progeny in the CNS. *Progress in Neurobiology* 83:2–23.
- Pinto L, Mader MT, Irmeler M, Gentilini M, Santoni F, Drechsel D, Blum R, Stahl R, Bulfone A, Malatesta P, Beckers J, Götz M (2008) Prospective isolation of functionally distinct radial glial subtypes—Lineage and transcriptome analysis. *Molecular and Cellular Neuroscience* 38:15–42.
- Pontious A, Kowalczyk T, Englund C, Hevner RF (2008) Role of Intermediate Progenitor Cells in Cerebral Cortex Development. *Dev Neurosci* 30:24–32.

- Qian X, Goderie SK, Shen Q, Stern JH, Temple S (1998) Intrinsic programs of patterned cell lineages in isolated vertebrate CNS ventricular zone cells. *Development* 125:3143–3152.
- Quinn JC, Molinek M, Martynoga BS, Zaki PA, Faedo A, Bulfone A, Hevner RF, West JD, Price DJ (2007) Pax6 controls cerebral cortical cell number by regulating exit from the cell cycle and specifies cortical cell identity by a cell autonomous mechanism. *Dev Biol* 302:50–65.
- Rainer J, Sanchez-Cabo F, Stocker G, Sturn A, Trajanoski Z (2006) CARMAweb: comprehensive R- and bioconductor-based web service for microarray data analysis. *Nucleic Acids Res* 34:W498–W503.
- Rakic P (1971) Guidance of neurons migrating to the fetal monkey neocortex. *Brain Res* 33:471–476.
- Rakic P (1972) Mode of cell migration to the superficial layers of fetal monkey neocortex. *J Comp Neurol* 145:61–83.
- Rakic P (1974) Neurons in rhesus monkey visual cortex: systematic relation between time of origin and eventual disposition. *Science* 183:425–427.
- Rakic P (1988) Specification of cerebral cortical areas. *Science* 241:170–176.
- Rakic P (2009) Evolution of the neocortex: a perspective from developmental biology. *Nat Rev Neurosci* 10:724–735.
- Rao MS, Jacobson M (2005) *Developmental Neurobiology*. Springer.
- Reillo I, Borrell V (2011) Germinal Zones in the Developing Cerebral Cortex of Ferret: Ontogeny, Cell Cycle Kinetics, and Diversity of Progenitors. *Cerebral Cortex*.
- Reillo I, de Juan Romero C, Garcia-Cabezas MA, Borrell V (2011) A Role for Intermediate Radial Glia in the Tangential Expansion of the Mammalian Cerebral Cortex. *Cerebral Cortex* 21:1674–1694.
- Rieger MA, Hoppe PS, Smejkal BM, Eitelhuber AC, Schroeder T (2009) Hematopoietic cytokines can instruct lineage choice. *Science* 325:217–218.
- Rieger MA, Schroeder T (2009) Analyzing cell fate control by cytokines through continuous single cell biochemistry. *J Cell Biochem* 108:343–352.
- Rossi F, Cattaneo E (2002) Opinion: neural stem cell therapy for neurological diseases: dreams and reality. *Nat Rev Neurosci* 3:401–409.
- Saito T (2006) In vivo electroporation in the embryonic mouse central nervous system. *Nat Protoc* 1:1552–1558.

- Sambrook J, Fritsch EF, Maniatis T (1989) *Molecular Cloning*.
- Sansom SN, Griffiths DS, Faedo A, Kleinjan D-J, Ruan Y, Smith J, van Heyningen V, Rubenstein JL, Livesey FJ (2009) The level of the transcription factor Pax6 is essential for controlling the balance between neural stem cell self-renewal and neurogenesis. Sansom SN, Griffiths DS, Faedo A, Kleinjan D-J, Ruan Y, Smith J, van Heyningen V, Rubenstein JL, Livesey FJ, eds. *PLoS Genet* 5:e1000511.
- Sasaki H, Matsui Y (2008) Epigenetic events in mammalian germ-cell development: reprogramming and beyond. *Nat Rev Genet* 9:129–140.
- Sauer ME, Walker BE (1959) Radioautographic study of interkinetic nuclear migration in the neural tube. *Proc Soc Exp Biol Med* 101:557–560.
- Sauvageau M, Sauvageau G (2010) Polycomb group proteins: multi-faceted regulators of somatic stem cells and cancer. *Cell Stem Cell* 7:299–313.
- Schermelleh L, Spada F, Easwaran HP, Zolghadr K, Margot JB, Cardoso MC, Leonhardt H (2005) Trapped in action: direct visualization of DNA methyltransferase activity in living cells. *Nat Meth* 2:751–756.
- Schuurmans C, Armant O, Nieto M, Stenman JM, Britz O, Klenin N, Brown C, Langevin LM, Seibt J, Tang H, Cunningham JM, Dyck R, Walsh C, Campbell K, Polleux F, Guillemot F (2004) Sequential phases of cortical specification involve Neurogenin-dependent and -independent pathways. *The EMBO Journal* 23:2892–2902.
- Seki T, Arai Y (1995) Age-related production of new granule cells in the adult dentate gyrus. *Neuroreport* 6:2479–2482.
- Sessa A, Mao C-A, Colasante G, Nini A, Klein WH, Broccoli V (2010) Tbr2-positive intermediate (basal) neuronal progenitors safeguard cerebral cortex expansion by controlling amplification of pallial glutamatergic neurons and attraction of subpallial GABAergic interneurons. *Genes & Development* 24:1816–1826.
- Sessa A, Mao C-A, Hadjantonakis A-K, Klein WH, Broccoli V (2008) Tbr2 directs conversion of radial glia into basal precursors and guides neuronal amplification by indirect neurogenesis in the developing neocortex. *Neuron* 60:56–69.
- Shen Q, Wang Y, Dimos JT, Fasano CA, Phoenix TN, Lemischka IR, Ivanova NB, Stifani S, Morrisey EE, Temple S (2006) The timing of cortical neurogenesis is encoded within lineages of individual progenitor cells. *Nature Neuroscience* 9:743–751.
- Shitamukai A, Konno D, Matsuzaki F (2011) Oblique Radial Glial Divisions in the Developing Mouse Neocortex Induce Self-Renewing Progenitors outside the Germinal Zone That Resemble Primate Outer Subventricular Zone Progenitors. *Journal of Neuroscience* 31:3683–3695.

References

- Sidman RL, Miale IL, Feder N (1959) Cell proliferation and migration in the primitive ependymal zone: an autoradiographic study of histogenesis in the nervous system. *Experimental Neurology* 1:322–333.
- Smart IH, McSherry GM (1986a) Gyrus formation in the cerebral cortex in the ferret. I. Description of the external changes. *J Anat* 146:141–152.
- Smart IH, McSherry GM (1986b) Gyrus formation in the cerebral cortex of the ferret. II. Description of the internal histological changes. *J Anat* 147:27–43.
- Sommer L, Ma Q, Anderson DJ (1996) neurogenins, a novel family of atonal-related bHLH transcription factors, are putative mammalian neuronal determination genes that reveal progenitor cell heterogeneity in the developing CNS and PNS. *Mol Cell Neurosci* 8:221–241.
- Stancik EK, Navarro-Quiroga I, Sellke R, Haydar TF (2010) Heterogeneity in Ventricular Zone Neural Precursors Contributes to Neuronal Fate Diversity in the Postnatal Neocortex. *Journal of Neuroscience* 30:7028–7036.
- Stoykova A, Fritsch R, Walther C, Gruss P (1996) Forebrain patterning defects in Small eye mutant mice. *Development* 122:3453–3465.
- Stoykova A, GOTZ M, Gruss P, Price J (1997) Pax6-dependent regulation of adhesive patterning, R-cadherin expression and boundary formation in developing forebrain. *Development* 124:3765–3777.
- Su Y, Deng B, Xi R (2011) Polycomb group genes in stem cell self-renewal: a double-edged sword. *Epigenetics* 6:16–19.
- Sun Y, Meijer DH, Alberta JA, Mehta S, Kane MF, Tien A-C, Fu H, Petryniak MA, Potter GB, Liu Z, Powers JF, Runquist IS, Rowitch DH, Stiles CD (2011) Phosphorylation state of Olig2 regulates proliferation of neural progenitors. *Neuron* 69:906–917.
- Talasz H, Helliger W, Sarg B, Debbage PL, Puschendorf B, Lindner H (2002) Hyperphosphorylation of histone H2A.X and dephosphorylation of histone H1 subtypes in the course of apoptosis. *Cell Death Differ* 9:27–39.
- Tao J, Van Esch H, Hagedorn-Greiwe M, Hoffmann K, Moser B, Raynaud M, Sperner J, Fryns J-P, Schwinger E, Gécz J, Ropers H-H, Kalscheuer VM (2004) Mutations in the X-linked cyclin-dependent kinase-like 5 (CDKL5/STK9) gene are associated with severe neurodevelopmental retardation. *Am J Hum Genet* 75:1149–1154.
- Tashiro A, Zhao C, Gage FH (2006) Retrovirus-mediated single-cell gene knockout technique in adult newborn neurons in vivo. *Nat Protoc* 1:3049–3055.
- Tate P, Skarnes W, Bird A (1996) The methyl-CpG binding protein MeCP2 is essential for embryonic development in the mouse. *Nat Genet* 12:205–208.

- Team RRDC (2005) [R] R Development Core Team: R: A language and environmen... - Google Scholar.
- Tiberi L, Vanderhaeghen P, van den Aemele J (2012) Cortical neurogenesis and morphogens: diversity of cues, sources and functions. *Curr Opin Cell Biol* 24:269–276.
- Tuoc TC, Radyushkin K, Tonchev AB, Piñon MC, Ashery-Padan R, Molnár Z, Davidoff MS, Stoykova A (2009) Selective cortical layering abnormalities and behavioral deficits in cortex-specific Pax6 knock-out mice. *Journal of Neuroscience* 29:8335–8349.
- van den Boom V, Kooistra SM, Boesjes M, Geverts B, Houtsmuller AB, Monzen K, Komuro I, Essers J, Drenth-Diephuis LJ, Eggen BJJ (2007) UTF1 is a chromatin-associated protein involved in ES cell differentiation. *J Cell Biol* 178:913–924.
- Villard L (2007) MECP2 mutations in males. *J Med Genet* 44:417–423.
- Volpe M, Shpungin S, Barbi C, Abrham G, Malovani H, Wides R, Nir U (2006) trnp: A conserved mammalian gene encoding a nuclear protein that accelerates cell-cycle progression. *DNA Cell Biol* 25:331–339.
- Wang X, Tsai J-W, Lamonica B, Kriegstein AR (2011) A new subtype of progenitor cell in the mouse embryonic neocortex. Nature Publishing Group.
- Wang Z, Shu W, Lu MM, Morrissey EE (2005) Wnt7b activates canonical signaling in epithelial and vascular smooth muscle cells through interactions with Fzd1, Fzd10, and LRP5. *Molecular and Cellular Biology* 25:5022–5030.
- Warren N, Caric D, Pratt T, Clausen JA, Asavaritikrai P, Mason JO, Hill RE, Price DJ (1999) The transcription factor, Pax6, is required for cell proliferation and differentiation in the developing cerebral cortex. *Cereb Cortex* 9:627–635.
- Weaving LS, Christodoulou J, Williamson SL, Friend KL, McKenzie OLD, Archer H, Evans J, Clarke A, Pelka GJ, Tam PPL, Watson C, Lahooti H, Ellaway CJ, Bennetts B, Leonard H, Gécz J (2004) Mutations of CDKL5 cause a severe neurodevelopmental disorder with infantile spasms and mental retardation. *Am J Hum Genet* 75:1079–1093.
- Weaving LS, Ellaway CJ, Gécz J, Christodoulou J (2005) Rett syndrome: clinical review and genetic update. *J Med Genet* 42:1–7.
- Williams BP, Price J (1995) Evidence for multiple precursor cell types in the embryonic rat cerebral cortex. *Neuron* 14:1181–1188.
- Williams BP, Read J, Price J (1991) The generation of neurons and oligodendrocytes from a common precursor cell. *Neuron* 7:685–693.

References

- Willis T (1664) *Cerebri anatome*.
- Xu J, Testa JR (2009) DLX5 (distal-less homeobox 5) promotes tumor cell proliferation by transcriptionally regulating MYC. *J Biol Chem* 284:20593–20601.
- Xu J, Watts JA, Pope SD, Gadue P, Kamps M, Plath K, Zaret KS, Smale ST (2009) Transcriptional competence and the active marking of tissue-specific enhancers by defined transcription factors in embryonic and induced pluripotent stem cells. *Genes & Development* 23:2824–2838.
- Yang A, Zhu Z, Kapranov P, McKeon F, Church GM, Gingeras TR, Struhl K (2006) Relationships between p63 binding, DNA sequence, transcription activity, and biological function in human cells. *Molecular Cell* 24:593–602.
- Yaworsky PJ, Kappen C (1999) Heterogeneity of neural progenitor cells revealed by enhancers in the nestin gene. *Dev Biol* 205:309–321.
- Yellajoshiyula D, Patterson ES, Elitt MS, Kroll KL (2011) Geminin promotes neural fate acquisition of embryonic stem cells by maintaining chromatin in an accessible and hyperacetylated state. *Proceedings of the National Academy of Sciences* 108:3294–3299.
- Yun K, Potter S, Rubenstein JL (2001) Gsh2 and Pax6 play complementary roles in dorsoventral patterning of the mammalian telencephalon. *Development* 128:193–205.
- Zaret KS, Carroll JS (2011) Pioneer transcription factors: establishing competence for gene expression. *Genes & Development* 25:2227–2241.
- Zhao Y et al. (2008) Two supporting factors greatly improve the efficiency of human iPSC generation. *Cell Stem Cell* 3:475–479.
- Zhou FC, Balaraman Y, Teng M, Liu Y, Singh RP, Nephew KP (2011) Alcohol alters DNA methylation patterns and inhibits neural stem cell differentiation. *Alcohol Clin Exp Res* 35:735–746.
- Zhou Q, Anderson DJ (2002) The bHLH transcription factors OLIG2 and OLIG1 couple neuronal and glial subtype specification. *Cell* 109:61–73.
- Zhou Z, Hong EJ, Cohen S, Zhao W-N, Ho H-YH, Schmidt L, Chen WG, Lin Y, Savner E, Griffith EC, Hu L, Steen JAJ, Weitz CJ, Greenberg ME (2006) Brain-specific phosphorylation of MeCP2 regulates activity-dependent Bdnf transcription, dendritic growth, and spine maturation. *Neuron* 52:255–269.

PUBLIKATIONEN

Teile dieser Arbeit sind oder werden wie folgt publiziert

Stahl R, Walcher T, De Juan Romero C, Irmeler M, Blum R, Borrell V, Götz M – „Trnp1 regulates expansion and folding of the mammalian cerebral cortex by control of radial glial fate” Manuscript in revision at Cell

Pinto L., Mader M.T., Irmeler M., Gentilini M., Santoni F., Drechsel D., Blum R., **Stahl R.**, Bulfone A., Malatesta P., Beckers J. and Götz M – „Prospective isolation of functionally distinct radial glial subtypes-Lineage and transcriptome analysis“ Mol Cell Neurosci. 2008, 38, 15-42

Stahl R, Soba P, Wagner K, Eggert S, Merdes G and Kins S – „Proteolytic processing modulates the cell adhesion properties of APP“ Manuscript in revision at Journal of Neuroscience Research